[redacted]

[redacted]

NASA-TM-X-6987

NIMBUS 1
HIGH RESOLUTION RADIATION DATA CATALOG AND USERS' MANUAL

Volume 1
Photofacsimile Film Strips

(NASA-TM-X-69876) NIMBUS 1 HIGH RESOLUTION RADIATION DATA CATALOG AND USERS' MANUAL. VOLUME 1: PHOTOFACSIMILE FILM STRIPS (NASA) 333 p N73-72523
Unclas
00/99 02724

GODDARD SPACE FLIGHT CENTER
GREENBELT, MARYLAND

NIMBUS I
HIGH RESOLUTION RADIATION DATA CATALOG AND USERS' MANUAL

Volume 1
Photofacsimile Film Strips

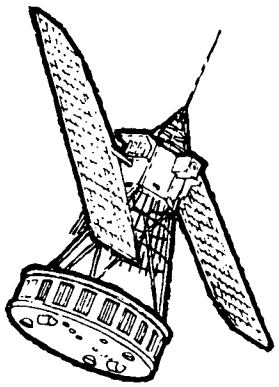

By

Staff Members

of the

Aeronomy and Meteorology Division

Goddard Space Flight Center

National Aeronautics and Space Administration

January 15, 1965

FOREWORD

This Volume, "Photofacsimile Film Strips," is the first of two volumes documenting the data from the High Resolution Infrared Radiometer (HRIR) experiment carried on the Nimbus I Meteorological Satellite. Volume 2, "Nimbus Meteorological Radiation Tapes – HRIR," to be published later, will document essentially the same data reduced to a magnetic tape format suitable for automatic processing on a large digital computer.

It is not feasible to list by name all of the many people who contributed to the success of the HRIR experiment, but their efforts are sincerely appreciated and gratefully acknowledged. The task of assembling the information contained herein into a form suitable for publication was largely accomplished by the following persons.

Aeronomy and Meteorology Division, Goddard Space Flight Center

Mr. L. Foshee, Experimenter
Mr. G. W. Nicholas, Editor
Mr. W. R. Bandeen
Mr. W. Fizell
Mr. P. S. Hoffrichter
Mr. David Rasmussen

ARACON Geophysics Company
(Under contract to the Goddard Space Flight Center) Contract No. NAS 5-3253

Mr. Robert Smith
Mr. Romeo R. Sabatini
Mr. Walter Smith
Mr. James Pike

ABSTRACT

The Nimbus I Meteorological Satellite contained a High Resolution Infrared Radiometer (HRIR) designed to map nighttime cloud cover and surface temperatures from emission within the 3.5 – 4.1 micron atmospheric window. HRIR data were acquired from a near-polar orbit during the period 28 August - 22 September 1964, after which a spacecraft malfunction occurred.

In this Volume the radiometer design, calibration, and performance, the photofacsimile processing, and the coverage and documentation of the data are discussed.

The successfully reduced data are documented in three forms. One form consists of an "Index of Available High Resolution Infrared Radiometer Film Strips (Photofacsimile)," a second of "Subpoint Track Summaries of Available Radiation Data," and a third of "Contact Prints of Available Photofacsimile Film Strips." The data documented in this Volume are available in the form of 70mm positive or negative transparencies or positive contact prints.

TABLE OF CONTENTS

	Page
Foreword	iii
Abstract	iv
List of Figures	vi
List of Tables	vii
List of Common Symbols	viii
I. INTRODUCTION	1
1.1 General	1
1.2 User Data Requests	2
II. DESCRIPTION OF THE HIGH RESOLUTION INFRARED RADIOMETER (HRIR) EXPERIMENT	5
2.1 Summary of the Experiment	5
2.2 Design of the Radiometer	8
2.3 HRIR Subsystem	9
III. CALIBRATION	12
3.1 Effective Spectral Response	12
3.2 Effective Radiance	12
3.3 Equivalent Blackbody Temperature	14
IV. RADIATION DATA PROCESSING (PHOTOFACSIMILE)	18
4.1 Photofacsimile Recorder	18
4.2 Gridding	18
V. RADIATION DATA COVERAGE AND DOCUMENTATION	20
5.1 Radiation Data Coverage	20
5.2 Documentation of the Data	32
VI. PERFORMANCE OF THE RADIATION EXPERIMENT	33
VII. CONCLUSIONS	42
VIII. REFERENCES AND BIBLIOGRAPHY	43
APPENDIX A - Index of Available High Resolution Infrared Radiometer Film Strips (Photofacsimile)	45
APPENDIX B – Subpoint Track Summaries of Available Radiation Data	62
APPENDIX C – Contact Prints of Available Photofacsimile Film Strips	89

LIST OF FIGURES

Figure		Page
1	A positive print of daytime HRIR data	3
2	Nimbus I spacecraft showing the position of the radiometer	5
3	Schematic showing (a) relevant scan angles and (b) the resulting data coverage	6
4	Schematic showing the content of a typical HRIR film strip	7
5	Nimbus I High Resolution Infrared Radiometer	8
6	Radiation cooling system for the HRIR lead selenide detector	9
7	Schematic of the HRIR optical system	10
8	Portion of an analog record showing nearly two HRIR scan cycles	10
9	Simplified block diagram of the HRIR subsystem	11
10	The effective spectral response of the HRIR vs. wavelength	13
11	Schematic illustrating the relationship between laboratory calibration and T_{BB} measurements made in orbit	14
12	$\overline{N}$ vs. T_{BB}	15
13	HRIR calibration	17
14	Data coverage strips for subpoint night portions of orbits 001 and 002 of Nimbus I	21
15	Subperigee latitude vs. orbit number for Nimbus I	22
16	Acquisition figures at Gilmore Creek, Alaska and Rosman, North Carolina, and 16 subpoint tracks	24
17	Diagrams showing the record and playback sequence of the HRIR tape recorder for 15 orbits - a through d	25
	Diagrams showing the record and playback sequence of the HRIR tape recorder for 15 orbits - e through h	26
	Diagrams showing the record and playback sequence of the HRIR tape recorder for 15 orbits - i through l	27
18	Typical HRIR data coverage for Nimbus I	31
19	HRIR lead selenide cell temperature vs. orbit number	34-41
A1	Time of descending node minus time of ascending node vs. orbit number	48

Figure		Page
A2	Longitude of the descending node minus the longitude of the ascending node vs. orbit number	49
C1	Block of forward mode data showing (a) the film positioned for reading the index display, and (b) correctly oriented for viewing	90
C2	Block of reverse mode data showing (a) the film positioned for reading the index display, and (b) correctly oriented for viewing	92
C3	Ten-Step Gray Scale Wedge	93

LIST OF TABLES

Table		Page
I	Orbital Characteristics of Nimbus I	1
II	Nimbus I HRIR Optics	13
III	Effective Spectral Response	13
IV	$\bar{N}$ vs. T_{BB}	15

LIST OF COMMON SYMBOLS

ϕ_λ - Effective spectral response

$\bar{N}$ - Effective radiance

T_{BB} - Blackbody target temperature (in the laboratory)
Equivalent blackbody temperature (in orbit)

R_λ - Spectral reflectivity

R_λ^{SC} - Spectral reflectivity of scan mirror

R_λ^{PM} - Spectral reflectivity of primary mirror

R_λ^{SM} - Spectral reflectivity of secondary mirror

R_λ^{R1} - Spectral reflectivity of relay mirror 1

R_λ^{R2} - Spectral reflectivity of relay mirror 2

f_λ - Spectral transmittance of the filter

A_λ - Spectral absorptivity of the detector

B_λ - Planck function (radiance) at wavelength λ

N_λ - Non-Planckian spectral radiance

E_P - Pitch error in spacecraft attitude

E_R - Roll error in spacecraft attitude

E_Y - Yaw error in spacecraft attitude

T_{CC} - Radiometer detector cell temperature

T_{HS} - Radiometer housing temperature

NATIONAL AERONAUTICS AND SPACE ADMINISTRATION

ERRATA

NIMBUS I HIGH RESOLUTION RADIATION DATA CATALOG AND USERS' MANUAL: VOLUME 1. PHOTOFACSIMILE FILM STRIPS

January 15, 1965

Page 43. The authors of Reference 5 should be changed to read: "Fujita, Tetsuya and William Bandeen..."

Page 43. The authors of Reference 8 should be changed to read: "Foshee, L., I. L. Goldberg, W. Nordberg, and C. Catoe..."

Page 91, first complete paragraph. The last line should be changed to read "...in error by more than 120 nautical miles."

Page 94, first complete paragraph. The third sentence which reads, "The prints have been arranged to avoid overlap from one page to a non-facing page," should be deleted. (A printing error shifted all even-numbered pages from left to right beginning with page 96, yielding instances where overlap of data does extend to a non-facing page. The only result, however, is a slight inconvenience to the reader.)

I. INTRODUCTION

1.1 General

The Nimbus I Meteorological Satellite was injected into orbit on August 28, 1964 at 8:52 UT. At that time its orbital elements were those shown in Table I.

TABLE I
Orbital Characteristics of Nimbus I

Perigee Height	423.2 km
Apogee Height	932.7 km
Anomalistic Period	98.31 min
Inclination	98.66 deg
Argument of Perigee	160.74 deg
Perigee Motion	-3.11 deg day^{-1}
Right Ascension of Ascending Node	150.20 deg
Motion of Line of Nodes	+1.06 deg day^{-1}

A circular orbit near the apogee height had been planned, but the elliptical orbit resulted from a shortened burning time of the second stage of the launch vehicle. The retrograde near-polar orbit was designed to be sun-synchronous, such that the eastward (+) motion of the line of nodes would equal 0.9856 deg day^{-1}, the mean motion of the Right Ascension of the sun. It is seen from Table I that this value was slightly exceeded. Also, the time of launch was planned such that the ascending node would always occur at local noon (and, therefore, the descending node at local midnight). This goal was not quite achieved inasmuch as the ascending node occurred at 11:34 a.m. local mean time at the time of injection (and the descending node at 11:34 p.m.). However, the slight excess in the motion of the line of nodes caused the times of the equator crossings to advance such that by orbit 368 on 22 September 1964 the ascending node occurred at 11:41 a.m. local mean time (and the descending node at 11:41 p.m.). A further discussion of the design parameters of the Nimbus orbit is given in Reference 1.

The experiments flown on the satellite consisted of an Advanced Vidicon Camera System (AVCS), an Automatic Picture Transmission (APT) system, and a High Resolution Infrared Radiometer (HRIR) system. This Volume is concerned only with an overall discussion of the HRIR experiment and the documentation of the HRIR data in the form of photofacsimile film strips. A second Volume will document essentially the same data reduced to a magnetic tape format suitable for automatic processing on a large digital computer (Reference 2). The data from the AVCS and APT systems will be documented in a separate volume (Reference 3).

Because of the relatively short lifetime of the spacecraft and, hence, the correspondingly limited amount of data, it was decided to publish contact prints of the HRIR photofacsimile data in their entirety. These prints, all but a few of which have been automatically "gridded" (i.e., correlated in Earth latitude and longitude), are presented in Appendix C. To aid further in their interpretation, pertinent documentary data are listed in an "Index of Available High Resolution Infrared Radiometer Film Strips (Appendix A)" and in the "Subpoint Track Summaries of Available Radiation Data (Appendix B)." Before attempting to interpret the HRIR photofacsimile data, the reader should give careful attention to all points discussed in this manual. An understanding of the significance of the equivalent blackbody temperatures, or effective radiance values, and a familiarity with the principle of the radiometer, the scan geometry, the calibration, and the photofacsimile data reduction are essential to an understanding of the data.

The data documented in this Volume are available in the form of 70 mm positive or negative transparencies or positive contact prints. (In our convention, a "positive" product is one in which the nighttime clouds in emission generally appear lighter than the land or water through clear skies, i.e., low values of radiance are light and high values of radiance are dark. However, when HRIR data are acquired in the daytime, strongly reflected solar radiation from the clouds, added to their emission, may yield the highest total radiance values in a strip, thus making the clouds appear darker than the land or water through clear skies. Such a daytime "positive" is shown in Figure 1. According to this convention all prints shown in Appendix C are "positives.")

1.2 User Data Requests

The HRIR data may be obtained by writing to:

Nimbus Data, Code 650
NASA Space Science Data Center
Goddard Space Flight Center
Greenbelt, Maryland 20771

As resources permit, limited quantities of data will be furnished to investigators without charge. Otherwise, data will be furnished for production costs or less. Whenever it is determined that a charge is required, a cost estimate will be provided to the user prior to filling the data request. The basic unit for furnishing data will be the "Data Orbit," i.e., even though only a single "Data Block" may be of primary interest, all Data Blocks making up the corresponding Data Orbit will be furnished in a single continuous strip. Also, a calibration gray scale wedge will normally be included on both transparancies and prints (see Figure C3). However, an important exception when a gray scale wedge will not be included is pointed out in item 5.b below. When requesting data, the following information should be given (all terms are discussed fully in subsequent parts of this manual):

1. Satellite (e.g., Nimbus I)
2. Data Orbit No. (cf. Appendix A)

Figure 1–A positive print of daytime HRIR data over Central America, Cuba, and Hurricane Dora showing the effects of reflected radiation in the 3.5 – 4.1 micron region

3. Calendar Date of Descending Node (cf. Appendix A)

4. Format Requested

   a. Photofacsimile 70mm Positive Transparency
   b. Photofacsimile 70mm Negative Transparency
   c. Photofacsimile 70mm Positive Print

5. Special Instructions

   a. If the primary interest of the investigator is in either clouds or land and ocean features, he should so indicate as a guide in achieving the proper density in the photographic processing.
   b. Unless otherwise specified a uniform density exposure will be employed, and a calibration gray scale will be included to permit the interpretation of the data in terms of absolute radiation values. However, the detail in a single transparency or print can be further enhanced photographically by automatically "dodging" or varying the exposure over the various light and dark portions of a given strip of data. (The data shown in Appendix C were dodged in this way). Persons who so specify, will be furnished data which include the automatic dodging feature. However, in the dodging process the uniformity of the calibration is altered, invalidating the gray scale wedge; hence, no calibration gray scale wedges will be furnished with such data.
   c. To the extent of our resources and capabilities, any other special requirements will be considered.

II. DESCRIPTION OF THE HIGH RESOLUTION INFRARED RADIOMETER (HRIR) EXPERIMENT

2.1 Summary of the Experiment

The Nimbus High Resolution Infrared Radiometer (HRIR) was designed to perform two functions. These functions were first to map the Earth's cloud cover at night, thus complementing the television (AVCS) coverage during the daytime portion of the orbit, and second to measure the radiative temperatures of cloud tops and terrain features. The interpretation of the HRIR data in terms of these physically significant quantities has already been discussed in the literature (References 4-11).

Normally the HRIR subsystem operates during "subpoint night," i.e., when the subpoint, and hence the general area of satellite observation, is on the dark side of the terminator. However, there are certain advantages occasionally in operating the HRIR subsystem during the daylight, e.g., comparing the HRIR film strips with AVCS cloud photographs of the same area at the same time. In addition it is of interest to observe the reflective characteristics of clouds and terrestrial features in the 3.5 - 4.1 micron region as shown in Figure 1. True surface and cloudtop temperatures are not revealed in this picture due to the reflected solar radiation which is added to the emitted radiation; however, the radiometer output is not saturated and a usable product is still obtained.

The radiometer is attached to the earth-oriented sensory ring of Nimbus I in such a manner that an unobstructed view of the earth is possible (Figure 2). As the satellite orbits the earth the radiometer scans the Earth's surface from horizon to horizon.

The scan mirror is inclined by 45 degrees to its axis of rotation which is coincident with the spacecraft velocity vector (assuming no attitude errors). Thus, the optical axis scans in a plane perpendicular to the spacecraft velocity vector.

The radiometer has an instantaneous field of view of 7.9 milliradians, which at a height of 930 km corresponds to a ground resolution of approximately 7.5 km at the nadir. The scan rate was chosen such that the scan mirror would rotate once every 1.3418 seconds, the time required for the satellite to advance the distance of one resolution element

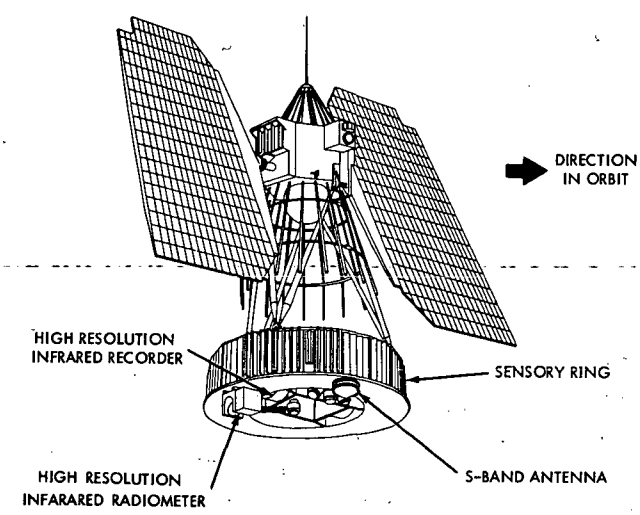

Figure 2—The Nimbus I spacecraft showing the position of the High Resolution Infrared Radiometer on the sensory ring

along the subsatellite track at the planned circular orbital height of 930 km. However, because of the eccentric orbit which was achieved, a condition of noncontiguous scans, separated by gaps near the subsatellite point, resulted from the lower orbital heights near perigee.

For a satellite height of 930 km, a complete nighttime data coverage strip would be approximately 6,500 km in width and 20,000 km in length (Figure 3). Because of the extreme perspective near the horizons, only data corresponding to the central 107° of the Earth scan were gridded. Again, for a satellite height of 930 km, the width of the gridded portion of the data strip would be approximately 3,200 km (Figure 3). For Nimbus I these dimensions are correspondingly reduced at heights below apogee.

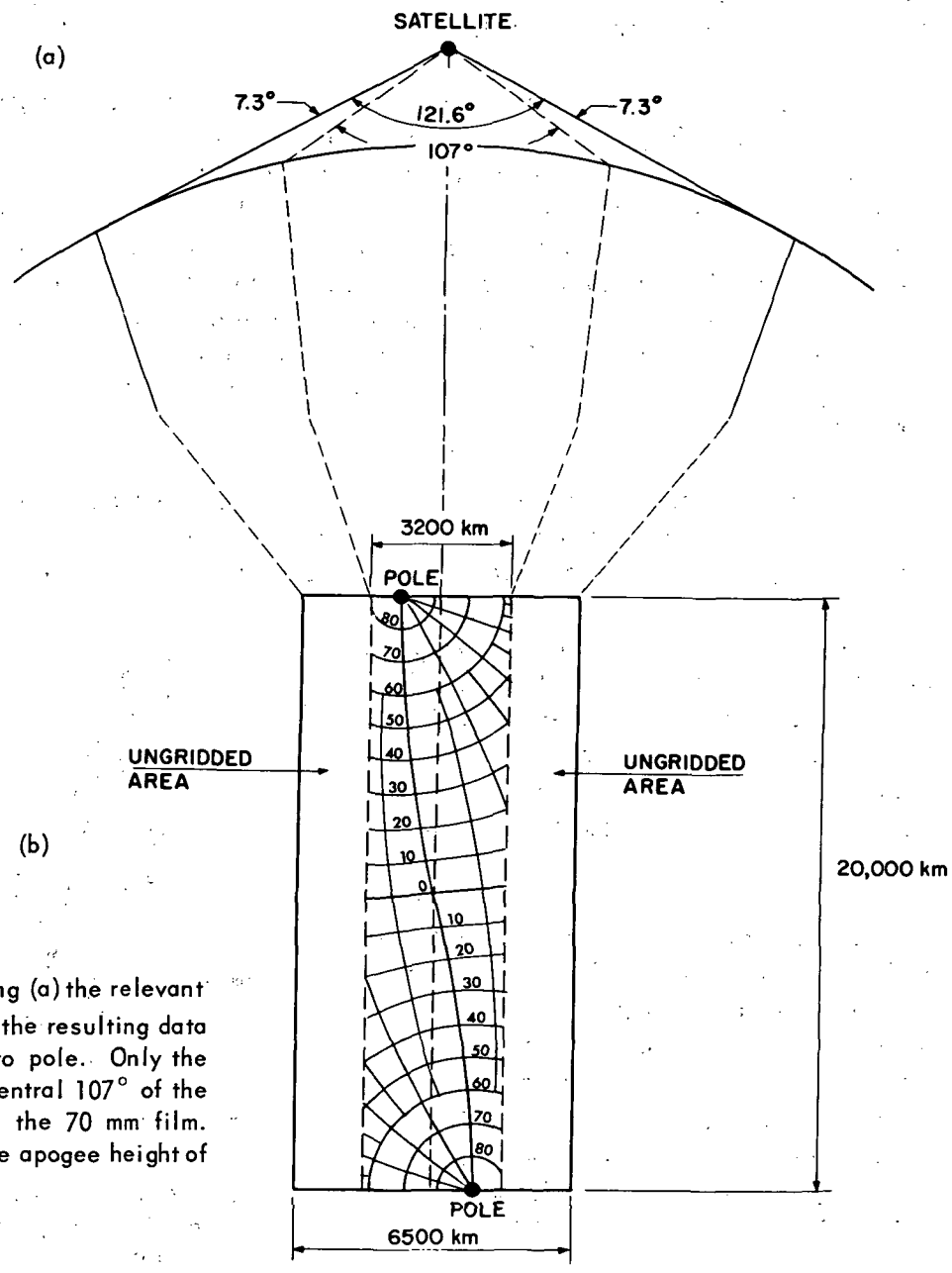

Figure 3—Schematic showing (a) the relevant HRIR scan angles and (b) the resulting data coverage strip from pole to pole. Only the data included within the central 107° of the Earth scan are gridded on the 70 mm film. This figure pertains to the apogee height of Nimbus I.

The photofacsimile recorder develops a visual readout for the HRIR subsystem. The data are presented on a film strip in the format shown in Figure 4. The data are normally presented as scales of gray in which higher temperatures are darker, and lower temperatures lighter, to correspond superficially with the conventional cloud photography to which we are already accustomed. The HRIR video data occupy 54mm of the 70mm film width. A two millimeter strip representing housing temperature (calibration) data is adjacent to the video. Also, depending upon the height of the satellite, the space-viewed response may be included in the 54mm of video data on the film strip (cf. Figures 3 and 4).

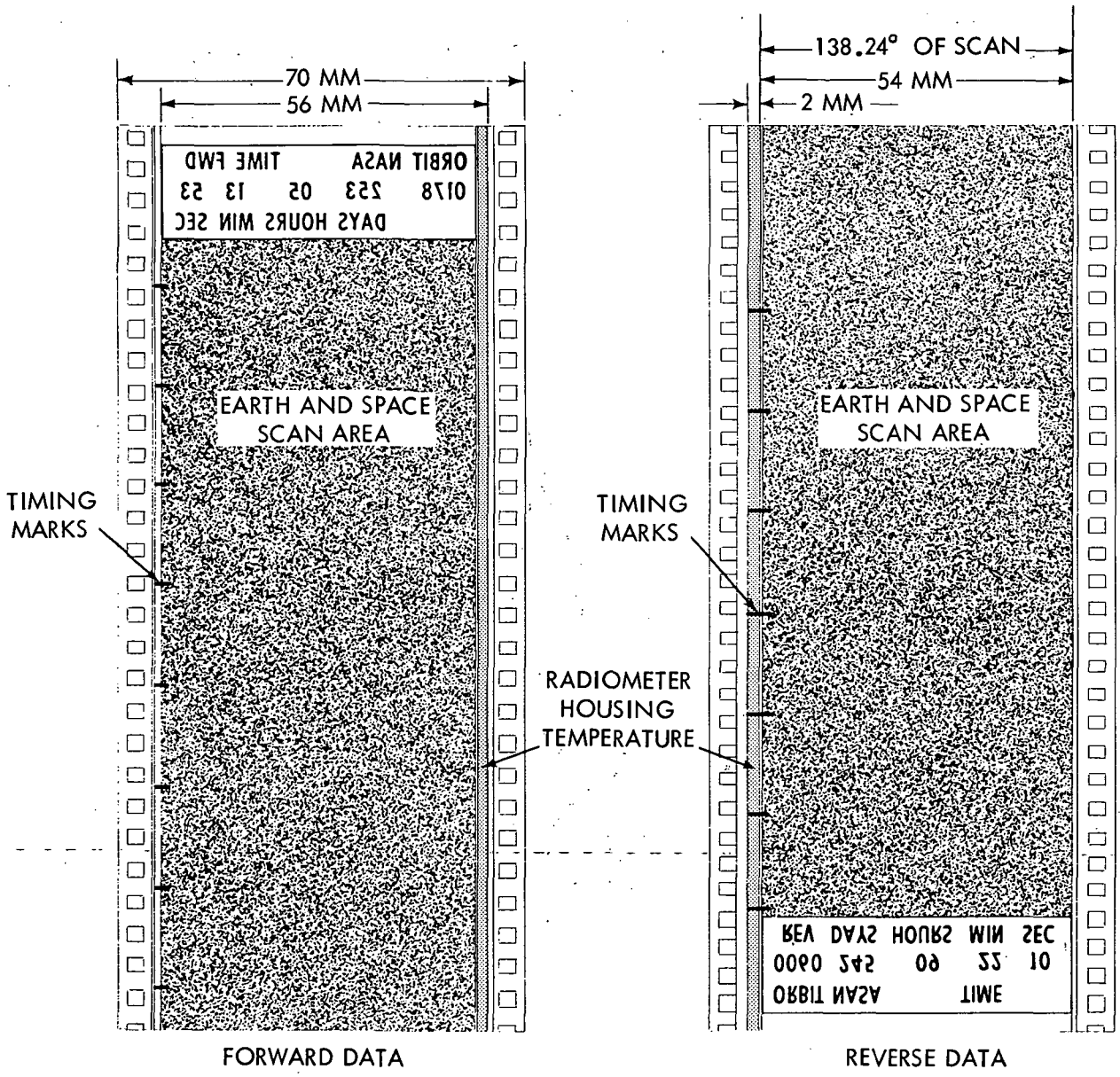

Figure 4—Schematic showing the content and appearance of typical HRIR nighttime data correctly oriented for viewing with north and east toward the top and right respectively. Both "FORWARD" and "REVERSE" data are shown. Note the backward orientation of the index information (cf. Figures C1 and C2).

2.2 Design of the Radiometer

The HRIR experiment incorporates a single channel scanning radiometer, built by the International Telephone and Telegraph Industrial Laboratories (ITTIL). The radiometer is shown in Figure 5. It contains a lead selenide (PbSe) photoconductive cell which is radiatively cooled to -75°C and operates in the 3.5 - 4.1 micron window region. The white collars shown in the figure are sun shields to prevent direct solar radiation from entering the optical cavity during spacecraft sunrise and sunset. The scan mirror is located between the sun shields.

The radiative cooling system is shown in Figure 6. Cooling is accomplished by means of a highly reflective gold coated pyramidal horn containing a black cooling patch at the bottom. The pyramidal horn is oriented to view outer space during the entire orbit, and the patch is suspended by thin wires to reduce heat conduction from the radiometer housing. The PbSe detector is connected to the cooling patch by a high-thermal-conductance transfer bar.

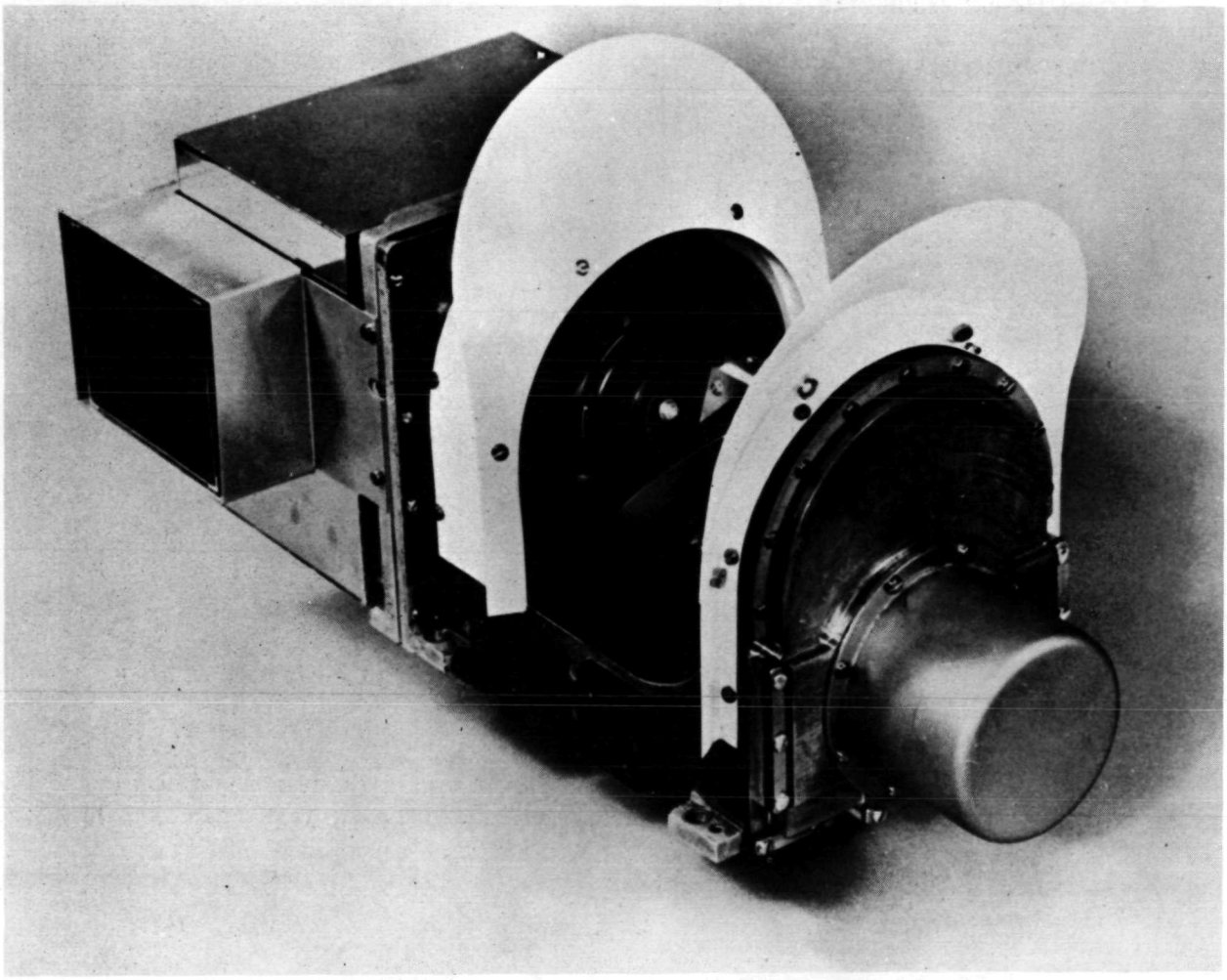

Figure 5–NIMBUS I High Resolution Infrared Radiometer

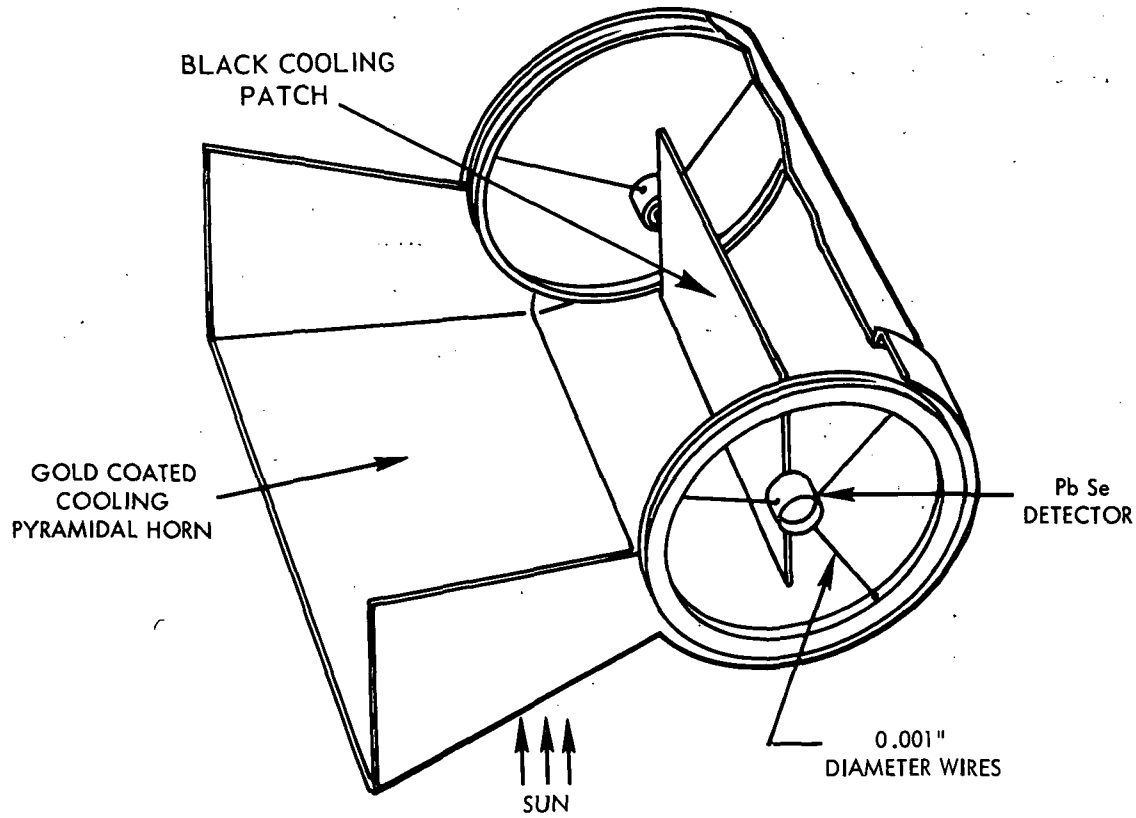

Figure 6-Radiative cooling system for the HRIR lead selenide detector

Figure 7 illustrates the HRIR optical system. The radiation reflected from the scan mirror is chopped at the rate of 1500 cps at the focus of a 4-inch f/1 modified Cassegrainian telescope. It is then refocused at the detector by means of a reflective relay optical system which contains the 3.5 - 4.1 micron interference filter. The resulting a.c. signal is amplified by a linear-logarithmic amplifier which is designed to begin compression when the detector output has increased to about 50 milliwatts RMS. The a.c. signal is rectified, resulting in a d.c. output varying from 0 to -6 volts and having a video bandwidth of 0 to 268 cps.

A typical scan cycle is shown in Figure 8. When outer space is viewed, the signal drops to the zero level. The temperature of the housing cavity, which is also viewed during each scan cycle, is telemetered separately to the ground. The space and housing measurements, then, yield two points for an in-flight check of calibration. During the space scan, a permanent magnet on the mirror axis (scan gear) triggers a gate and a multivibrator so that seven pulses are generated, serving to synchronize ground equipment for recomposing the picture.

2.3 HRIR Subsystem

A simplified block diagram of the HRIR subsystem is shown in Figure 9. The HRIR radiometer output or the video output from IR scanner A (Nimbus horizon-scanner

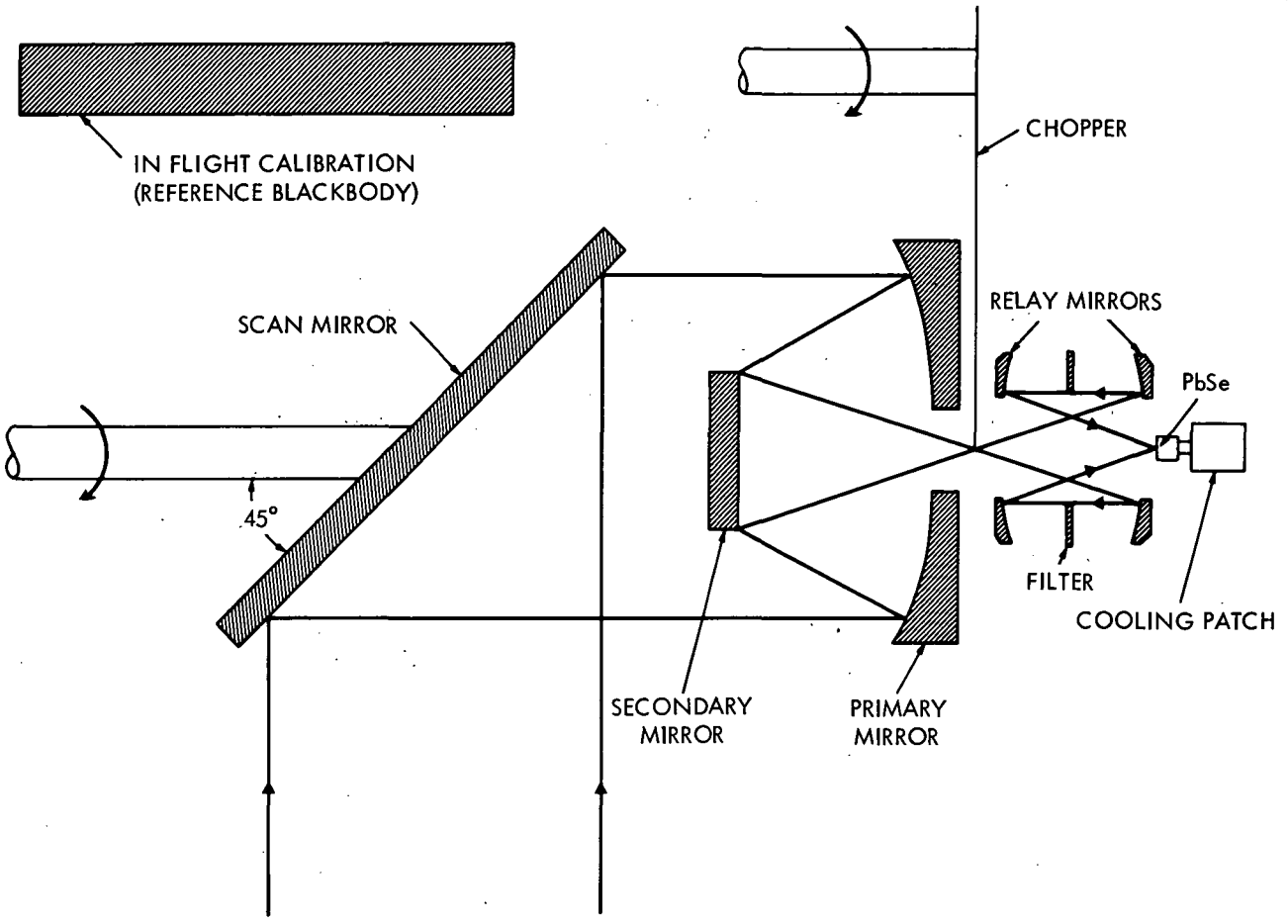

Figure 7–Schematic of the HRIR optical system

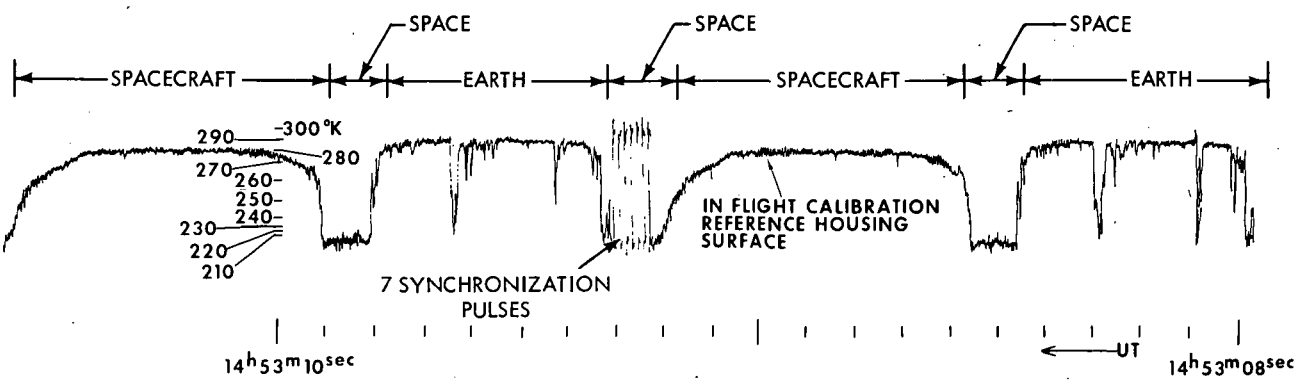

Figure 8–A portion of an analog record showing nearly two HRIR scan cycles. The scan progresses from right to left. Calibrated equivalent blackbody temperature levels are shown for comparison.

sensor) may be selected to be applied to the recording circuits of the tape recorder; however, only one video at a time is selected for recording.

The radiometer output and the radiometer sync pulse are applied to an FM modulator where they are converted to a frequency modulated signal with a maximum frequency deviation of 8.25 to 10 kcs. The space level corresponds to 10 kcs, and the

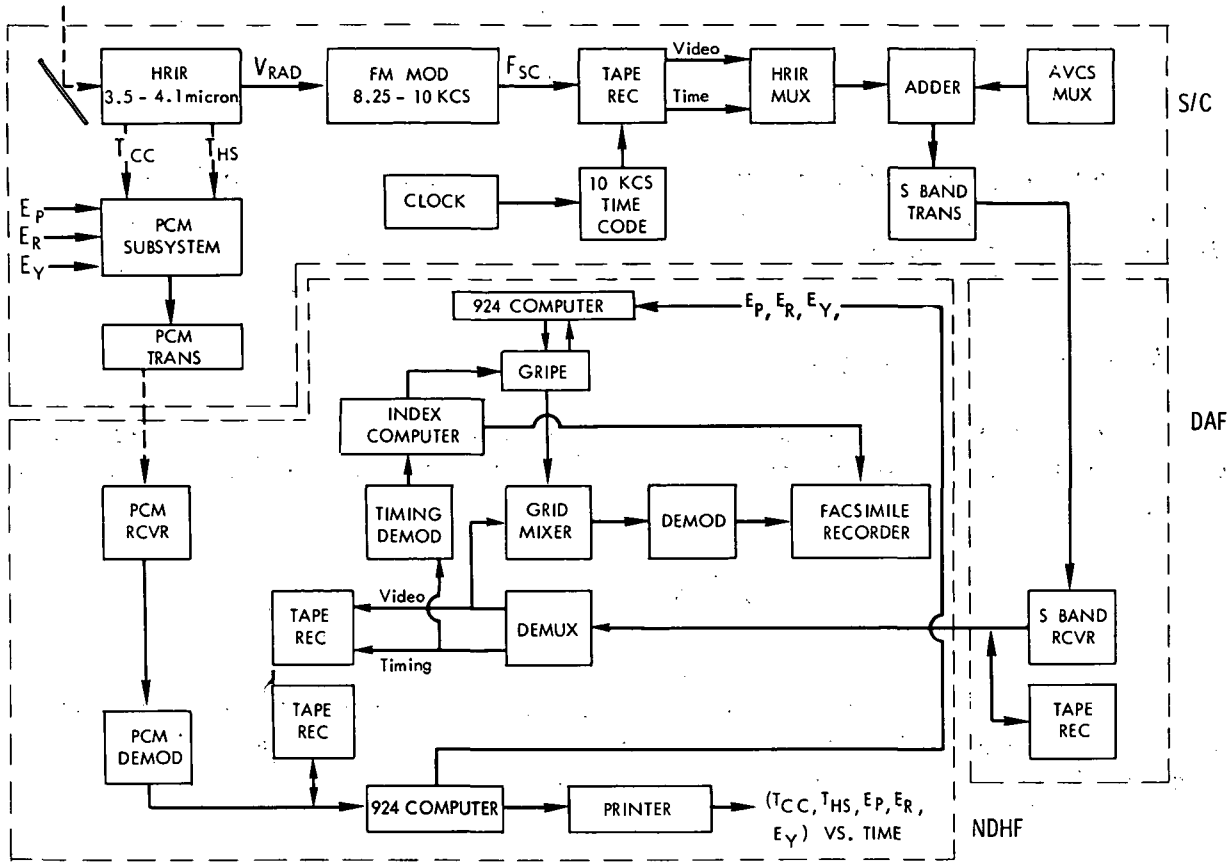

Figure 9–Simplified block diagram of the HRIR subsystem

hottest signal deviates to 8.25 kcs. The frequency modulated radiometer video signal combined with the sync signal and a 10 kcs time signal, amplitude modulated by the standard NASA time code, are simultaneously recorded on two of the four tape tracks at a tape speed of 3.75 inches per second. The 10 kc time signal provides a time reference for the radiometer video signal. When these two tracks have been completely recorded, the direction of the tape travel is automatically reversed by the end-of-tape signals and the recording continues on the other two tracks. When the playback command is received, record power is removed from the record circuits, and playback power is applied to the playback circuits in the tape recorder and multiplexer. The direction of the tape reverses and all four tracks are played back simultaneously at an eightfold increased speed of 30 inches per second. This means that if all four tracks have been recorded, two tracks will be played back in the same direction in which they are recorded, while the other two will be played back in the opposite direction. The most recent data will be played back in the opposite direction to that in which they were recorded. Provisions are made in the ground equipment to detect and to identify the most recently recorded data for display first. This is accomplished by using the time code accompanying the radiometer signal. All HRIR subsystem data are recorded in the ground equipment on magnetic tape which in turn serves as the master copy from which additional data processing can be accomplished. Additional information concerning the design of the HRIR experiment and its integration on the Nimbus spacecraft is contained in References 12-15.

III. CALIBRATION

In discussing the calibration three fundamental quantities must be defined: these are the effective spectral response, ϕ_λ, the effective radiance, $\overline{N}$, and the equivalent blackbody temperature, T_{BB}.

3.1 Effective Spectral Response

The radiation received by the radiometer is modified by five front-surfaced aluminized mirrors and a filter before reaching the PbSe detector. The effective spectral response, ϕ_λ, is defined as

$$\phi_\lambda = R_\lambda^{SC} R_\lambda^{PM} R_\lambda^{SM} R_\lambda^{R1} f_\lambda R_\lambda^{R2} A_\lambda. \tag{1}$$

In the actual computation of ϕ_λ, the spectral reflectivities, R_λ, of all mirrored surfaces were assumed to be constant over the pass band of the filter and, hence, were normalized to unity. The resultant equation used in computing ϕ_λ, therefore, was

$$\phi_\lambda = f_\lambda A_\lambda. \tag{2}$$

The materials used in the optics are given in Table II. The function, f_λ, was taken from International Telephone and Telegraph Industrial Laboratories (ITTIL) measurements of the filter used in HRIR Unit F-2, the instrument flown on Nimbus I, and the function, A_λ, was taken from several typical laboratory curves of PbSe detectors. The effective spectral response is given in Figure 10 and Table III.

3.2 Effective Radiance

Because of its narrow field of view, the HRIR essentially measures beam radiation or radiance toward the satellite along the optical axis. In the preflight laboratory calibration, the radiometer's field of view was filled by a blackbody target whose temperature could be varied and accurately measured over a range of 190°K to 340°K. From the temperature of the blackbody target, T_{BB}, the spectral radiance of the target is determined by the Planck function, B_λ. The integration of this function over the effective spectral response, ϕ_λ, yields that portion of the radiance of the target to which the radiometer responds, the "effective radiance, $\overline{N}$," given by

$$\overline{N} = \int_0^\infty B_\lambda (T_{BB}) \phi_\lambda \, d\lambda. \tag{3}$$

TABLE II
Nimbus I HRIR Optics

I. Filter

Type : Multilayer wide band-pass interference
Substrate: Germanium
Transmission: 0.76 (calculated)

II. Scan Mirror

Type: Evaporated SiO over hard coated aluminum
Substrate: Aluminum
Reflectivity: 0.96 (estimated)

III. Cassegrainian telescope (primary and secondary)

Type: Front surface AlO with SiO protective coating
Substrate: Glass

IV. Relay Optics

Type: Front surface gold coated with SiO protective coatings
Substrate: Glass
Reflectivity of the 4 mirror surfaces (Cassegrainian telescope and relay optics): 0.92 (estimated)

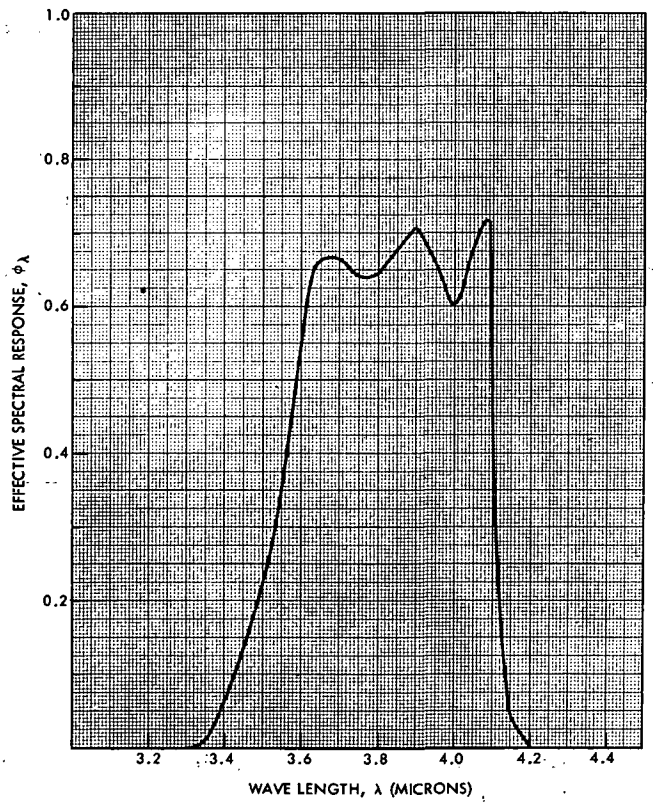

Figure 10–The effective spectral response of the HRIR vs. wavelength

TABLE III
Effective Spectral Response

λ	ϕ_λ
3.30	0.000
3.35	0.007
3.40	0.065
3.45	0.136
3.50	0.223
3.55	0.366
3.60	0.512
3.65	0.664
3.70	0.665
3.75	0.640
3.80	0.644
3.85	0.679
3.90	0.708
3.95	0.661
4.00	0.601
4.05	0.690
4.10	0.426
4.15	0.043
4.20	0.000

3.3 Equivalent Blackbody Temperature

The effective radiance to which the orbiting radiometer responds may be expressed by

$$\overline{N} = \int_0^\infty N_\lambda \, \phi_\lambda \, d\lambda \tag{4}$$

where N_λ is the generally non-Planckian spectral radiance in the direction of the satellite from the Earth and its atmosphere. It is convenient to express the measurement from orbit in terms of an equivalent temperature of a blackbody filling the field of view which would cause the same response from the radiometer. From Equations (3) and (4) it is seen that this "equivalent blackbody temperature" is simply the primary measurement of the laboratory calibration, the target temperature, T_{BB}. This relationship is expressed schematically in Figure 11. Therefore, the radiometer measurements can be expressed either as values of effective radiance, $\overline{N}$, or as equivalent blackbody temperatures, T_{BB}. The $\overline{N}$ vs. T_{BB} function from Equation (3) is given in Figure 12 and Table IV.

The only independent parameter of consequence in the calibration was the cooled PbSe cell temperature. All other temperature and voltage variations were automatically

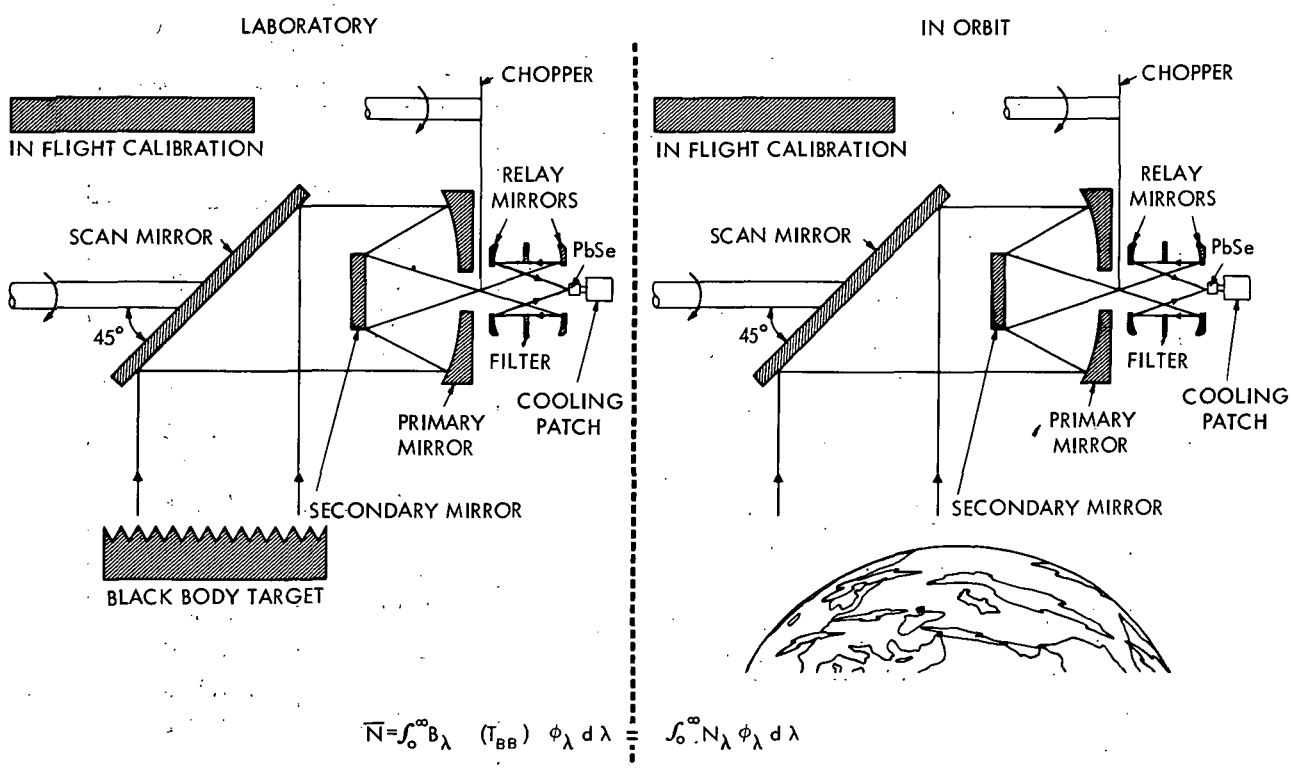

Figure 11–Schematic illustrating the relationship between the laboratory calibration and the equivalent blackbody temperature measurements made in orbit

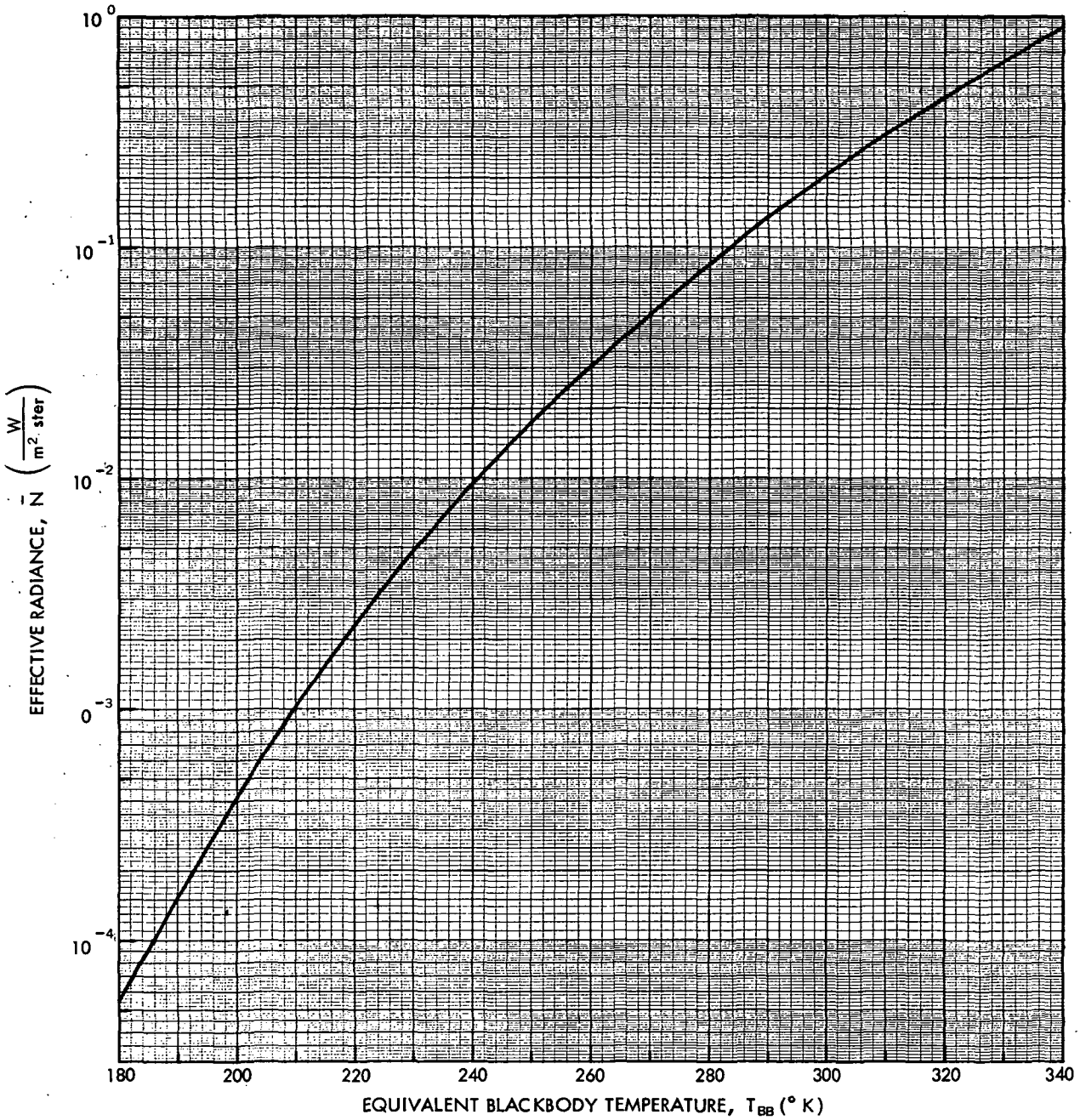

Figure 12—Effective radiance versus equivalent blackbody temperature

TABLE IV

$\bar{N}$ vs. T_{BB}

$\bar{N}$ (watts $m^{-2}ster^{-1}$)	T_{BB} (°K)	$\bar{N}$ (watts m^{-2} $ster^{-1}$)	T_{BB}(°K)	$\bar{N}$ (watts m^{-2} $ster^{-1}$)	T_{BB}(°K)
0.16291×10^{-3}	190	0.17228×10^{-1}	250	0.20483	300
0.04289×10^{-2}	200	0.30472×10^{-1}	260	0.30570	310
0.10311×10^{-2}	210	0.05169	270	0.44500	320
0.22916×10^{-2}	220	0.08449	280	0.64650	330
0.04755×10^{-1}	230	0.13355	290	0.89810	340
0.09294×10^{-1}	240				

compensated for and/or regulated between very narrow limits. Therefore, a separate calibration run was made for several different cell temperatures. The blackbody target temperature, T_{BB}, was varied between 190°K and 340°K in 10°K steps, and the radiometer output voltage was recorded after the temperature at each step had stabilized. After the radiometer output voltages had been obtained for all the target temperatures, the PbSe cell was stabilized at a new temperature, and the target temperature was cycled again from 190°K to 340°K.

After the unit was integrated in the spacecraft at the General Electric Company and subjected to vacuum-thermal environmental testing, a check of calibration was performed. These data were obtained approximately eight months after the original laboratory calibration of the radiometer. Essentially the same techniques were employed in obtaining these data points as were used in the original laboratory calibration of the individual unit. The blackbody target temperature was varied from 190°K to 340°K in 20°K steps, and the subcarrier frequency from the associated FM modulator and a timing signal were simultaneously recorded on the system tape recorder (cf. Figure 9). After the various target temperatures had been obtained, the data were played back through the entire system and transmitted via the S-band transmitter in the spacecraft. The data were received at the ground station, demultiplexed, demodulated, and displayed in the form of an analog trace on an oscillographic record. Close examination of both sets of calibration data revealed no significant changes over the eight months of handling and testing at the integrator's plant; therefore, we have high confidence in the validity of the calibration. The definitive calibration data for the HRIR F-2 unit which was flown on Nimbus I are shown in Figure 13. Parametric curves for different values of the PbSe cell temperature are given. Values of T_{BB} can be converted to $\bar{N}$ from Figure 12 or Table IV.

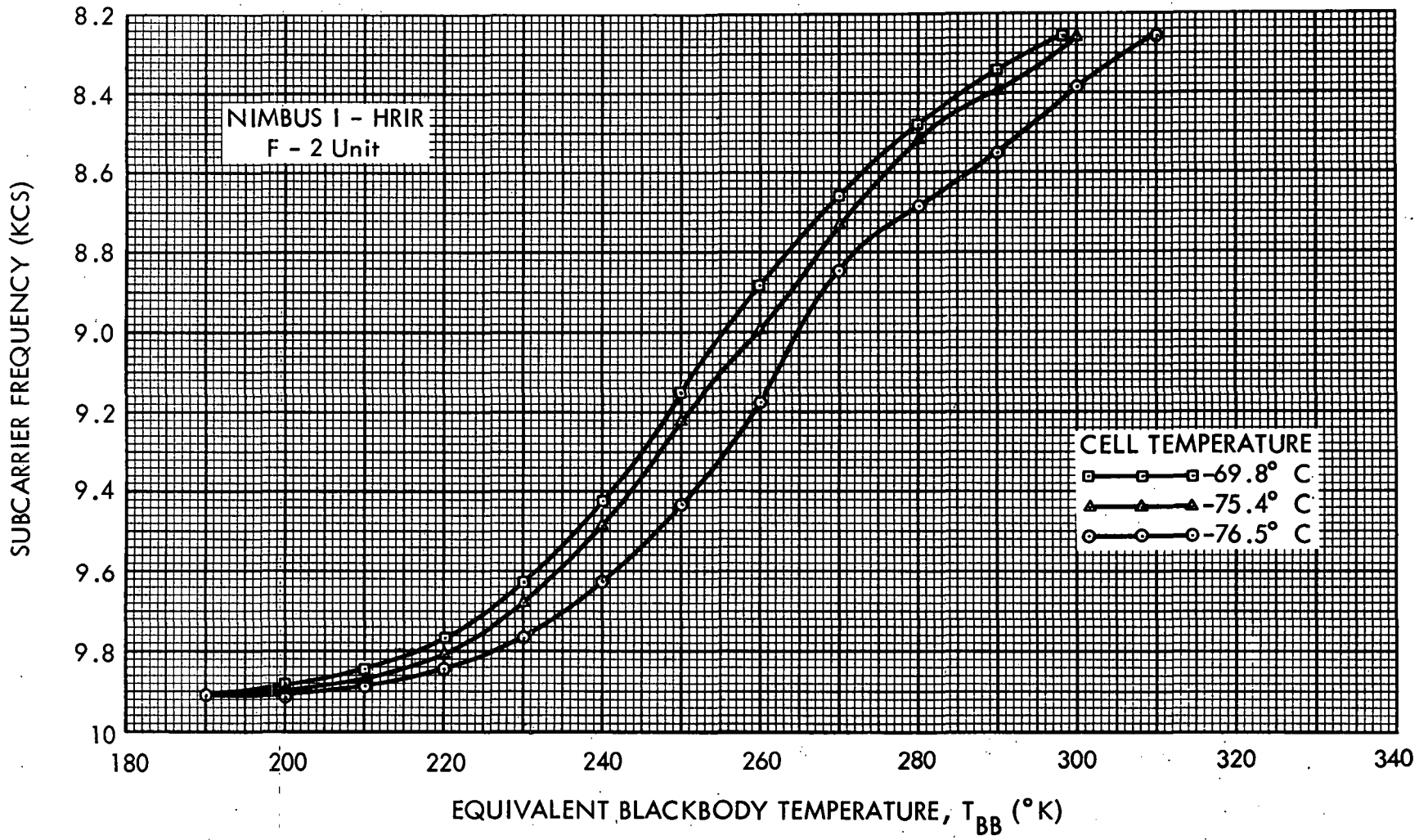

Figure 13-HRIR calibration showing subcarrier frequency versus equivalent blackbody temperature. Parametric curves for three lead selenide cell temperatures are shown.

IV. RADIATION DATA PROCESSING (PHOTOFACSIMILE)

4.1 Photofacsimile Recorder

At the ground station the video and timing signals are demultiplexed and recorded on magnetic tape. Simultaneously the video and time code of the most recent data are usually displayed in "real time" (cf. Figure 9).

In the recorder, the radiometer generated data are recorded on strips of photographic film with fine resolution and continuous gray scale. Either a positive or negative image can be produced as required. Horizontal sync signals derived from the radiometer (cf. Figure 8) are provided as a reference to bring about phase coincidence between the scan mechanism of the recorder and the infrared radiation scan mirror in the spacecraft. The horizontal sync signals consist of negative going pulses of -5.75 V DC amplitude and 78 microseconds in pulse width. The leading edge of the horizontal sync pulse is coincident with the start of the space video signal from the HRIR and, when phasing has occurred, the video recorded by the photofacsimile recorder represents the earth scan.

The timing signal is a clock reference signal derived from the satellite clock, and is used to drive the synchronous motor of the recorder in synchronism with the motor driving the scan mirror in the spacecraft.

The signal amplifier circuit of the photofacsimile receives video information from the ground receiving station demodulation equipment, amplifies it and uses it to modulate the light beam of the recorder lamp while it is scanned across the face of the advancing film. There is an automatic sync-speed circuit which brings the synchronous motor up to speed to drive the optical scan system and the film feed mechanism.

There are additional circuits which blank out all unwanted portions of the video signal; only the video representing the Earth scan, outer space, and the housing are recorded on the film output.

The recorder is provided with means for automically producing a ten-step calibration scale. Progressive voltage levels from a manually adjusted ten-step potentiometer network are sequentially selected by a ten-step motor driven cam operated by a timed program selector switch, and recorded on the synchronously-fed film. This ten-step calibration gray scale can, then, be related to equivalent blackbody temperatures.

4.2 Gridding

Because the satellite's motion is an integral part of the scanning system, the absolute and relative geographical location of each picture element is dependent upon the

Nimbus control system which has demonstrated a stability of about ±1° along all three axes. A pointing error of 1 degree corresponds to a location error of approximately 16 km when viewing near the nadir from apogee. On a global basis, this is probably an acceptable error for meteorological analysis.

The Grid Point Equipment (GRIPE) facilitates the generation of the conventional latitude and longitude grids and the electronic superposition of these grids on the cloud-cover picture. During transmission of the data, GRIPE receives HRIR start times and outputs this time to the CDC 924 computer. The computer uses these data along with orbital elements and spacecraft attitude data to compute the grid-point coordinates. After transmission, the computer inputs the grid-point coordinates to GRIPE which generates grid-point signals. These signals are then electronically mixed with the video signals in analog form, demodulated, and displayed in a strip map [cf. Figures C1(b) and C2(b)]. It should be pointed out, however, that the gridding of all Nimbus I data has been accomplished assuming no attitude errors. For this reason and because of other systematic effects, errors in the location of the data may considerably exceed 16 km near the nadir (cf. Appendix C).

V. RADIATION DATA COVERAGE AND DOCUMENTATION

5.1 Radiation Data Coverage

The HRIR system was designed to record primarily when the satellite was over the nighttime half of the Earth, although there were occasional periods when the system was programmed to operate during daylight. The following general discussion pertains to only the acquisition of nighttime data. The latitudinal extent of the nighttime subpoint track is a function of the time of year. The HRIR successfully acquired data from August 28, 1964 to September 22, 1964; it follows that nighttime data were recorded at all latitudes between 84°N and 90°S at the beginning of the period (see Figure 14), and, between 90°N and 90°S at the end of the period (near the Autumnal Equinox). Data were recorded for all longitudes when the HRIR system operated normally. The areas near the two Data Acquisition (DA) Facilities were generally excluded, however, since data could not be recorded during playback. Figure 14 shows the latitudinal extent of orbits 001 and 002, plotted on northern and southern hemisphere polar stereographic projections. The subpoint tracks begin at 78°N on the descending portions of the orbits, the beginning of subpoint night, and end at 78°S on the ascending portions of the orbits, the end of subpoint night. The radiometer scan mirror scans the Earth's surface from horizon to horizon in a plane perpendicular to the velocity vector of the satellite (assuming that the spacecraft is stabilized without error along the yaw and pitch axes). The length of the resulting scan line from horizon to horizon, then, is a function of only the height of the satellite. The boundaries of the horizon-to-horizon data coverage strips as the spacecraft moves in orbit are shown in Figure 14. The scan line, for a subsatellite point at 78°N, includes data acquisition to a latitude of 84°N. For a subsatellite point at 78°S on the ascending leg of the orbits, data are acquired to 52°S. The lateral extent of the data coverage strips of the two adjacent orbits shows there is considerable overlap from orbit to orbit even at the subperigee latitude, which is 19.1°N on the descending leg of the orbit. Also shown is the width of the data coverage strip for the central 107° of Earth scan (i.e., for a scan nadir angle maximum of 53.5°). The 53.5° scan nadir angle corresponds to the lateral extent for which grid points are calculated and reproduced on the photofacsimile film strips. The data on the film strips having a scan nadir angle greater than 53.5° are greatly distorted and compressed making interpretation of the data very difficult.

Two basic limitations reduced the amount of data coverage. One limitation was the locations of the DA Facilities. The other was the reduced amount of time available to read out the data which were recorded due to the low height of the satellite near perigee. The height of perigee of the elliptical orbit was less than half of the height of the planned circular orbit. Thus, when perigee occurred over a DA Facility, the readout time was reduced by about half, resulting in the loss of about half of the recorded data.

Figure 15 shows the subperigee latitude (more precisely, the latitude of minimum satellite height) and whether perigee occurred on the ascending or descending leg of the orbit, versus orbit number. Perigee occurred over 19.1°N on the descending leg of

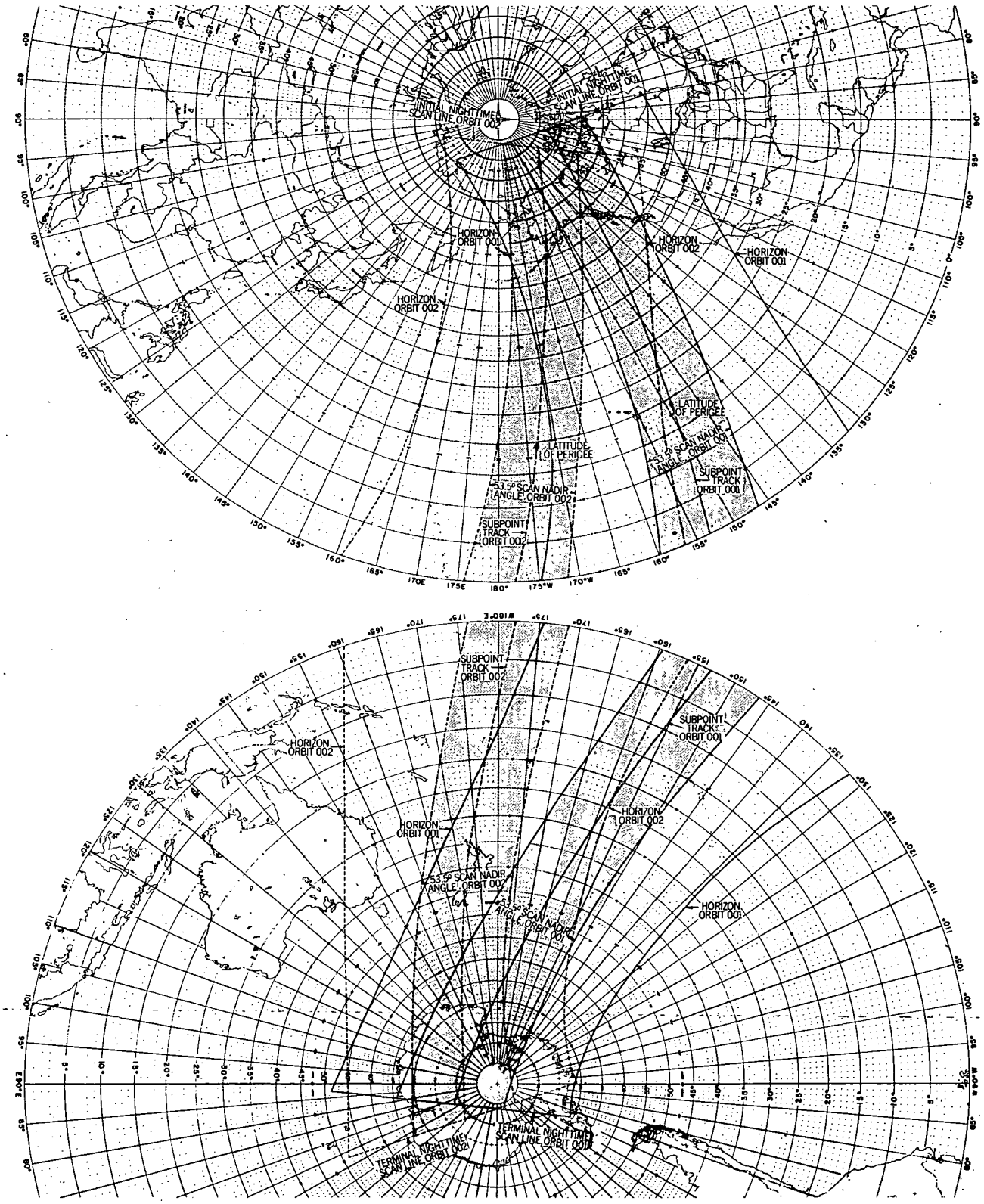

Figure 14–Data coverage strips for subpoint night portions of orbits 001 and 002 of Nimbus I. The solid lines refer to orbit 001 and the dashed lines to orbit 002. The two sets of outside lines delineate the horizon boundaries. The shaded strips represent the central 107° of the scan over the Earth where the data are gridded.

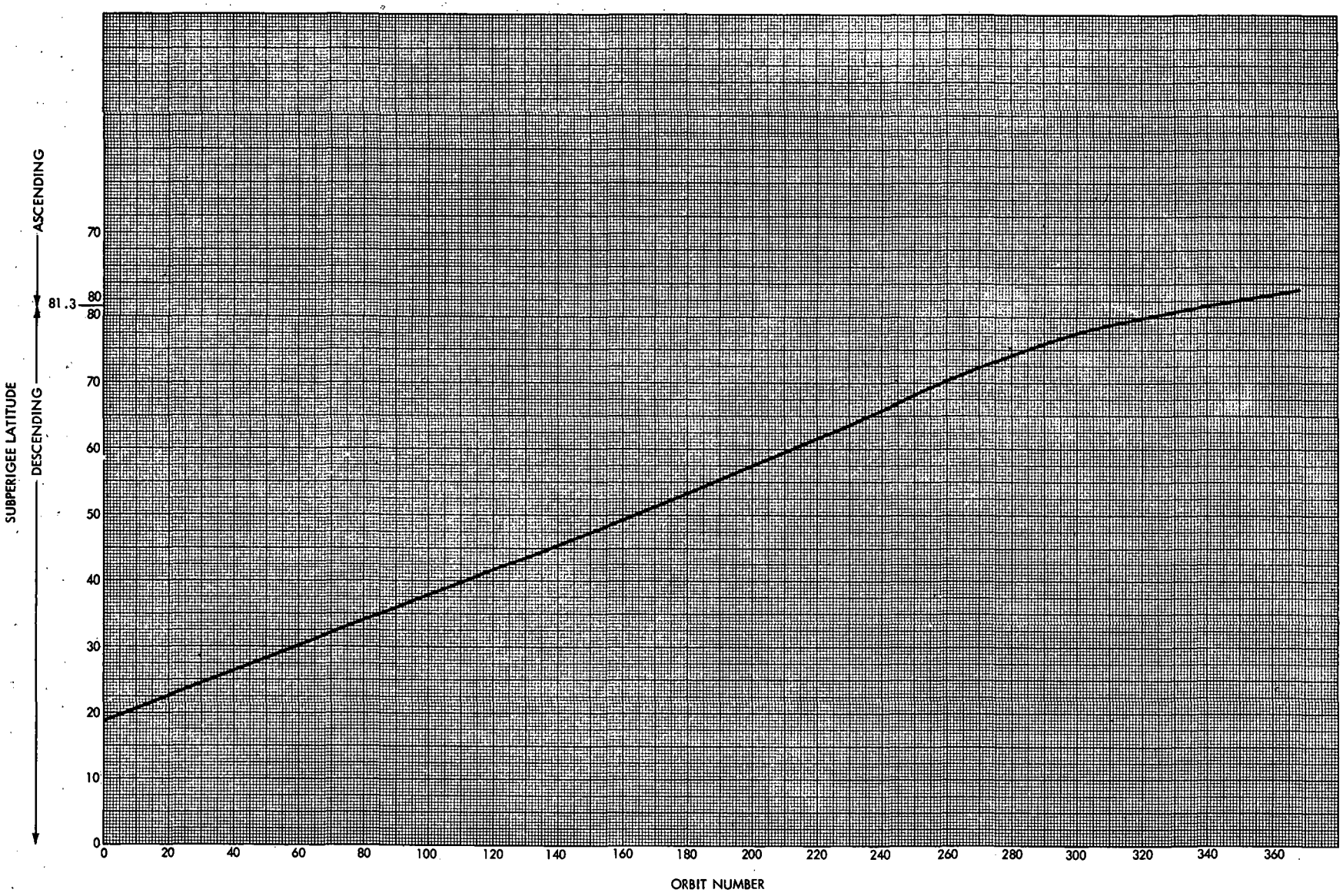

Figure 15–Subperigee latitude versus orbit number for Nimbus I. "Descending" and "Ascending" refer to the leg of the orbit where perigee occurred.

orbit 001, moved northward to 81.3°N by orbit 330, and thereafter moved southward on the ascending leg through orbit 368, the end of successful data acquisition.

A four-track tape recorder in the satellite recorded the radiation data. One track received the radiometer signals; another recorded the 10 kc timing signal from a master satellite clock. When one tape reel was fully unwound, the movement reversed and the signals switched to the remaining two tracks. The recorder functioned in this way, erasing just prior to recording, until a command was executed to end the recording. With the execution of a playback command, the direction of the recorder reversed, and the speed increased eightfold, reading out all four tracks simultaneously. Playback ended either automatically when the end of the tracks were reached or by commanding the satellite S-band transmitter off. The latter was done routinely 30 seconds before the satellite moved out of the range of a DA Facility. The tape recorder was capable of storing 114 minutes of data – 57 minutes on each track. These 114 minutes represented data recorded during the nighttime portions of approximately 2-1/3 orbits, a full nighttime portion being about 49 minutes long. At the eightfold playback speed, 7.125 minutes were required to recover all of the data on the recorder and 6.125 minutes to recover the 49 minutes of data from one nighttime portion of an orbit if all 49 minutes of data were recorded on one track. When a playback was commanded, the recorder reversed its direction and played back to the other end of the track, where it stopped even though additional playback time was available. Upon recording again, the data on the tape that were not read out could be erased. Because of the elliptical orbit and the design of the recorder, the record and playback sequence resulted in a very complex arrangement of data coverage.

Two acquisition figures for each of the two DA Facilities, Gilmore Creek, Alaska, and Rosman, North Carolina, are shown in Figure 16. The departure of these figures from a circle is caused by considering the masking of the line of sight to the satellite by local terrain features and mechanical constraints of the antenna mount. The outer figure at Rosman was computed using a satellite height of 900 km which is the greatest height over that station during the life of Nimbus I and occurred on the ascending leg of orbit 001. The inner figure at Rosman was computed using the height of perigee which occurred over Rosman on the descending leg of orbit 001. The outer figure at Gilmore Creek was determined by using 800 km which occurred on the ascending leg of orbit 001 and represents the greatest height over that station during the life of the satellite. The inner figure was computed for the height of perigee. The total amount of acquisition time, considering both ascending and descending leg acquisitions, decreased after orbit 001. Figure 16 also shows 16 subpoint tracks, constituting slightly more than 24 hours. Each track is marked by one-minute time intervals across the acquisition figures. At least four minutes of total acquisition time were required before an HRIR playback was attempted. Forty-five seconds were required for the S-band transmitter to warm-up before an HRIR playback started. The transmitter was commanded off 30 seconds before the satellite moved out of range of a DA Facility; thus, of the four minutes minimum required before attempting an HRIR playback, only two minutes and forty-five seconds were available to playback the radiation data.

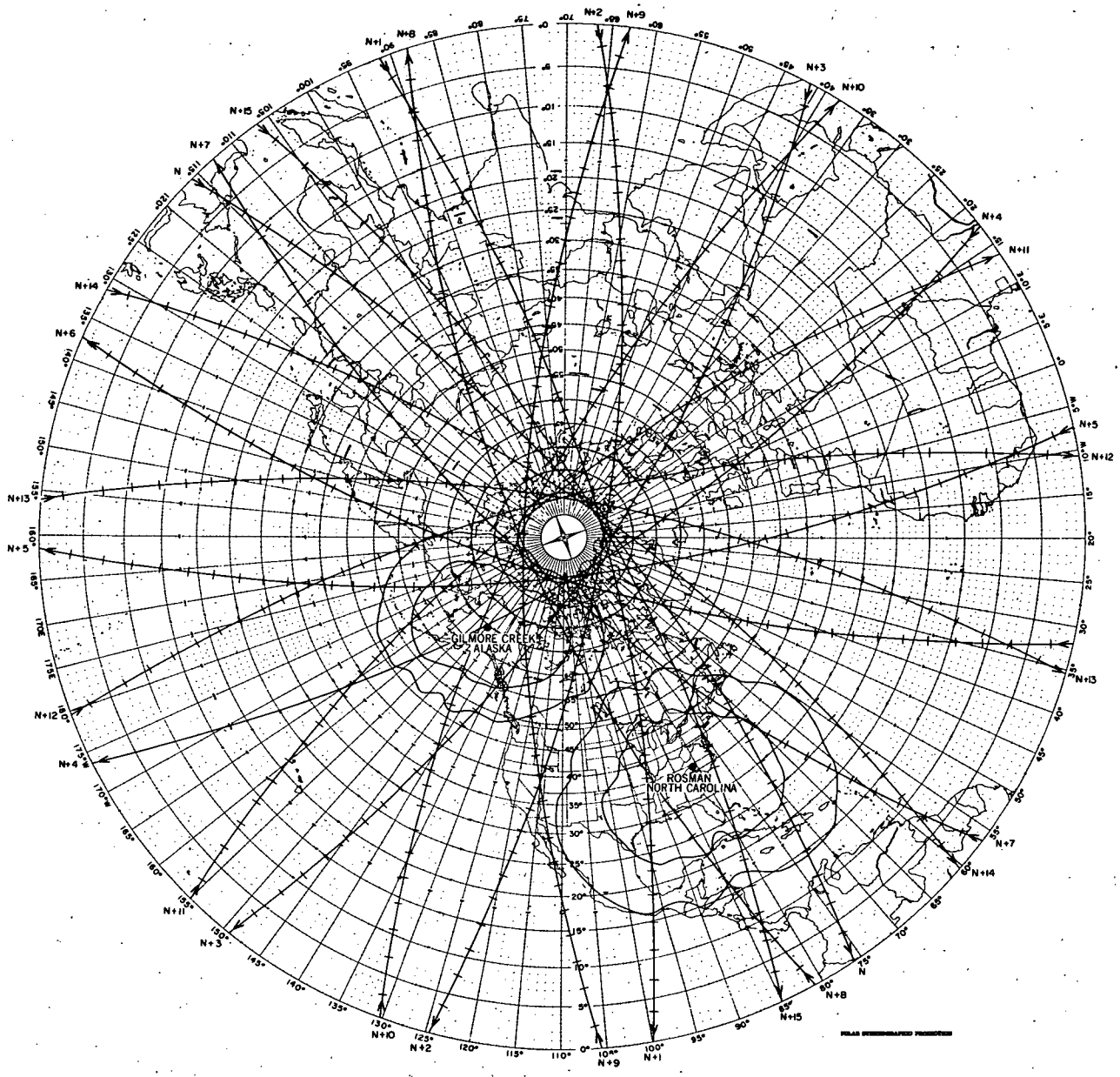

Figure 16—Northern hemisphere polar sterographic projection showing the acquisition figures pertaining to the two Data Acquisition Facilities at Rosman, North Carolina and Gilmore Creek, Alaska. Also shown are 16 subpoint tracks with one minute time marks.

We shall now consider a typical record and playback sequence of 15 orbits assuming that the orbital geometry of launch day prevails. The results of this example are derived from Figure 16 and illustrated in Figures 17 and 18.

[Refer to Figures 16 and 17(a)]

Considering the inner figure at Rosman, which applies for an acquisition on the descending (nighttime) portion of the orbit, and the minimum acquisition time of four minutes, orbit N can just be acquired. After playback the tape recorder is at the end of one of the two tracks and records 32 minutes of data to the end of subpoint night on orbit N,

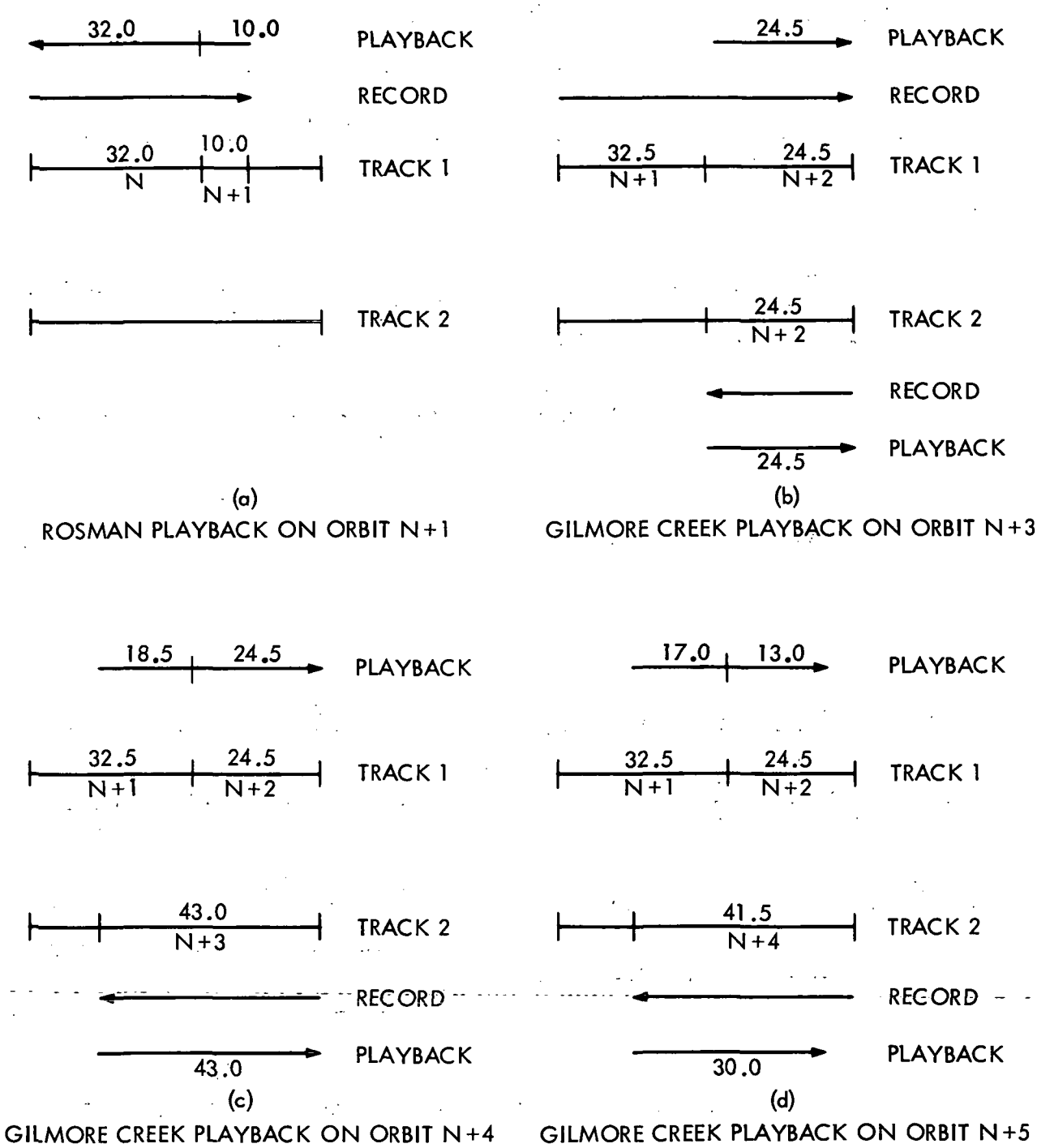

Figure 17(a-d)—Diagrams showing the record and playback sequence of the Nimbus I HRIR tape recorder for 15 orbits

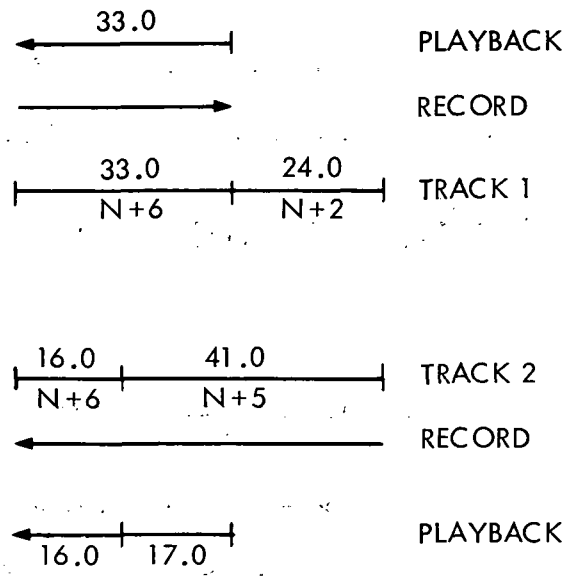

(e)

ROSMAN PLAYBACK ON ORBIT N+7

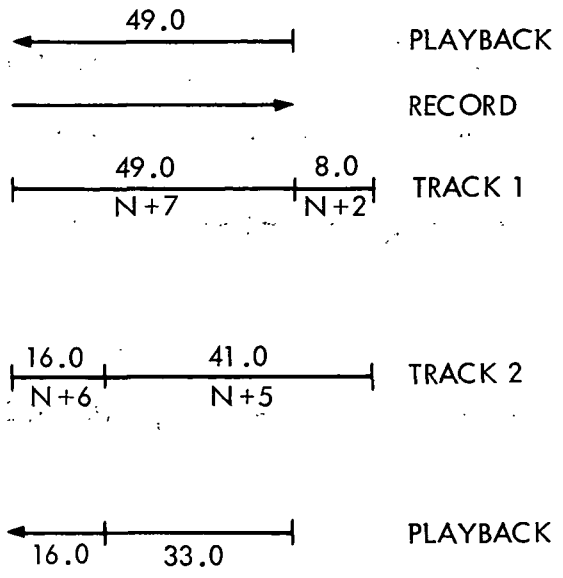

(f)

ROSMAN PLAYBACK ON ORBIT N+8

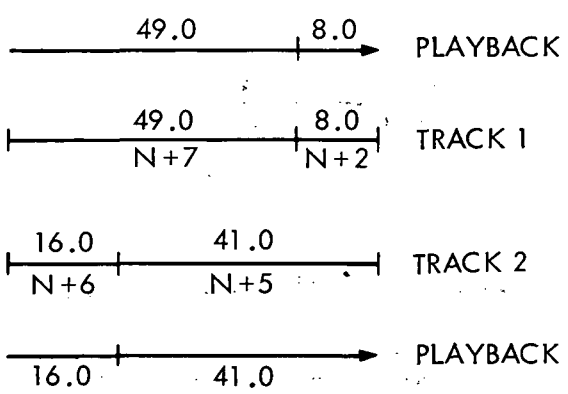

(g)

GILMORE CREEK PLAYBACK ON ORBIT N+8

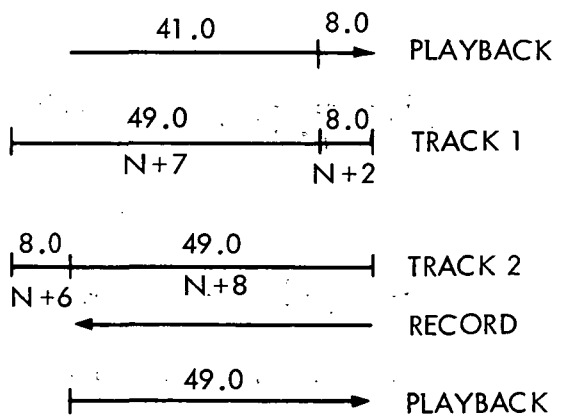

(h)

GILMORE CREEK PLAYBACK ON ORBIT N+9

Figure 17(e-h)—Diagrams showing the record and playback sequence of the Nimbus I HRIR tape recorder for 15 orbits

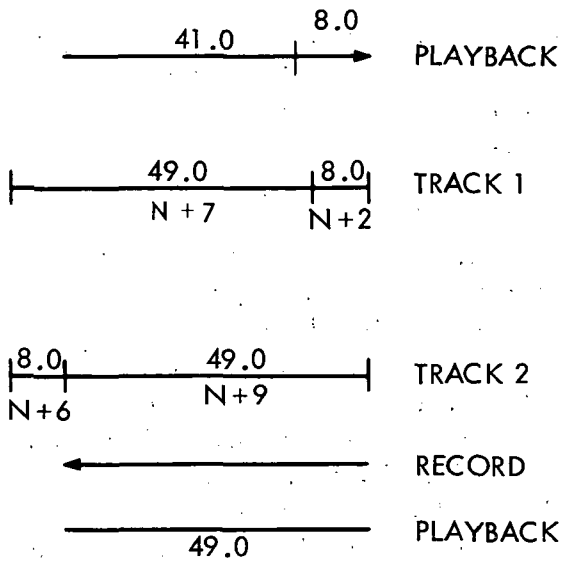

(i)

GILMORE CREEK PLAYBACK ON ORBIT N+10

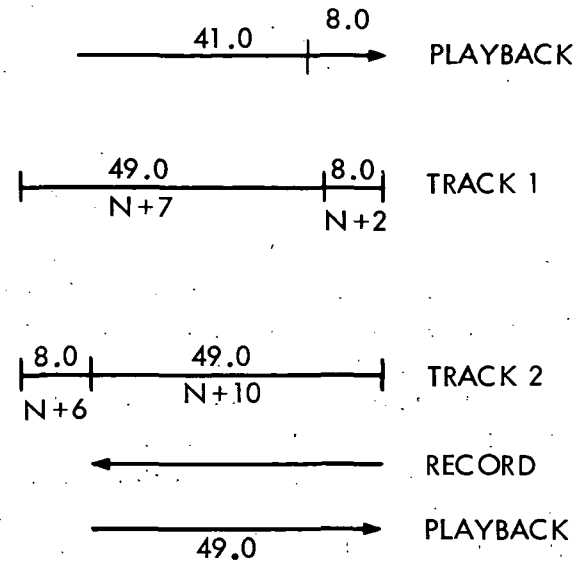

(j)

GILMORE CREEK PLAYBACK ON ORBIT N+11

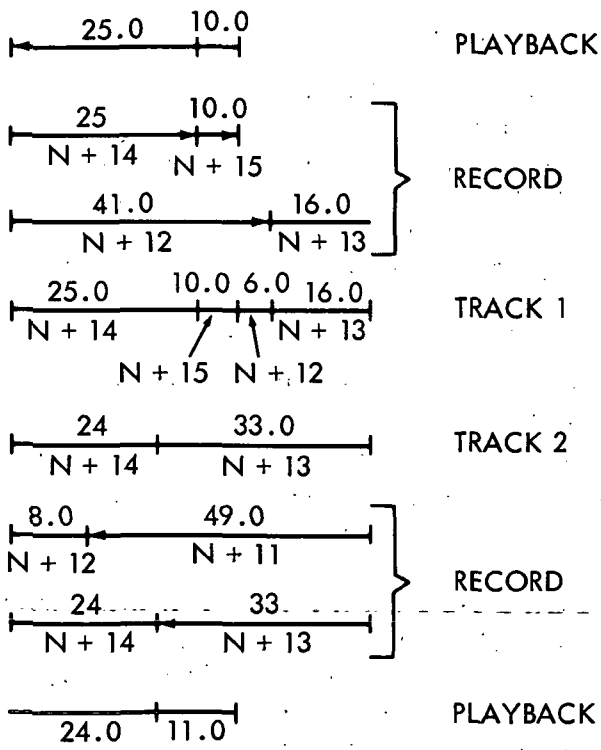

(k)

ROSMAN PLAYBACK ON ORBIT N + 15

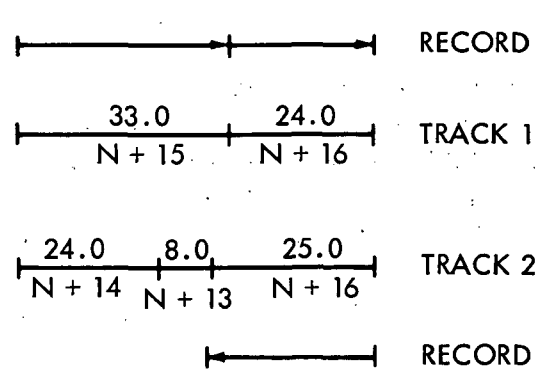

(l)

TAPE RECORDER IMMEDIATELY BEFORE GILMORE CREEK PLAYBACK ON ORBIT N + 17

Figure 17(i-l)—Diagrams showing the record and playback sequence of the Nimbus I HRIR tape recorder for 15 orbits

plus 10 minutes on orbit N + 1 from the beginning of subpoint night to the start of playback at Rosman. Orbit N + 1 has an acquisition period of 6.5 minutes, or 5.25 minutes of HRIR playback time, which will permit the playback of all 42 minutes of recorded data. The playback returns the recorder to the start position on Track 1.

[Refer to Figures 16 and 17(b)]

At this point the recorder reverses direction and records 32.5 minutes of data on orbit N + 1 from the end of acquisition to the end of subpoint night. The acquisition figure at Gilmore Creek for the descending portion of orbit N + 2 is slightly larger than the inner figure, but not enough larger to permit an acquisition; therefore, 49 minutes of data, from the beginning to the end of subpoint night, will be recorded on orbit N + 2. Of the 49 minutes, 24.5 minutes will be recorded on Track 1 and the remaining 24.5 minutes in the opposite direction on Track 2, leaving the recorder 32.5 minutes from the end of Track 2. The satellite comes within range of Gilmore Creek at the beginning of subpoint night so data are not recorded on orbit N + 3 before playback. This orbit has an acquisition period of 6 minutes, of which 4.75 minutes are for HRIR playback. Upon execution of the playback command, the recorder reverses direction and plays back to the end where it stops, playing back the 24.5 minutes of data on each of the two tracks. Thus, only the data recorded on orbit N + 2 are read out, while the 32.5 minutes of data recorded on orbit N + 1 are not read out.

[Refer to Figures 16 and 17(c)]

After the orbit N + 3 playback, data are recorded for 43 minutes on Track 2 to the end of subpoint night. Acquisition time for orbit N + 4 at Gilmore Creek is 7.5 minutes, of which 6.25 minutes are available for playback; therefore, all of the 43 minutes recorded on orbit N + 3 are read out from Track 2. The last 18.5 minutes of data recorded on orbit N + 1, plus the first 24.5 minutes of data recorded on orbit N + 2 are read out from Track 1. The 24.5 minutes of data from orbit N + 2 are read out the second time.

[Refer to Figures 16 and 17(d)]

After playback 41.5 minutes of data are recorded on Track 2, extending to the end of subpoint night on orbit N + 4. Orbit N + 5 has an acquisition period of 5 minutes, of which 3.75 minutes are available for playback, permitting read out of the last 30 minutes of data recorded on Track 2 from orbit N + 4, missing the first 11.5 minutes. The last 17.0 minutes of data recorded on orbit N + 1 will be read out from Track 1, the second readout of these data. Also, the first 13.0 minutes of data recorded on orbit N + 2 will be read out for the third time, although missing 11.5 minutes from this orbit that were read out the previous two times. This playback was ended, before the recorder played back to the end of the track, by commanding off the S-band transmitter power before the satellite passed over the horizon. With the execution of this command, the tape recorder automatically continues to the end of the track, where, upon receiving a record command, it records in the opposite direction.

[Refer to Figures 16 and 17(e)]

After playback at Gilmore Creek on orbit N + 5, 41 minutes of data are recorded to the end of subpoint night. An acquisition figure which applies to orbit N + 6 falls nearly halfway between the two plotted for Gilmore Creek. The total acquisition time is only

about two minutes, which is not enough time for a playback; therefore, none is executed, and data are recorded from the beginning to the end of subpoint night on orbit N + 6, 16 minutes, of which, are recorded on Track 2. The recorder switches tracks and the remaining 33 minutes are recorded on Track 1, where it is now ready for playback on orbit N + 7 at Rosman. The orbital pattern has now shifted so that acquisition takes place on the ascending leg of the orbit and the outer acquisition figure applies. Rosman has a total acquisition period of 9.25 minutes, 8 minutes, of which, are available for playback. The satellite also comes within range of Gilmore Creek, but the acquisition time is too short for a playback. At Rosman, then, upon command the recorder plays back 33.0 minutes of orbit N + 6 data from Track 1 and the last 17.0 minutes of orbit N + 5 data, plus the first 16.0 minutes of orbit N + 6 data, from Track 2.

[Refer to Figures 16 and 17(f)]

Data are recorded on Track 1 for orbit N + 7 for the entire 49 minutes of subpoint night. Ten minutes of acquisition time are available at Rosman and 8.5 minutes at Gilmore Creek for orbit N + 8. At Rosman all 49.0 minutes of orbit N + 7 data are read out from Track 1 and the last 33.0 minutes of orbit N + 5 data (17.0 minutes of which are read out for the second time) and the first 16.0 minutes of orbit N + 6 data (all of which are read out for the second time) from Track 2.

[Refer to Figures 16 and 17(g)]

Data are not recorded between Rosman and Gilmore Creek since this portion of the orbit is in daylight. At Gilmore Creek there are 7.25 minutes available for playback. The recorder reverses direction and plays back to the other end of the track. All of the data are read out at this acquisition, 49.0 minutes of orbit N + 7 data are read out for the second time from Track 1. Also, 8.0 minutes of orbit N + 2 data are read out from Track 1 for the third time. The readout of Track 2 will result in the recovery of 16.0 minutes of orbit N + 6 data for the third time and 41.0 minutes of orbit N + 5 data, of which, 17.0 minutes will be read out for the third time, 16.0 minutes for the second time and the remaining 8.0 minutes for the first time.

[Refer to Figures 16 and 17(h)]

After the Gilmore Creek acquisition, 49.0 minutes of orbit N + 8 data are recorded on Track 2. Orbit N + 9 has a total acquisition period of 9.0 minutes, considering the outer acquisition figure at Gilmore Creek. The 49.0 minutes of orbit N + 8 data are read out from Track 2. From Track 1, 41.0 minutes of orbit N + 7 data are received for the third time and 8.0 minutes of orbit N + 2 data are received for the fourth time.

[Refer to Figures 16 and 17(i)]

After the orbit N + 9 acquisition, 49.0 minutes of data are again recorded for the subpoint night portion of the orbit. The orbit N + 10 playback is similar to the orbit N + 9 playback since the same amount of new data is recorded and the N + 10 acquisition time of 9.5 minutes allows the recorder to play back to the end of the track.

[Refer to Figures 16 and 17(j)]

Again 49.0 minutes of orbit N + 10 data are recorded on Track 2 and the orbit N + 11 playback is similar to the orbits N + 9 and N + 10 playbacks. The orbit N + 11 playback

will recover 49.0 minutes of orbit N + 10 data from Track 2, as well as 41.0 minutes of orbit N + 7 data for the fifth time, and 8.0 minutes of orbit N + 2 data for the sixth time from Track 1.

[Refer to Figures 16 and 17(k)]

Orbits N + 12, N+ 13, and N + 14 do not come within range of either DA Facility, and acquisitions are not possible. The next orbit which can be acquired is orbit N + 15 with an acquisition time of 6.0 minutes, of which, 4.75 minutes are available for playback. After the orbit N + 11 playback, data are recorded continuously during subpoint night, beginning on orbit N + 11 and ending at the start of playback on orbit N + 15. The recorder erases old data on the tape just prior to recording new data. All of orbit N + 11 data and the first 43.0 minutes of orbit N + 12 data were erased. The orbit N + 15 playback reads out the 10.0 minutes of data recorded on orbit N + 15 and the last 25.0 minutes of orbit N + 14 data from Track 1. Also, the first 24.0 minutes of orbit N + 14 data and the last 11.0 minutes of orbit N + 13 data are received from Track 2.

[Refer to Figures 16 and 17(l)]

Orbit N + 16 does not come within range of a DA Facility; therefore, after the N + 15 playback, data are recorded so that by the orbit N + 17 acquisition at Gilmore Creek, all of the data recorded on orbits N + 12 and N + 13 that were not read out at the orbit N + 15 playback have been erased and lost forever.

The record and playback sequence of a complete series of 15 orbits has been demonstrated, starting at the end of the Rosman playback on orbit N and ending with the Rosman playback on orbit N + 15. This series represents the best possible for the life of Nimbus I (i.e., the most acquisition time is available for this series). Of the total of 735 minutes that the satellite spent in subpoint night, 700 minutes of data were recorded. During the remaining 35 minutes, data were not recorded due to playbacks. Of the 700 minutes of data recorded, 538.5 minutes were read out and the remaining 161.5 minutes were erased before they could be read out. Of the total 735 minutes of data, then, 73.3 percent were recovered.

The portions of the subpoint tracks of the orbits discussed in the example of Figure 17 along which HRIR data were successfully recovered are shown in Figure 18. It is seen that the eastern U.S. and Alaska are not covered due to acquisitions over these areas. The general areas of western Europe, western Africa, the eastern Atlantic Ocean, and eastern South America are not covered since these areas are covered by orbits which cannot be acquired. This coverage of the Nimbus I data is typical during the early part of the satellite's life. The general coverage pattern remains the same throughout its life, although the amount of recorded data recovered decreased to about 50 percent due to the changing position of perigee. Late in the life of the spacecraft, stored commands to the HRIR system were used to cover those areas which were routinely missed and to take advantage of all the acquisition time available. The DA Facilities were used to track another satellite during four periods, and the HRIR system was not operated, reducing the data coverage. These four periods were during orbits 94 through 103, 111 through 117, 125 through 132, and 148 through 158. Also, the HRIR

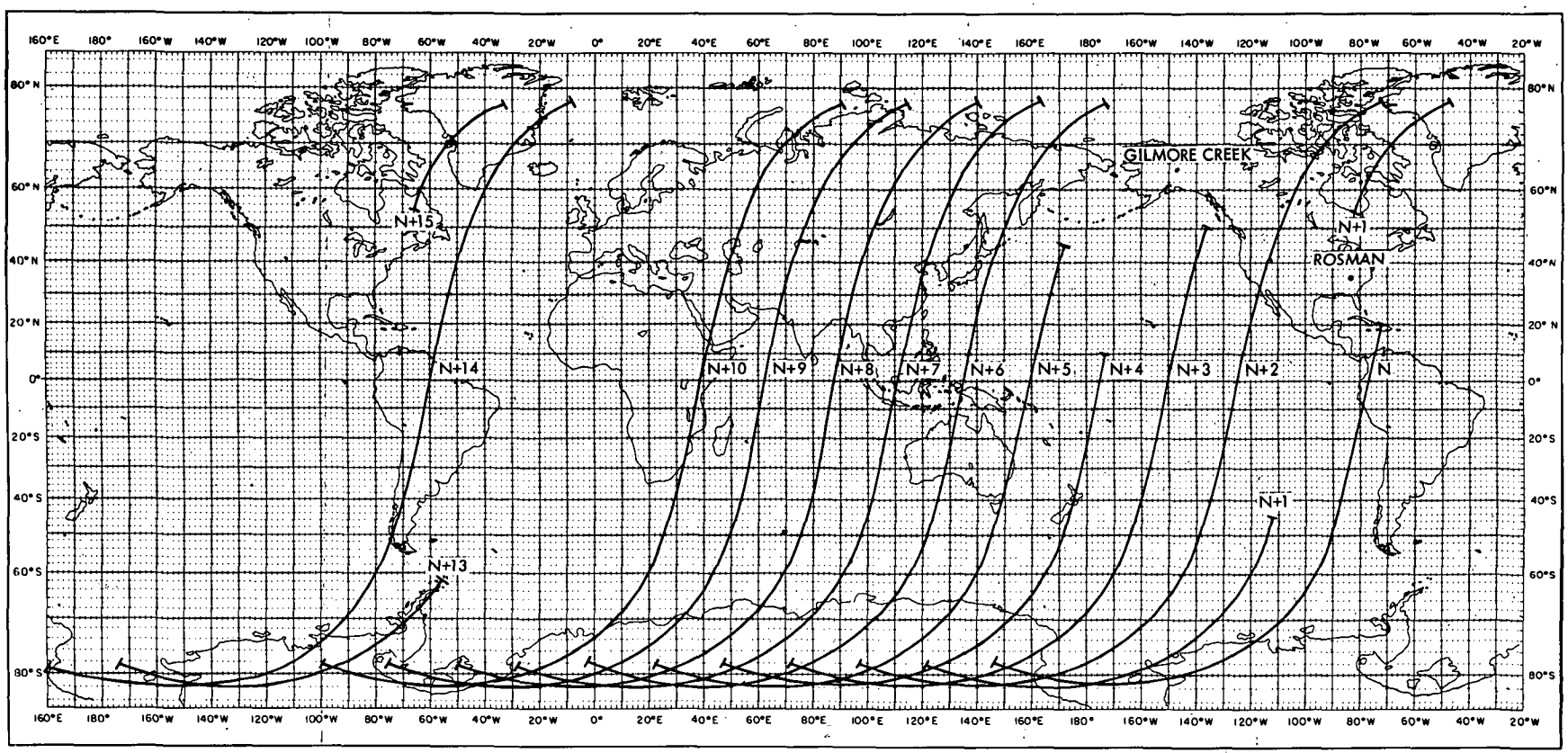

Figure 18—Typical HRIR data coverage for Nimbus I shortly after launch. Subpoint tracks are shown corresponding to those portions of the orbits discussed in the example of Figure 17 from which data were successfully recovered

system was used only sparingly during the first two days of the satellite's life because at that time primary emphasis was given to validating the engineering aspects of the various spacecraft subsystems.

5.2 Documentation of the Data

The radiation data available on the 70mm film strips are documented in an "Index of Available High Resolution Infrared Radiometer Film Strips (Photofacsimile)." This Index, which is found in Appendix A, lists information for the orbital descending node, the time interval for which data are available, the mode of playback, and the readout orbit and station for every Nimbus I orbit for which radiation data are available.

The time interval for the radiation data on film strips is summarized diagrammatically in Appendix B, "Subpoint Track Summaries of Available Radiation Data." Every orbit, from which data were successfully recovered, with a descending node within a calendar day is presented on a separate page for that calendar day. With the data in this form, the user can quickly find the orbits of interest to him and approximate the geographical area of data coverage.

All of the available 70mm film strips from Nimbus I are presented in Appendix C, "Contact Prints of Available Photofacsimile Film Strips." All of the film strips are shown as positive prints in their original size, and most are shown with grid points. Only those which were too noisy to grid are shown without gridding. Information is given with each data block within a film strip to allow the user to identify it with the proper information in the Index and the Subpoint Track Summaries. A description of the film strips and the information they contain is also given in Appendix C.

VI. PERFORMANCE OF THE RADIATION EXPERIMENT

One of the unique features of this experiment is the radiative cooling technique. The cell cooled to its desired temperature of -75°C within less than 3 hours after launch and remained at a satisfactory temperature thereafter (Figure 19). There were no indications of degradation in the gold coated cell cooling horn nor was there any difficulty experienced in the cell-patch suspension system. The suspension system had been extensively tested prior to launch, having withstood satisfactorily some 95 minutes of the various types of vibration tests to which the radiometer had been subjected in the testing program.

The radiometer housing stabilized at its anticipated temperature of 11°C and remained there within ±2.5°C throughout its lifetime. The temperature stability of the housing contributed in large part to the corresponding stability of the PbSe cell temperature. The temperature of the motor end of the casting stayed well above -5°C which is the lower limit for the successful operation of the motor.

The calibration of the radiometer remained stable throughout its lifetime, and there was no discernable degradation of the characteristics of the detector cell, cooling horn, scanning mirror, or interference filter.

Results have shown that radiance levels corresponding to the equivalent blackbody temperature in the range from 210°K to 320°K were resolved with an accuracy of 2°K or better. Some smoothing of the analog traces of the radiometer signal is required to achieve this accuracy. An arbitrary point measurement taken from the analog trace without smoothing can deviate an additional 2°K due to noise superimposed on the signal, making the overall uncertainty of a point measurement about ±4°K (References 5 and 10).

Results from aircraft flights at night with a modified HRIR during January and February 1964 from an altitude of 12 km indicated that stratocumulus and altocumulus cloud equivalent blackbody temperatures were about 2°C cooler than actual cloud temperatures while ocean equivalent blackbody temperatures were approximately 5°C cooler than measured sea surface temperatures. The over-water flights were made near the Bahamas where the measured water temperature varied between 23°C and 25°C. Data from Nimbus I show approximately the same results (Reference 6).

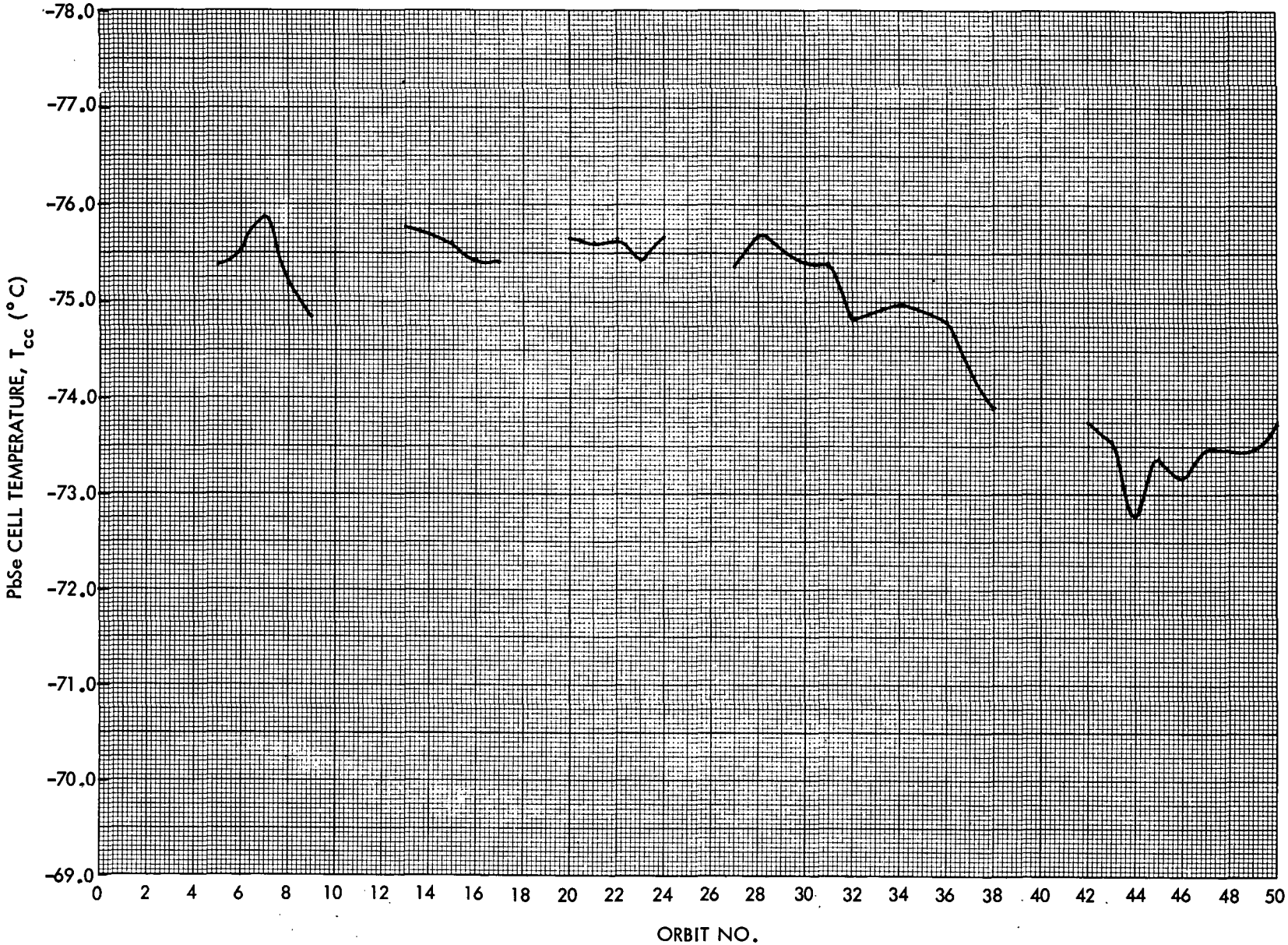

Figure 19(a)–HRIR lead selenide cell temperature vs. orbit number

Figure 19(b)–HRIR lead selenide cell temperature vs. orbit number

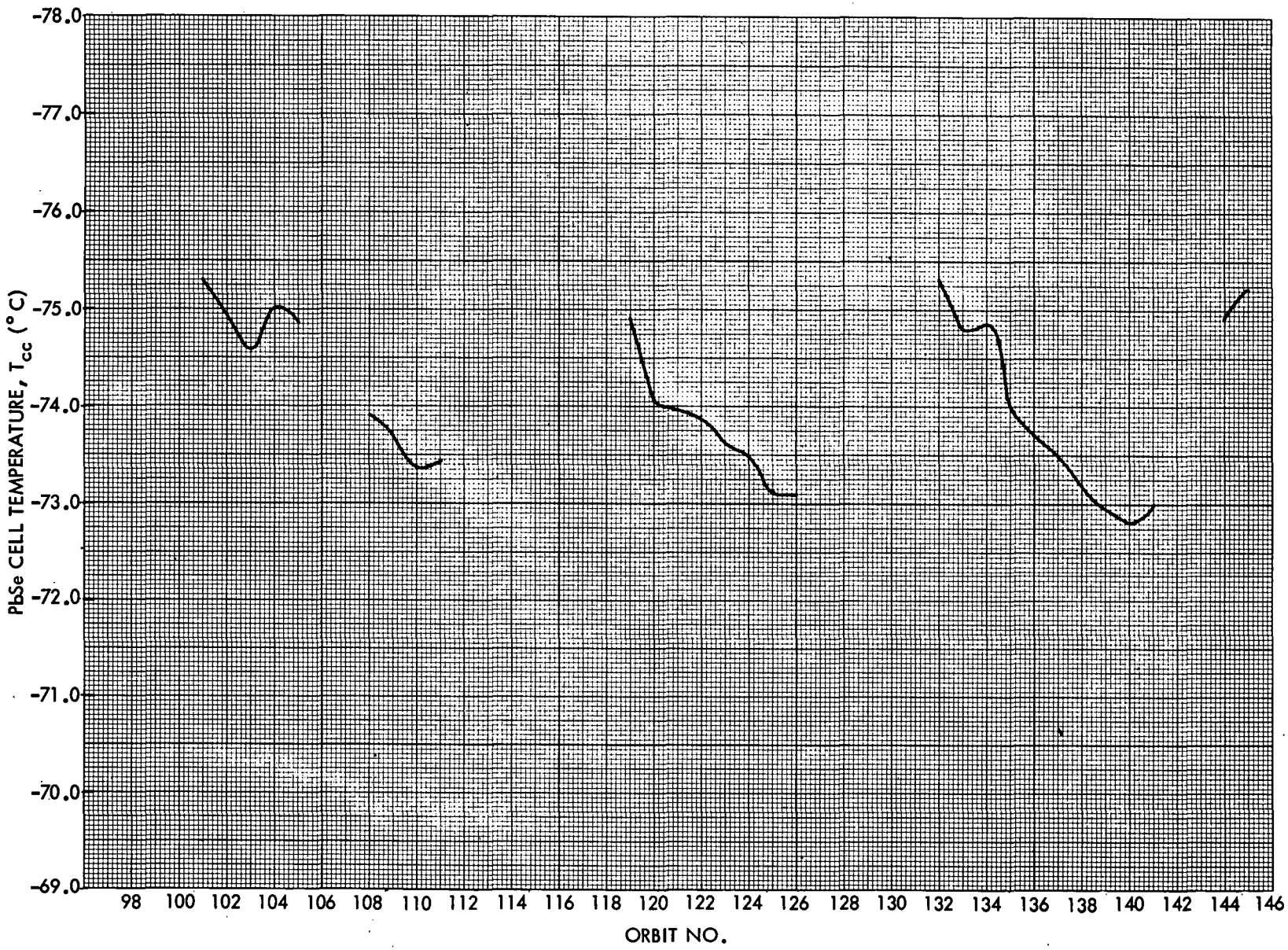

Figure 19(c)—HRIR lead selenide cell temperature vs. orbit number

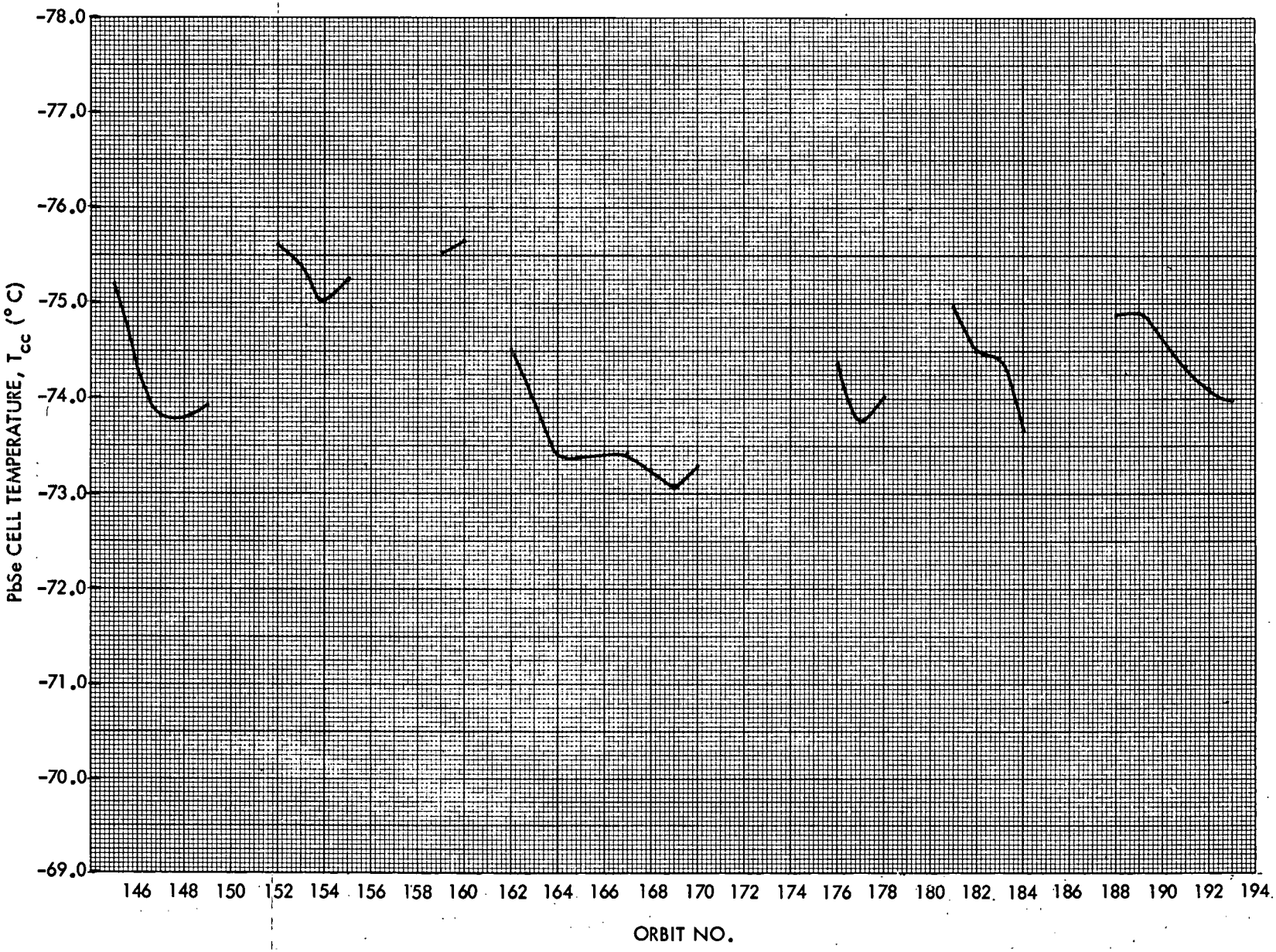

Figure 19(d)—HRIR lead selenide cell temperature vs. orbit number

Figure 19(e)–HRIR lead selenide cell temperature vs. orbit number

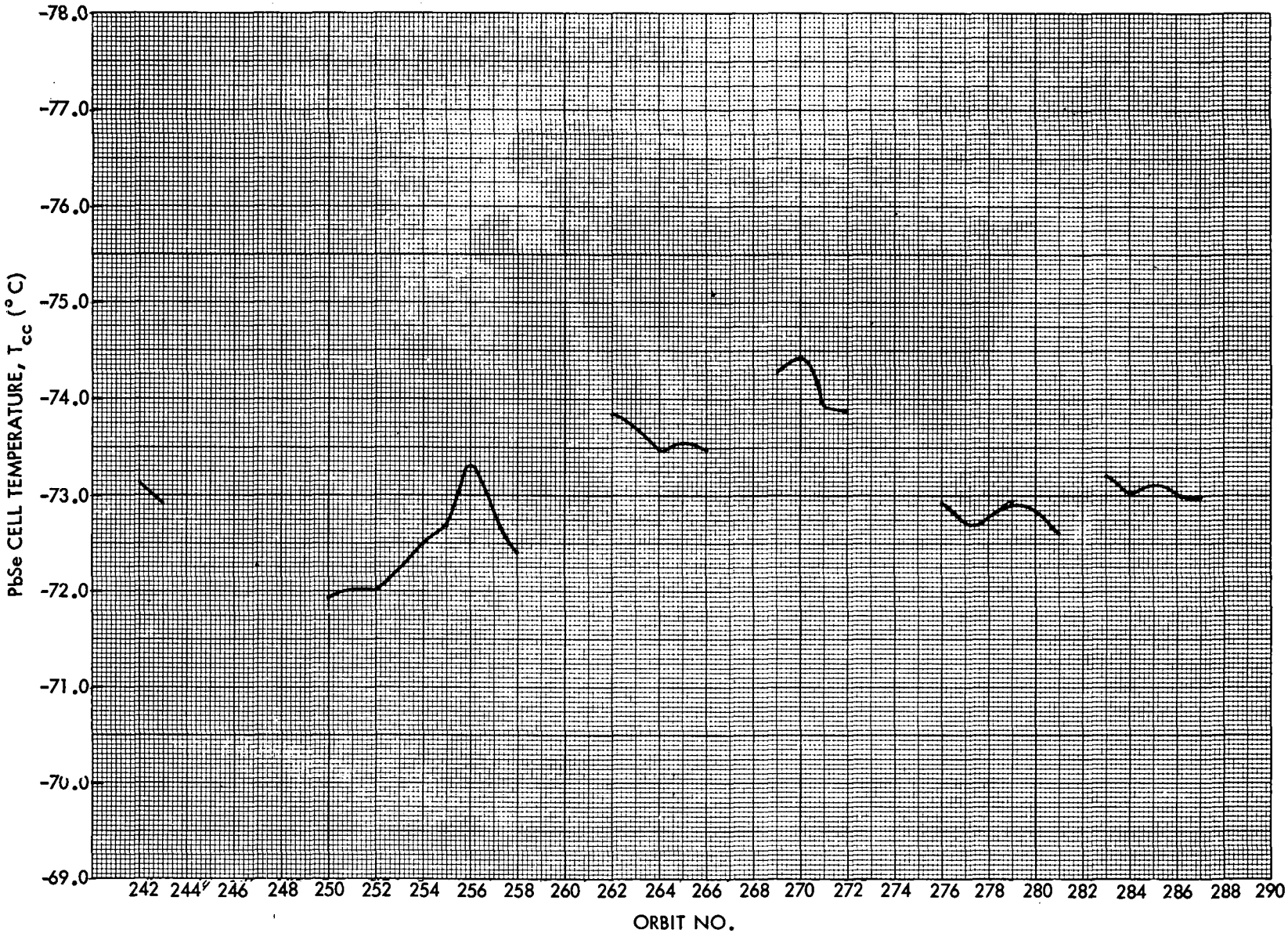

Figure 19(f)–HRIR lead selenide cell temperature vs. orbit number

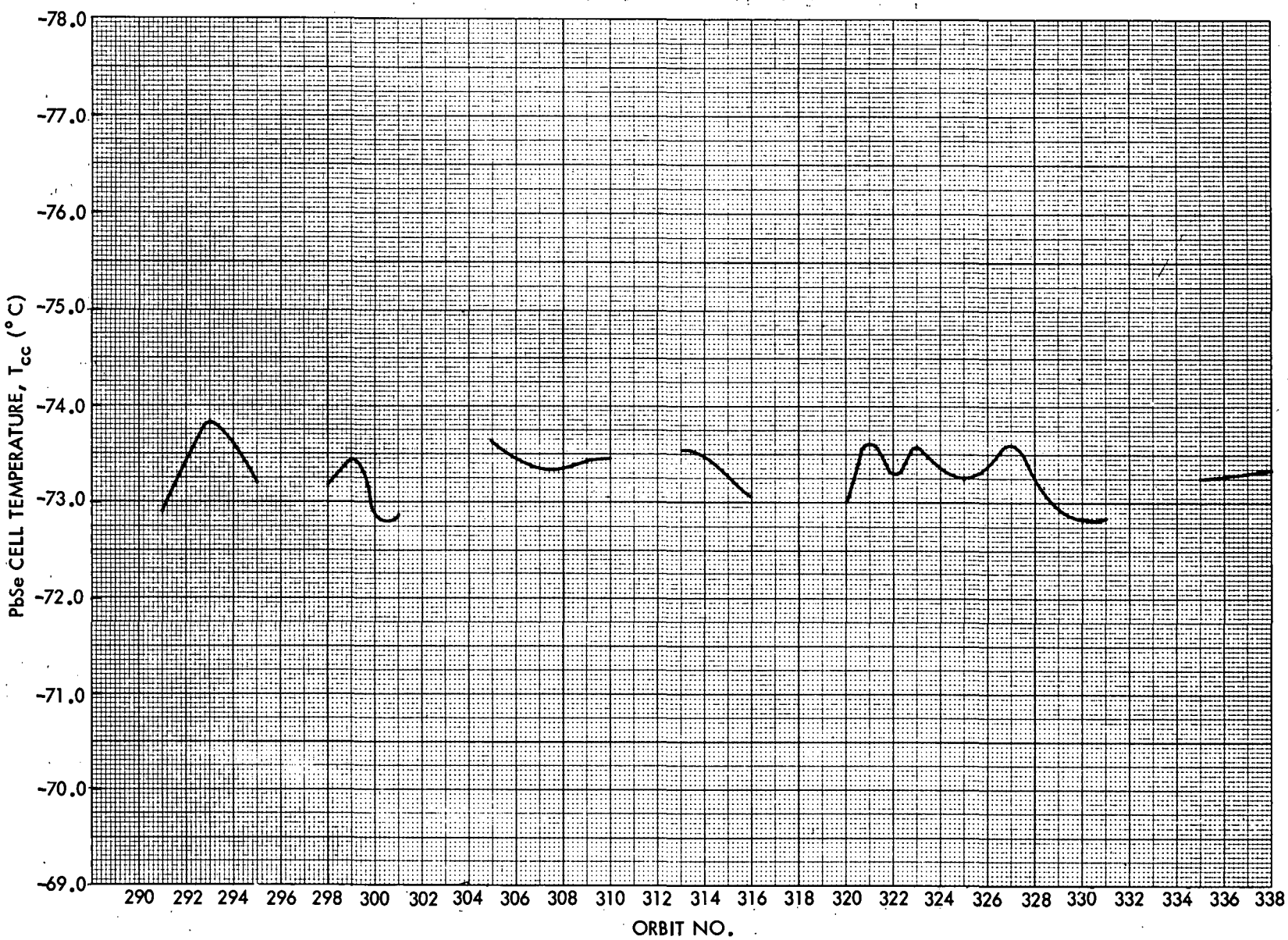

Figure 19(g)—HRIR lead selenide cell temperature vs. orbit number

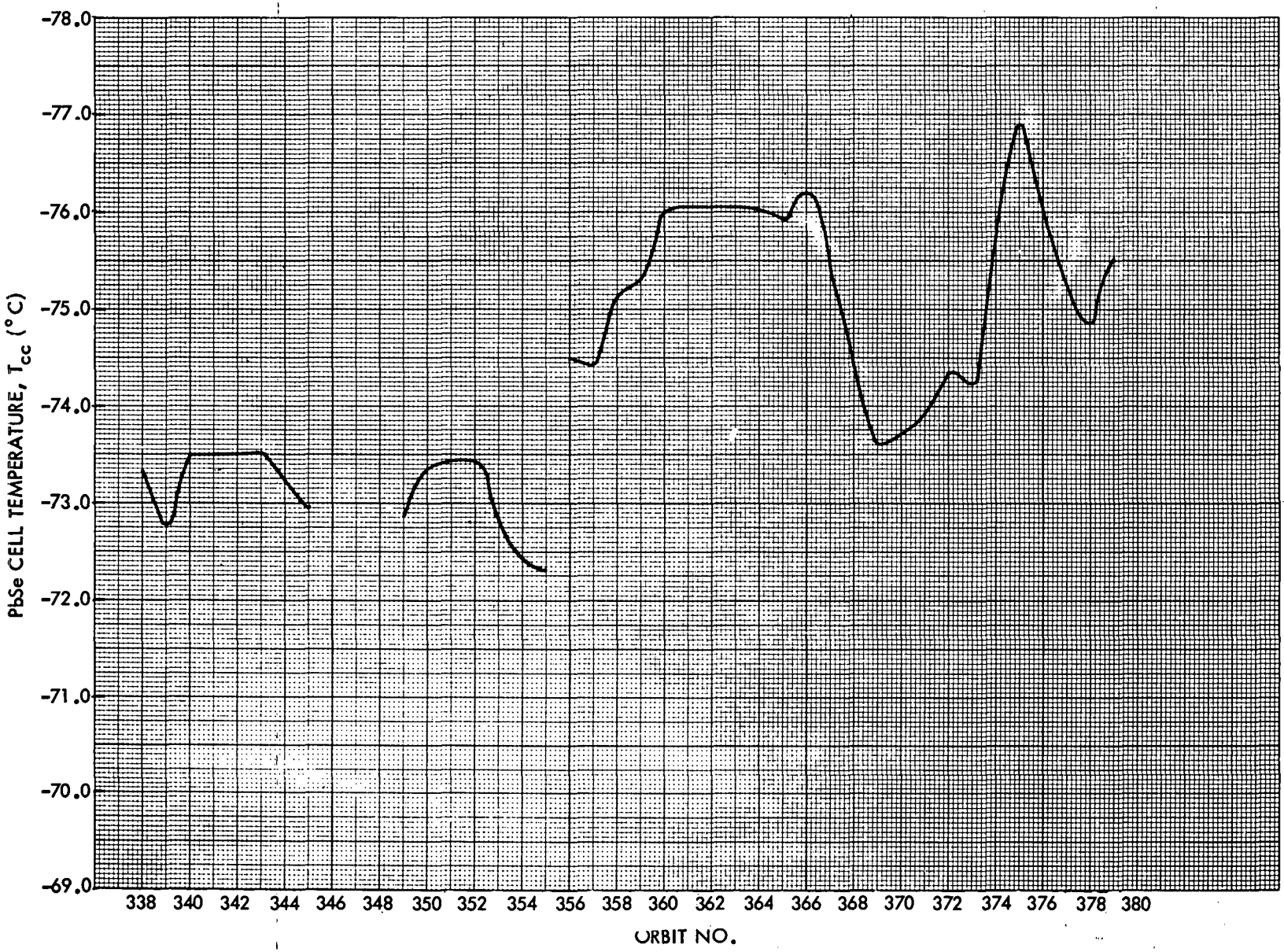

Figure 19(h)–HRIR lead selenide cell temperature vs. orbit number

VII. CONCLUSIONS

The Nimbus I High Resolution Infrared Radiometer experiment has provided extensive coverage over the world of radiation in an atmospheric window from the tops of clouds and from land, sea, and ice surfaces. With a resolution approaching that of the better TIROS television pictures and with a far simpler scanning geometry than the scanning radiometers previously flown on TIROS, the Nimbus HRIR significantly increases the ability of meteorological satellites to make detailed and accurately placed measurements of emitted radiation and, thereby, infer characteristics of the horizontal and vertical structure of the Earth-atmosphere system. In interpreting the photofacsimile data, one must initially exert some effort to associate the visible contrasts with variations in the radiating temperatures of surfaces (and, hence, their heights and emissivities), instead of variations in the reflectivity of sunlight as in conventional television pictures which the HRIR film strips superficially resemble.

The data from this experiment, in both the photofacsimile format discussed in this Volume and the magnetic tape format to be discussed in Volume 2, should be of interest not only to the meteorologist in providing a new tool for operational use and research into the behavior of large and small scale weather systems, but also to the oceanographer, geologist, glaciologist, and other geophysicists in investigating temperature gradients in ocean currents, thermal emission properties of various terrains, the structure and thickness of continental and floating ice in the polar caps, and other geophysical phenomena.

VIII. REFERENCES AND BIBLIOGRAPHY

(Numbered entries are referenced in the text)

1. Bandeen, W.R., 1961: "Earth Oblateness and Relative Sun Motion Considerations in the Determination of an Ideal Orbit for the Nimbus Meteorological Satellite," NASA Technical Note D-1045 (July).

2. "Nimbus I High Resolution Radiation Data Catalog and Users' Manual: Volume 2. Nimbus Meteorological Radiation Tapes - HRIR," 1965: Goddard Space Flight Center, Greenbelt, Maryland (to be published).

3. "Nimbus I Users' Catalog: AVCS and APT," 1965: Goddard Space Flight Center, Greenbelt, Maryland (to be published).

4. Nordberg, W. and Harry Press, 1964: "The Nimbus I Meteorological Satellite," Bulletin of the American Meteorological Society, 45, 684-687 (November).

5. Feyita, Tetsuya and William Bandeen, 1965: "Resolution of the Nimbus High Resolution Infrared Radiometer," Satellite and Mesometeorology Research Project Research Paper No. 40, The University of Chicago (February).

6. Goldberg, I.L., L. Foshee, W. Nordberg, and C. Catoe, 1964: "Nimbus High Resolution Infrared Measurements," Paper presented at the Third Symposium on Remote Sensing of Environment, October 14-16, 1964, Institute of Science and Technology, The University of Michigan, Ann Arbor (to be published in Proceedings).

7. Kunde, V., 1965: "Theoretical Relationship Between the HRIR Equivalent Blackbody Temperatures and Surface Temperatures," in Symposium on Geophysical and Meteorological Observations with the Nimbus I Satellite. (Group of papers presented at the Fourth Western National Meeting of the American Geophysical Union in Seattle, Washington, December 1964. To be published as a NASA Special Publication.)

8. Foshee, L., L. Goldberg, W. Nordberg, and C. Catoe, 1965: "Mapping of Emitted Radiation at 4 Microns from Nimbus I," in Symposium on Geophysical and Meteorological Observations with the Nimbus I Satellite. (Group of papers presented at the Fourth Western National Meeting of the American Geophysical Union in Seattle, Washington, December 1964. To be published as a NASA Special Publication.)

9. Nicholas, G.W., J.S. Kennedy, and L.J. Allison, 1965: "Nimbus Views the Weather," in Symposium on Geophysical and Meteorological Observations with the Nimbus I Satellite. (Group of papers presented at the Fourth Western National Meeting of the American Geophysical Union in Seattle, Washington, December 1964. To be published as a NASA Special Publication.)

10. Nordberg, W. and R.E. Samuelson, 1965: "Terrestrial Features Observed through the 4 Micron 'Window' by Nimbus I," in Symposium on Geophysical and Meteorological Observations with the Nimbus I Satellite. (Group of papers presented at the Fourth Western National Meeting of the American Geophysical Union in Seattle, Washington, December 1964. To be published as a NASA Special Publication.)

11. Popham, R. and R.E. Samuelson, 1965: "Polar Exploration with Nimbus," in Symposium on Geophysical and Meteorological Observations with the Nimbus I Satellite. (Group of papers presented at the Fourth Western National Meeting of the American Geophysical Union in Seattle, Washington, December 1964. To be published as a NASA Special Publication.)

12. Press, Harry and W.B. Huston, 1965: "The Nimbus I Flight," in Symposium on Geophysical and Meteorological Observations with the Nimbus I Satellite. (Group of papers presented at the Fourth Western National Meeting of the American Geophysical Union in Seattle, Washington, December 1964. To be published as a NASA Special Publication.)

13. Hanel, Rudolf A., 1962: "Radiometric Measurements from Satellites," Aerospace Engineering, 21, No. 7, 34-39 (July).

14. Stampfl, Rudolf and Harry Press, 1962: "Nimbus Spacecraft System," Aerospace Engineering, 21, No. 7, 16-28 (July).

15. Stampfl, Rudolf A., 1963: "The Nimbus Spacecraft and its Communication System as of September 1961," NASA Technical Note D-1422 (January).

Goldshlak, Leon and Robert B. Smith, 1964: "Nimbus Backup Gridding: AVCS and HRIR," Technical Report No. 1, Contract No. NAS 5-3253, Aracon Geophysics Company, Concord, Mass. (January).

Widger, William K., Jr., Paul E. Sherr, and C.W.C. Rogers, 1964: "Practical Interpretation of Meteorological Satellite Data," Final Report, Contract No. AF 19(628)-2471, Aracon Geophysics Company, Concord, Mass. (September).

APPENDIX A

INDEX OF AVAILABLE HIGH RESOLUTION INFRARED RADIOMETER FILM STRIPS (PHOTOFACSIMILE)

Each film strip contains several "blocks" of data. A block of data is defined to be a piece of a film strip with continuous, uninterrupted data. A data block may extend over the entire nighttime portion of an orbit or it may extend over only a few minutes, in which case several blocks may be included in one data orbit. Multiple blocks of data in a given orbit may result from the data being readout out at different times or from continuously obtained data of one interrogation being broken up by noise in the timing signal and/or noise in the video signal.

All of the 323 blocks containing data from 194 individual orbits of Nimbus I are tabulated on the following pages. The data blocks are numbered from 1 through 323. The Index is designed to be used with the Subpoint Track Summaries in Appendix B and the HRIR Photofacsimile Displays in Appendix C.

It has been pointed out in Section V that the same recorded data can be and often were read out several times. When two or more blocks of different interrogations contained exactly the same data, only the best one was chosen for archiving in this Manual. However, in many instances, portions of two or more blocks contained the same data while other portions contained data which were unique to a single block. All of these overlapping blocks are needed to complete the data archive and are, therefore, indexed in this Appendix.

The index is divided into two basic sections. One contains information concerning the orbit and time interval when the data were recorded in the satellite. The other section gives information about the readout of these data. The nomenclature used in the Index is defined below.

INDEX NOMENCLATURE

HEADING	EXPLANATION
Data Orbit Number	The orbit number increases by one at each ascending node, orbit zero covering the period from launch to the first ascending node. The data orbit number is the number of the orbit at the time the HRIR data were recorded in the satellite.

INDEX NOMENCLATURE (Continued)

HEADING	EXPLANATION
DESCENDING NODE	
Longitude	The longitude on earth at which the satellite crossed the equatorial plane going from north to south, measured in degrees from 0° to 180° East or West.
Universal Time (UT)	Universal time of the occurrence of the descending node in months, days, hours, minutes and seconds.
Calendar Day	Calendar days are numbered consecutively beginning with January 1, 1964, which was calendar day 1.
Data Block Number	Each continuous piece of film strip containing HRIR data with no time discontinuities makes up a data block. Two or more data blocks may contain part of the same data, but all of the data in one block are never duplicated exactly in any other block. The data blocks are numbered sequentially from 1 through 323.
BEGIN	
Latitude	The subsatellite latitude corresponding to the beginning time listed for the data block. Latitude is shown in degrees north, N, or south, S. The lower case "a" or "d" following "N" or "S" indicates that the data began while the satellite was on the ascending or descending leg of the orbit, respectively.
Universal Time	The beginning time of the HRIR data in a data block to the nearest minute.
END	
Latitude	The subsatellite latitude corresponding to the ending time listed for the data block. Latitude is shown in degrees north, N, or south, S. The lower case "a" or "d" following the "N" or "S" indicates that the data ended while the satellite was on the ascending or descending leg of the orbit, respectively.
Universal Time	The ending time of the HRIR data in a data block to the nearest minute.

INDEX NOMENCLATURE (Continued)

HEADING	EXPLANATION
Playback Mode	The playback mode indicates the playback direction of the tape recorder. Forward (FWD) means the data were played back from the tape recorder in the same direction as that in which they were recorded. Reverse (REV) means the data were played back in the opposite direction from the direction in which they were recorded.
Readout Orbit Number	The number of the orbit at the time the data were read out from the satellite.
DAF	The Data Acquisition Facility which read out the data. "G" is the Gilmore Creek, Alaska station and "R" is the Rosman, North Carolina station.

The Index was designed to tabulate the HRIR data acquired during the nighttime (descending) legs of the orbits. However, the HRIR system operated during daylight on a few occasions. These data are also tabulated in the Index and are identified in the Remarks column. All orbits are identified by the longitude and time of the descending node since most of the nighttime data were acquired on the descending leg of the orbit. In those cases for which daytime data were acquired when the satellite crossed the equatorial plane north bound and the orbit number increased by one, both orbit numbers are given. In these cases, the orbit number to which the descending node information applies, is underlined. (The underlined orbit is also the one for which a descending node notation is entered on the subpoint tracks in Appendix B.) For example, Data Block Number 46 contains daytime data acquired while the satellite crossed the equatorial plane going northbound on orbits 065 and 066. The descending node information applies to orbit 065.

Figure A1 gives the difference in time of the descending and ascending nodes versus orbit number for Nimbus I and Figure A2 gives the difference in longitude of the descending and ascending nodes versus orbit number. Using the descending node time and longitude given in the Index and these two figures, one can obtain the ascending node time and longitude.

To illustrate the use of the tabulated material, the entry in the row for data block 93 indicates that data were recorded in the satellite during orbit 145. The descending node of orbit 145 was over longitude 95.9°W when Nimbus I crossed the equatorial plane going from north to south at 06:00:38 UT on September 7, 1964. The calendar day was the 251st day of 1964. The Index also shows that the data began to be recorded when the satellite was over 17.8 North latitude on the descending leg of orbit 145. The beginning time of the data was 05:56 UT to the nearest minute. The data ended when the satellite

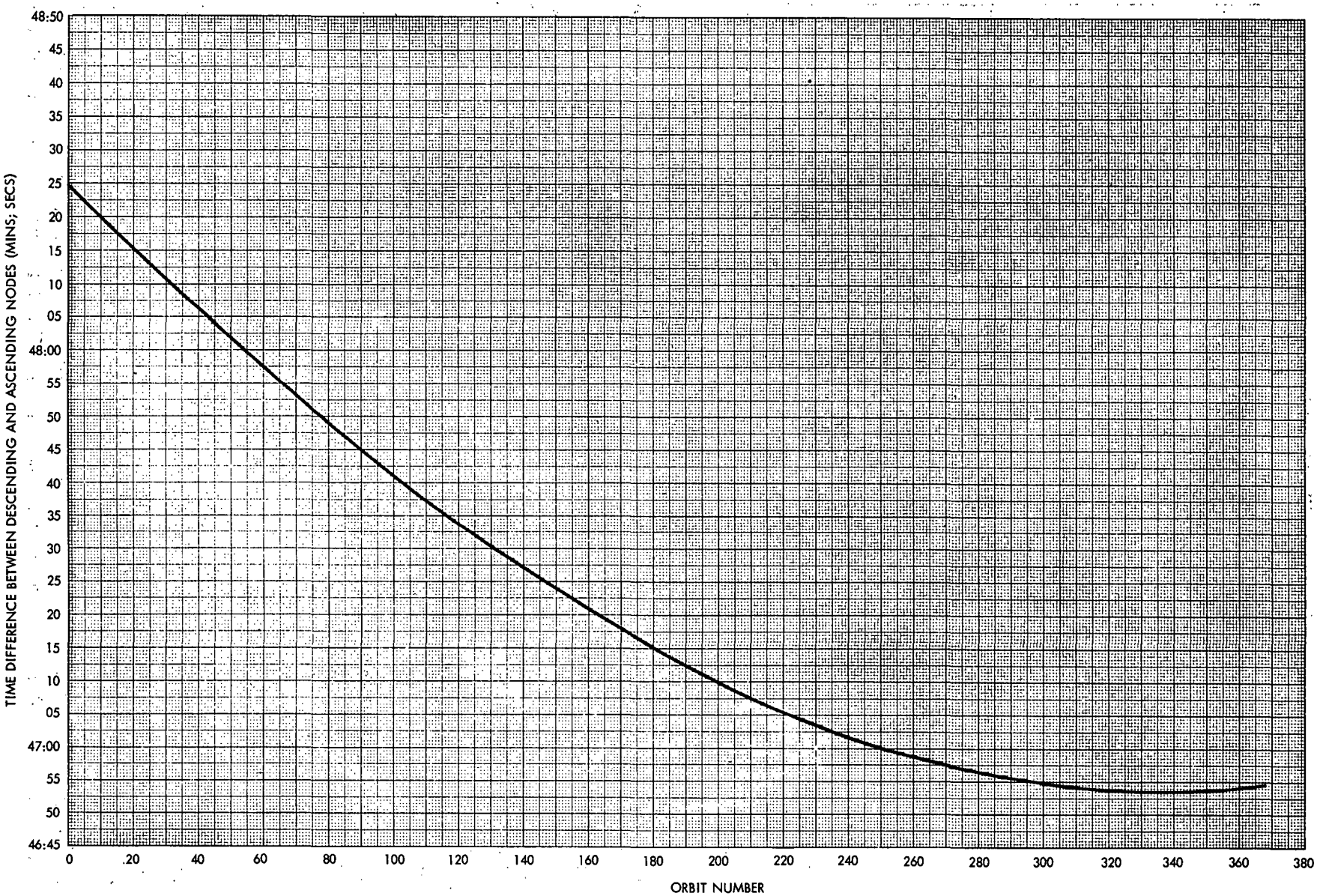

Figure A1—Time of the descending node minus the time of the ascending node vs. orbit number

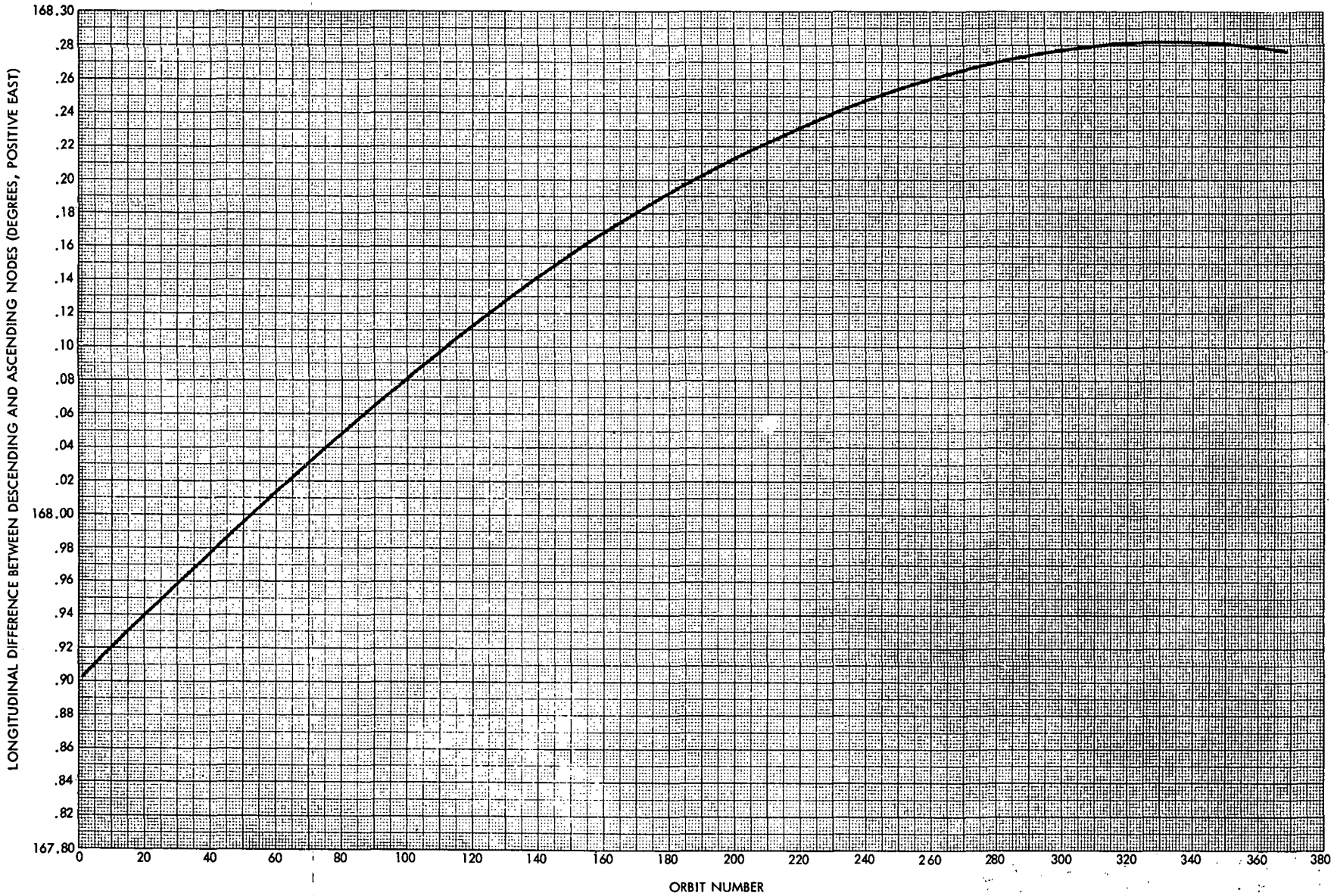

Figure A2—Longitude of the descending node minus the longitude of the ascending node (positive east) vs. orbit number

was over 74.9 South latitude on the ascending portion of the orbit at 06:29 UT. These data were read out in the forward mode, i.e., they were read out when the tape recorder traveled in the same direction as it traveled when recording the data. It is also seen that the data were read out when the satellite passed within range of the Gilmore Creek, Alaska, Data Acquisition Facility (abbreviated G) on orbit 154.

The entry in the next row for block 94 indicates that the data were recorded when the satellite traveled northbound across the equatorial plane and the orbit number increased from 145 to 146. The descending node of orbit 146 occurred over longitude 120.5° West at 07:39:04 UT on September 7, 1964. The data began at 06:48 when the satellite was over 12.6°S on the ascending leg of the orbit. The data ended at 07:07 over 54.7°N when the satellite was still northbound. These data also were read out in the forward mode. A Remark indicates that the grid is in error and that the data were recorded on the daylight side of the Earth. The data were read out over the Gilmore Creek DA Facility during orbit 162.

INDEX OF AVAILABLE HIGH RESOLUTION INFRARED RADIOMETER FILM STRIPS (PHOTOFACSIMILE)

DATA											READOUT	
DATA ORBIT NUMBER	DESCENDING NODE			DATA BLOCK NUMBER	BEGIN		END		PLAYBACK MODE	REMARKS	READOUT ORBIT NUMBER	DAF
	LONGITUDE (DEG)	UNIVERSAL TIME (MO D H M S)	CALENDAR DAY		LATITUDE (DEG)	UNIVERSAL TIME (H M)	LATITUDE (DEG)	UNIVERSAL TIME (H M)				
007	59.3 E	AUG 28 19:37:27	241	1	9.9 Sd	19:40	77.5 Sa	20:04	REV		008	G
023	25.6 E	AUG 29 21:52:19	242	2	16.8 Nd	21:48	74.7 Sa	22:20	FWD		028	R
024	1.0 E	AUG 29 23:30:45	242	3	71.4 Nd	23:12	53.3 Nd	23:16	FWD		031	G
				4	49.5 Nd	23:18	30.2 Nd	23:23	REV		031	G
				5	26.3 Nd	23:24	78.4 Sa	23:57	REV		028	R
031	171.2 W	AUG 30 10:59:45	243	6	34.1 Nd	10:51	73.1 Sa	11:28	FWD		036	G
034	115.0 E	AUG 30 15:55:02	243	7	78.4 Nd	15:34	50.6 Nd	15:42	FWD		036	G
				8	78.4 Nd	15:34	46.8 Nd	15:43	FWD		035	R
				9	46.8 Nd	15:43	80.5 Sd	16:18	REV		035	R
				10	81.4 Sd	16:19	76.8 Sa	16:22	REV	UNGRIDDED	035	R
035	90.4 E	AUG 30 17:33:28	243	11	76.9 Nd	17:13	80.0 Sa	17:59	REV		036	G
036	65.8 E	AUG 30 19:11:53	243	12	71.9 Nd	18:53	78.9 Sa	19:38	REV		037	G
037	41.2 E	AUG 30 20:50:19	243	13	79.1 Nd	20:29	79.8 Sa	21:16	REV		038	G
040	32.6 W	AUG 31 01:45:36	244	14	28.3 Sd	01:53	71.1 Sd	02:05	FWD		043	R
041	57.2 W	AUG 31 03:24:02	244	15	75.6 Nd	03:04	19.6 Nd	03:19	FWD		042	R
				16	37.9 Sd	03:34	80.9 Sa	03:49	REV		042	R
043	106.4 W	AUG 31 06:40:54	244	17	80.3 Nd	06:19	42.4 Nd	06:30	REV		043	R
				18	38.5 Sd	06:51	73.8 Sa	07:09	FWD		046	G
044	131.0 W	AUG 31 08:19:19	244	19	73.4 Nd	08:00	14.2 Sd	08:23	FWD		046	G
				20	21.8 Sd	08:25	79.9 Sa	08:45	REV		045	G
045	155.6 W	AUG 31 09:57:45	244	21	57.0 Nd	09:43	81.4 Sa	10:22	REV	Erroneous grid. For correct position, move grid down 4.0 mm and left 3.0 mm.	046	G
046	179.8 E	AUG 31 11:36:11	244	22	0.7 Nd	11:36	80.2 Sd	11:59	REV		047	G
047	155.2 E	AUG 31 13:14:36	244	23	39.5 Sd	13:25	75.9 Sa	13:42	FWD		049	R
048	130.6 E	AUG 31 14:53:02	244	24	75.6 Nd	14:33	27.4 Nd	14:46	FWD		049	R
				25	27.4 Nd	14:46	81.0 Sa	15:18	REV	UNGRIDDED	049	R
				26	23.5 Nd	14:47	81.0 Sa	15:18	REV		049	R
049	106.0 E	AUG 31 16:31:28	244	27	56.0 Nd	16:17	69.6 Sa	17:01	FWD	Erroneous grid. For correct position, move grid down 3.0 mm and left 3.0 mm.	052	G
049/050	106.0 E	AUG 31 16:31:28	244	28	63.2 Sa	17:03	7.3 Na	17:24	REV	ALL DAYTIME DATA	050	R
050	81.3 E	AUG 31 18:09:54	244	29	35.1 Na	17:32	45.7 Na	17:35	REV	ALL DAYTIME DATA	050	G
				30	49.2 Na	17:36	59.7 Na	17:39	REV	ALL DAYTIME DATA	050	G

INDEX OF AVAILABLE HIGH RESOLUTION INFRARED RADIOMETER FILM STRIPS (PHOTOFACSIMILE)

DATA											READOUT	
DATA ORBIT NUMBER	DESCENDING NODE			DATA BLOCK NUMBER	BEGIN		END		PLAYBACK MODE	REMARKS	READOUT ORBIT NUMBER	DAF
	LONGITUDE (DEG)	UNIVERSAL TIME (MO D H M S)	CALENDAR DAY		LATITUDE (DEG)	UNIVERSAL TIME (H M)	LATITUDE (DEG)	UNIVERSAL TIME (H M)				
050	81.3 E	AUG 31 18:09:54	244	31	53.8 Nd	17:56	19.6 Sd	18:15	REV		051	G
				32	27.2 Sd	18:17	56.5 Sd	18:25	REV		051	G
051	56.7 E	AUG 31 19:48:19	244	33	79.2 Nd	19:27	81.2 Sd	20:12	REV		052	G
055	41.7 W	SEPT 1 02:22:02	245	34	66.2 Sd	02:40	77.2 Sa	02:49	FWD		057	R
056	66.3 W	SEPT 1 04:00:28	245	35	70.5 Nd	03:42	17.4 Nd	03:56	FWD		057	R
				36	43.6 Sd	04:12	78.2 Sa	04:27	REV		057	R
057	90.9 W	SEPT 1 05:38:54	245	37	80.3 Nd	05:17	46.2 Nd	05:27	REV		057	R
				38	30.9 Sd	05:47	76.8 Sa	06:06	FWD		060	G
058	115.5 W	SEPT 1 07:17:19	245	39	76.5 Nd	06:57	2.6 Sd	07:18	FWD		064	R
				40	44.1 Sd	07:29	80.0 Sa	07:43	REV		059	G
059	140.1 W	SEPT 1 08:55:45	245	41	49.5 Nd	08:43	38.9 Sd	09:06	REV		060	G
				42	45.7 Nd	08:44	78.9 Sa	09:22	REV		060	G
060	164.7 W	SEPT 1 10:34:11	245	43	39.6 Nd	10:24	81.2 Sa	10:59	REV		064	R
064	96.9 E	SEPT 1 17:07:54	245	44	53.8 Nd	16:54	78.5 Sd	17:30	FWD	UNGRIDDED	065	R
				45	78.5 Sd	17:30	15.0 Sa	17:54	REV	UNGRIDDED / PARTLY DAYTIME DATA	065	R
065/066	72.3 E	SEPT 1 18:46:20	245	46	74.7 Sd	19:07	7.4 Na	19:39	REV	PARTLY DAYTIME DATA	066	G
066	47.7 E	SEPT 1 20:24:45	245	47	6.3 Nd	20:23	76.6 Sa	20:52	FWD		067	G
066/067	47.7 E	SEPT 1 20:24:45	245	48	64.5 Sa	20:56	44.4 Na	21:28	REV	ALL DAYTIME DATA	067	R
069	26.1 W	SEPT 2 01:20:02	246	49	4.0 Nd	01:19	79.6 Sa	01:46	REV		075	G
070	50.7 W	SEPT 2 02:58:28	246	50	77.0 Nd	02:38	2.1 Sd	02:59	REV		075	G
073	124.5 W	SEPT 2 07:53:45	246	51	71.5 Nd	07:35	35.1 Sd	08:03	FWD		075	G
				52	26.3 Nd	07:47	81.4 Sd	08:18	REV		074	G
				53	38.7 Sd	08:04	79.1 Sa	08:20	FWD		075	G
075	173.7 W	SEPT 2 11:10:37	246	54	2.4 Nd	11:10	76.4 Sa	11:38	FWD	Erroneous grid. For correct position, move grid down 3.5 mm.	079	R
078	112.5 E	SEPT 2 16:05:54	246	55	72.0 Nd	15:47	79.5 Sa	16:32	REV		079	R
079/080	63.3 E	SEPT 2 19:22:45	246	56	50.4 Sa	18:20	49.3 Na	18:49	REV	ALL DAYTIME DATA	080	G
080	63.3 E	SEPT 2 19:22:45	246	57	2.9 Nd	19:22	71.1 Sa	19:52	FWD		081	G
080/081	63.3 E	SEPT 2 19:22:45	246	58	68.0 Sa	19:53	44.2 Na	20:26	REV	ALL DAYTIME DATA	081	G
081	38.7 E	SEPT 2 21:01:11	246	59	80.3 Na	20:37	79.8 Sd	21:24	REV		082	G
084	35.1 W	SEPT 3 01:56:28	247	60	13.5 Sd	02:00	76.2 Sa	02:24	FWD		089	G

INDEX OF AVAILABLE HIGH RESOLUTION INFRARED RADIOMETER FILM STRIPS (PHOTOFACSIMILE)

DATA											READOUT	
DATA ORBIT NUMBER	DESCENDING NODE			DATA BLOCK NUMBER	BEGIN		END		PLAYBACK MODE	REMARKS	READOUT ORBIT NUMBER	DAF
	LONGITUDE (DEG)	UNIVERSAL TIME (MO D H M S)	CALENDAR DAY		LATITUDE (DEG)	UNIVERSAL TIME (H M)	LATITUDE (DEG)	UNIVERSAL TIME (H M)				
085	59.7 W	SEPT 3 03:34:54	247	61	75.3 Nd	03:15	38.5 Nd	03:25	FWD		086	R
				62	72.0 Nd	03:16	15.1 Nd	03:31	FWD		090	G
				63	19.5 Sd	03:40	79.6 Sa	04:01	REV		086	R
086	84.3 W	SEPT 3 05:13:20	247	64	79.2 Nd	04:52	59.2 Nd	04:58	REV		086	R
088	133.6 W	SEPT 3 08:30:11	247	65	47.3 Nd	08:18	80.1 Sa	08:56	REV		089	G
089	158.6 W	SEPT 3 10:08:37	247	66	48.9 Nd	09:56	79.0 Sa	10:35	REV		090	G
091	152.6 E	SEPT 3 13:25:28	247	67	9.7 Sd	13:28	76.3 Sa	13:53	FWD		105	G
092	128.0 E	SEPT 3 15:03:54	247	68	75.3 Nd	14:44	15.1 Nd	15:00	FWD		105	G
				69	75.3 Nd	14:44	4.2 Sd	15:05	FWD	Erroneous grid. For correct position, move grid left 2.0 mm.	093	R
				70	8.1 Sd	15:06	79.6 Sa	15:30	REV		093	R
104	167.2 W	SEPT 4 10:45:03	248	71	50.5 Nd	10:32	80.0 Sa	11:11	REV		105	G
106	143.6 E	SEPT 4 14:01:54	248	72	4.2 Sd	14:03	77.6 Sa	14:29	FWD		110	G
107	119.0 E	SEPT 4 15:40:20	248	73	76.6 Nd	15:20	6.4 Sd	15:42	FWD		110	G
				74	10.2 Sd	15:43	80.5 Sa	16:06	REV		108	R
108	94.4 E	SEPT 4 17:18:46	248	75	64.4 Nd	17:02	81.0 Sa	17:44	REV		109	R
109	69.8 E	SEPT 4 18:57:12	248	76	80.3 Na	18:33	80.3 Sa	19:23	REV	Erroneous grid. For correct position, move grid down 4.0 mm.	110	G
118	151.6 W	SEPT 5 09:43:03	249	77	69.1 Nd	09:25	81.3 Sa	10:08	REV		119	G
119	176.2 W	SEPT 5 11:21:29	249	78	5.7 Nd	11:20	80.8 Sa	11:47	REV		120	G
120	159.2 E	SEPT 5 12:59:55	249	79	19.0 Nd	12:55	77.9 Sa	13:27	FWD		123	R
121	134.6 E	SEPT 5 14:38:20	249	80	76.6 Nd	14:18	28.4 Nd	14:31	FWD		123	R
				81	2.5 Sd	14:39	80.6 Sa	15:04	REV		122	R
122	110.0 E	SEPT 5 16:16:46	249	82	77.8 Nd	15:56	79.7 Sa	16:43	REV		123	R
				83	53.2 Nd	16:03	77.5 Sa	16:44	FWD		124	G
123	85.4 E	SEPT 5 17:55:12	249	84	78.9 Nd	17:34	80.5 Sa	18:21	REV		124	G
124	60.8 E	SEPT 5 19:33:37	249	85	81.1 Na	19:10	79.5 Sa	20:00	REV		125	G
133	160.7 W	SEPT 6 10:19:29	250	86	70.5 Nd	10:01	81.4 Sa	10:44	REV		134	G
135	150.1 E	SEPT 6 13:36:21	250	87	10.1 Sd	13:39	76.7 Sa	14:04	FWD		139	G
136	125.5 E	SEPT 6 15:14:46	250	88	74.8 Nd	14:55	4.7 Sd	15:16	FWD		139	G
				89	12.3 Sd	15:18	79.9 Sa	15:41	REV		137	R
137	100.9 E	SEPT 6 16:53:12	250	90	73.0 Nd	16:34	81.4 Sa	17:18	REV		138	R

INDEX OF AVAILABLE HIGH RESOLUTION INFRARED RADIOMETER FILM STRIPS (PHOTOFACSIMILE)

DATA											READOUT	
DATA ORBIT NUMBER	DESCENDING NODE			DATA BLOCK NUMBER	BEGIN		END		PLAYBACK MODE	REMARKS	READOUT ORBIT NUMBER	DAF
	LONGITUDE (DEG)	UNIVERSAL TIME (MO D H M S)	CALENDAR DAY		LATITUDE (DEG)	UNIVERSAL TIME (H M)	LATITUDE (DEG)	UNIVERSAL TIME (H M)				
138	76.3 E	SEPT 6 18:31:38	250	91	79.9 Nd	18:10	79.7 Sa	18:58	REV		139	G
139	51.7 E	SEPT 6 20:10:03	250	92	80.5 Na	19:46	81.0 Sd	20:34	REV		140	G
145	95.9 W	SEPT 7 06:00:38	251	93	17.8 Nd	05:56	74.9 Sa	06:29	FWD		154	G
145/146	120.5 W	SEPT 7 07:39:04	251	94	12.6 Sa	06:48	54.7 Na	07:07	FWD	Erroneous grid. For correct position, move grid down 4.0 mm and left 2.0 mm. All dcytime data	162	G
146	120.5 W	SEPT 7 07:39:04	251	95	22.4 Na	06:58	15.6 Nd	07:35	FWD	PARTLY DAYTIME DATA	160	R
159	80.3 W	SEPT 8 04:58:38	252	96	10.1 Nd	04:56	79.9 Sa	05:25	REV		160	R
160	104.9 W	SEPT 8 06:37:04	252	97	80.6 Nd	06:15	54.1 Nd	06:23	REV		160	R
161	129.5 W	SEPT 8 08:15:30	252	98	38.9 Sd	08:26	81.1 Sa	08:41	REV		162	G
163	178.7 W	SEPT 8 11:32:21	252	99	21.2 Sd	11:38	81.0 Sa	11:58	REV		164	G
164	156.6 E	SEPT 8 13:10:47	252	100	29.9 Nd	13:03	75.7 Sa	13:39	FWD	UNGRIDDED	169	G
				101	18.3 Nd	13:06	75.7 Sa	13:39	FWD		168	G
165	132.0 E	SEPT 8 14:49:13	252	102	80.8 Nd	14:27	23.8 Nd	14:43	FWD	UNGRIDDED	166	R
				103	78.9 Nd	14:28	27.7 Nd	14:42	FWD		169	G
				104	20.0 Nd	14:44	80.8 Sa	15:15	REV		166	R
166	107.4 E	SEPT 8 16:27:38	252	105	79.8 Nd	16:06	81.2 Sa	16:53	REV		167	R
167	82.8 E	SEPT 8 18:06:04	252	106	50.3 Nd	17:53	80.7 Sa	18:32	REV		168	G
168	58.2 E	SEPT 8 19:44:30	252	107	81.2 Nd	19:21	81.1 Sa	20:10	REV		169	G
174	89.4 W	SEPT 9 05:35:04	253	108	72.4 Nd	05:16	67.7 Sd	05:54	FWD		178	G
				109	11.1 Sd	05:38	73.9 Sd	06:04	REV	Erroneous grid. For correct position, move grid down 3.0 mm.	181	R
175	114.0 W	SEPT 9 07:13:30	253	110	55.7 Nd	06:59	52.8 Sd	07:28	FWD		181	R
				111	28.8 Nd	07:06	46.6 Sa	07:51	FWD	PARTLY DAYTIME DATA	183	G
181	98.4 E	SEPT 9 17:04:04	253	112	46.4 Nd	16:52	78.9 Sd	17:27	REV		182	R
182	73.8 E	SEPT 9 18:42:30	253	113	76.9 Nd	18:22	81.2 Sa	19:08	REV		183	G
183	49.2 E	SEPT 9 20:20:56	253	114	26.3 Sd	20:28	81.4 Sa	20:46	REV		184	G
187	49.2 W	SEPT 10 02:54:39	254	115	37.0 Nd	02:45	5.1 Sd	02:56	FWD		192	G
188	73.8 W	SEPT 10 04:33:04	254	116	75.6 Nd	04:13	7.3 Sd	04:35	FWD		192	G
				117	50.2 Nd	04:20	3.5 Sd	04:34	REV		193	G
189	98.4 W	SEPT 10 06:11:30	254	118	76.9 Nd	05:51	40.3 Nd	06:01	REV		193	G
				119	73.8 Nd	05:52	28.7 Nd	06:04	FWD		195	R

INDEX OF AVAILABLE HIGH RESOLUTION INFRARED RADIOMETER FLIM STRIPS (PHOTOFACSIMILE)

DATA											READOUT	
DATA ORBIT NUMBER	DESCENDING NODE			DATA BLOCK NUMBER	BEGIN		END		PLAYBACK MODE	REMARKS	READOUT ORBIT NUMBER	DAF
	LONGITUDE (DEG)	UNIVERSAL TIME (MO D H M S)	CALENDAR DAY		LATITUDE (DEG)	UNIVERSAL TIME (H M)	LATITUDE (DEG)	UNIVERSAL TIME (H M)				
189	98.4 W	SEPT 10 06:11:30	254	120	21.0 Nd	06:06	1.9 Sd	06:12	REV		195	R
				121	17.2 Nd	06:07	5.6 Sd	06:13	FWD		193	G
190	123.0 W	SEPT 10 07:49:56	254	122	75.1 Nd	07:30	0.3 Sd	07:50	REV		192	G
				123	71.8 Nd	07:31	4.0 Sd	07:51	FWD		193	G
191	147.6 W	SEPT 10 09:28:22	254	124	69.8 Nd	09:10	1.4 Nd	09:28	REV		192	G
195	114.0 E	SEPT 10 16:02:05	254	125	54.5 Na	15:30	25.7 Sd	16:09	FWD	PARTLY DAYTIME DATA	197	G
				126	80.5 Na	15:38	67.3 Sd	16:21	FWD		198	G
				127	76.3 Sd	16:24	68.3 Sa	16:33	REV	UNGRIDDED / PARTLY DAYTIME DATA	196	G
195/196	114.0 E	SEPT 10 16:02:05	254	128	62.0 Sa	16:35	31.0 Na	17:02	REV	ALL DAYTIME DATA	196	R
196	89.4 E	SEPT 10 17:40:30	254	129	51.8 Nd	17:27	81.2 Sa	18:06	REV		197	G
197	64.8 E	SEPT 10 19:18:56	254	130	80.3 Nd	18:57	73.9 Sd	19:40	REV		198	G
201	33.7 W	SEPT 11 01:52:39	255	131	68.6 Sd	02:12	78.4 Sa	02:20	FWD		203	R
202	58.3 W	SEPT 11 03:31:05	255	132	78.4 Nd	03:10	7.2 Sd	03:33	FWD		203	R
				133	18.3 Sd	03:36	81.4 Sa	03:56	REV		203	R
203	82.9 W	SEPT 11 05:09:31	255	134	81.1 Nd	04:47	44.1 Nd	04:58	REV		203	R
205	132.1 W	SEPT 11 08:26:22	255	135	73.2 Nd	08:07	47.3 Nd	08:14	FWD		206	G
				136	43.5 Nd	08:15	17.3 Sd	08:31	FWD		206	G
				137	17.3 Sd	08:31	81.2 Sa	08:52	REV		206	G
206	156.7 W	SEPT 11 10:04:48	255	138	6.8 Nd	10:03	76.9 Sd	10:27	FWD	UNGRIDDED	208	G
				139	19.4 Sd	10:10	34.8 Sa	10:46	FWD	PARTLY DAYTIME DATA	207	G
206/207	156.7 W	SEPT 11 10:04:48	255	140	34.8 Sa	10:46	61.3 Na	11:13	REV	ALL DAYTIME DATA	207	G
207	178.7 E	SEPT 11 11:43:14		141	64.9 Na	11:14	78.8 Nd	11:22	REV	ALL DAYTIME DATA	207	G
				142	28.7 Sd	11:51	81.1 Sa	12:09	REV		208	G
208	154.1 E	SEPT 11 13:21:39	255	143	44.9 Sd	13:34	78.5 Sa	13:49	FWD		210	R
209	129.5 E	SEPT 11 15:00:05	255	144	78.4 Nd	14:39	46.2 Nd	14:48	FWD		213	G
				145	25.6 Sd	15:07	81.4 Sd	15:25	REV		210	R
210	104.9 E	SEPT 11 16:38:31	255	146	28.6 Nd	16:31	62.4 Sd	16:56	REV		211	G
				147	77.5 Sd	17:01	13.4 Sa	17:26	FWD	PARTLY DAYTIME DATA	211	G
210/211	104.9 E	SEPT 11 16:38:31	255	148	69.9 Sa	17:09	25.7 Na	17:37	FWD	ALL DAYTIME DATA	212	G
211	80.3 E	SEPT 11 18:16:57	255	149	53.3 Nd	18:03	80.8 Sa	18:43	REV		212	G

INDEX OF AVAILABLE HIGH RESOLUTION INFRARED RADIOMETER FILM STRIPS (PHOTOFACSIMILE)

DATA											READOUT	
DATA ORBIT NUMBER	DESCENDING NODE			DATA BLOCK NUMBER	BEGIN		END		PLAYBACK MODE	REMARKS	READOUT ORBIT NUMBER	DAF
	LATITUDE (DEG)	UNIVERSAL TIME (MO D H M S)	CALENDAR DAY		LATITUDE (DEG)	UNIVERSAL TIME (H M)	LATITUDE (DEG)	UNIVERSAL TIME (H M)				
212	55.7 E	SEPT 11 19:55:22	255	150	69.7 Nd	19:37	80.0 Sd	20:19	REV		213	G
216	42.7 W	SEPT 12 02:29:05	256	151	60.4 Sd	02:46	77.3 Sa	02:57	FWD		218	R
217	67.3 W	SEPT 12 04:07:31	256	152	79.4 Nd	03:46	5.6 Sd	04:09	FWD		218	R
				153	13.0 Sd	04:11	81.3 Sa	04:33	REV		218	R
218	91.9 W	SEPT 12 05:45:57	256	154	80.3 Nd	05:24	49.5 Nd	05:33	REV		218	R
				155	3.9 Sd	05:47	79.3 Sa	06:13	FWD		222	G
219	116.5 W	SEPT 12 07:24:23	256	156	79.1 Nd	07:03	28.1 Nd	07:17	FWD		220	G
				157	9.0 Nd	07:22	1.4 Nd	07:24	FWD		221	G
				158	28.1 Sd	07:32	81.3 Sa	07:50	REV		220	G
220	141.1 W	SEPT 12 09:02:48	256	159	80.0 Nd	08:41	71.2 Nd	08:44	REV		220	G
221	165.7 W	SEPT 12 10:41:14	256	160	81.4 Nd	10:18	78.7 Nd	10:20	REV		221	G
				161	12.2 Nd	10:38	81.2 Sa	11:07	REV		222	G
222	169.7 E	SEPT 12 12:19:40	256	162	81.2 Nd	11:57	77.2 Nd	11:59	REV		222	G
				163	55.1 Sd	12:35	80.6 Sa	12:46	FWD		227	G
223	145.1 E	SEPT 12 13:58:06	256	164	80.5 Nd	13:36	75.4 Nd	13:38	FWD	UNGRIDDED	227	G
				165	72.1 Nd	13:39	30.8 Nd	13:50	FWD	UNGRIDDED	227	G
224	120.5 E	SEPT 12 15:36:31	256	166	79.4 Nd	15:15	2.0 Nd	15:36	FWD		225	R
				167	5.5 Sd	15:38	81.3 Sa	16:02	REV		225	R
				168	20.3 Sd	15:42	78.5 Sa	16:04	FWD		226	G
225	95.9 E	SEPT 12 17:14:57	256	169	22.6 Nd	17:09	80.9 Sa	17:41	REV		226	R
226	71.3 E	SEPT 12 18:53:23	256	170	80.9 Nd	18:31	58.6 Nd	18:38	REV	UNGRIDDED	227	G
				171	79.1 Nd	18:32	81.3 Sa	19:19	REV		227	G
229	2.5 W	SEPT 12 23:48:40	256	172	1.4 Na	23:02	6.3 Nd	23:47	REV	PARTLY DAYTIME DATA	236	G
236	174.7 W	SEPT 13 11:17:40	257	173	1.6 Sd	11:18	80.7 Sa	11:44	REV		237	G
237	160.6 E	SEPT 13 12:56:06	257	174	26.9 Nd	12:49	79.8 Sa	13:23	FWD		242	G
238	136.0 E	SEPT 13 14:34:32	257	175	81.1 Nd	14:12	32.4 Nd	14:26	FWD		240	R
				176	2.0 Nd	14:34	74.4 Sd	14:56	REV	UNGRIDDED	239	R
239	111.4 E	SEPT 13 16:12:58	257	177	77.9 Nd	15:52	47.0 Sd	16:26	REV		240	R
				178	50.4 Sd	16:27	78.5 Sd	16:36	REV		240	R
240	86.8 E	SEPT 13 17:51:23	257	179	47.1 Nd	17:39	81.3 Sa	18:17	REV		241	G
241	62.2 E	SEPT 13 19:29:49	257	180	79.9 Nd	19:08	78.8 Sd	19:53	REV		242	G

INDEX OF AVAILABLE HIGH RESOLUTION INFRARED RADIOMETER FILM STRIPS (PHOTOFACSIMILE)

DATA											READOUT	
DATA ORBIT NUMBER	DESCENDING NODE			DATA BLOCK NUMBER	BEGIN		END		PLAYBACK MODE	REMARKS	READOUT ORBIT NUMBER	DAF
	LONGITUDE (DEG)	UNIVERSAL TIME (MO D H M S)	CALENDAR DAY		LATITUDE (DEG)	UNIVERSAL TIME (H M)	LATITUDE (DEG)	UNIVERSAL TIME (H M)				
242	37.6 E	SEPT 13 21:08:15	257	181	50.4 Nd	20:55	77.8 Sd	21:31	REV	UNGRIDDED	243	G
245	36.2 W	SEPT 14 02:03:32	258	182	30.9 Sd	02:12	78.8 Sa	02:31	FWD		247	R
246	60.8 W	SEPT 14 03:41:58	258	183	77.9 Nd	03:21	11.1 Nd	03:39	FWD		247	R
				184	3.6 Nd	03:41	81.1 Sa	04:08	REV		247	R
247	85.4 W	SEPT 14 05:20:24	258	185	81.3 Nd	04:57	47.1 Nd	05:08	REV		247	R
248	110.0 W	SEPT 14 06:58:49	258	186	43.9 Sd	07:11	81.4 Sd	07:24	FWD		251	G
249	134.6 W	SEPT 14 08:37:15	258	187	78.6 Nd	08:16	24.7 Sd	08:44	FWD		251	G
				188	38.9 Nd	08:27	28.3 Sd	08:45	FWD	UNGRIDDED	250	G
				189	28.3 Sd	08:45	81.3 Sa	09:03	REV	UNGRIDDED	250	G
250	159.2 W	SEPT 14 10:15:41	258	190	79.6 Nd	09:54	77.0 Nd	09:55	REV		250	G
				191	52.0 Nd	10:02	47.8 Sd	10:29	REV		251	G
				192	58.0 Sd	10:32	81.4 Sa	10:41	REV		251	G
251	176.2 E	SEPT 14 11:54:07	258	193	81.4 Nd	11:31	78.2 Nd	11:33	REV		251	G
				194	53.2 Sd	12:09	80.0 Sa	12:21	FWD		266	G
252	151.6 E	SEPT 14 13:32:32	258	195	79.3 Nd	13:11	28.5 Nd	13:25	FWD		266	G
				196	79.3 Nd	13:11	24.7 Sd	13:26	FWD	Erroneous grid. For correct position, move grid down 4.0 mm and right 3.0 mm.	262	R
				197	20.1 Sd	13:38	81.4 Sa	13:58	REV		256	G
253	127.0 E	SEPT 14 15:10:58	258	198	81.3 Nd	14:48	7.4 Nd	15:09	REV		256	G
				199	80.2 Nd	14:49	3.6 Nd	15:10	FWD	UNGRIDDED	255	G
				200	0.1 Sd	15:11	81.3 Sd	15:36	REV		255	G
				201	39.9 Sd	15:22	79.7 Sa	15:38	FWD		264	G
258	4.0 E	SEPT 14 23:23:07	258	202	75.7 Na	22:57	59.7 Sd	23:40	REV		262	R
262	94.4 W	SEPT 15 05:56:50	259	203	70.2 Sd	06:17	81.0 Sa	06:23	REV		264	G
263	119.0 W	SEPT 15 07:35:16	259	204	80.6 Nd	07:13	31.2 Nd	07:27	REV		264	G
				205	80.6 Nd	07:13	23.6 Nd	07:29	REV	UNGRIDDED	264	G
264	143.6 W	SEPT 15 09:13:42	259	206	44.3 Nd	09:02	12.2 Sd	09:17	REV		265	G
265	168.2 W	SEPT 15 10:52:07	259	207	49.7 Nd	10:39	75.2 Sd	11:14	REV		266	G
266	167.2 E	SEPT 15 12:30:33	259	208	76.5 Nd	12:10	58.9 Nd	12:15	FWD	UNGRIDDED	271	G
269	93.4 E	SEPT 15 17:25:50	259	209	81.3 Nd	17:03	15.3 Sd	17:30	REV		270	G
270	68.8 E	SEPT 15 19:04:16	259	210	68.8 Nd	18:46	81.3 Sa	19:30	REV		271	G

INDEX OF AVAILABLE HIGH RESOLUTION INFRARED RADIOMETER FILM STRIPS (PHOTOFACSIMILE)

DATA											READOUT	
DATA ORBIT NUMBER	DESCENDING NODE			DATA BLOCK NUMBER	BEGIN		END		PLAYBACK MODE	REMARKS	READOUT ORBIT NUMBER	DAF
	LONGITUDE (DEG)	UNIVERSAL TIME (MO D H M S)	CALENDAR DAY		LATITUDE (DEG)	UNIVERSAL TIME (H M)	LATITUDE (DEG)	UNIVERSAL TIME (H M)				
271	44.2 E	SEPT 15 20:42:42	259	211	55.6 Nd	20:28	37.1 Sd	20:53	REV		272	G
274	29.7 W	SEPT 16 01:37:59	260	212	71.3 Nd	01:19	60.4 Nd	01:22	FWD	UNGRIDDED	277	R
				213	52.9 Nd	01:24	18.3 Sd	01:44	FWD	UNGRIDDED	277	R
275	54.3 W	SEPT 16 03:16:25	260	214	41.6 Sd	03:28	81.4 Sa	03:42	REV		277	R
276	78.9 W	SEPT 16 04:54:51	260	215	81.2 Nd	04:32	52.4 Nd	04:41	REV		277	R
				216	59.9 Nd	04:39	40.9 Nd	04:44	FWD		277	R
277	103.5 W	SEPT 16 06:33:16	260	217	45.5 Sd	06:46	62.2 Sd	06:51	FWD		280	G
				218	68.6 Sd	06:53	80.4 Sa	07:00	FWD		280	G
278	128.1 W	SEPT 16 08:11:42	260	219	79.5 Nd	07:50	73.7 Nd	07:52	FWD		279	G
				220	70.3 Nd	07:53	44.2 Nd	08:00	FWD		280	G
				221	59.3 Nd	07:56	12.1 Sd	08:15	FWD		279	G
				222	15.7 Sd	08:16	78.6 Sd	08:35	REV		279	G
279	152.7 W	SEPT 16 09:50:08	260	223	53.4 Nd	09:36	23.0 Nd	09:44	REV		280	G
				224	11.7 Nd	09:47	4.2 Nd	09:49	REV		280	G
				225	6.9 Sd	09:52	32.0 Sd	09:59	REV		280	G
				226	42.5 Sd	10:02	69.0 Sd	10:10	REV		280	G
				227	77.6 Sd	10:13	81:3 Sa	10:16	REV		280	G
281	158.1 E	SEPT 16 13:07:00	260	228	49.1 Nd	12:54	53.2 Sd	13:22	FWD	Erroneous grid. For correct position, move grid left 3.5 mm.	284	R
282	133.5 E	SEPT 16 14:45:25	260	229	78.8 Nd	14:24	9.0 Nd	14:43	FWD		285	G
				230	46.9 Nd	14:33	5.3 Nd	14:44	FWD		287	G
				231	13.1 Sd	14:49	44.9 Sd	14:58	REV		284	R
283	108.9 E	SEPT 16 16:23:51	260	232	81.1 Na	16:00	15.2 Sd	16:28	REV		284	R
284	84.3 E	SEPT 16 18:02:17	260	233	80.6 Nd	17:40	35.0 Sd	18:12	REV		285	G
285	59.7 E	SEPT 16 19:40:43	260	234	79.7 Na	19:16	50.7 Sd	19:55	REV		286	G
286	35.1 E	SEPT 16 21:19:08	260	235	81.4 Nd	20:56	42.0 Nd	21:08	REV		287	G
287	10.5 E	SEPT 16 22:57:34	260	236	76.4 Nd	22:37	67.6 Sd	23:17	FWD		291	R
				237	13.3 Nd	22:54	79.3 Sa	23:25	FWD		294	G
288	14.1 W	SEPT 17 00:36:00	261	238	80.1 Nd	00:14	67.7 Nd	00:18	FWD		295	G
				239	18.7 Nd	00:31	81.3 Sa	01:02	REV		291	R
289	38.7 W	SEPT 17 02:14:26	261	240	80.8 Nd	01:52	46.8 Nd	02:02	REV		291	R

INDEX OF AVAILABLE HIGH RESOLUTION INFRARED RADIOMETER FILM STRIPS (PHOTOFACSIMILE)

DATA											READOUT	
DATA ORBIT NUMBER	DESCENDING NODE			DATA BLOCK NUMBER	BEGIN		END		PLAYBACK MODE	REMARKS	READOUT ORBIT NUMBER	DAF
	LONGITUDE (DEG)	UNIVERSAL TIME (MO D H M S)	CALENDAR DAY		LATITUDE (DEG)	UNIVERSAL TIME (H M)	LATITUDE (DEG)	UNIVERSAL TIME (H M)				
293	137.1 W	SEPT 17 08:48:09	261	241	53.3 Nd	08:34	77.4 Sd	09:11	REV		294	G
294	161.7 W	SEPT 17 10:26:35	261	242	47.4 Nd	10:14	78.7 Sd	10:50	REV		295	G
295	173.7 E	SEPT 17 12:05:00	261	243	41.4 Nd	11:54	3.6 Sd	12:06	FWD		298	R
296	149.1 E	SEPT 17 13:43:26	261	244	54.4 Nd	13:29	51.5 Sd	13:58	FWD		298	R
				245	43.0 Nd	13:32	61.5 Sd	14:01	REV		299	G
297	124.5 E	SEPT 17 15:21:52	261	246	81.2 Nd	14:59	80.1 Sd	15:46	REV		298	R
298	99.9 E	SEPT 17 17:00:18	261	247	78.3 Nd	16:39	27.8 Sd	17:08	FWD		299	G
				248	12.2 Nd	16:57	78.9 Sa	17:28	FWD	Erroneous grid. For correct position, move grid left 3.0 mm.	300	G
299	75.3 E	SEPT 17 18:38:43	261	249	79.4 Nd	18:17	53.8 Sd	18:54	REV		300	G
300	50.7 E	SEPT 17 20:17:09	261	250	80.8 Na	19:53	55.7 Sd	20:33	REV		301	G
304	47.7 W	SEPT 18 02:50:52	262	251	21.9 Nd	02:45	81.2 Sd	03:16	FWD		308	G
305	72.3 W	SEPT 18 04:29:18	262	252	81.4 Nd	04:06	78.3 Nd	04:08	FWD		309	G
				253	75.4 Nd	04:09	19.7 Nd	04:24	FWD	UNGRIDDED	309	G
				254	68.6 Nd	04:11	19.7 Nd	04:24	FWD		309	G
				255	16.0 Nd	04:25	27.7 Sd	04:37	REV		309	G
				256	41.6 Sd	04:41	48.5 Sd	04:43	REV		309	G
				257	51.8 Sd	04:44	80.8 Sd	04:54	REV		308	G
306	96.9 W	SEPT 18 06:07:44	262	258	81.1 Nd	05:45	32.7 Nd	05:59	REV		308	G
				259	17.6 Nd	06:03	6.4 Nd	06:06	REV		308	G
309	170.8 W	SEPT 18 11:03:01	262	260	48.9 Nd	10:50	49.4 Sd	11:17	FWD		313	R
310	164.6 E	SEPT 18 12:41:27	262	261	78.6 Nd	12:20	61.8 Nd	12:25	FWD		313	R
				262	50.5 Nd	12:28	12.9 Sd	12:45	FWD		313	R
				263	12.9 Sd	12:45	47.9 Sd	12:55	REV		313	R
				264	16.5 Sd	12:46	81.4 Sd	13:07	REV		313	R
311	140.0 E	SEPT 18 14:19:53	262	265	81.2 Nd	13:57	11.3 Sd	14:23	REV		313	R
				266	21.9 Nd	14:14	22.1 Sd	14:26	REV	UNGRIDDED	313	R
313	90.8 E	SEPT 18 17:36:44	262	267	81.1 Nd	17:14	26.1 Sd	17:44	REV		314	G
314	66.2 E	SEPT 18 19:15:10	262	268	78.9 Na	18:50	55.5 Sd	19:31	REV		315	G
315	41.6 E	SEPT 18 20:53:36	262	269	80.1 Na	20:29	23.1 Sd	21:00	REV		316	G

INDEX OF AVAILABLE HIGH RESOLUTION INFRARED RADIOMETER FILM STRIPS (PHOTOFACSIMILE)

DATA											READOUT	
DATA ORBIT NUMBER	DESCENDING NODE			DATA BLOCK NUMBER	BEGIN		END		PLAYBACK MODE	REMARKS	READOUT ORBIT NUMBER	DAF
	LONGITUDE (DEG)	UNIVERSAL TIME (MO D H M S)	CALENDAR DAY		LATITUDE (DEG)	UNIVERSAL TIME (H M)	LATITUDE (DEG)	UNIVERSAL TIME (H M)				
317	7.6 W	SEPT 19 00:10:27	263	270	16.4 Sd	00:15	79.4 Sa	00:38	FWD		323	G
318	32.2 W	SEPT 19 01:48:53	263	271	79.6 Nd	01:27	55.8 Nd	01:34	FWD		323	G
				272	59.6 Nd	01:33	52.1 Nd	01:35	FWD	UNGRIDDED	320	R
				273	52.1 Nd	01:35	40.7 Nd	01:38	REV	UNGRIDDED	320	R
321	106.0 W	SEPT 19 06:44:10	263	274	22.9 Nd	06:38	8.0 Nd	06:42	REV		323	G
322	130.6 W	SEPT 19 10:01:02	263	275	81.3 Nd	07:59	1.4 Sd	08:23	REV		323	G
323	155.2 W	SEPT 19 10:01:02	263	276	33.7 Nd	09:52	26.1 Nd	09:54	FWD		328	R
				277	18.6 Nd	09:56	3.8 Nd	10:00	FWD		328	R
324	179.8 W	SEPT 19 11:39:28	263	278	80.6 Nd	11:17	65.3 Nd	11:22	FWD		328	R
				279	80.6 Nd	11:17	61.6 Nd	11:23	FWD	UNGRIDDED	328	R
				280	39.1 Nd	11:29	5.6 Sd	11:41	FWD		330	G
325	155.6 E	SEPT 19 13:17:54	263	281	81.2 Nd	12:55	66.9 Nd	13:00	FWD		330	G
				282	81.2 Nd	12:55	63.2 Nd	13:01	FWD	UNGRIDDED	328	R
				283	55.8 Nd	13:03	10.7 Nd	13:15	FWD		331	G
				284	36.9 Nd	13:08	7.0 Nd	13:16	FWD		337	G
326	131.0 E	SEPT 19 14:56:19	263	285	61.1 Nd	14:40	2.4 Sd	14:57	REV		328	R
327	106.4 E	SEPT 19 16:34:45	263	286	81.3 Nd	16:11	32.6 Nd	16:26	REV		328	R
328	81.8 E	SEPT 19 18:13:11	263	287	76.2 Na	17:47	34.9 Sd	18:23	REV	UNGRIDDED	329	G
329	57.2 E	SEPT 19 19:51:37	263	288	80.2 Na	19:27	36.9 Sd	20:02	REV		330	G
330	32.6 E	SEPT 19 21:30:03	263	289	76.6 Na	21:04	67.3 Nd	21:12	REV		337	G
				290	79.3 Na	21:05	45.0 Nd	21:18	REV		331	G
333	41.2 W	SEPT 20 02:25:20	264	291	42.3 Nd	02:14	51.4 Sd	02:40	REV		338	G
				292	16.8 Sd	02:30	54.7 Sd	02:41	FWD		337	G
334	65.8 W	SEPT 20 04:03:46	264	293	72.4 Sd	04:25	81.2 Sd	04:29	REV		337	G
				294	75.3 Sd	04:26	80.1 Sa	04:31	FWD		338	G
335	90.4 W	SEPT 20 05:42:11	264	295	80.1 Nd	05:20	22.9 Nd	05:36	FWD		338	G
339	171.2 E	SEPT 20 12:15:55	264	296	76.9 Nd	11:55	70.3 Nd	11:57	FWD		344	G
				297	63.1 Nd	11:59	3.4 Nd	12:15	FWD		344	G
340	146.6 E	SEPT 20 13:54:20	264	298	80.3 Nd	13:32	16.0 Nd	13:50	FWD		344	G
				299	80.3 Nd	13:32	12.3 Nd	13:51	FWD		345	G

INDEX OF AVAILABLE HIGH RESOLUTION INFRARED RADIOMETER FILM STRIPS (PHOTOFACSIMILE)

DATA											READOUT	
DATA ORBIT NUMBER	DESCENDING NODE			DATA BLOCK NUMBER	BEGIN		END		PLAYBACK MODE	REMARKS	READOUT ORBIT NUMBER	DAF
	LONGITUDE (DEG)	UNIVERSAL TIME (MO D H M S)	CALENDAR DAY		LATITUDE (DEG)	UNIVERSAL TIME (H M)	LATITUDE (DEG)	UNIVERSAL TIME (H M)				
342	97.4 E	SEPT 20 17:11:12	264	300	71.3 Nd	16:52	11.8 Nd	17:08	REV		343	R
343	72.8 E	SEPT 20 18:49:38	264	301	77.9 Na	18:24	36.7 Sd	19:00	REV		344	G
344	48.1 E	SEPT 20 20:28:04	264	302	76.7 Na	20:02	38.6 Sd	20:39	REV		345	G
345	23.5 E	SEPT 20 22:06:29	264	303	68.7 Nd	21:48	57.4 Sd	22:23	FWD		349	R
				304	67.0 Sd	22:26	81.1 Sa	22:33	FWD		350	R
346	1.1 W	SEPT 20 23:44:55	264	305	79.5 Nd	23:23	63.0 Nd	23:28	FWD		350	R
				306	59.3 Nd	23:29	0.3 Sd	23:45	REV		350	R
				307	11.1 Sd	23:48	79.6 Sd	00:09	REV		349	R
				308	14.6 Sd	23:49	81.0 Sd	00:10	REV		349	R
347	25.7 W	SEPT 21 01:23:21	265	309	80.7 Na	00:59	42.2 Nd	01:12	REV		349	R
350	99.5 W	SEPT 21 06:18:38	265	310	46.8 Sd	06:32	81.2 Sa	06:45	FWD	UNGRIDDED	353	G
351	124.1 W	SEPT 21 07:57:04	265	311	79.7 Nd	07:35	52.1 Sd	08:12	FWD	UNGRIDDED	353	G
				312	79.7 Nd	07:35	44.9 Nd	07:45	FWD		369	G
				313	41.1 Nd	07:46	7.6 Nd	07:55	FWD		369	G
				314	6.9 Sd	07:59	65.1 Sd	08:16	FWD		367	R
				315	79.2 Sd	08:21	81.4 Sd	08:23	REV		353	G
352	148.7 W	SEPT 21 09:35:30	265	316	80.5 Nd	09:13	68.7 Nd	09:17	REV		353	G
				317	50.2 Nd	09:22	73.0 Sd	09:57	REV		353	G
353	173.3 W	SEPT 21 11:13:56	265	318	44.3 Nd	11:02	14.4 Nd	11:10	REV		367	G
				319	10.7 Nd	11:11	3.4 Nd	11:13	REV		367	G
367	157.7 W	SEPT 22 10:11:57	266	320	59.2 Nd	09:56	80.9 Sd	10:37	REV		368	G
368	177.7 E	SEPT 22 11:50:23	266	321	74.9 Nd	11:30	64.4 Nd	11:33	REV	UNGRIDDED	368	G
				322	20.0 Sd	11:56	54.1 Sd	12:06	REV		369	G
				323	57.4 Sd	12:07	81.3 Sd	12:16	REV		369	G

APPENDIX B

SUBPOINT TRACK SUMMARIES OF AVAILABLE RADIATION DATA

In this Appendix, the time intervals for which radiation data are available on the photofacsimile-produced 70 mm film are summarized diagrammatically by means of subpoint tracks. All orbits from which data were acquired with descending nodes falling within a given calendar day beginning at 00 UT are included on a single map base for that day. This method of presentation enables a user to quickly apprise himself of the orbits containing data in a particular area of interest.

On the subpoint track summaries, the nighttime data are shown by a solid line and the daytime data by a dotted line. A dashed line is used to extend either the solid or dotted line to the equator for ease in identifying the relevant data orbit number. The dashed line should not be misinterpreted to mean that data exist along that portion of the track. Each orbit is identified by orbit number and the time of occurrence of the descending node to the nearest minute of UT. Each portion of the subpoint track along which data were acquired is further identified by the beginning and ending times of the data to the nearest minute of UT.

To illustrate the use of the subpoint track summaries, we use the same examples as in Appendix A. The subpoint track for orbit 145 is drawn on page 73. It can be seen that orbit 145 has a descending node at 95.9°W and occurred at 06:01 UT. The nighttime data began at 05:56 and ended at the end of subpoint night. Daytime data began at the end of subpoint night and ended at 06:29. No data were recovered from 06:29 to 06:48. Daytime data began again at 06:48 on orbit 145 and ended at the beginning of subpoint night on orbit 146 at which time nighttime acquisition of data began again and ended at 07:35. These two parts of the subsatellite track for orbits 145 and 146 summarize diagrammatically the information pertaining to data blocks 93 through 95.

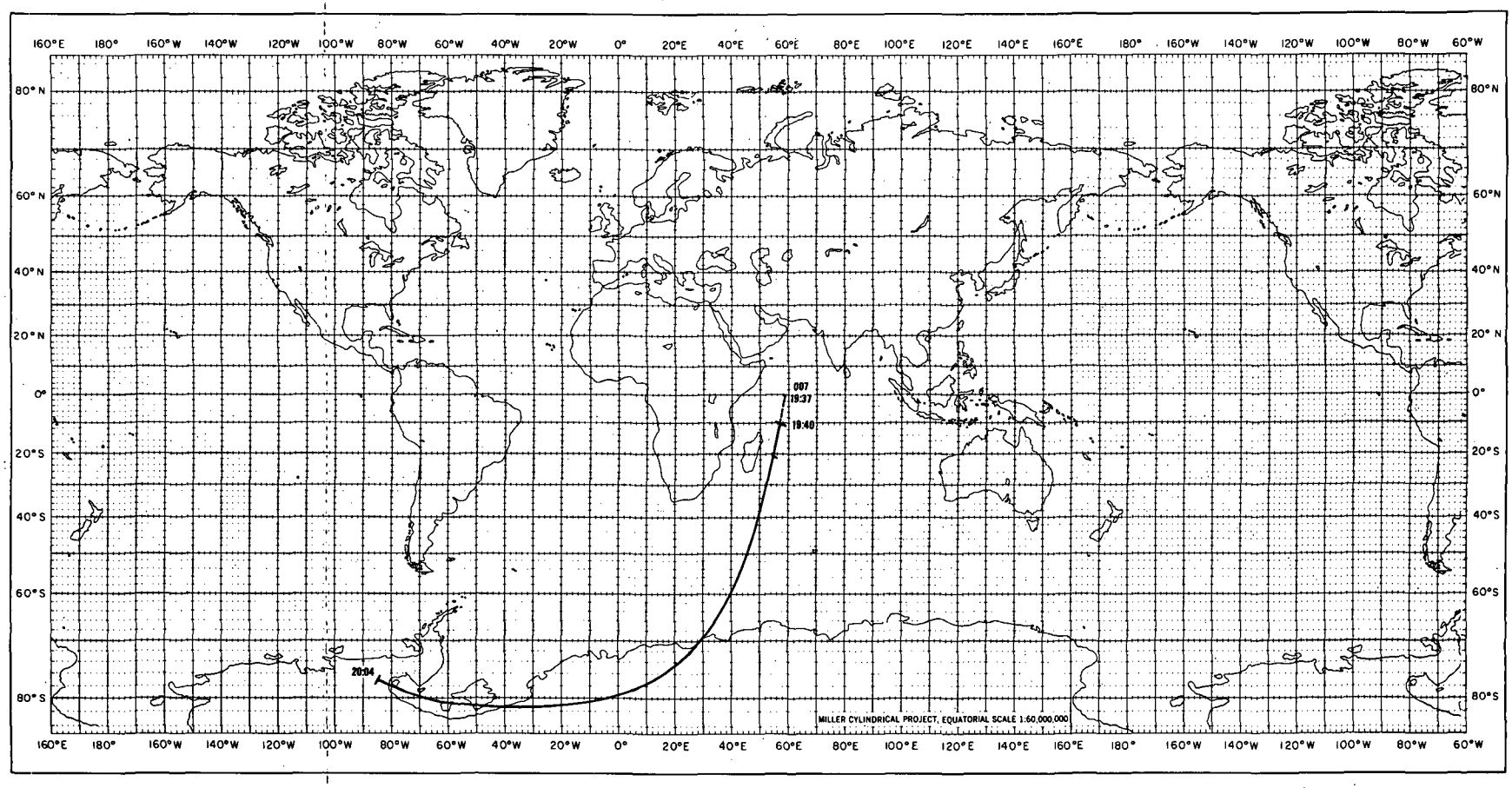

AUGUST 28, 1964

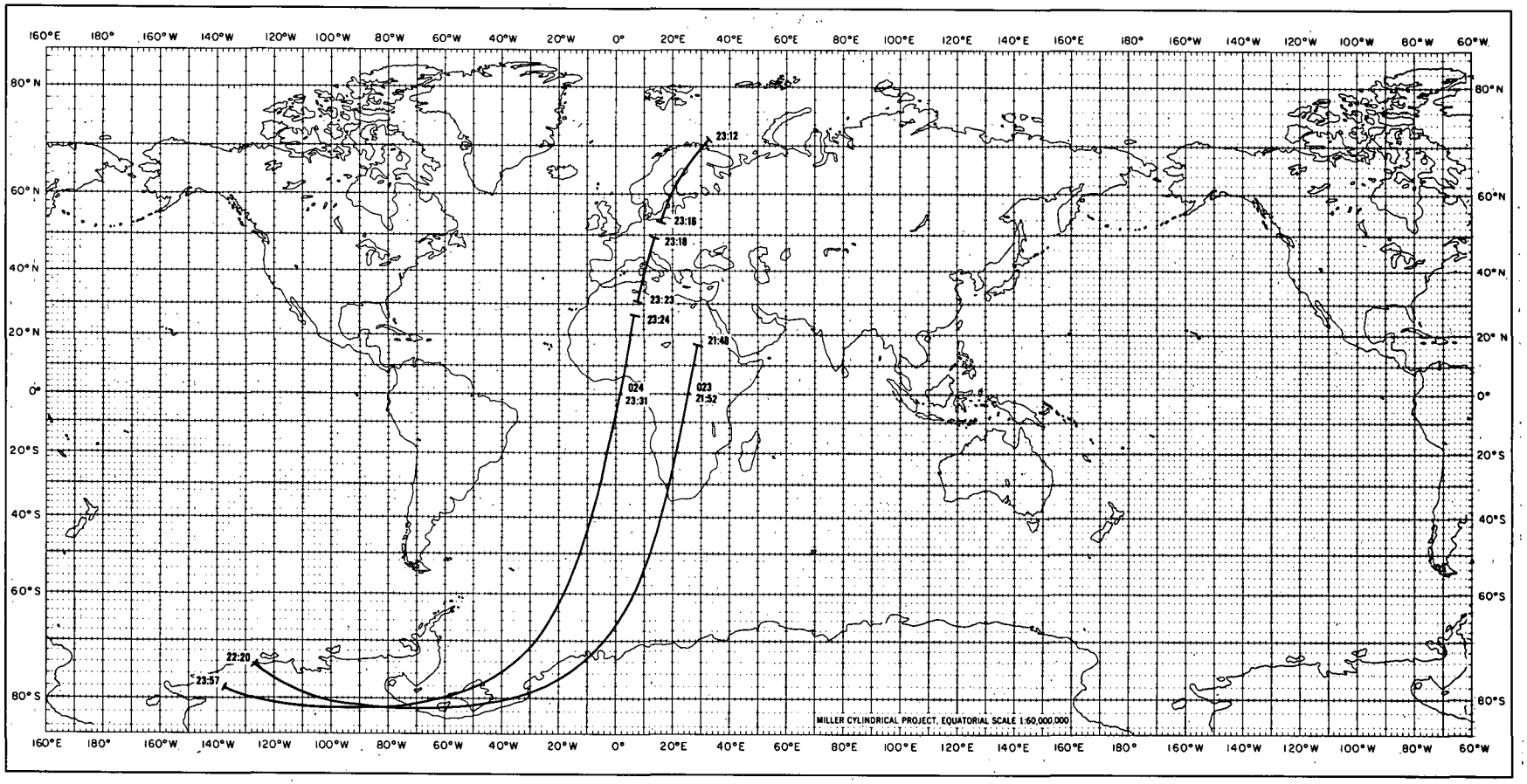

AUGUST 29, 1964

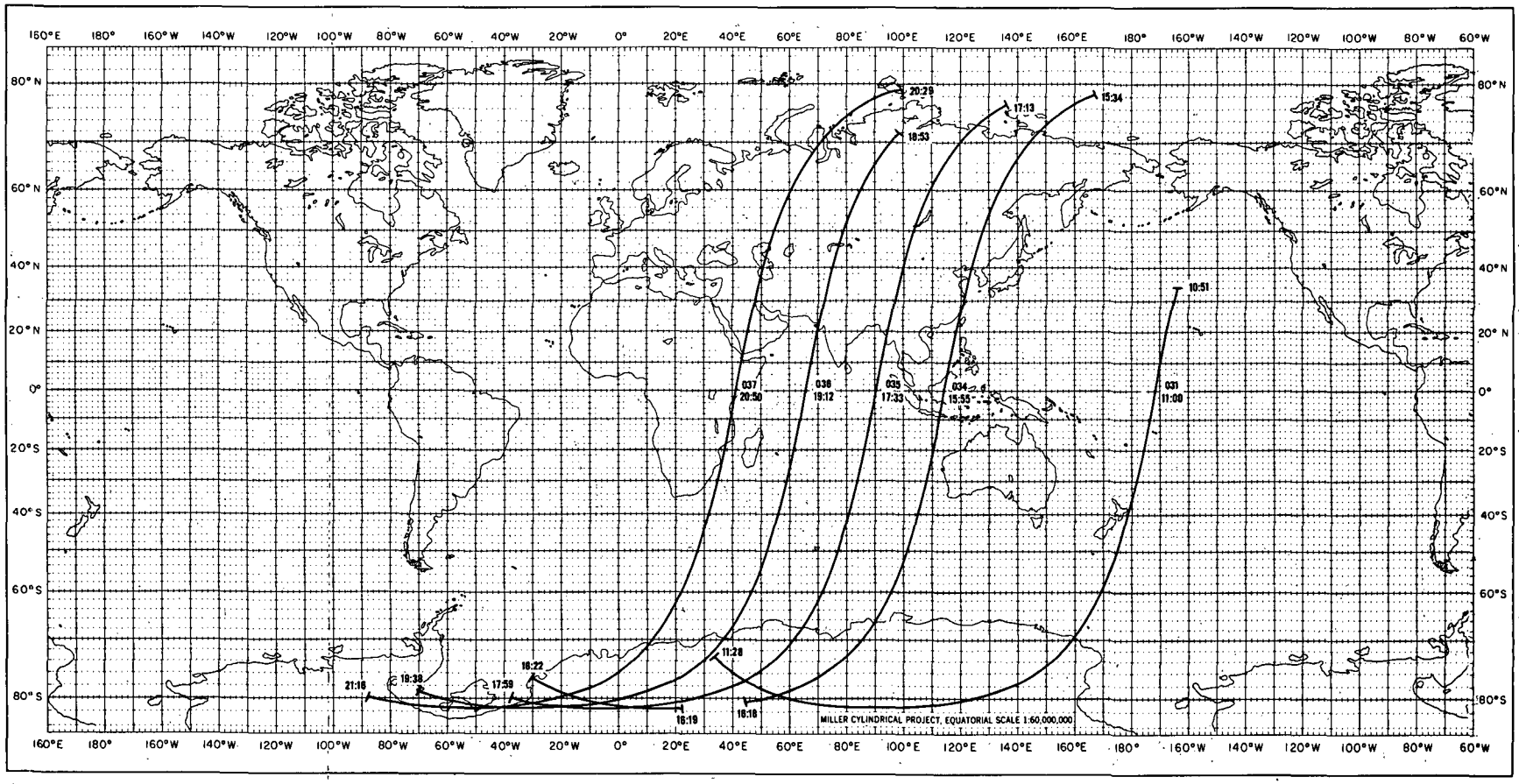

AUGUST 30, 1964

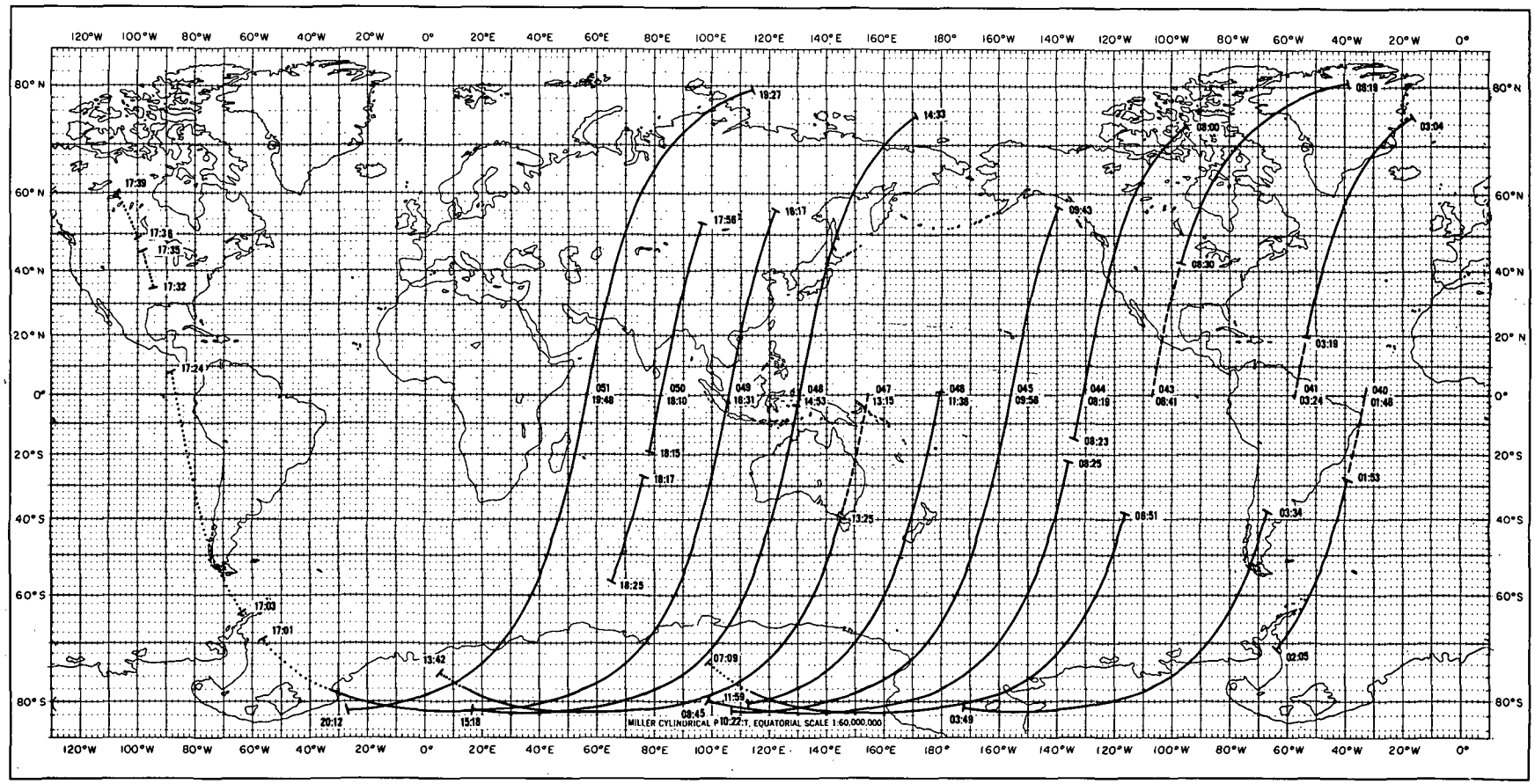

AUGUST 31, 1964

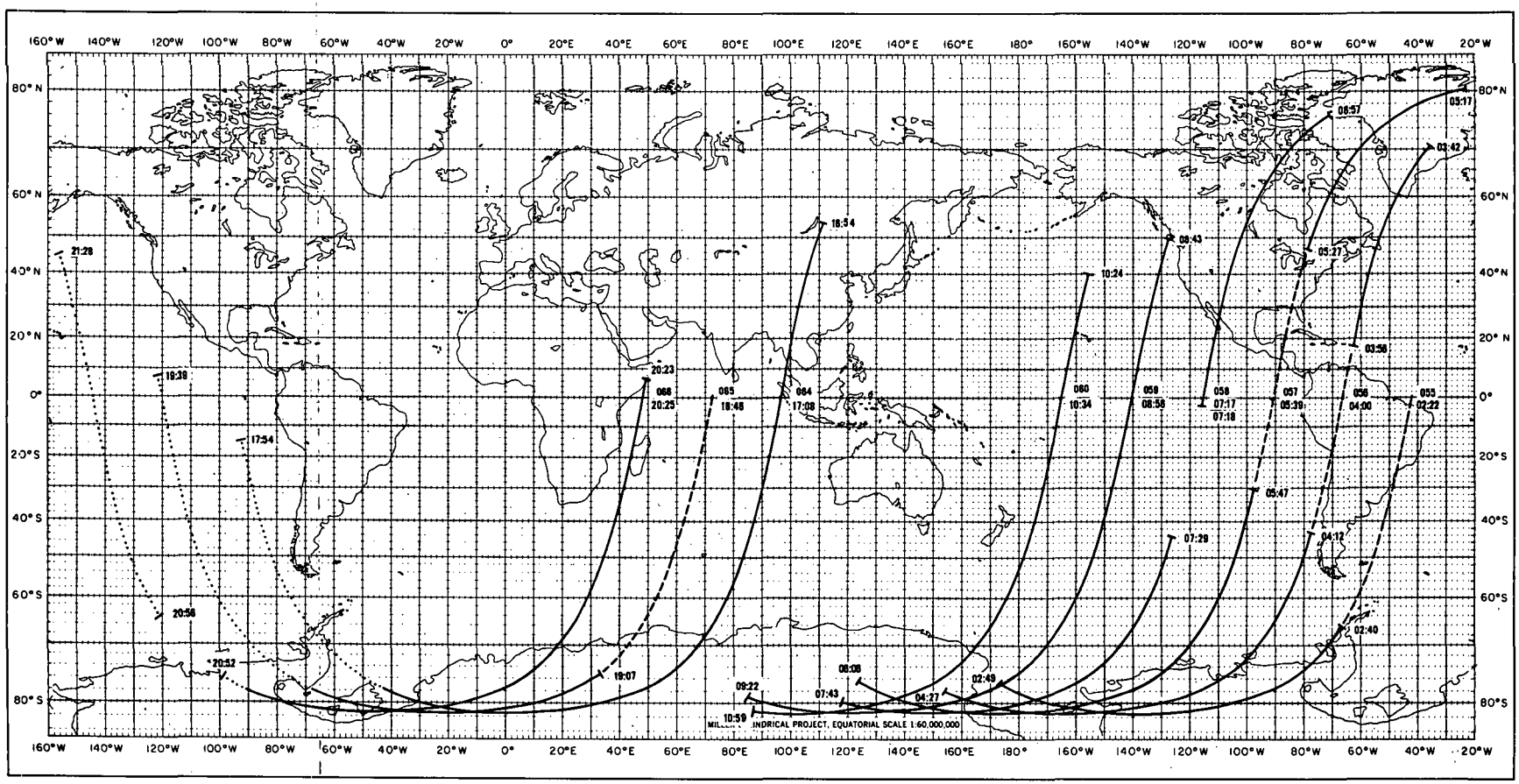

SEPTEMBER 1, 1964

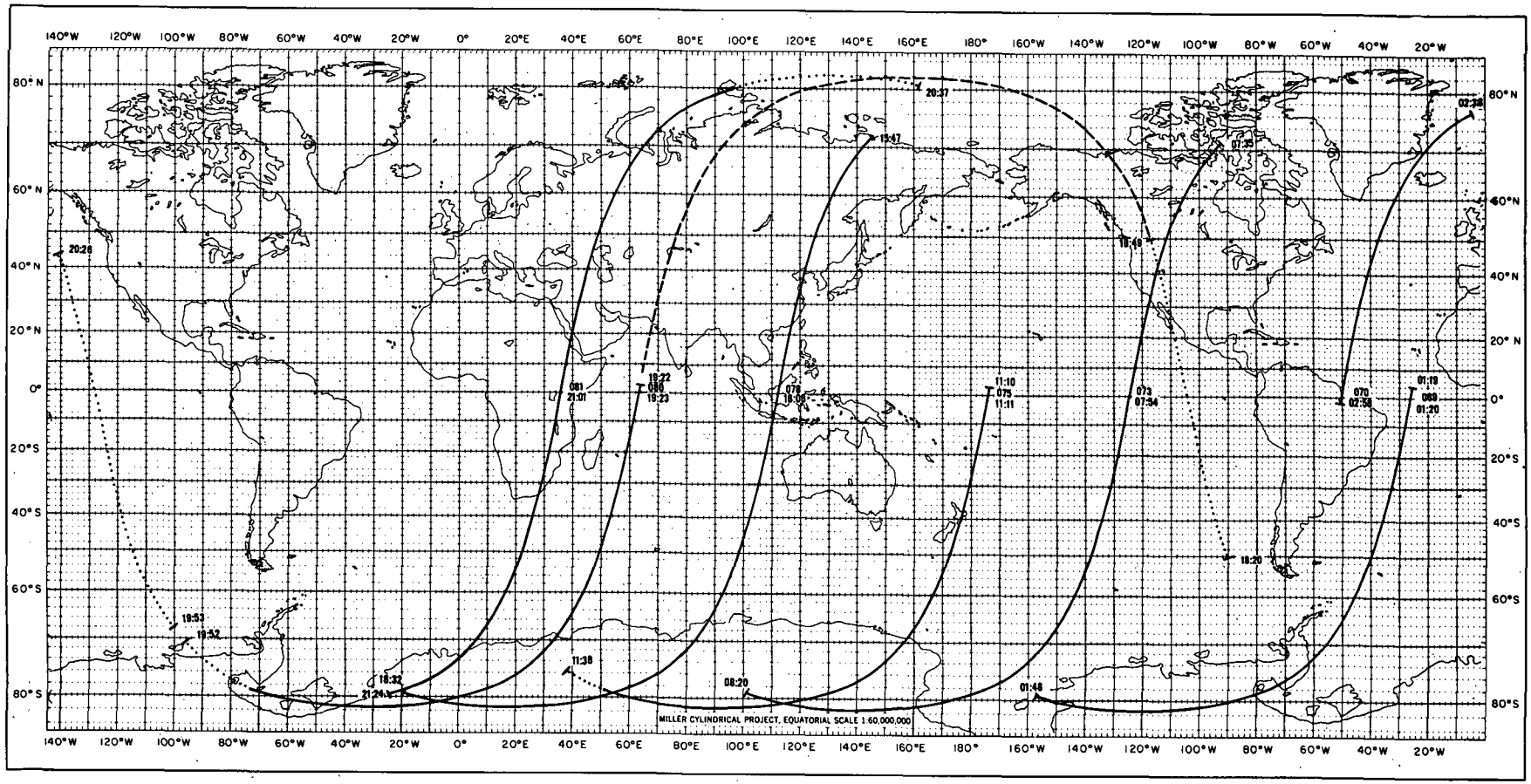

SEPTEMBER 2, 1964

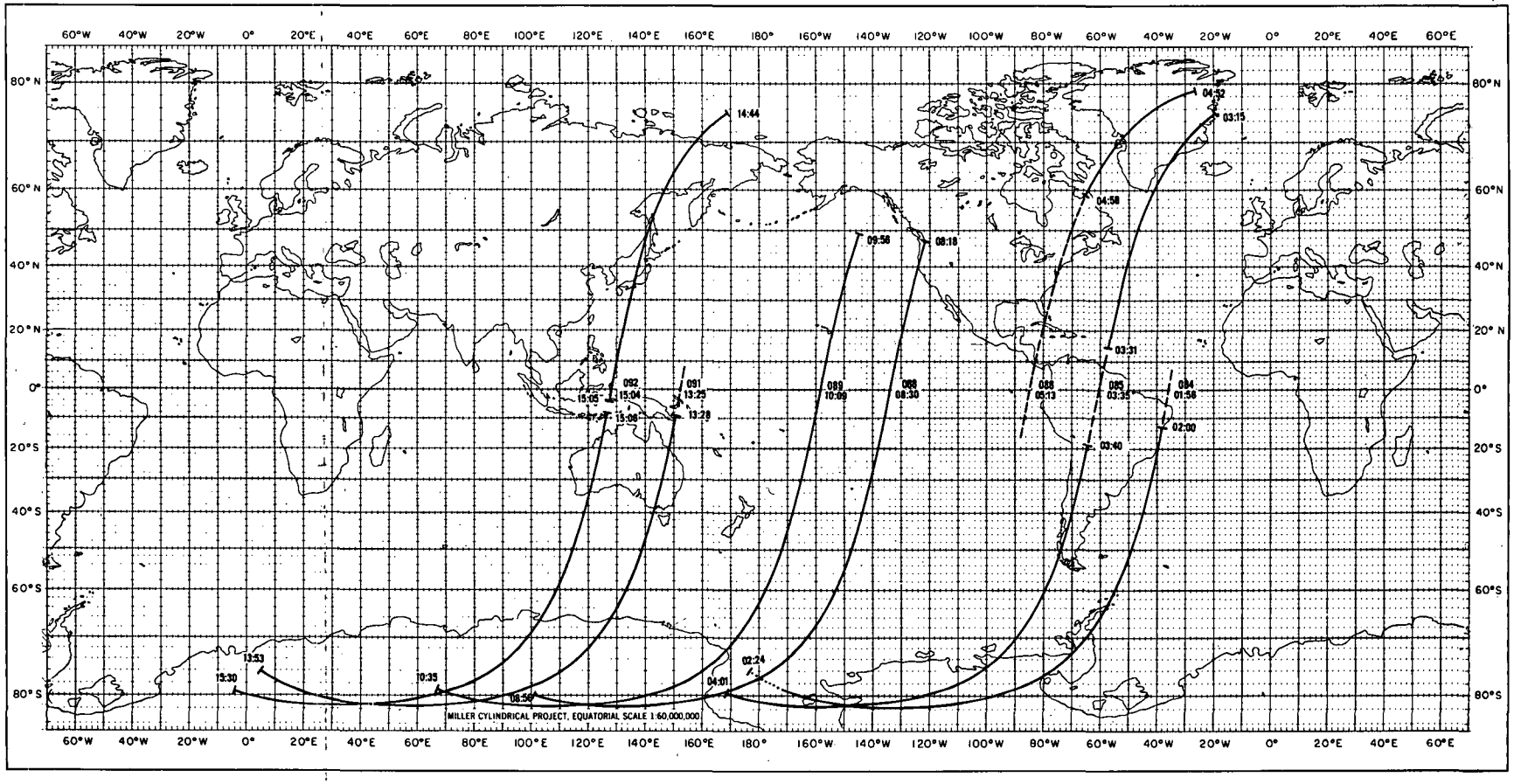

SEPTEMBER 3, 1964

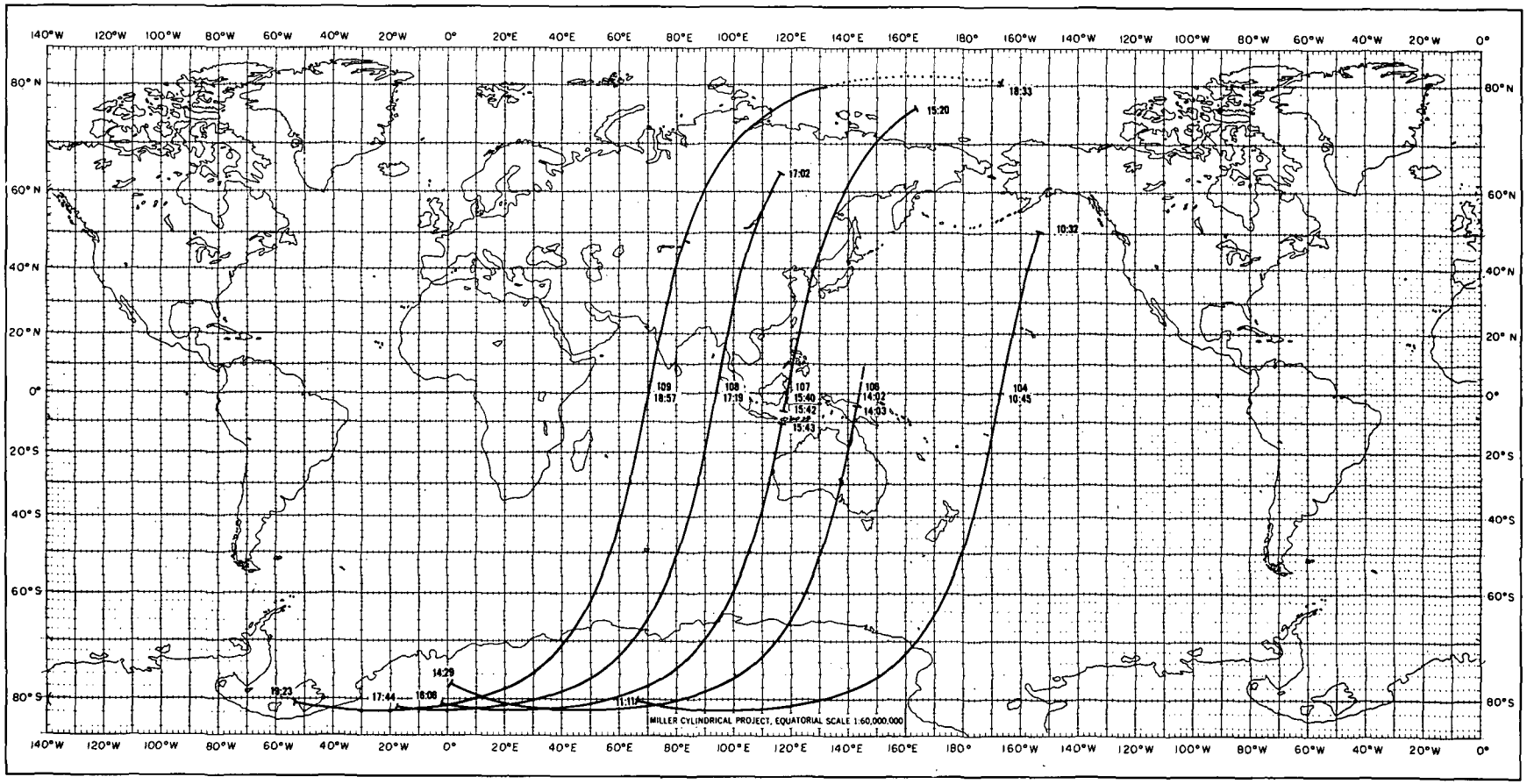

SEPTEMBER 4, 1964

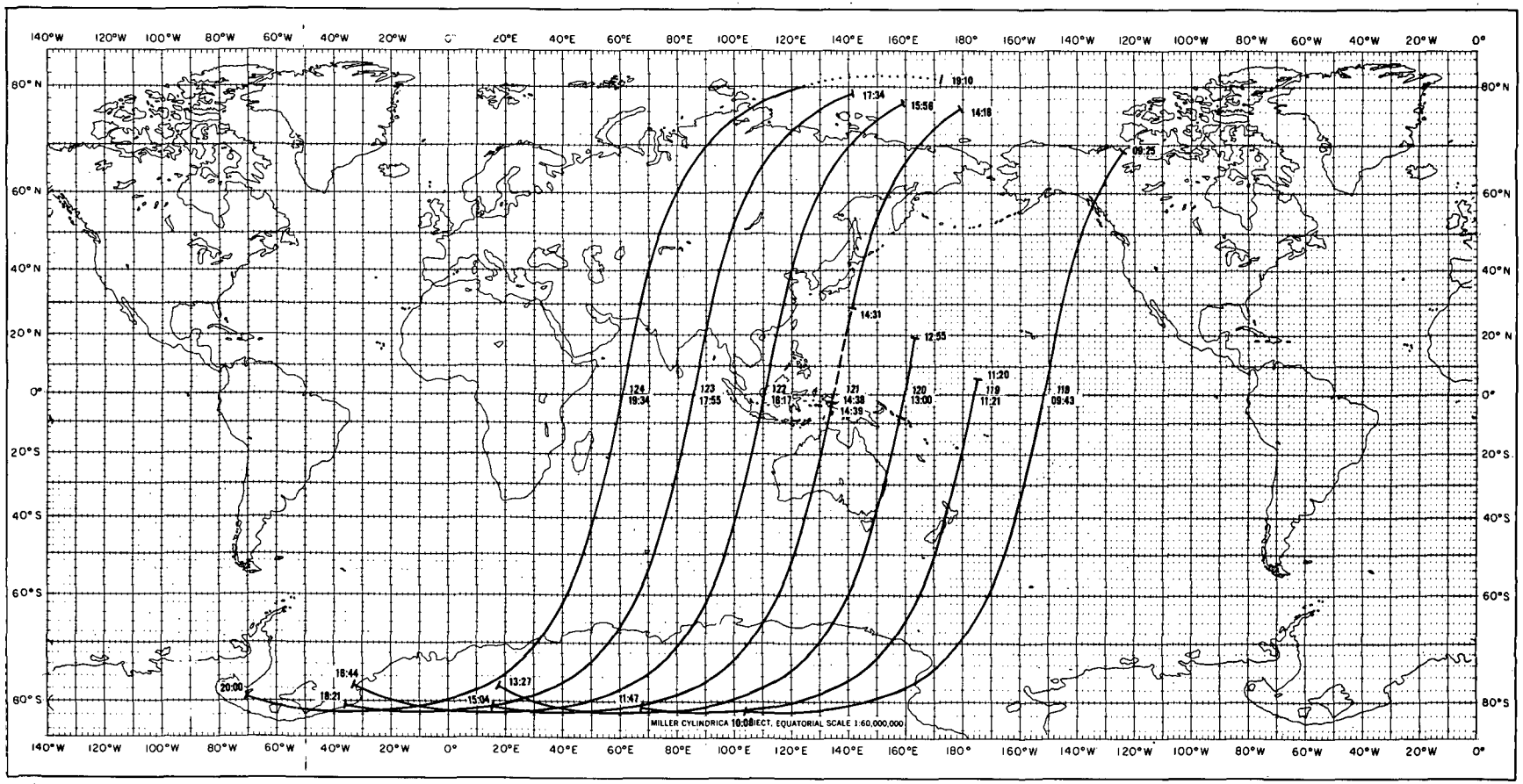

SEPTEMBER 5, 1964

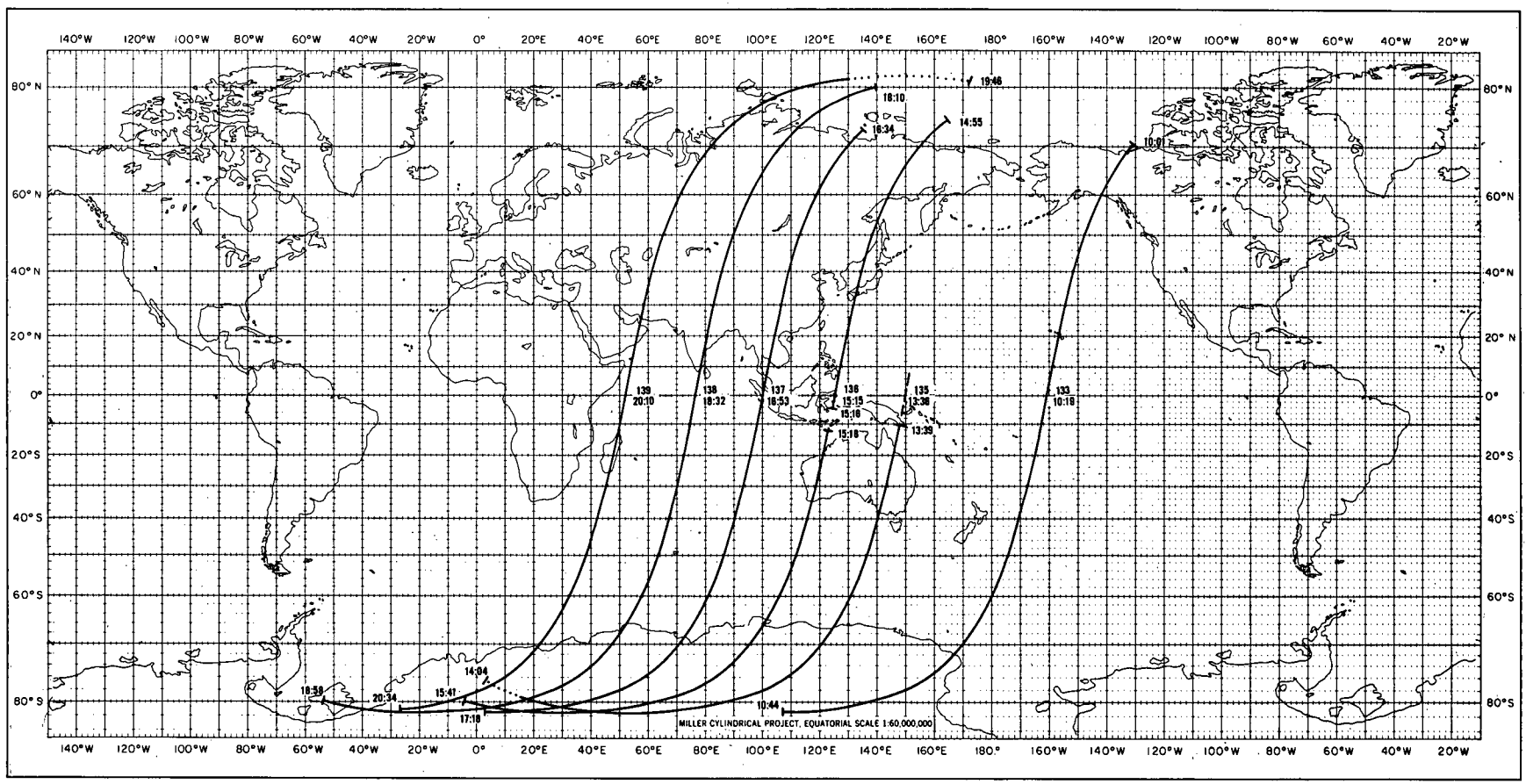

SEPTEMBER 6, 1964

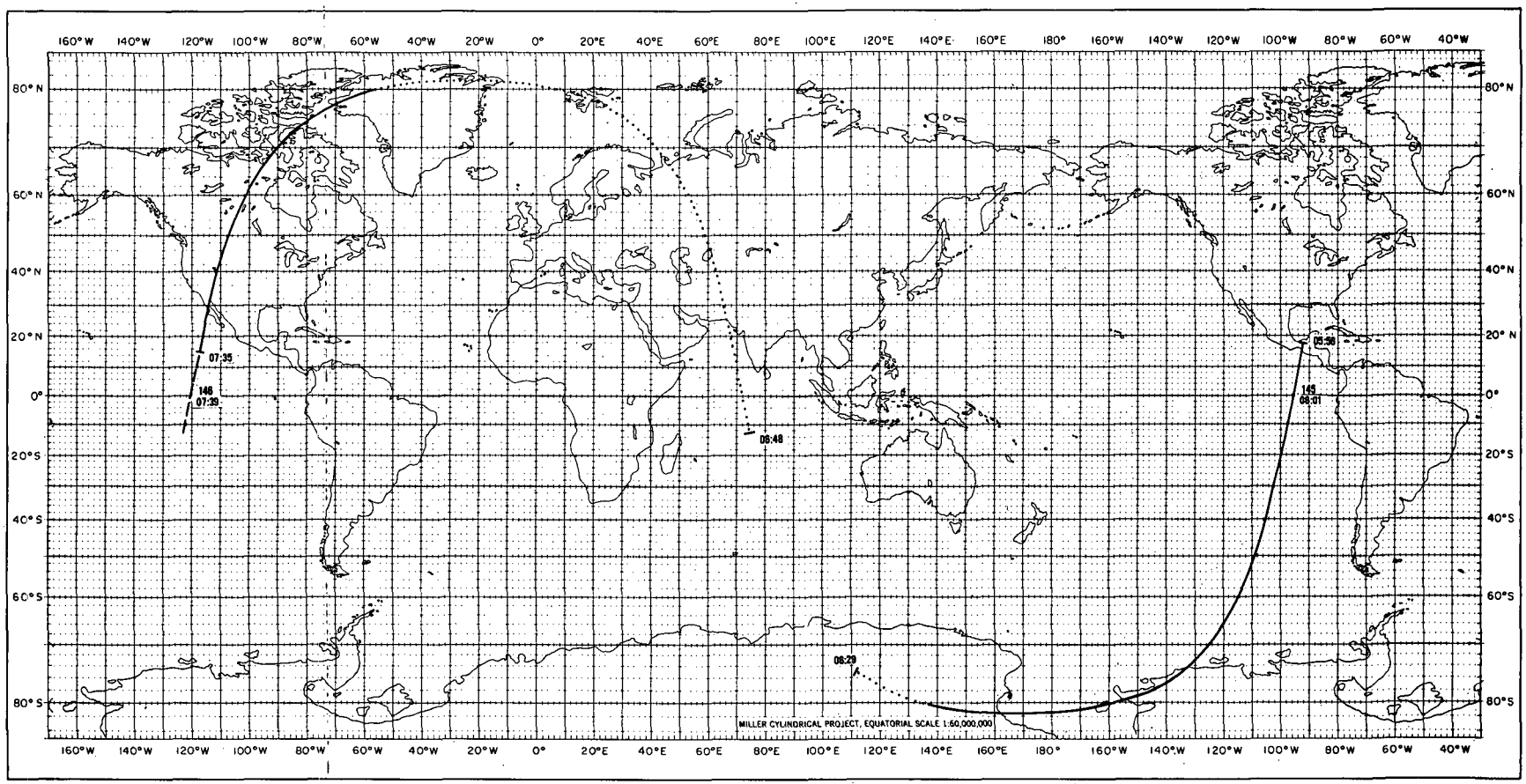

SEPTEMBER 7, 1964

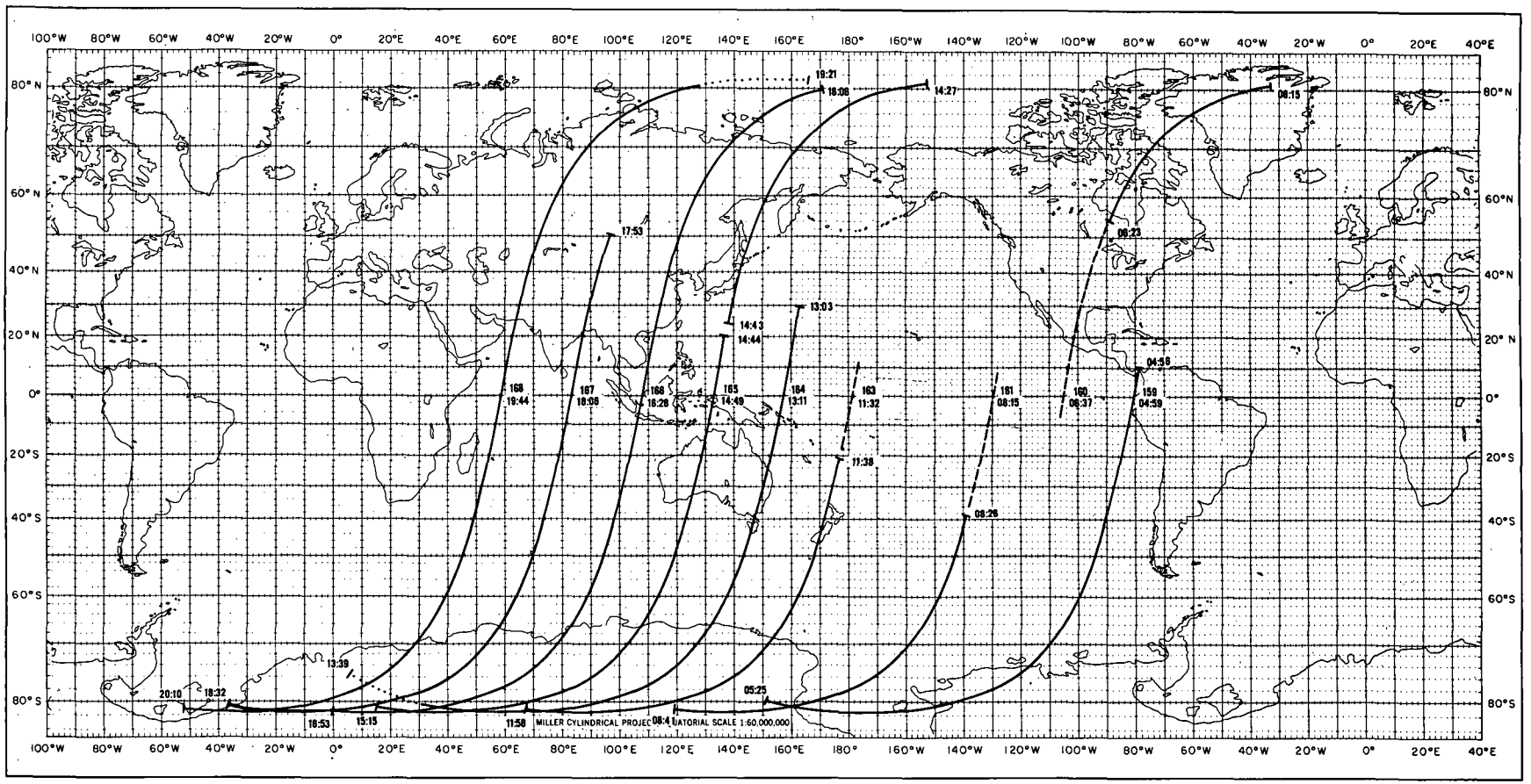

SEPTEMBER 8, 1964

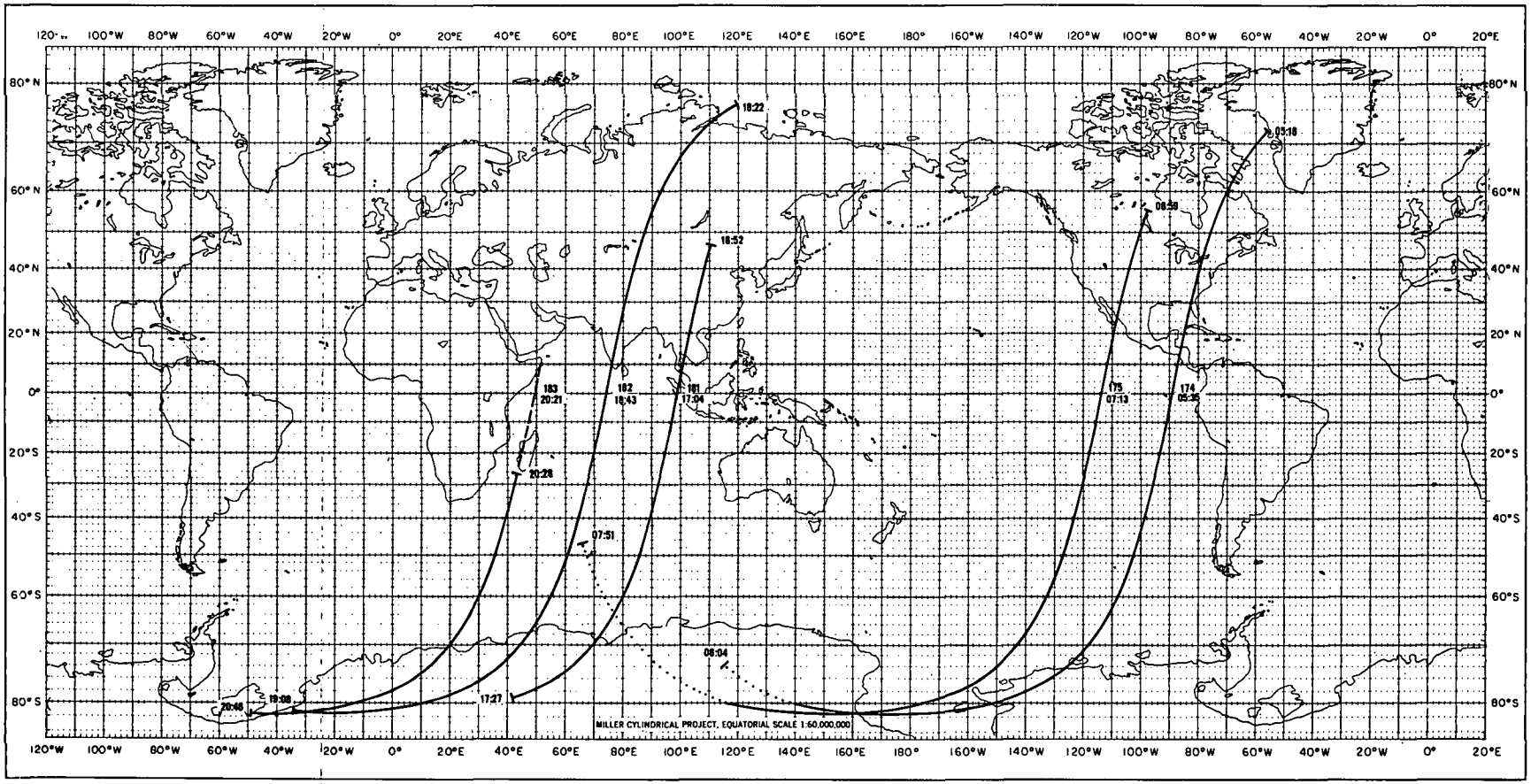

SEPTEMBER 9, 1964

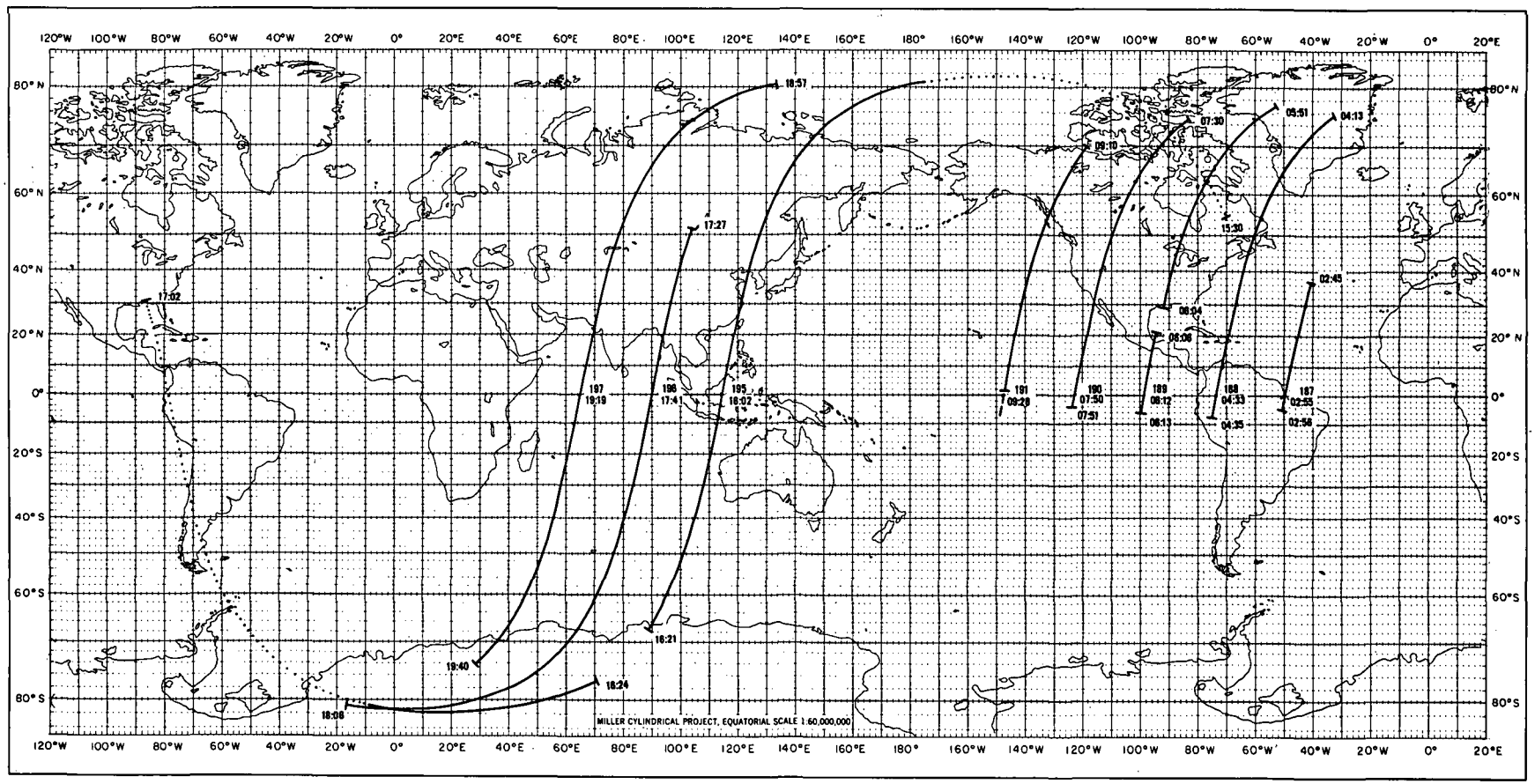

SEPTEMBER 10, 1964

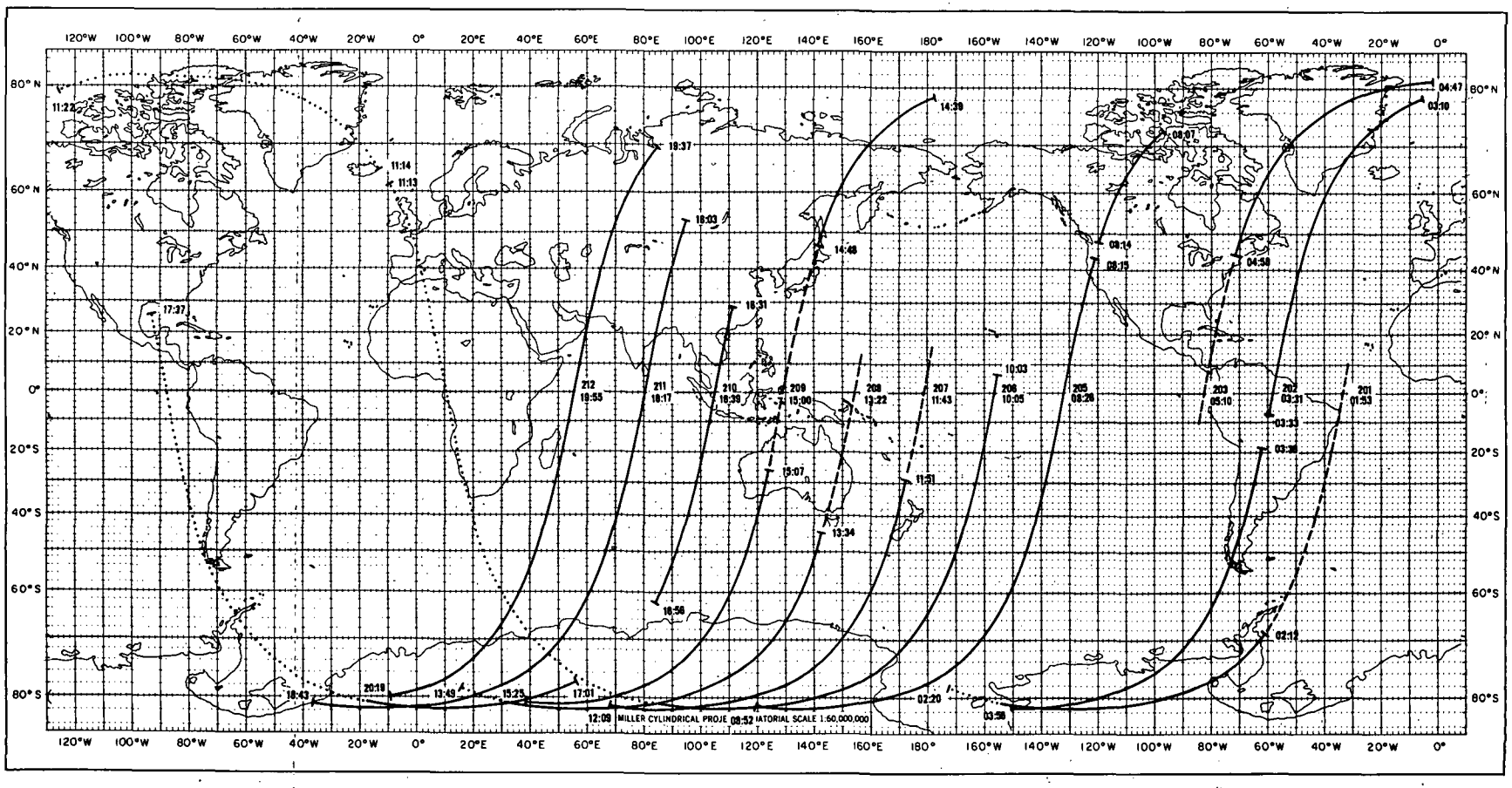

SEPTEMBER 11, 1964

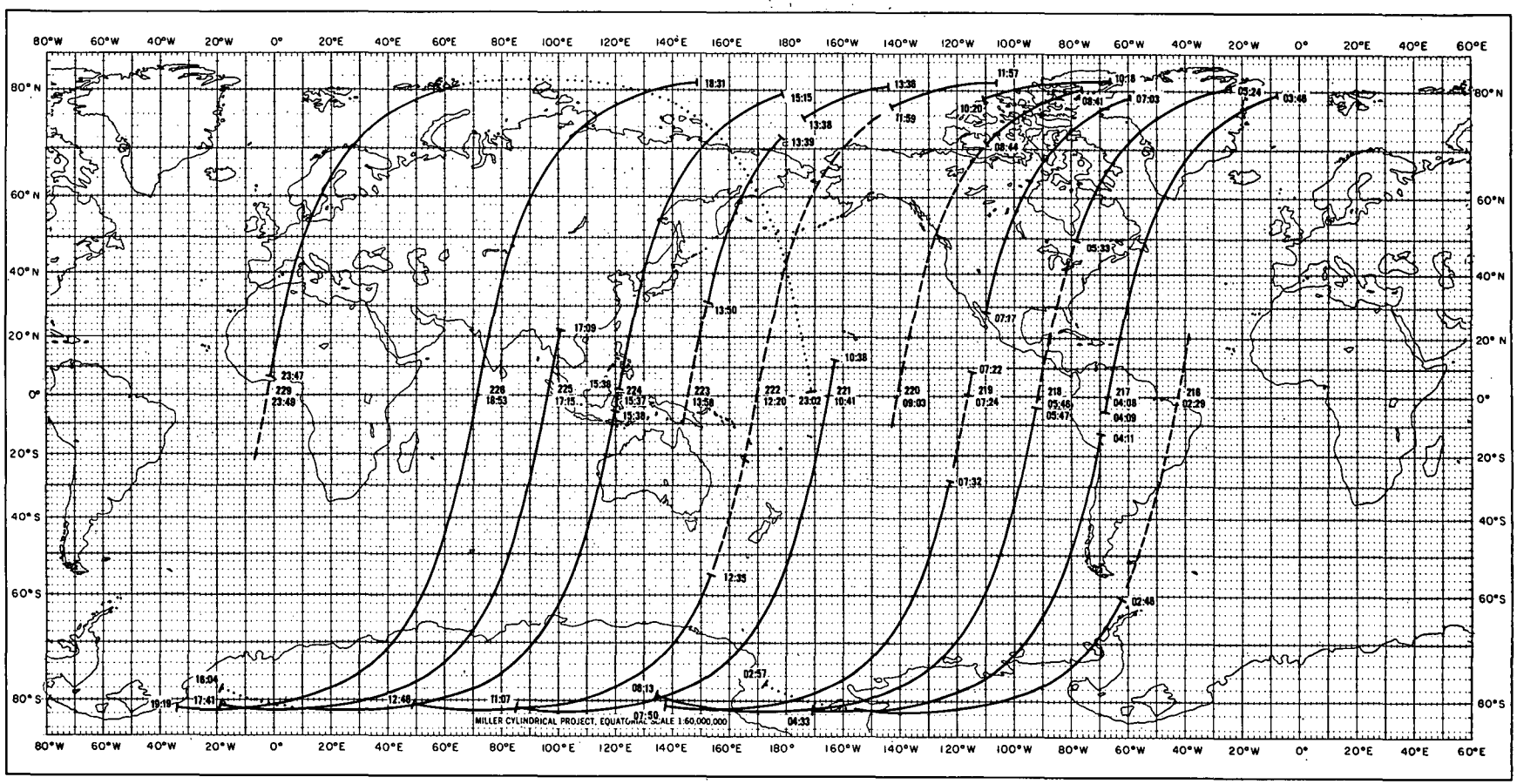

SEPTEMBER 12, 1964

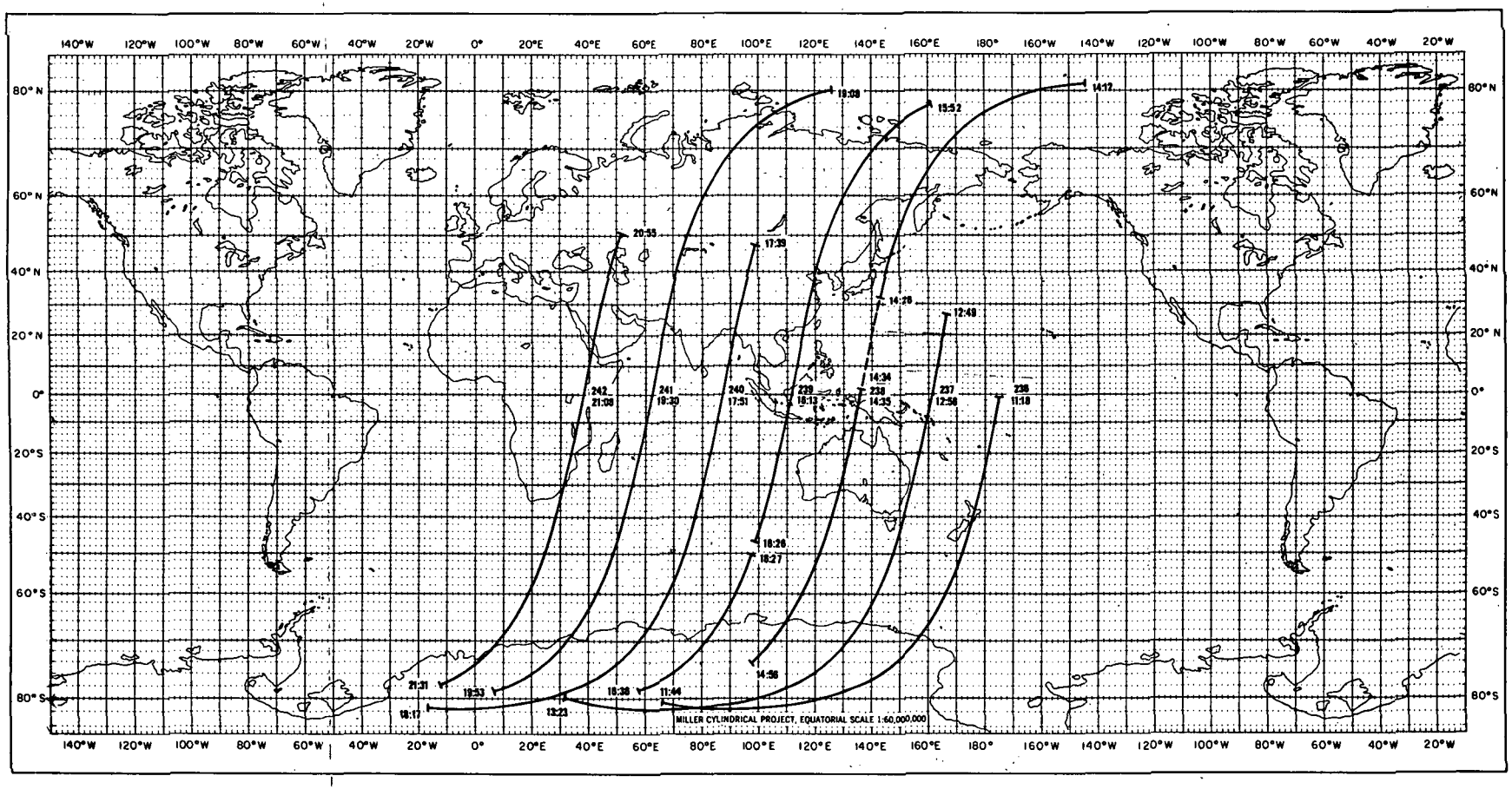

SEPTEMBER 13, 1964

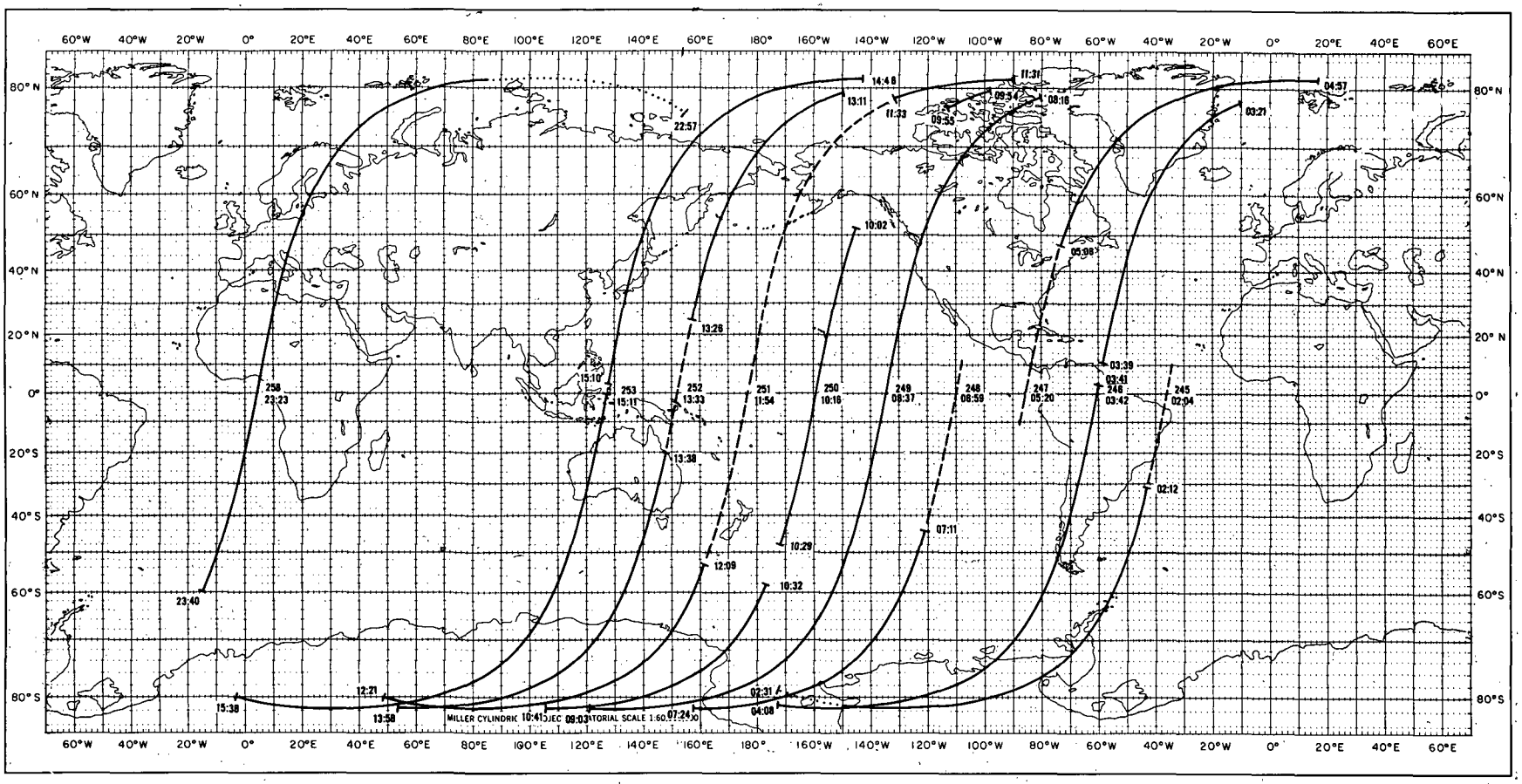

SEPTEMBER 14, 1964

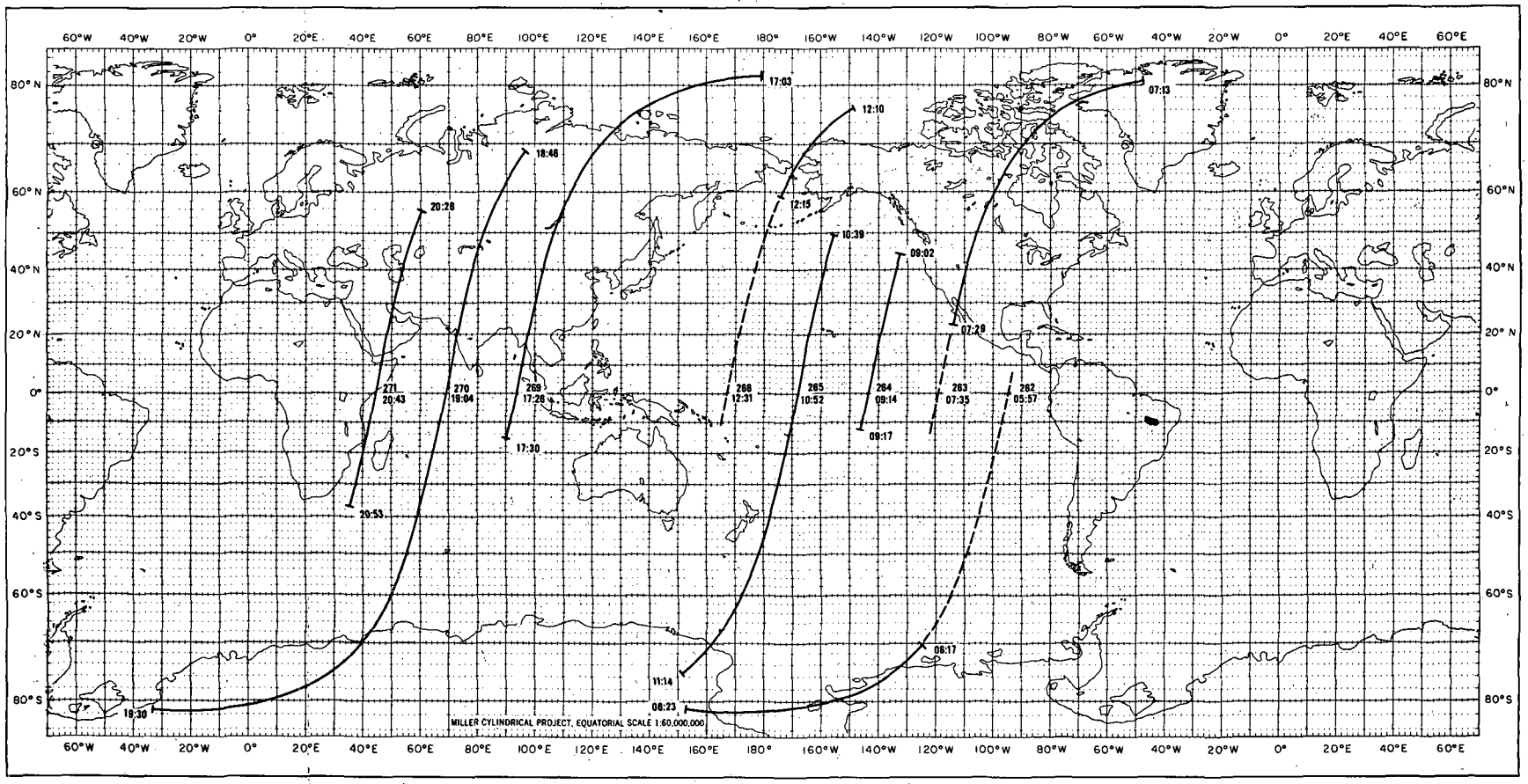

SEPTEMBER 15, 1964

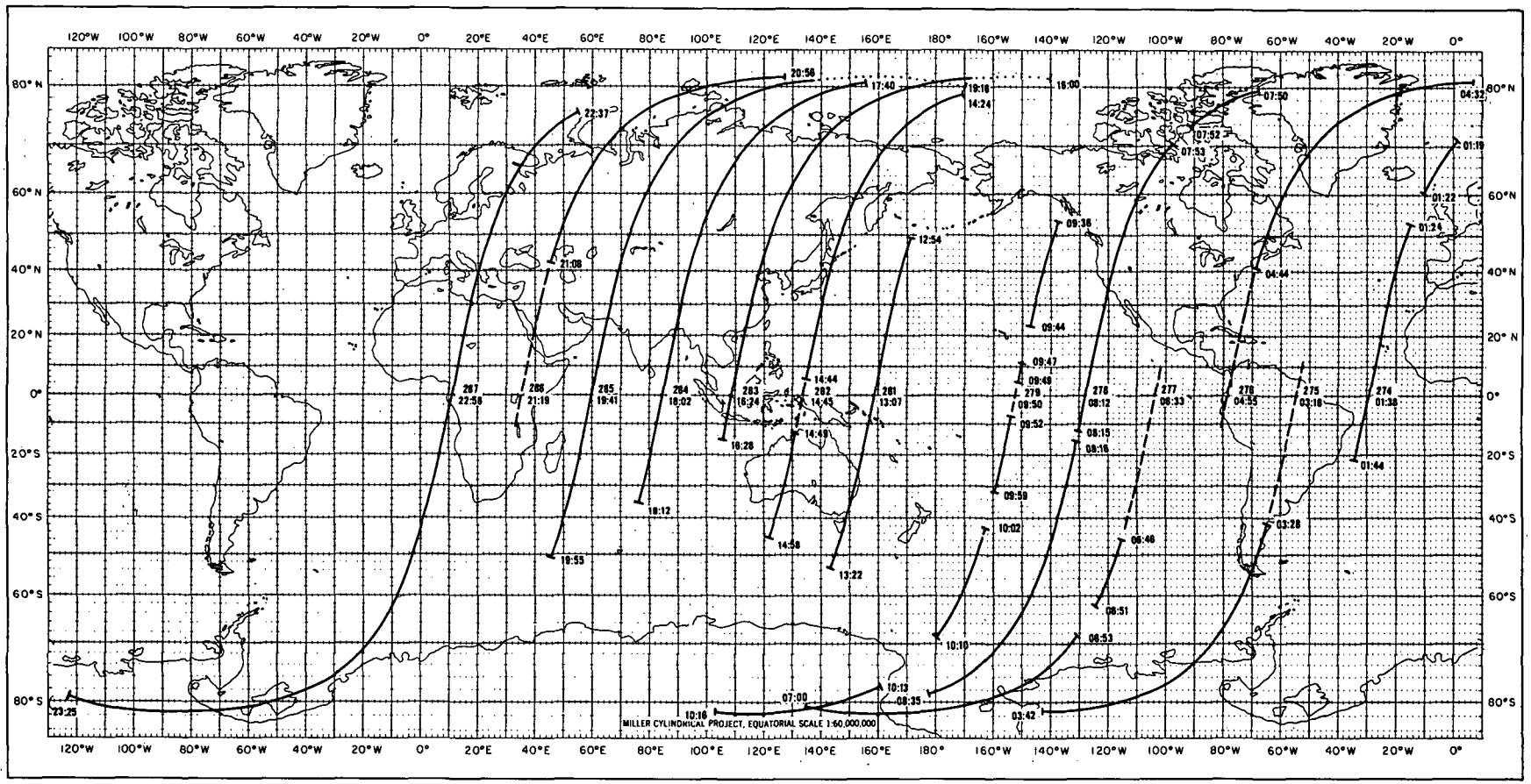

SEPTEMBER 16, 1964

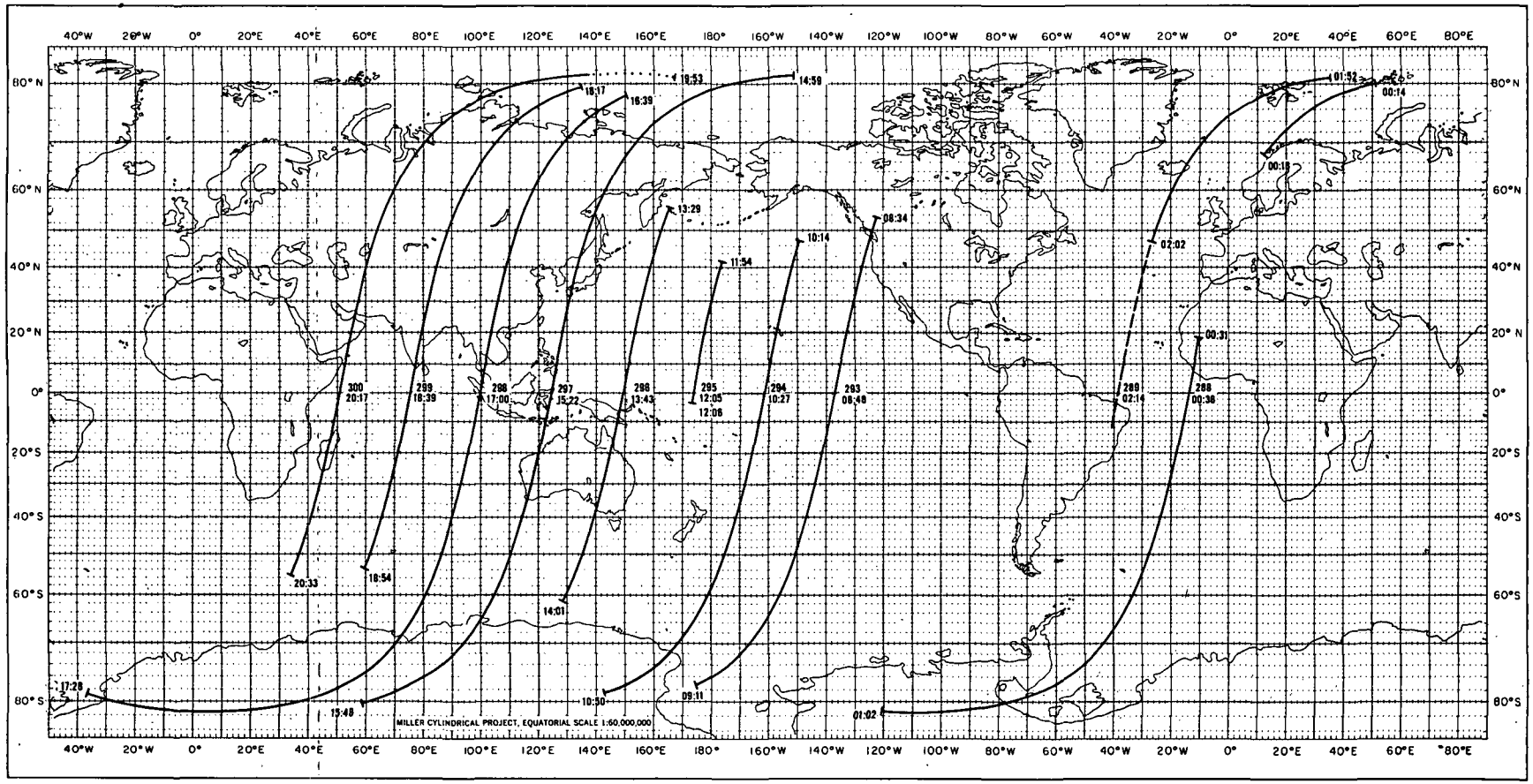

SEPTEMBER 17, 1964

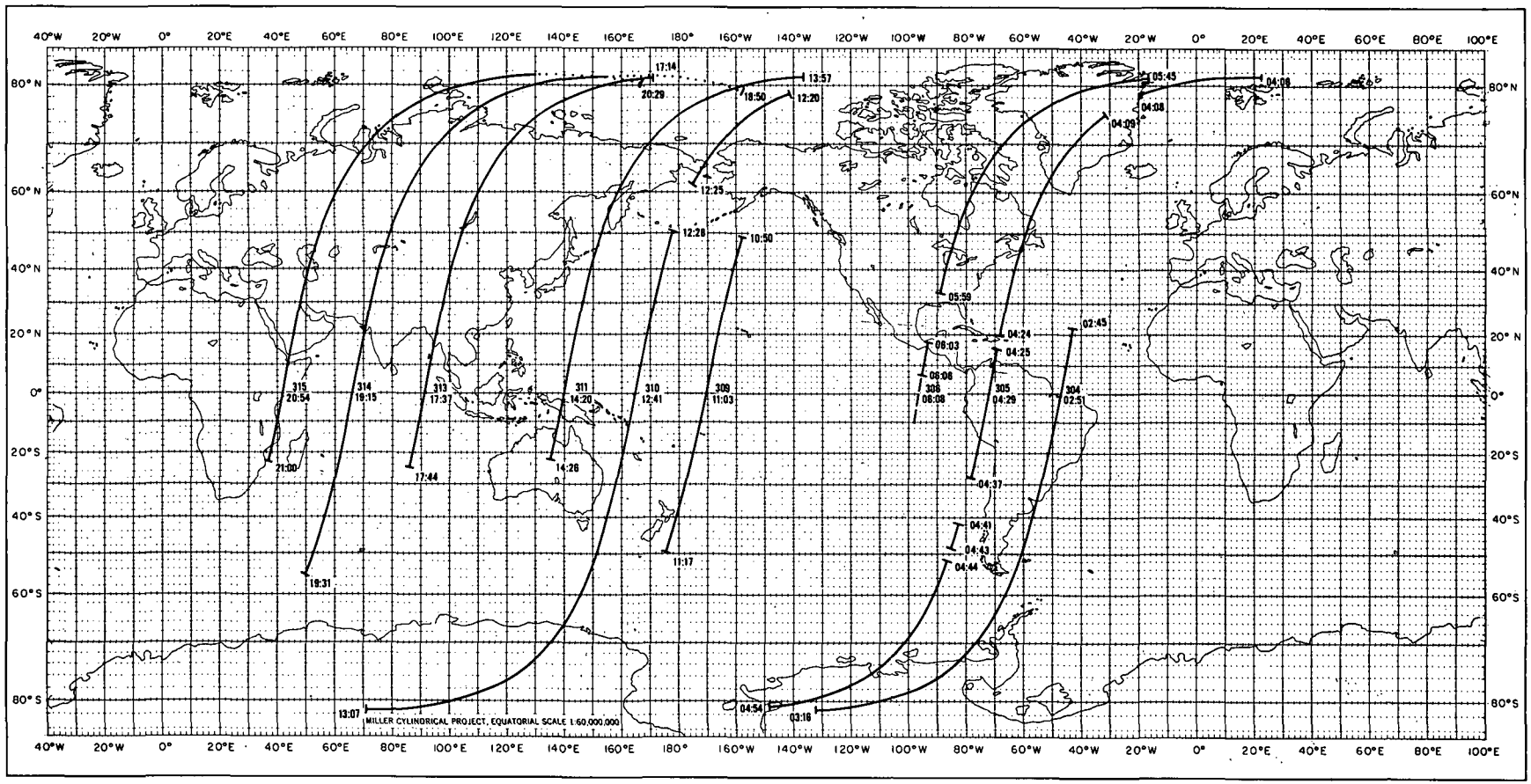

SEPTEMBER 18, 1964

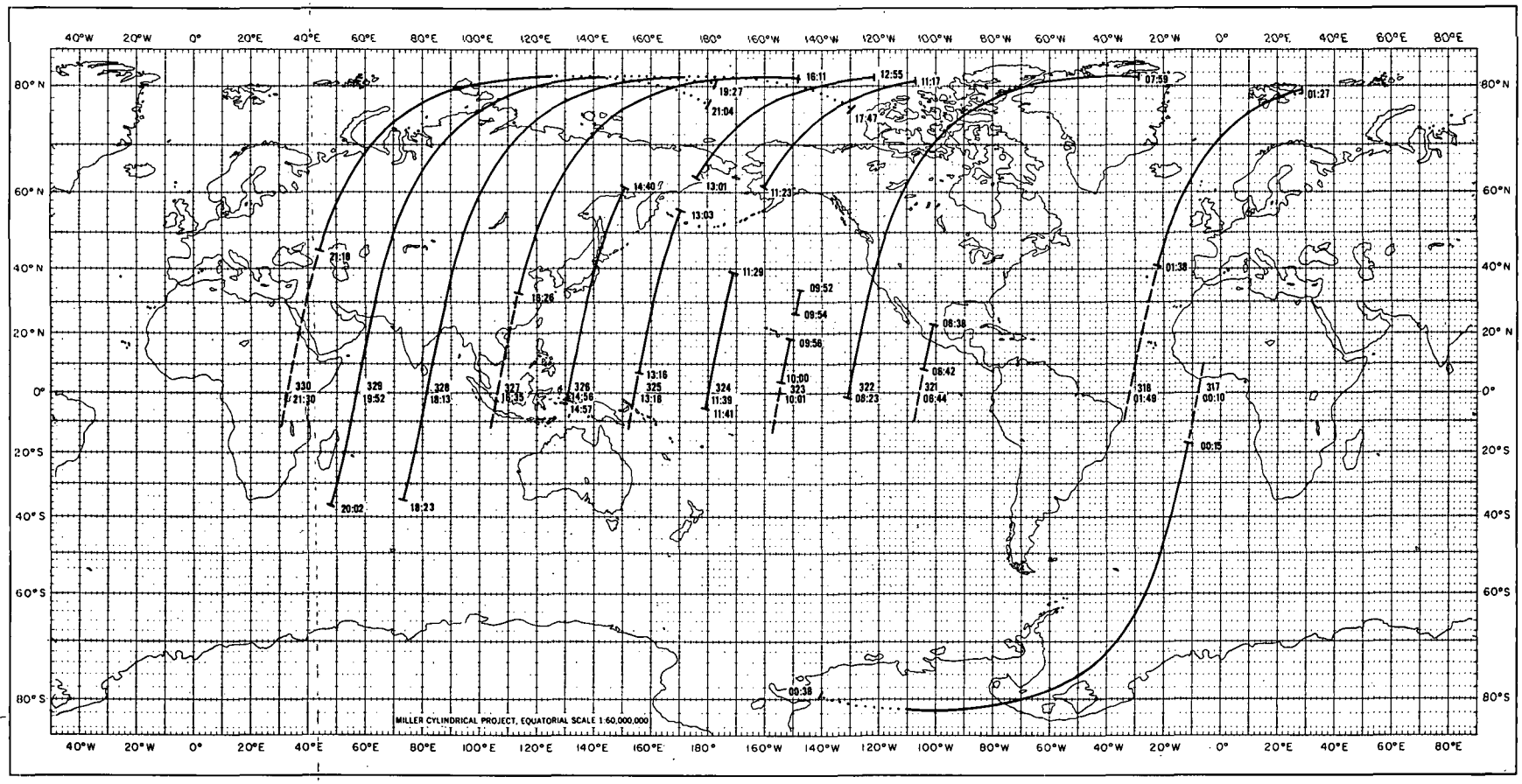

SEPTEMBER 19, 1964

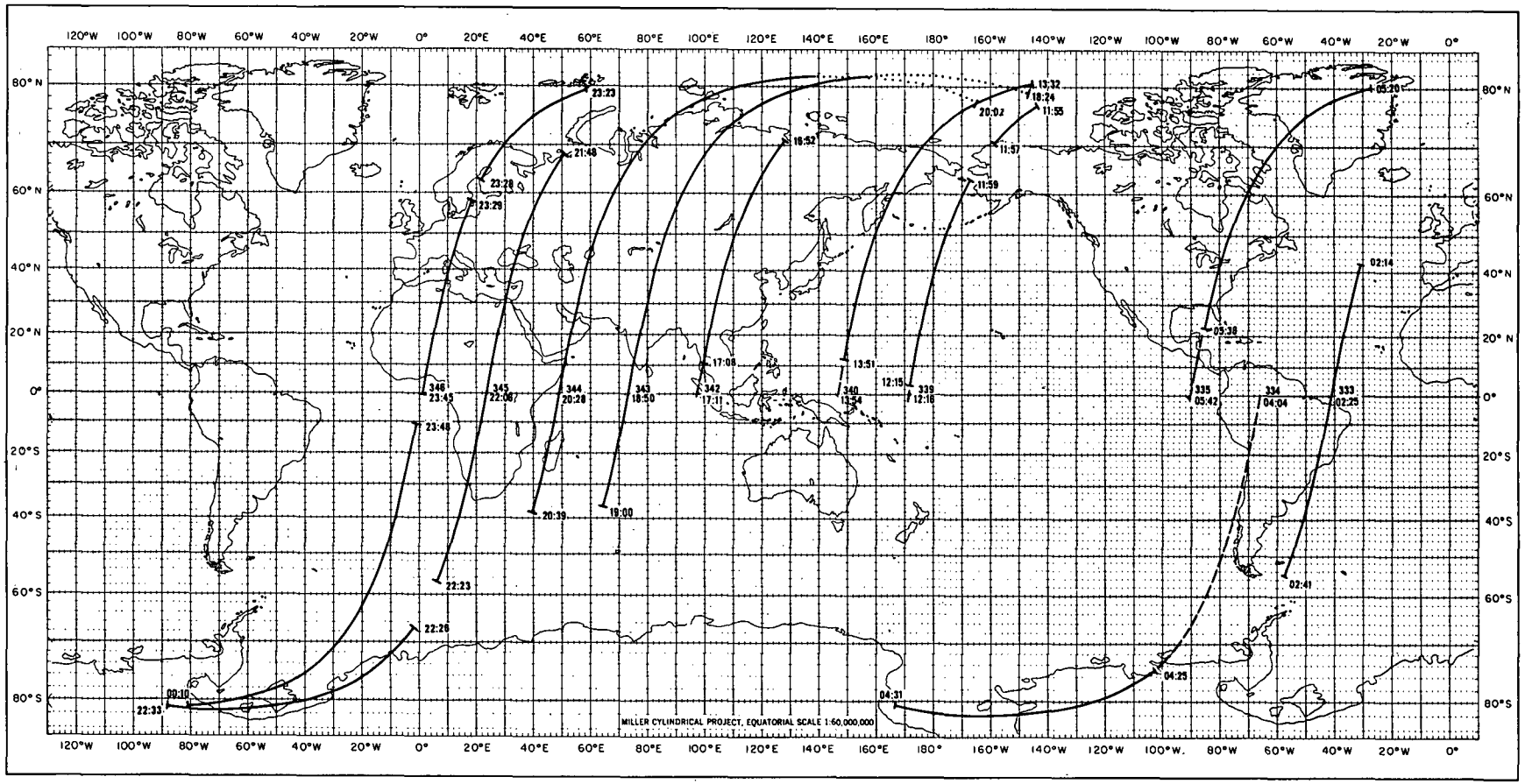

SEPTEMBER 20, 1964

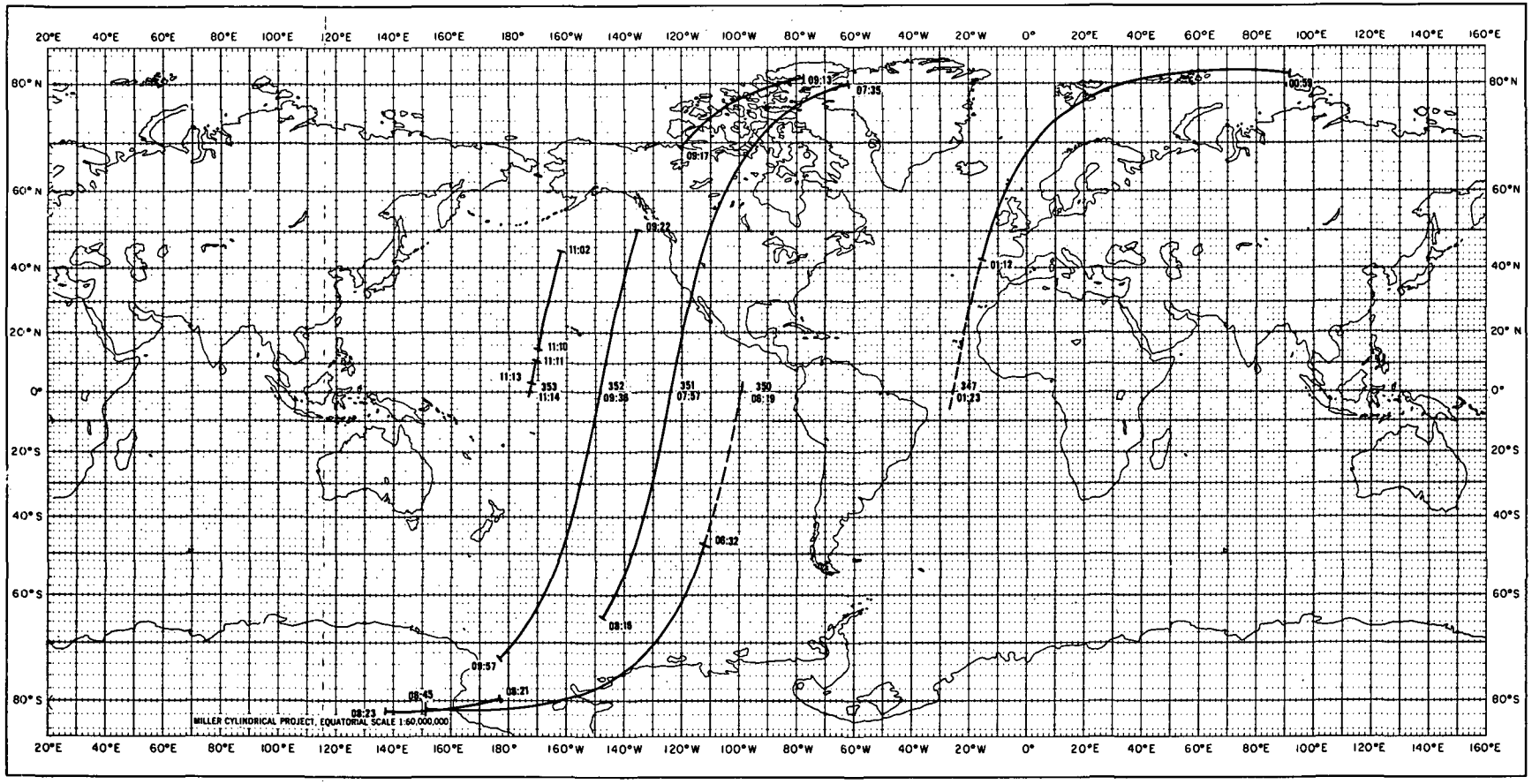

SEPTEMBER 21, 1964

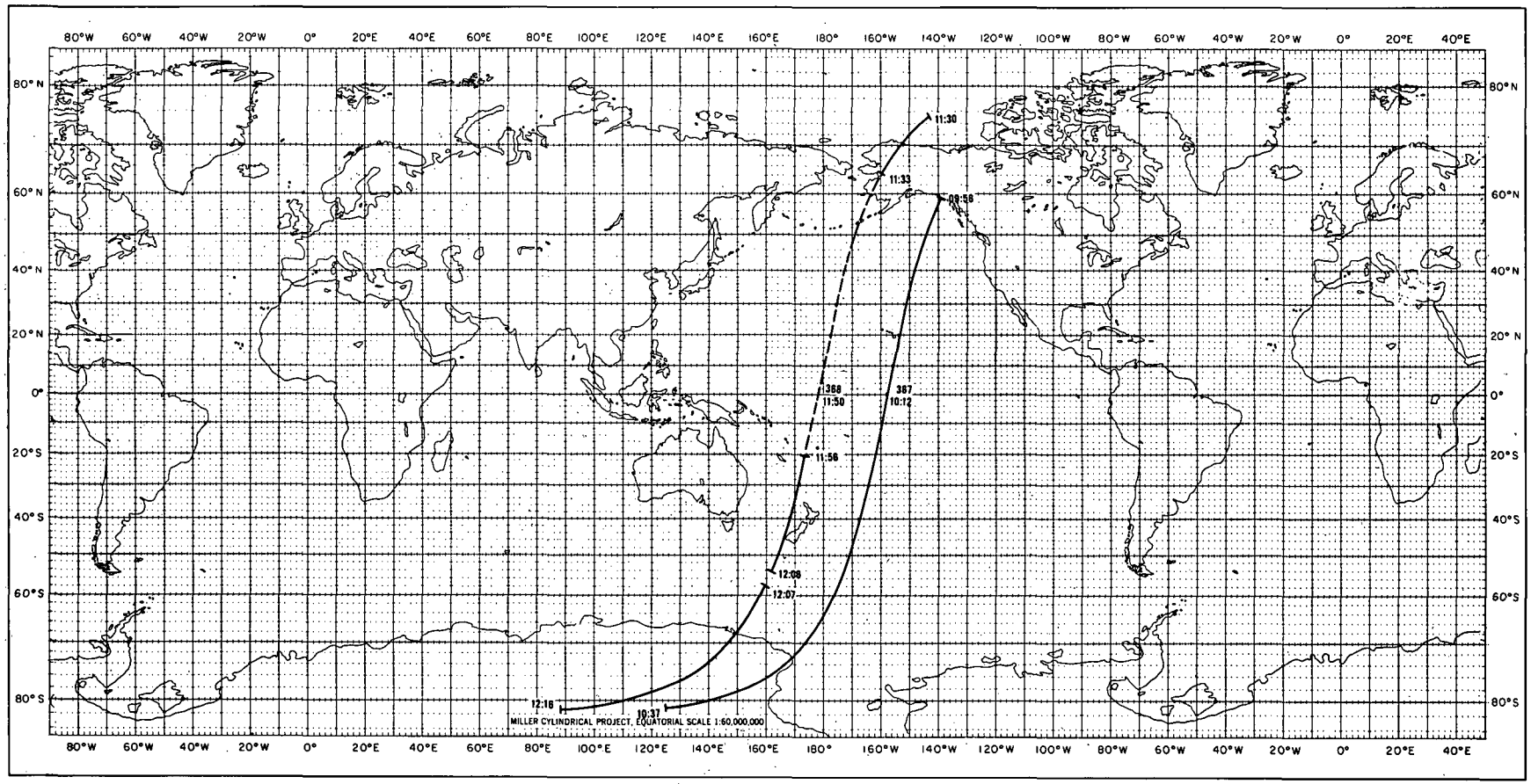

SEPTEMBER 22, 1964

APPENDIX C

CONTACT PRINTS OF AVAILABLE PHOTOFACSIMILE FILM STRIPS

All of the Nimbus I HRIR data on photofacsimile film strips are presented in this Appendix in the form of positive prints. The production of these films is described in Section IV and will not be repeated here. However, an explanation of the content and annotation on the film will be given, followed by a discussion of the content of the prints reproduced in this Appendix.

Each block of data on a film strip is provided with an index display which identifies the data. The index display contains three pieces of information: the readout orbit number, the approximate beginning (for forward mode) or ending (for reverse mode) time, and the playback mode. Figure C1(a) shows a block of "forward mode" data, i.e., data read out with the tape recorder traveling in the same direction as it traveled while the data were being recorded. The orbit number 301 refers to the number of the orbit at the time the data were read out from the satellite. The time is the first time code associated with the data "read" from the magnetic tape and is the time of a satellite clock when recording of the data began in the satellite. The time given in the index display is 17:12:26 UT on the 261st day of the year or September 17, 1964. The letters "FWD" indicate the "forward" playback mode.

A series of time marks in increments of two minutes is found on the right side of the film. These marks represent even minutes of time. The first time mark is the first even minute after the index display time; i.e., 17:14 UT, the second is 17:16, etc., and the last time mark is 17:26. The data do not begin at the time given in the index display, but begin from 40 to 120 seconds later. The time marks are used to determine the beginning time of the data. In producing the film the index display is first presented; then, the film is advanced rapidly about 0.5 of an inch. It remains in this position normally for approximately six seconds during which time the photofacsimile recorder is phased so that the correct video is presented on the film, i.e., the 138.24° of mirror rotation is centered around the subsatellite point. Normally from 40 to 64 seconds of the data are lost during this phasing period, and the data on the film begin an equivalent length of time after the index time. There are cases in which the phasing time is as long as 120 seconds. If the first even minute, after the index display time occurs during the phasing period, the first time mark can be positioned erroneously. When this happens, the spacing between the first and second time marks is different from subsequent spacings. However, by working backwards from the second time mark, the correct time for the beginning of the data and the time for data prior to the second mark can be found. In this case the data begin at 17:13:42 and end at 17:27:20. The beginning time of the data is 76 seconds later than the index display time. The time identifies the data to have been recorded during orbit 298, although they were read out during orbit 301.

The data are correctly oriented when the film is viewed from the opposite side (i.e., shiny side toward the viewer), keeping the index display at the top for forward

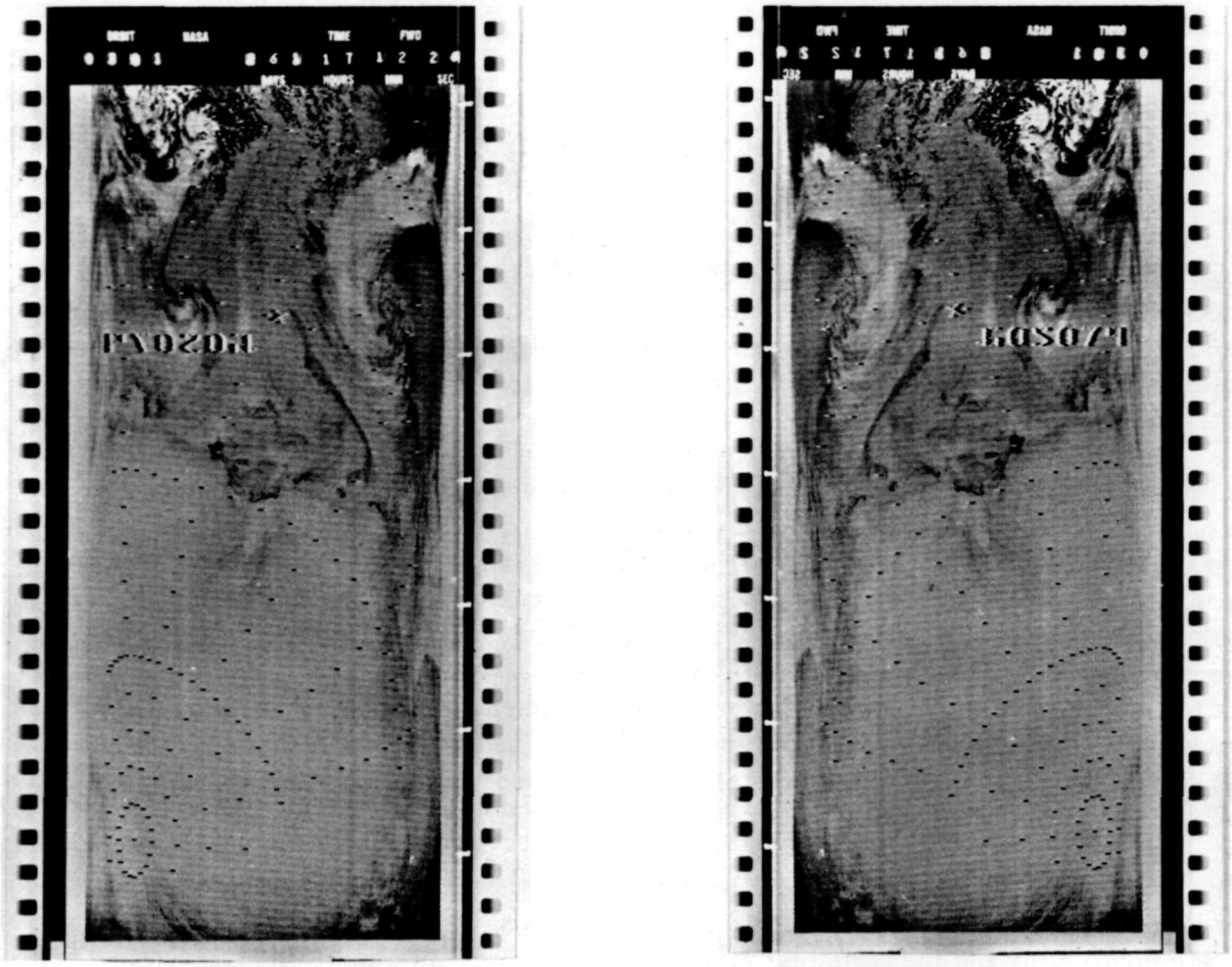

(a) (b)

Figure C1–A block of Forward mode data showing (a) the film strip positioned for reading the index display, and (b) the film strip with the nighttime data correctly oriented for viewing with north and east toward the top and right, respectively.

mode data as shown in Figure C1(b). From left to right across the film, the 138.24° of arc, centered at the subsatellite point, includes space, Earth, and space; plus, 2mm of the radiometer housing temperature measured by the radiometer. The width of the space portion of the scan increases with increasing height of the satellite since less of the 138.24° of arc is included in the Earth portion of the scan. This is seen in Figure C1(b); the space portion becomes wider from top to bottom of the strip.

A CDC 924 computer uses start times from the magnetic tapes along with orbital elements and spacecraft attitude information to compute latitude and longitude grid point coordinates. These grid points are electronically superpositioned on the film. The latitude grid points appear every 2° from pole to pole. The grid point array makes up lines for every 10° of latitude between 80°N and 80°S and every 2° between 80° and the poles. The longitude grid points are in increments of 2° between 60°N and 60°S and of 5° between 60° and the poles. The longitude lines appear for every 10° between 60°North and 60°South and every 20° from 60° to the poles. The grid points are superpositioned on

the film from 0° to 53.5° of scan nadir angle. The annotation for the grid is given 60° North and South, 30°North and South and the equator. The annotation applies at the small "x" near the center of the film. East longitude is given to the nearest degree from 0° to 360°. In figure C1(b) the only annotation which appears is at 60°S and 079°E and applies at the small "x" to the left and above the annotation.

The CDC 924 computer-produced latitude-longitude grids, which do not take into account satellite attitude errors have been verified for accuracy against landmarks, where possible, and/or against graphically obtained latitude-longitude points on a picture from a knowledge of the subsatellite track with time. Spot-check verifications of the grids (at least three per data block) were made up to ten degrees of arc from the subsatellite track. A note has been made in the Remarks column in the Index of Appendix A whenever either the latitude or longitude within 10° of the subsatellite track was in error by more that 120 nautical miles.

Figure C2(a) shows a block of "reverse mode" (REV) data, i.e., data read out with the tape recorder traveling in the opposite direction from the direction it traveled while recording the data. The index display at the top of the film shows that the data were read out during orbit 123. The first time code received by the photofacsimile recorder was Day 249 (September 5, 1964) at 16:43:44 UT. This time code is the <u>last</u> time code associated with the data. The time marks are found on the <u>left</u> side of the film when viewed from this position. The first time mark represents the first even minute <u>before</u> the index display time. In this case the first time mark is 16:42, the second is 16:40, etc., and the last is 16:30. Using the second time mark and extrapolating forward and backward in time, it is found that the data ended at 16:42:35 and began at 16:28:14. Thus, the difference between the end time and the index display time is 69 seconds. The time identifies the data to have been recorded during orbit 122. The data are properly oriented when the film is viewed from the opposite side (shiny side toward the viewer) with the index display at the <u>bottom</u> as shown in Figure C2(b). For properly oriented film, the time marks appear on the left for both forward and reverse mode data. From left to right across the film of reverse mode data, 2mm of housing temperature, space, Earth, and space are seen.

The grid-point array for reverse mode data is the same as that for forward mode data. In Figure C2(b) the annotation is given at 60°S and 089°E. This annotation applies at the small "x" to the right and above the annotation.

It should be emphasized that the information given in the index display and the time marks can be, and often are, in error. When an error occurs in the index display time or the time marks, the correct time can often be found by correlating the data showing land features and orbital information. In cases of data not showing land features, a knowledge of the beginning and end times of the recording of the data and length of the playback helps to correlate the data with time. Also helpful are the grids on the film which are established using the time codes associated with the data, but they can also be in error. All available diagnostic sources were consulted and cross-checked in establishing the beginning and ending times and other information listed for each data

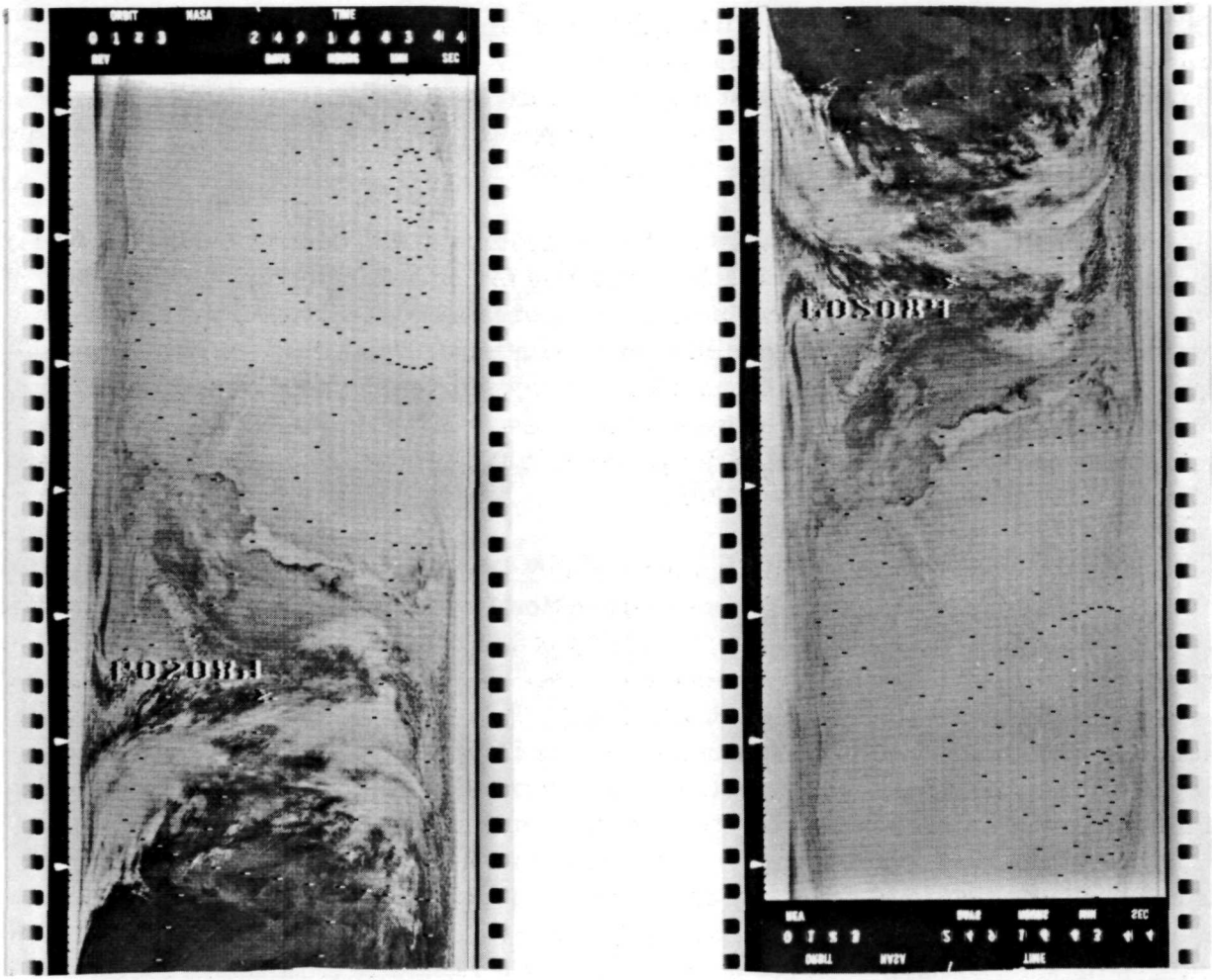

(a) (b)

Figure C2–A block of Reverse mode data showing (a) the film strip positioned for reading the index display, and (b) the film strip with the nighttime data correctly oriented for viewing with north and east toward the top and right, respectively.

block in Appendix A. Therefore, whenever there appears to be a discrepancy, the index display information should be considered to be in error, and the Appendix A information should be considered to be correct.

Concurrently with the preparation of this Manual, the HRIR data are being processed to eliminate duplication and noisy areas. The end result of this processing will be a reconstituted and condensed library of magnetic tapes and film strips to serve as the final archive of the data. This additional processing may result in minor variations in the archival products compared to the documentation shown in Appendices A, B, and C (e.g., beginning or ending times may be altered by a few seconds or two separate blocks shown in this Manual may occasionally be combined into one archival data block or vice versa). However, a user can readily apply the documentation information of Appendix A to any data which he may request simply by comparing like features of the data with the contact prints shown in Appendix C to determine whether any such minor variations exist.

The photofacsimile recorder is provided with the means for automatically producing a ten-step calibration gray scale wedge. Progressive voltage levels, from a manually adjusted ten-step potentiometer network, are sequentially selected by a ten-step motor driven cam operated by a timed program selector switch and are recorded on the film. The ten voltage levels correspond to the ten equivalent blackbody temperatures shown in Figure C3. The gray scale wedge shown in Figure C3 is for illustrative purposes only, and no attempt should be made to calibrate the positive prints of Appendix C by means of this gray scale. As mentioned in Section 1.2, the data shown in Appendix C were enhanced by an automatic dodging technique. This process, plus variations in photographic reproduction and printing, make it impossible to calibrate absolutely the data in Appendix C with a gray scale wedge. However, unless otherwise specified, a uniform-density exposure will be employed in producing copies requested by a user, and a calibration gray scale wedge will be included with each data orbit to permit the interpretation of the data in terms of absolute equivalent blackbody temperature values.

All of the Nimbus I HRIR gridded data, on positive prints of 70mm film strips constituting 323 separate blocks of data from 194 individual orbits, are presented in this Appendix. The positive prints are shown at actual size, although the 14mm of the film provided for the sprocket holes on both edges have been trimmed off to conserve space. The index display and the repetitious gray scale have also been trimmed off and only

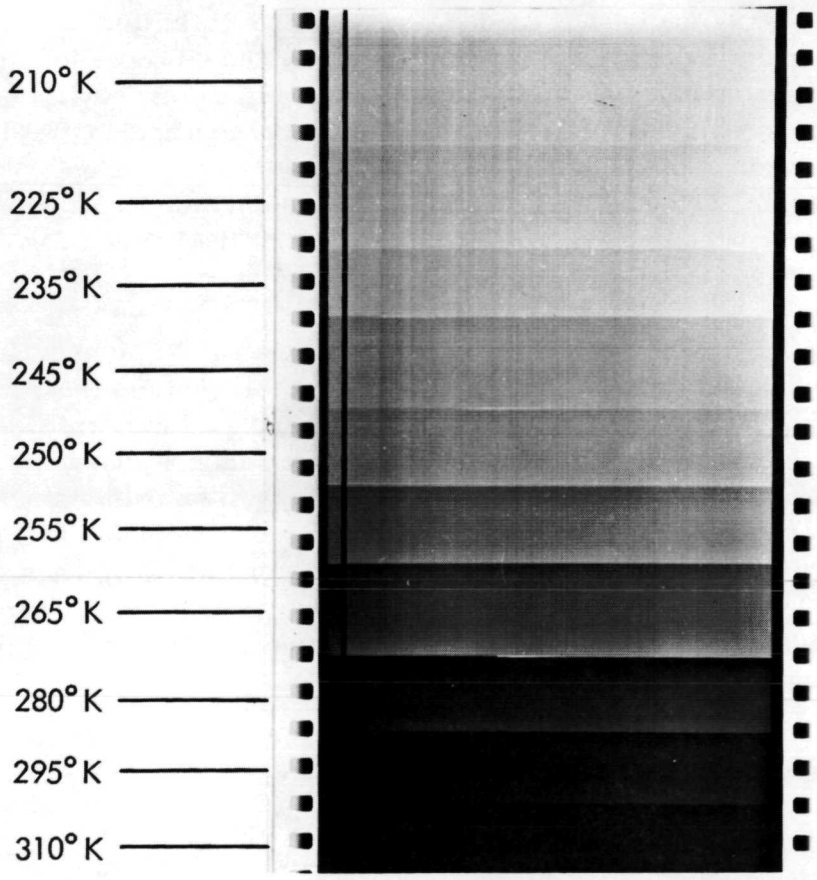

Figure C3—The ten-step gray scale wedge for the photofacsimile produced film strips showing the corresponding equivalent blackbody temperatures

the actual data, portions of space, and the housing temperatures are shown. Two or more of the data blocks may contain portions of the same data. In this Appendix the archival prints were edited such that repetitious portions of the data appear only once, but the data which are contained in the separate data blocks on the archival film are indicated by the brackets to the right of the prints on even numbered pages and to the left on odd numbered pages.

When it was necessary to place one continuous piece of film on two columns, the film was overlapped from the bottom of one column to the top of the next column to provide for the continuation of the data and to provide for easy appraisement of the content of the data. The vertical line beside the print is dashed to indicate that portion of the data which is overlapped. The prints have been arranged to avoid overlap from one page to a non-facing page. Each data block is identified by its relevant data orbit number (top) and the data block number (bottom), and both numbers are placed beside the data block to which they apply.

A feature of the gridding program provides for the presentation of the annotation for the grids on the film in such a manner that it is properly oriented when the latest recorded data are at the bottom and the earliest recorded data are at the top of the film. For data recorded at night when the satellite travels from north to south, this presentation of the annotation is natural, with north at the top and south at the bottom of the film. However, in the case of daylight recorded data when the satellite travels from south to north, the latest recorded are the northern most data and a properly oriented film strip shows the annotation upside down. If a data block contains only daytime data, the print is shown in this Appendix correctly oriented with the annotation upside down. However, if a data block contains both nighttime and daytime data, the print is arranged such that the nighttime data are oriented correctly, forcing the daytime data to appear with the southern most data at the top and northern most data at the bottom, for example, see data block 95 on page 144.

To illustrate the use of this Appendix, we use page 144. The print in the left column contains data for two data blocks indicated by the two brackets to the right of the print. The bracket nearest to the print shows the extent of the data for orbit 145/146, block 94. The second bracket, which continues on the right column, shows the extent of orbit 146, block 95. The dashed portion of this line shows that the print overlaps from the left to the right column. The extent of the second bracket indicates that the data for block 95 starts before the end of the data on block 94, but block 95 ends much later; therefore, both blocks are necessary to complete the record of the data. The data orbit (top) and the data block (bottom) numbers allow the user to find quickly the associated information in Appendices A and B.

Following are 131 pages of

CONTACT PRINTS OF AVAILABLE
PHOTOFACSIMILE FILM STRIPS

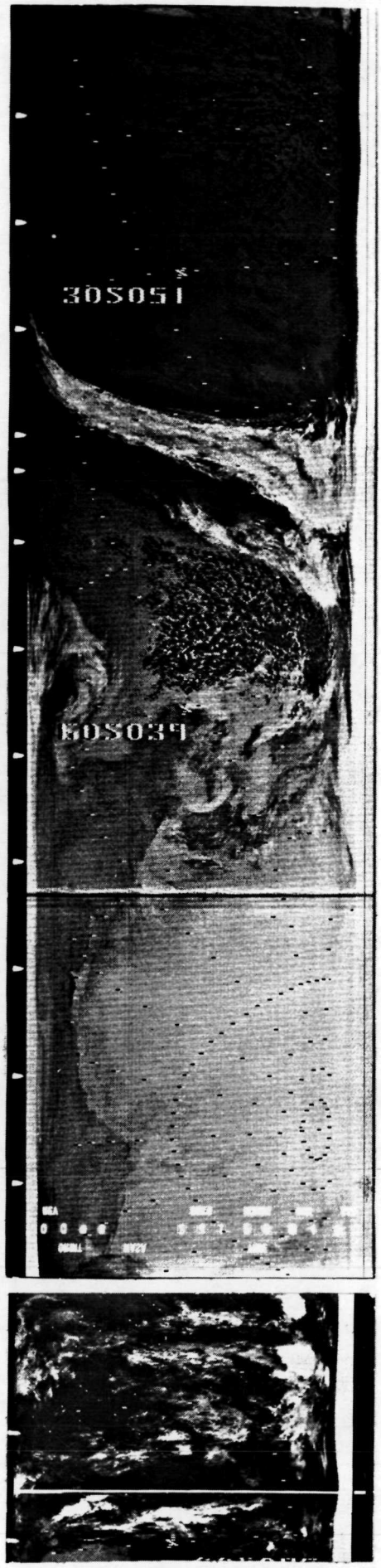

007

023
2

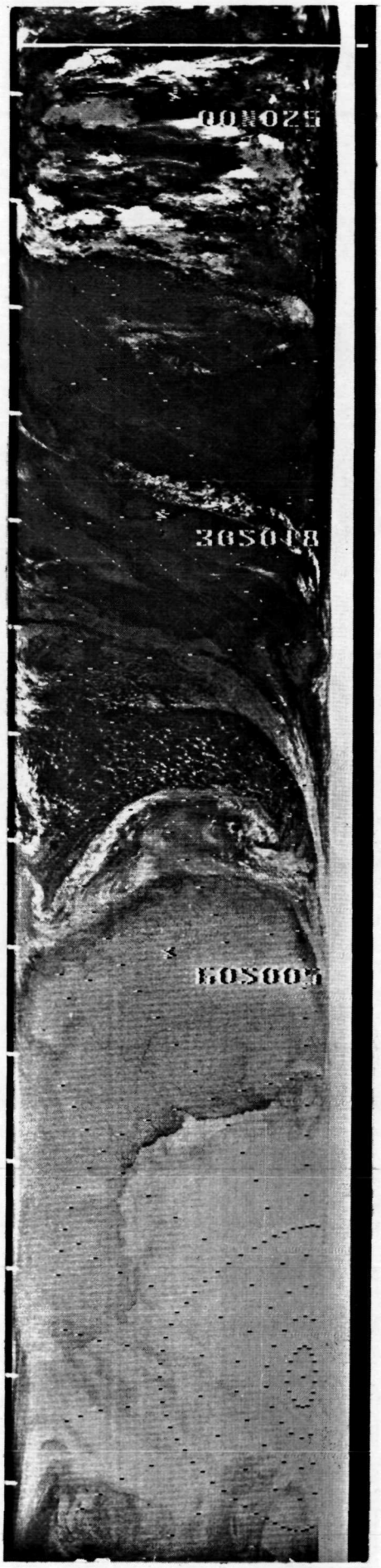

023
2

024
3

024
4

024
5

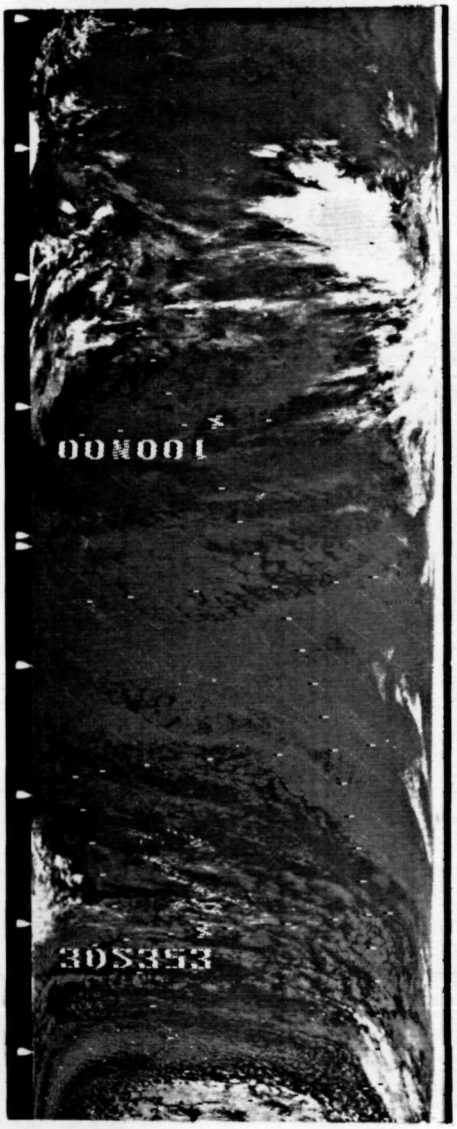

024
5

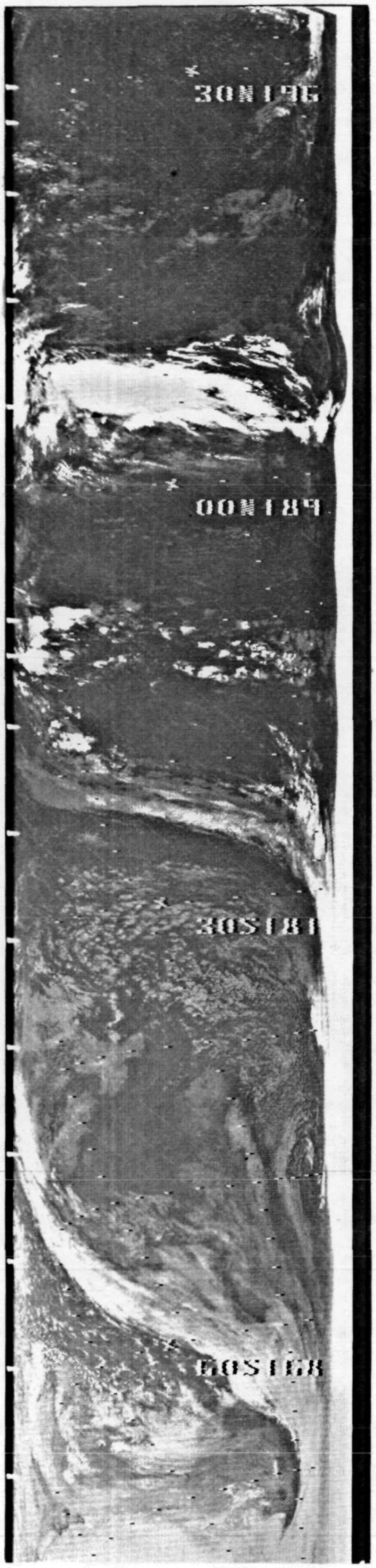

031
6

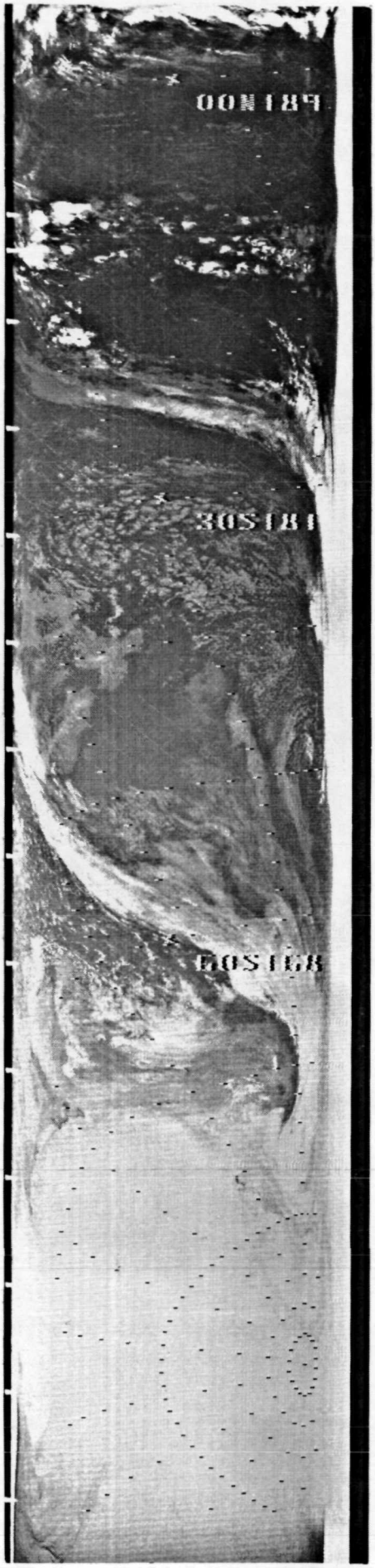

031
6

034
7

034
8

034
9

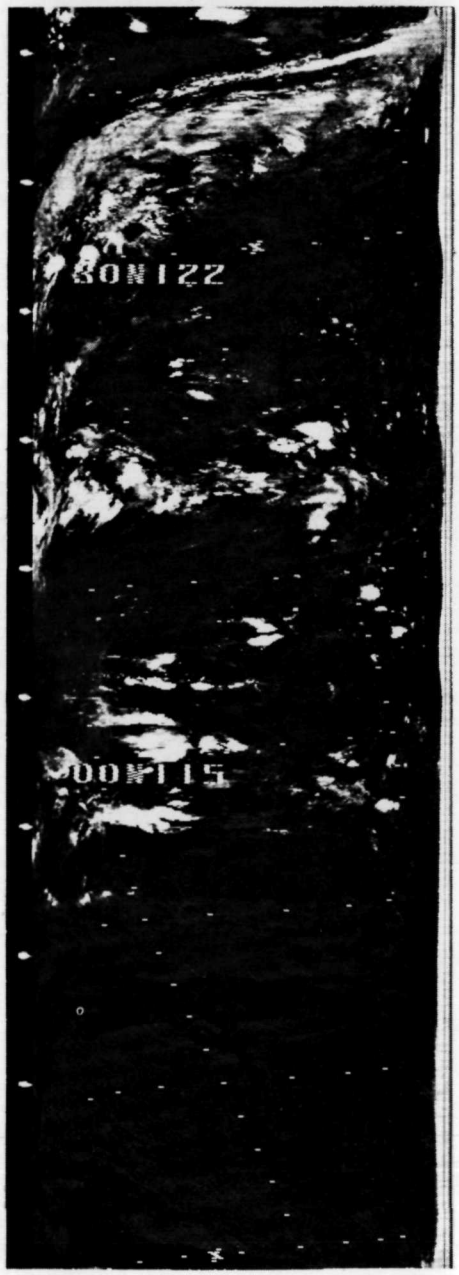

034
9

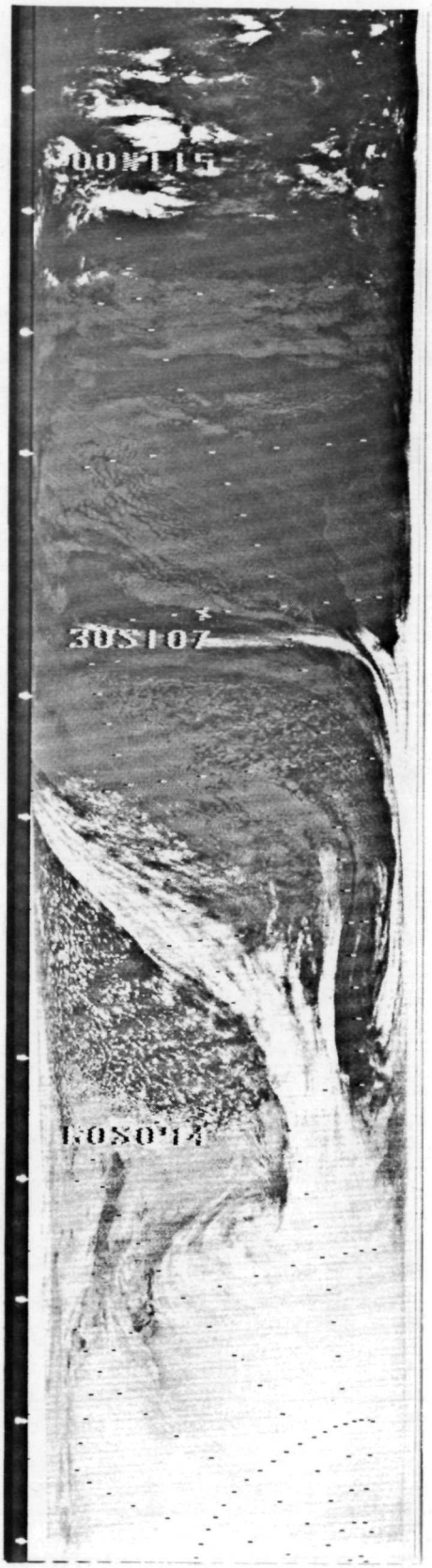

034
10

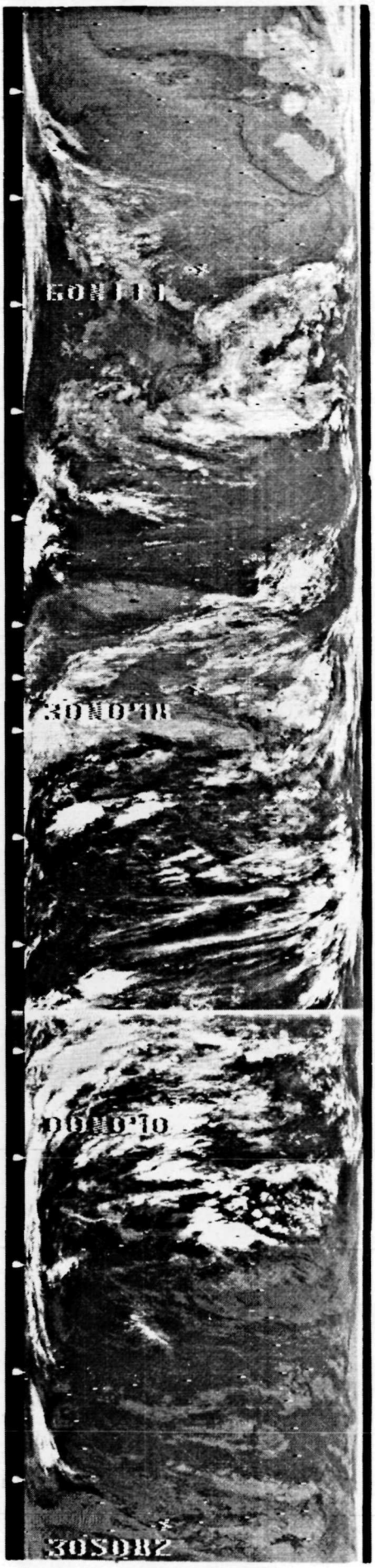

035
11

035
11

036
12

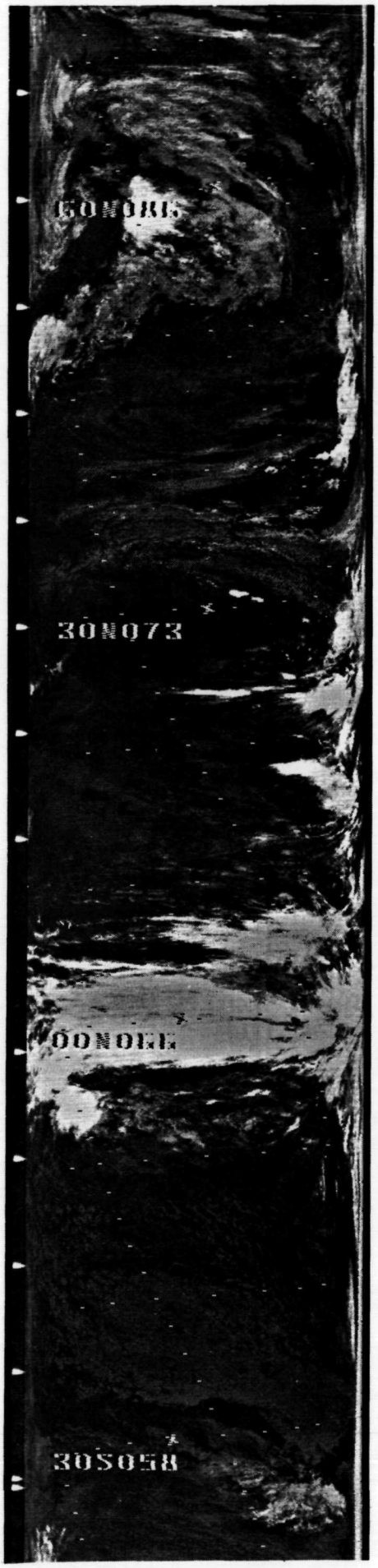

036
12

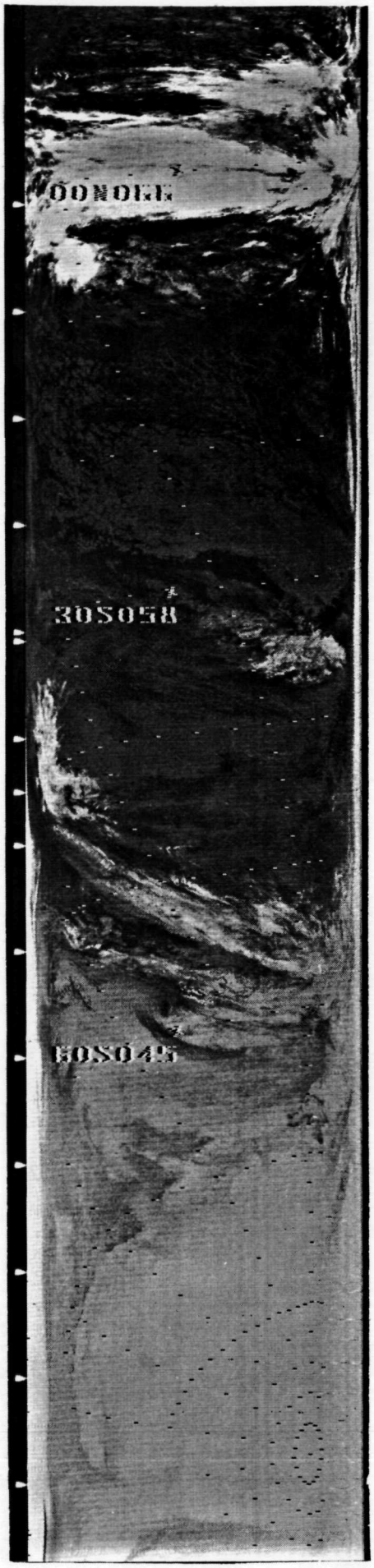

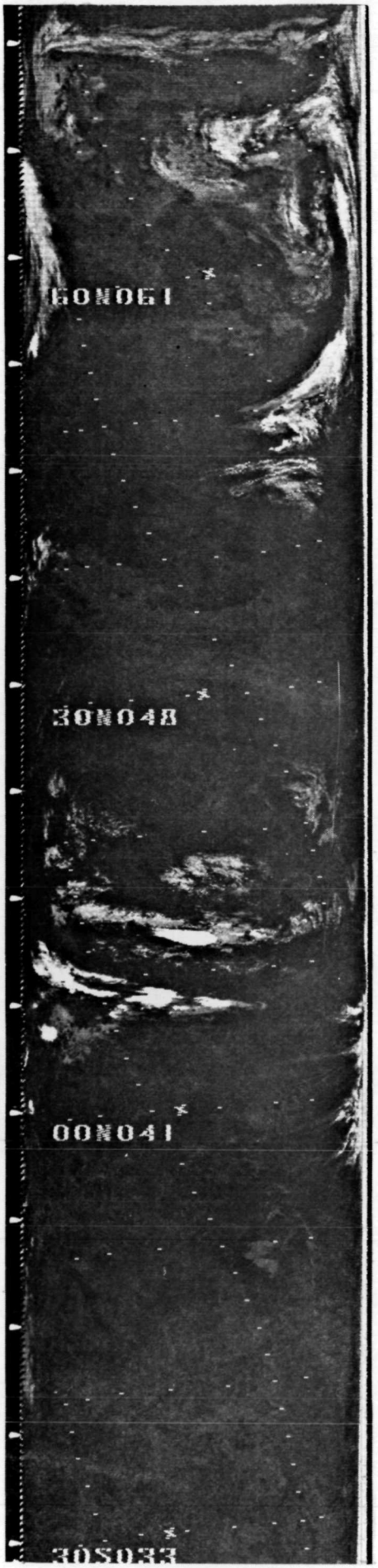

037
13

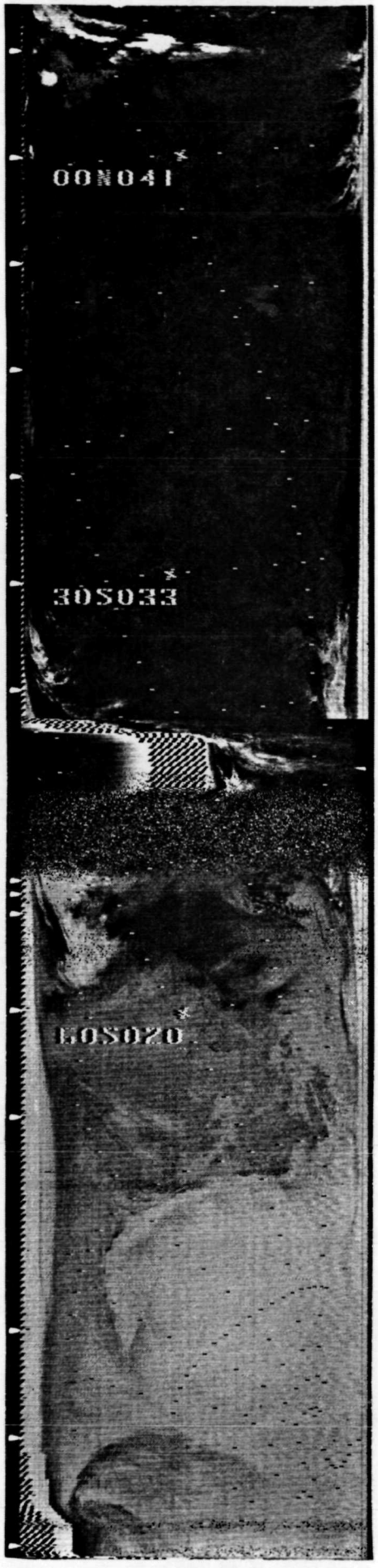

037
13

040
14

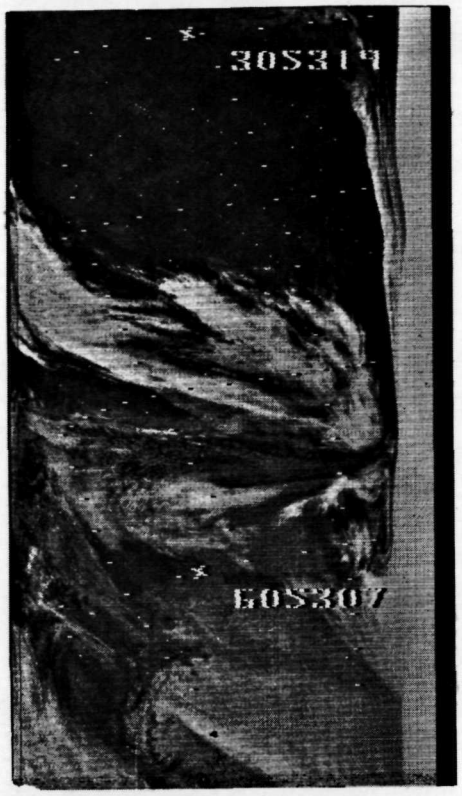

041
16

041
15

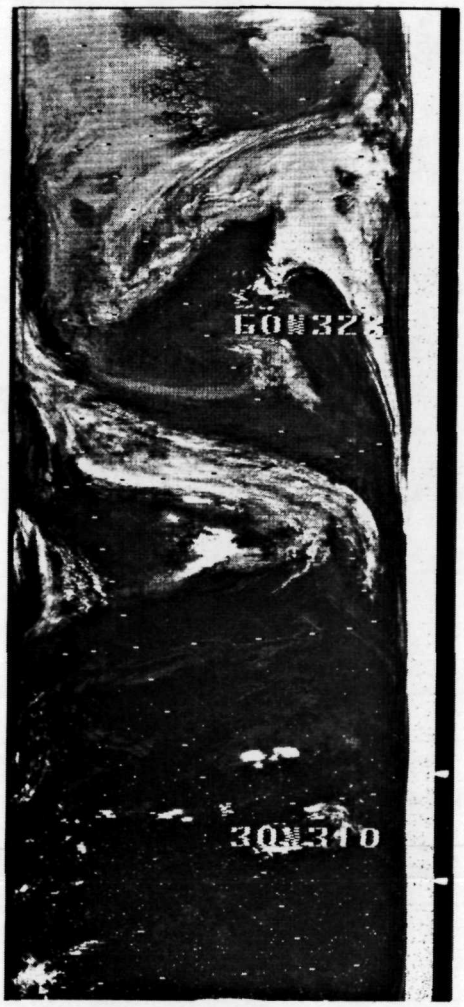

043
17

043
18

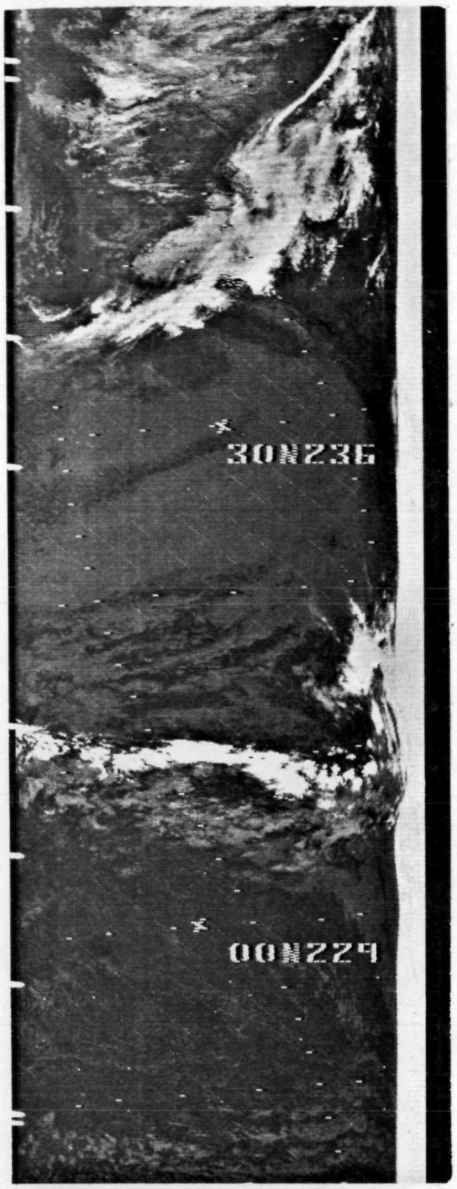

044
19

044
19

044
20

044
20

045
21

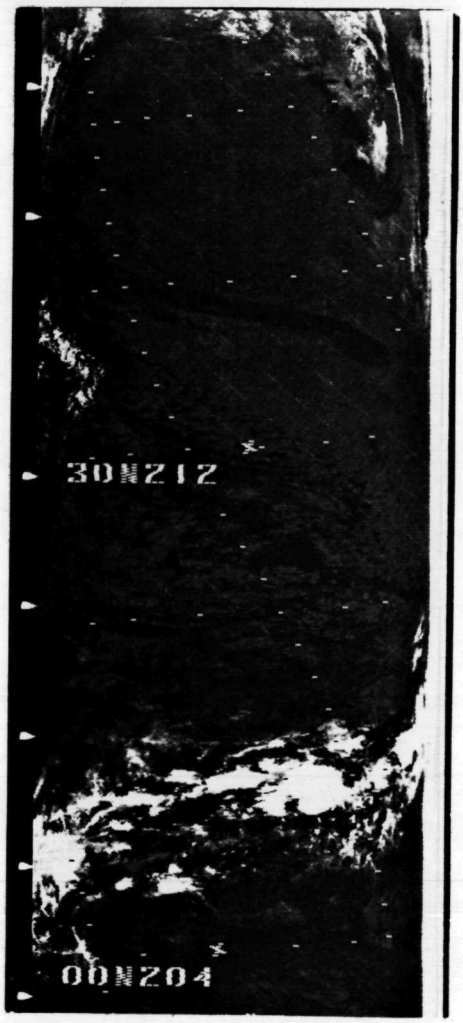

045
21

046
22

047
23

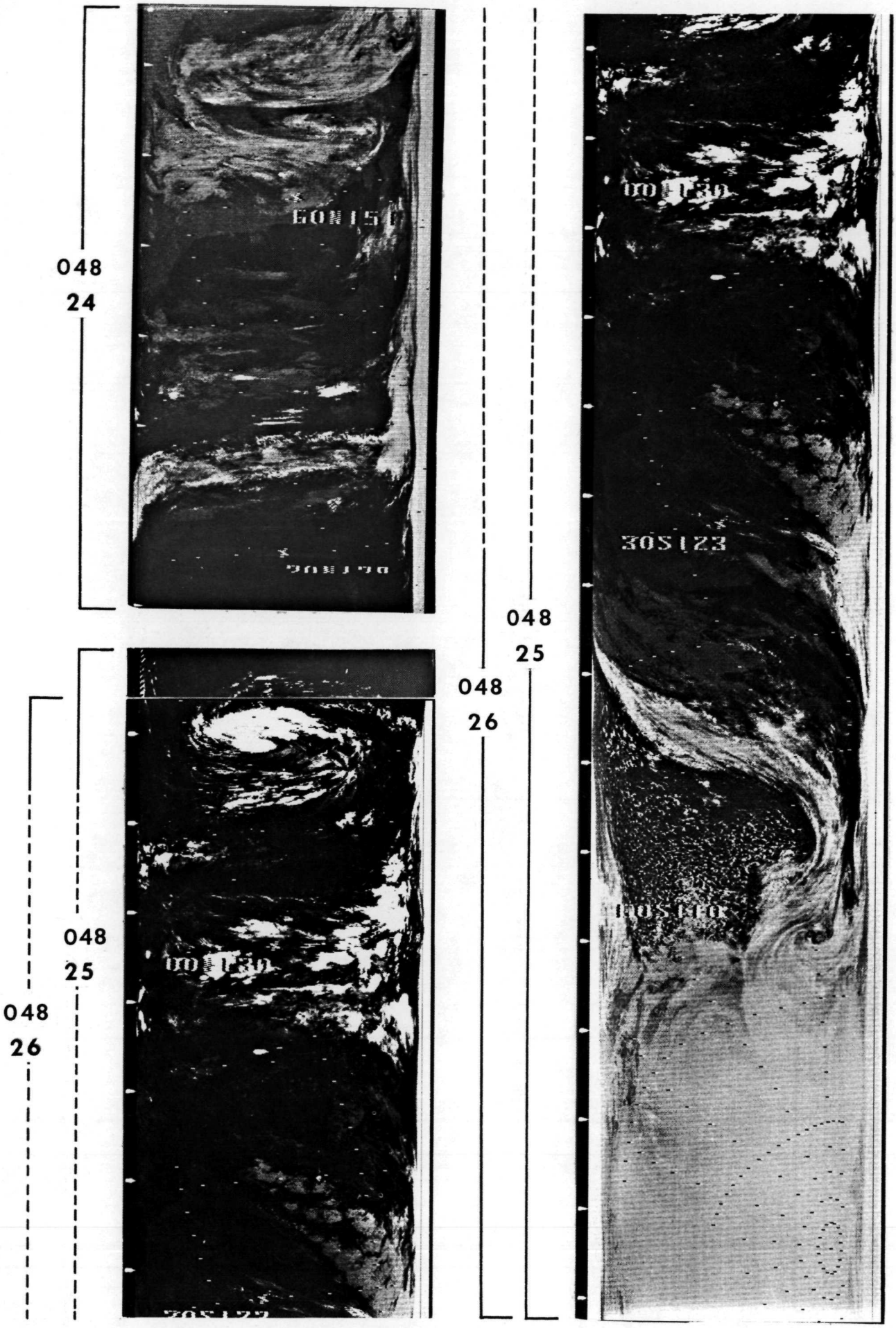
048
24
048
25
048
26
048
25
048
26

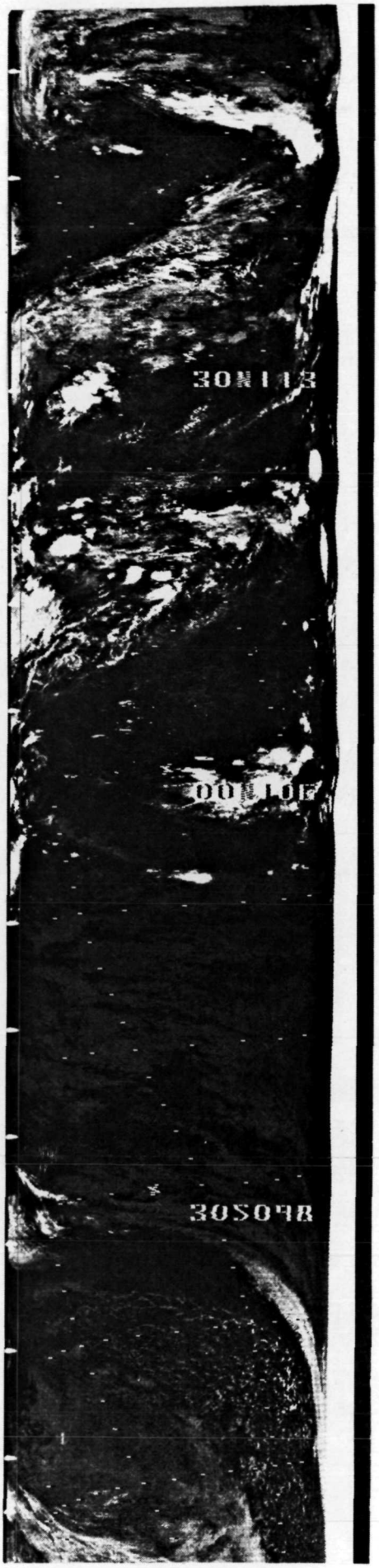

049
27

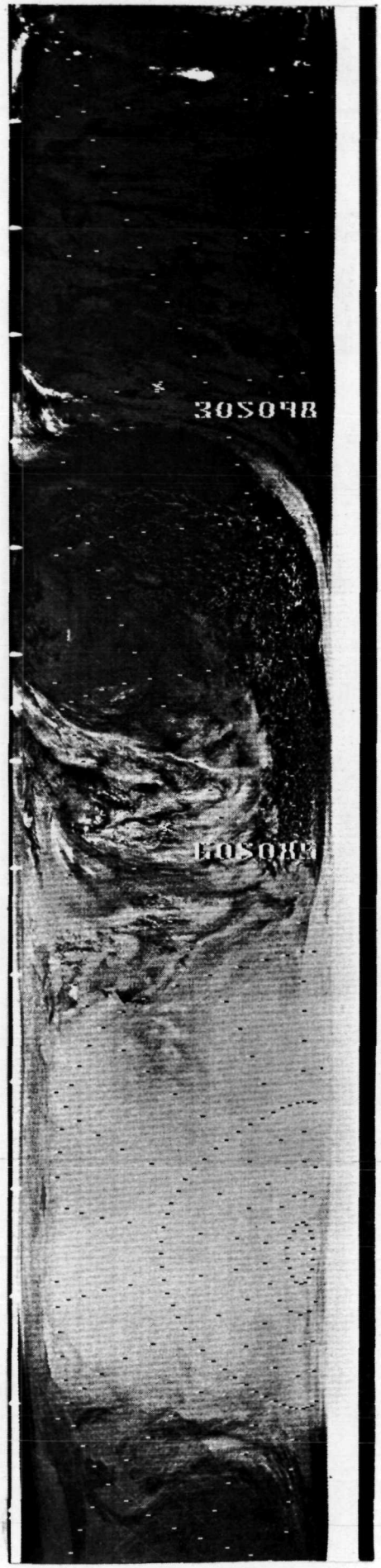

049
27

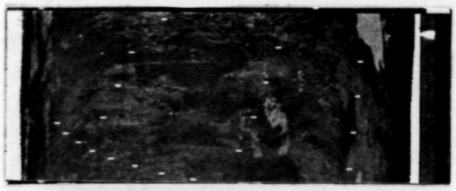

050
30

050
29

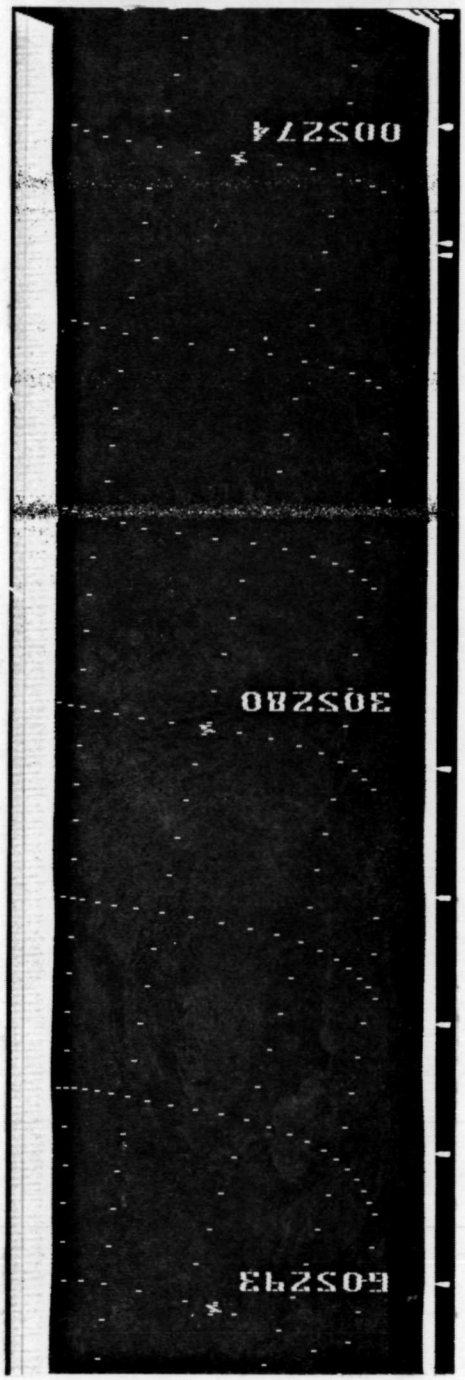

049/050
28

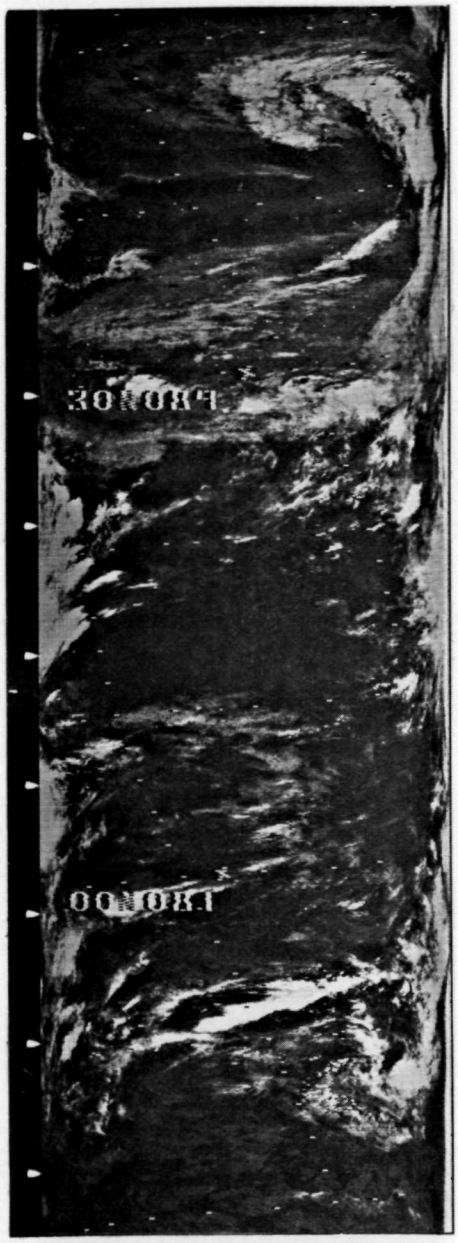

050
31

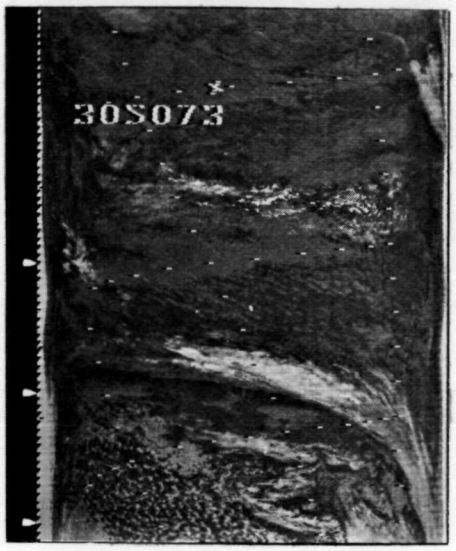

050
32

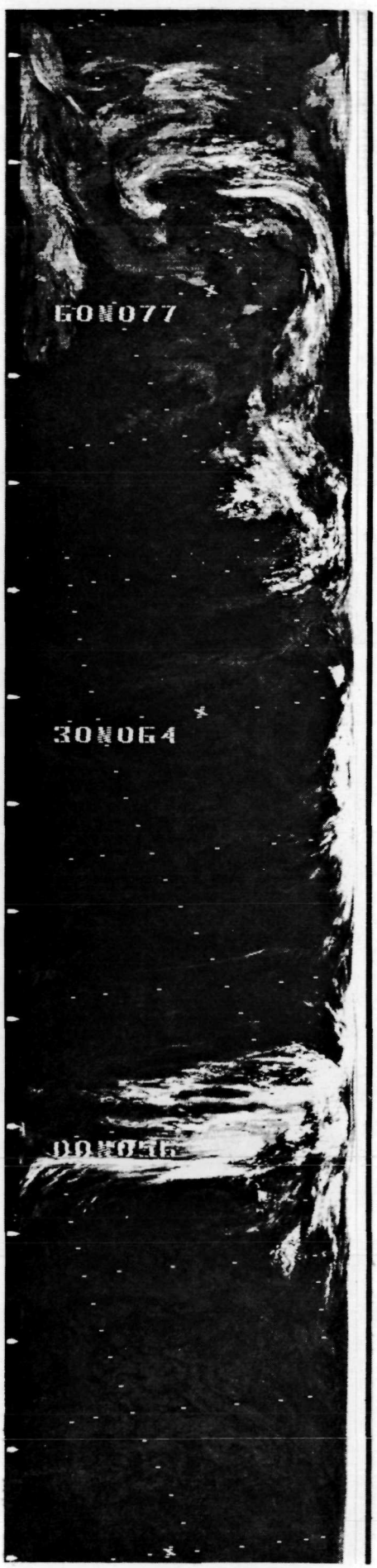

051
33

051
33

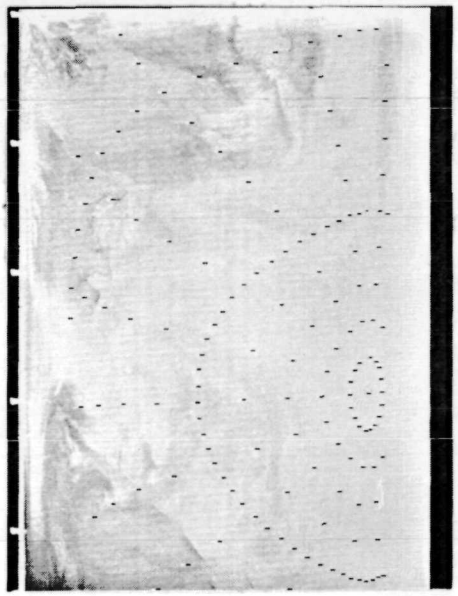

055
34

056
35

057
37

056
36

057
38

058
39

058
40

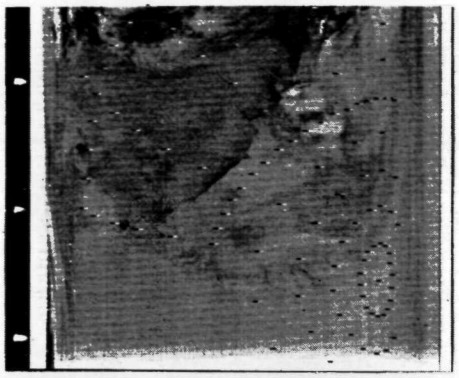

058
40

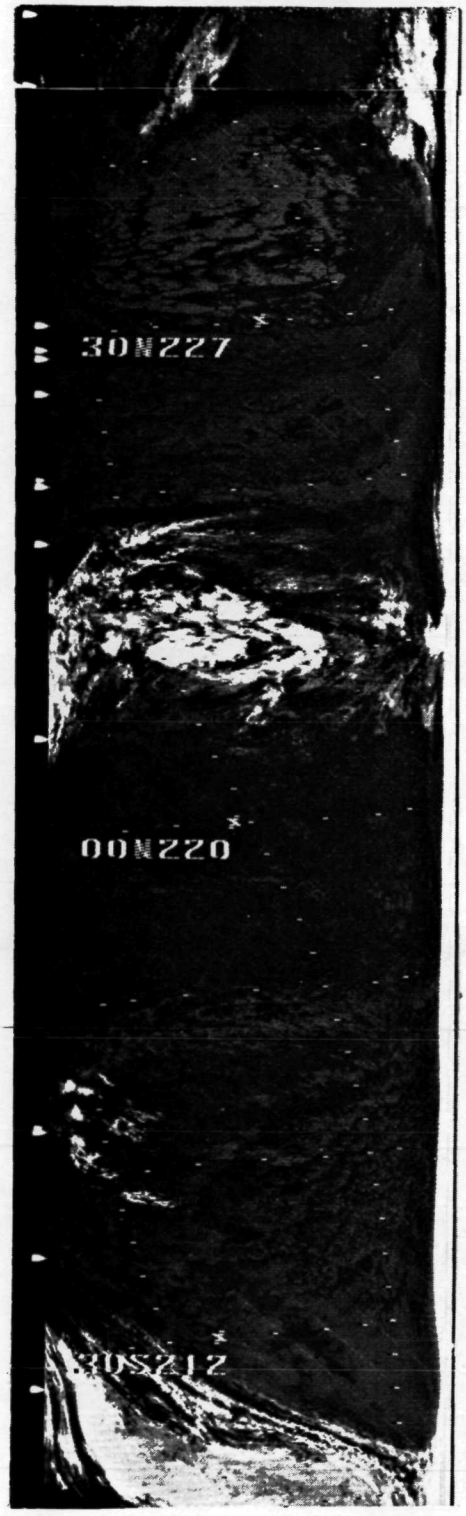

059
41

059
42

059
42

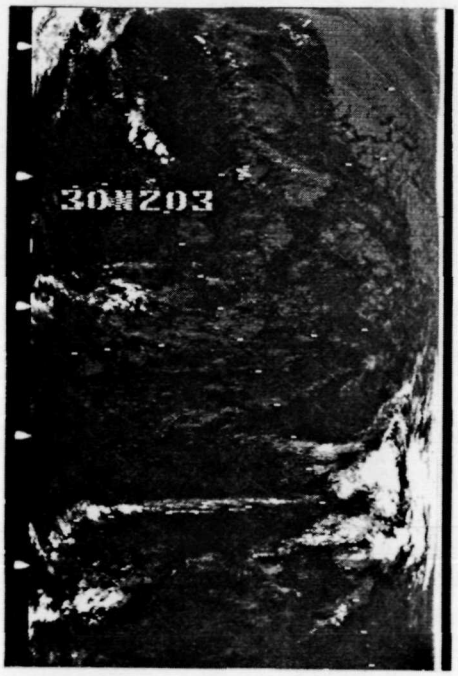

060
43

060
43

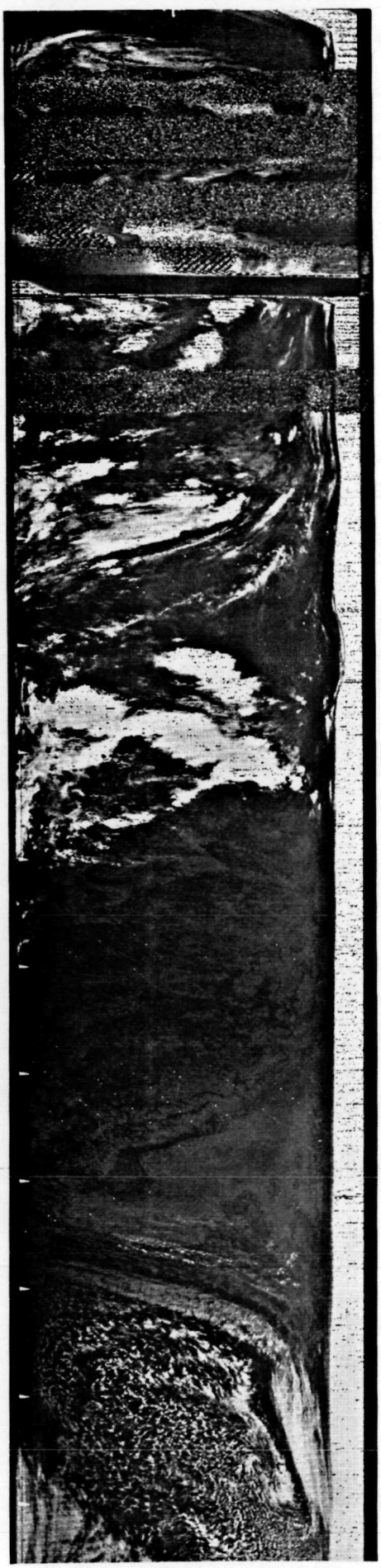

064
44

064
44

064
45

065/066
46
005240
305246
605249

065/066
46
305246
605249

066
47

066 / 067
48

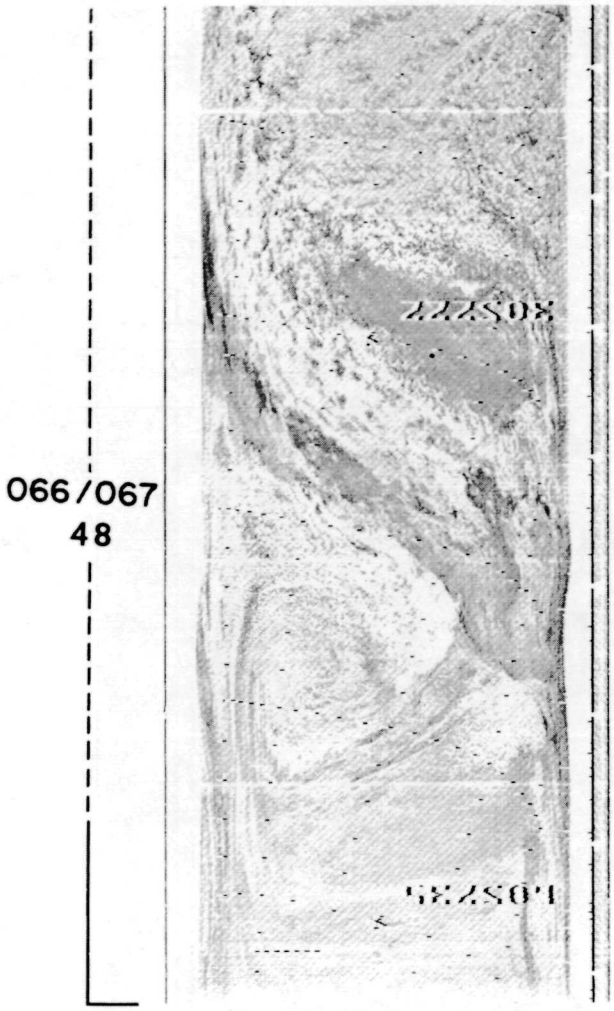
066/067
48

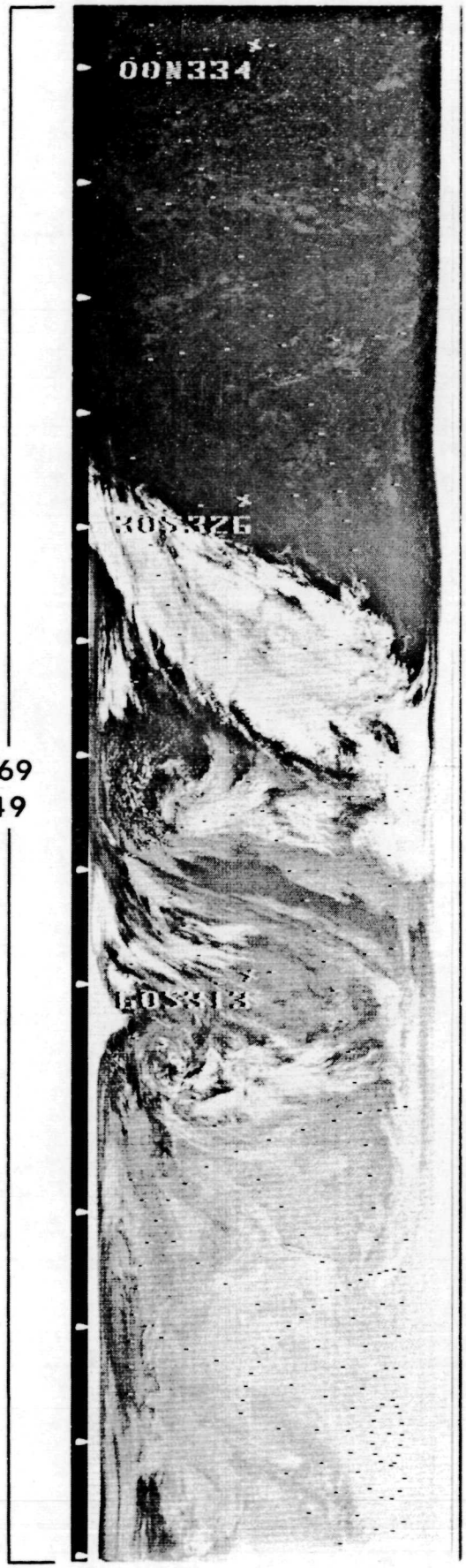
00N334
069
49

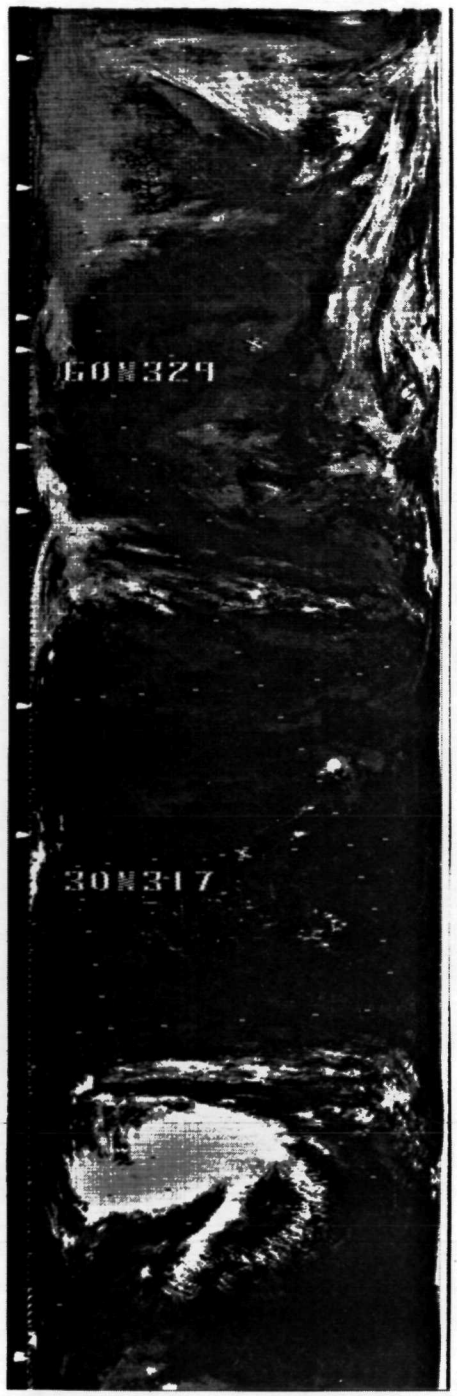

070
50

073
51

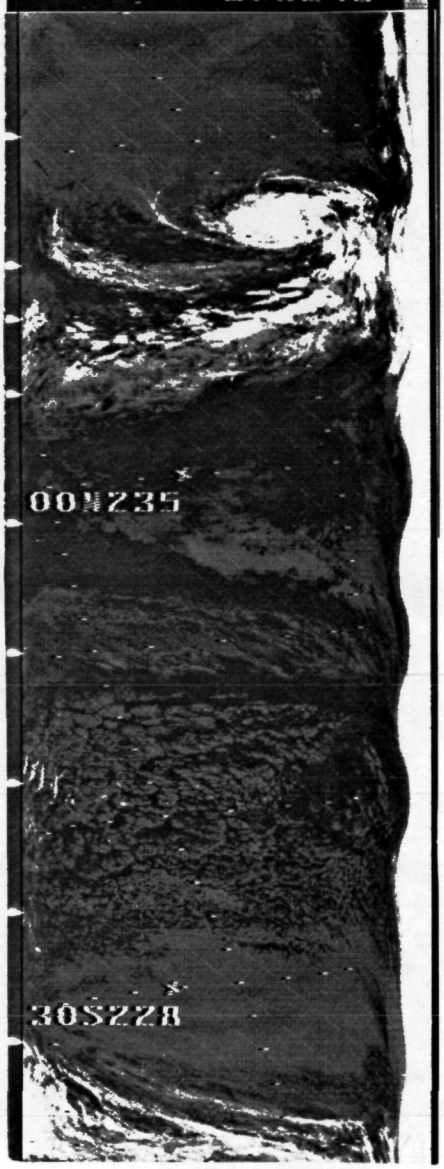

073
52

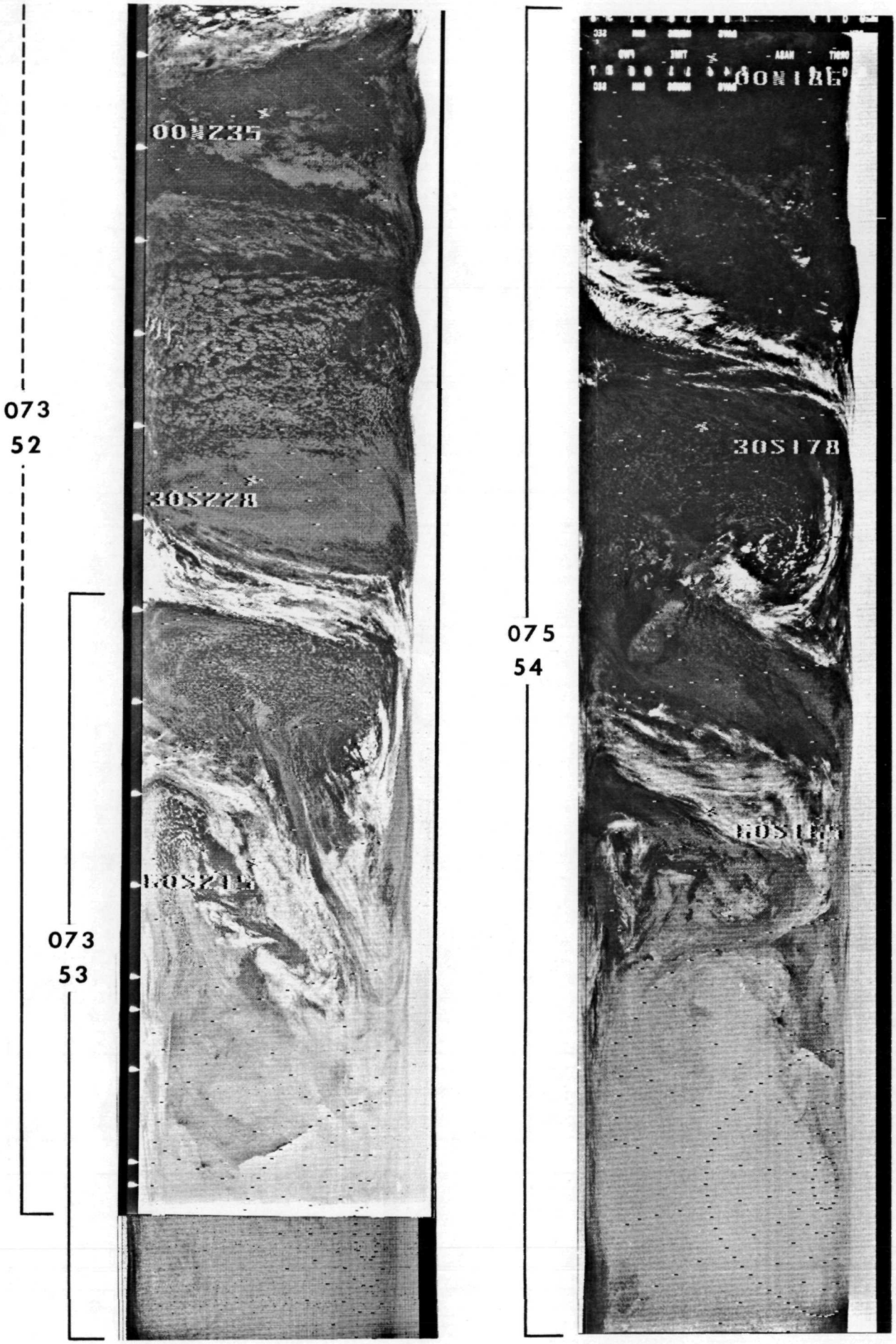
073
52
00N235
30S228
073
53
075
54
00N186
30S178

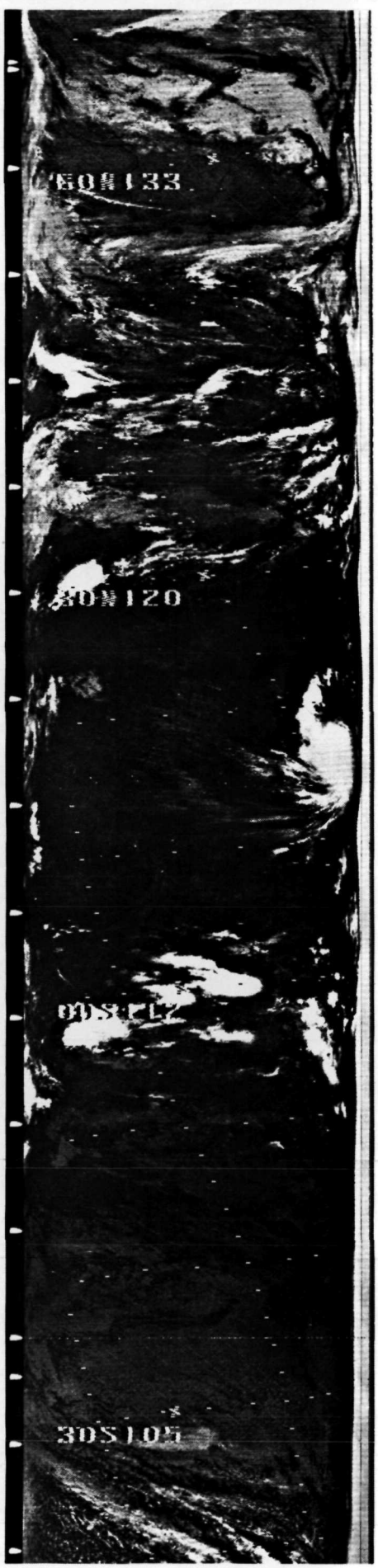

078
55

078
55

079/080
56

080
57

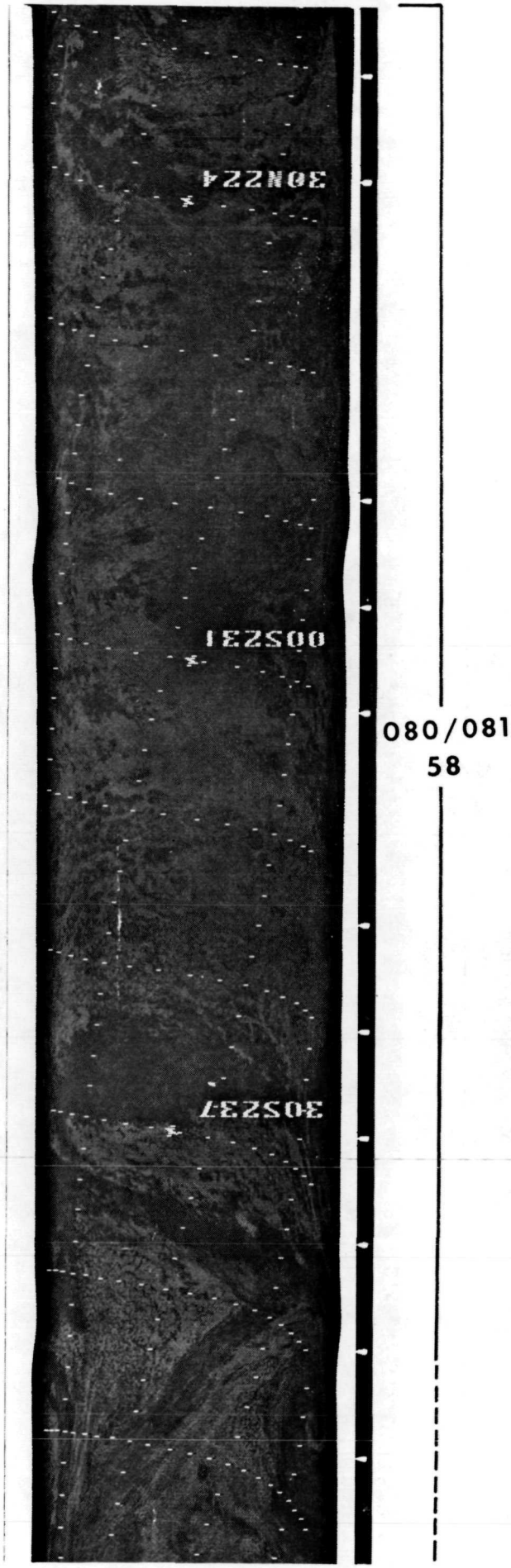

080/081
58

080/081
58

081
59

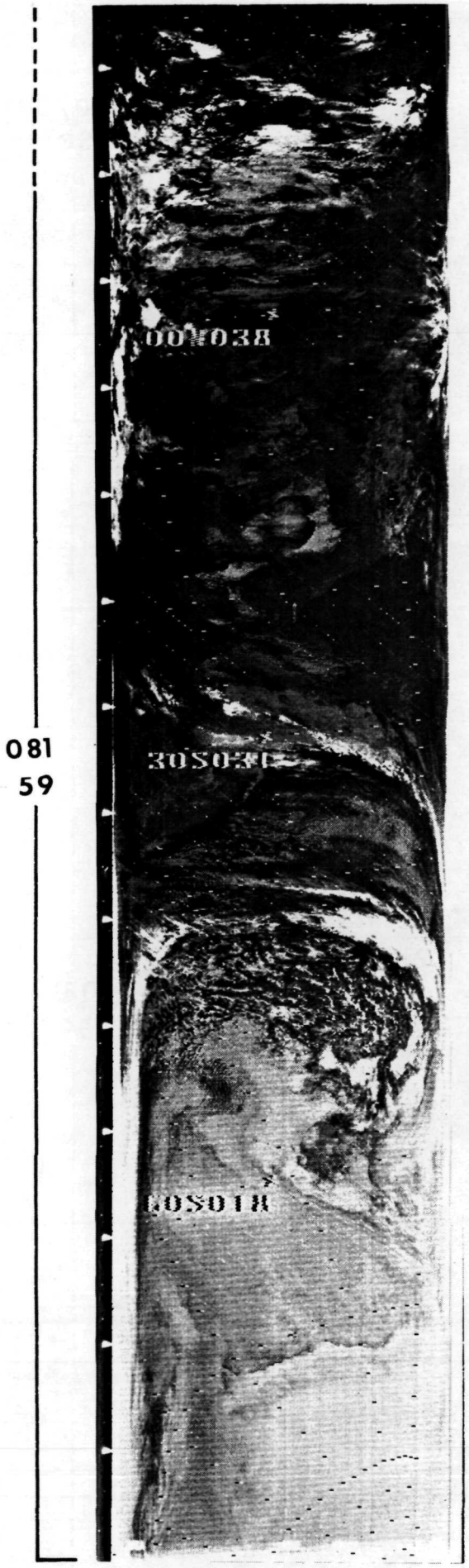
081
59
00N038
30S030
60S018

084
60
30S317
60S304

085
61

085
62

085
63

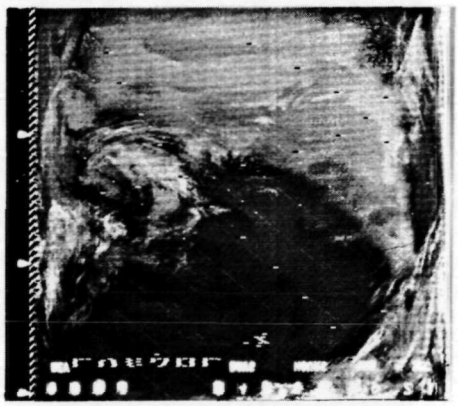

086
64

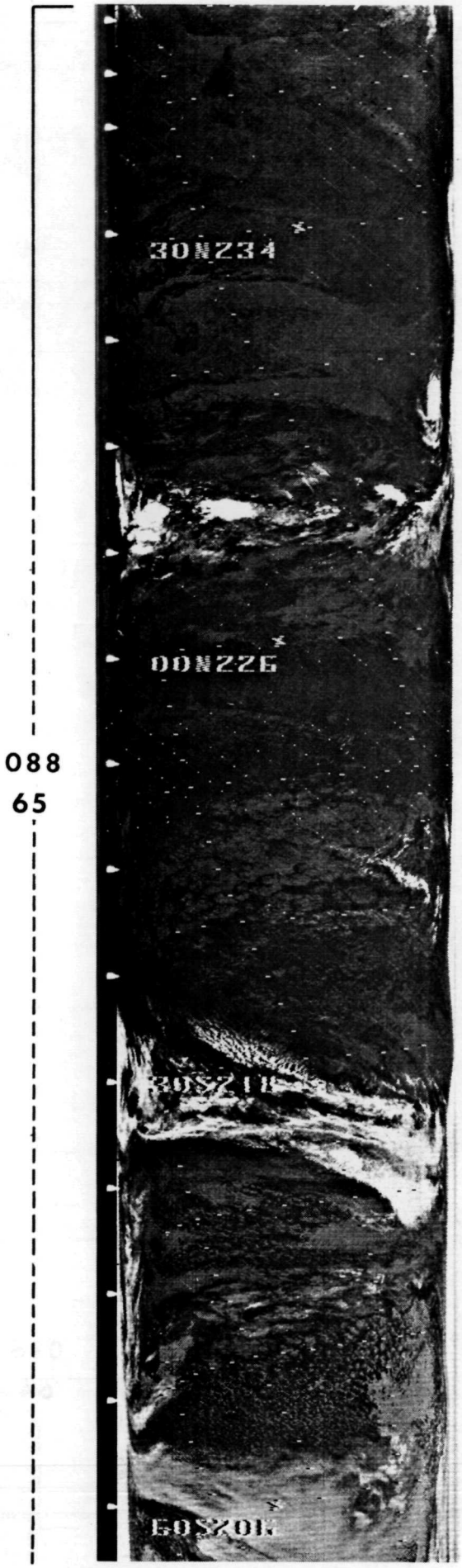
088
65

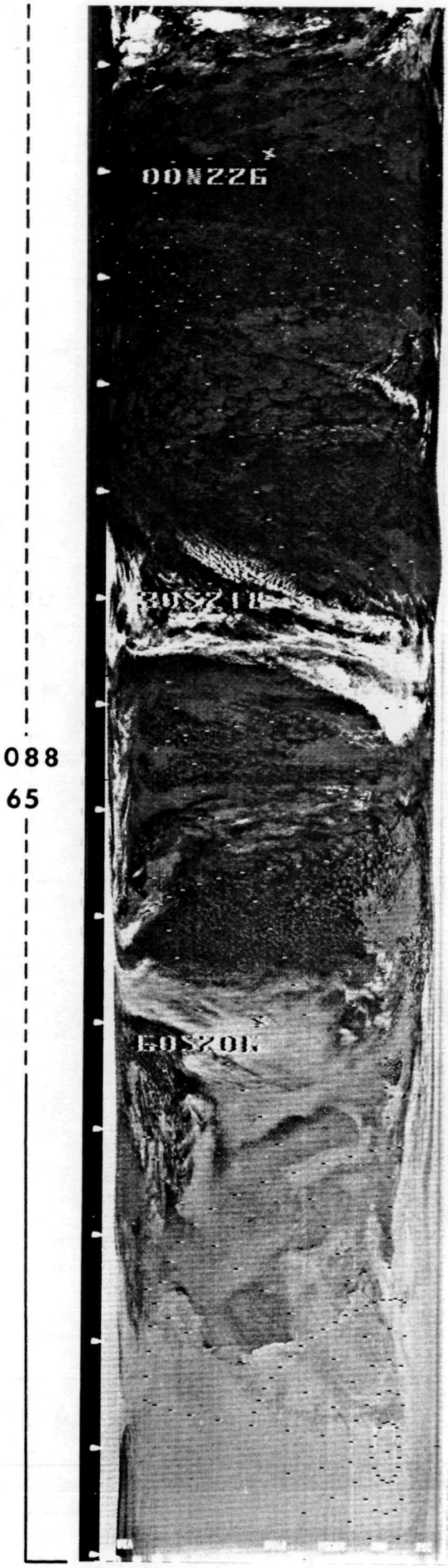
088
65

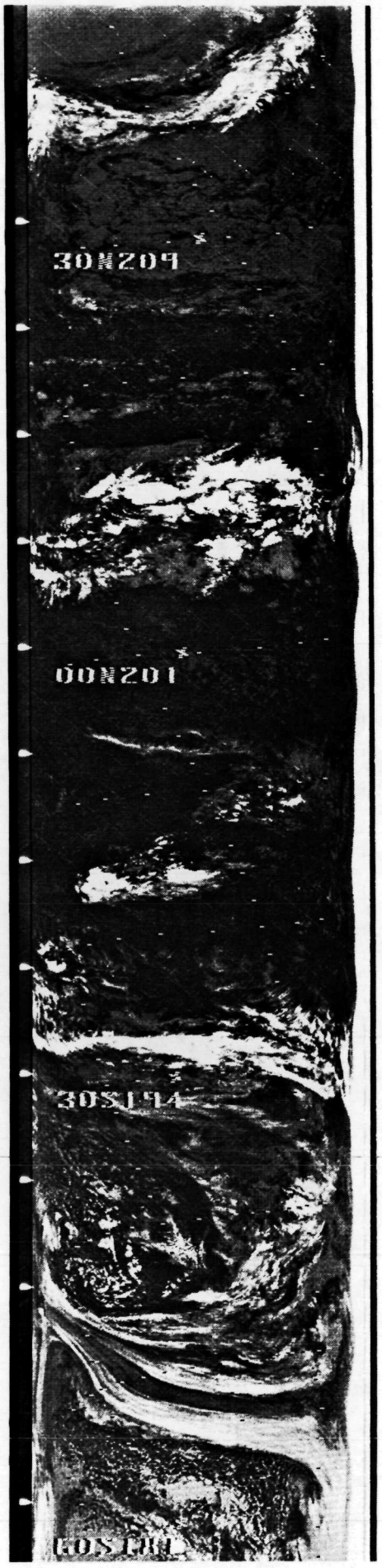

089
66

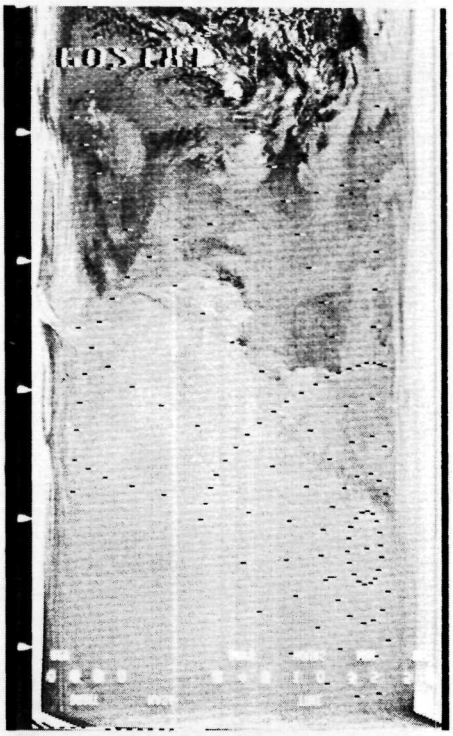

089
66

091
67

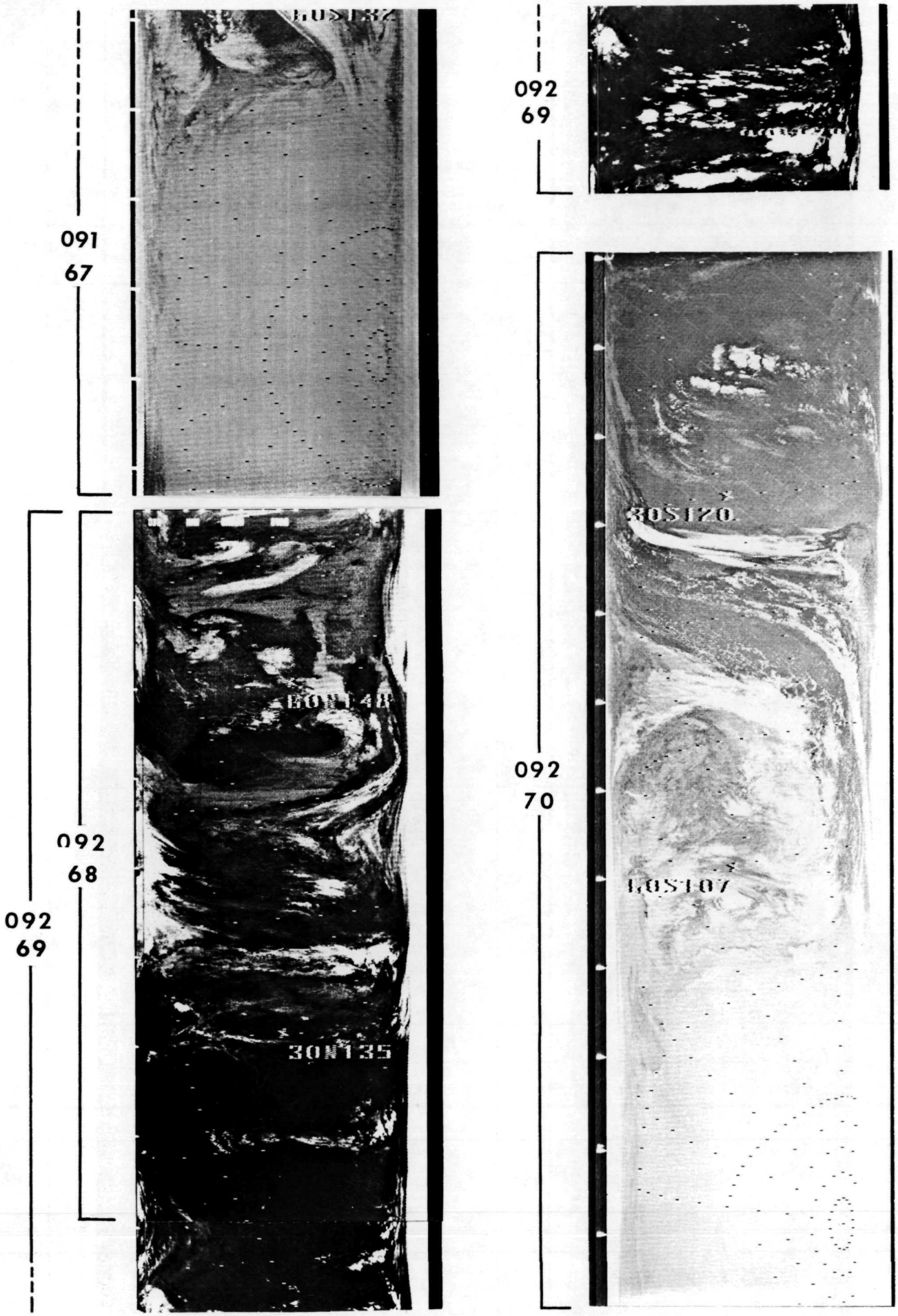
091
67
092
68
092
69
30N148
30N135
092
69
092
70
30S170
10S107

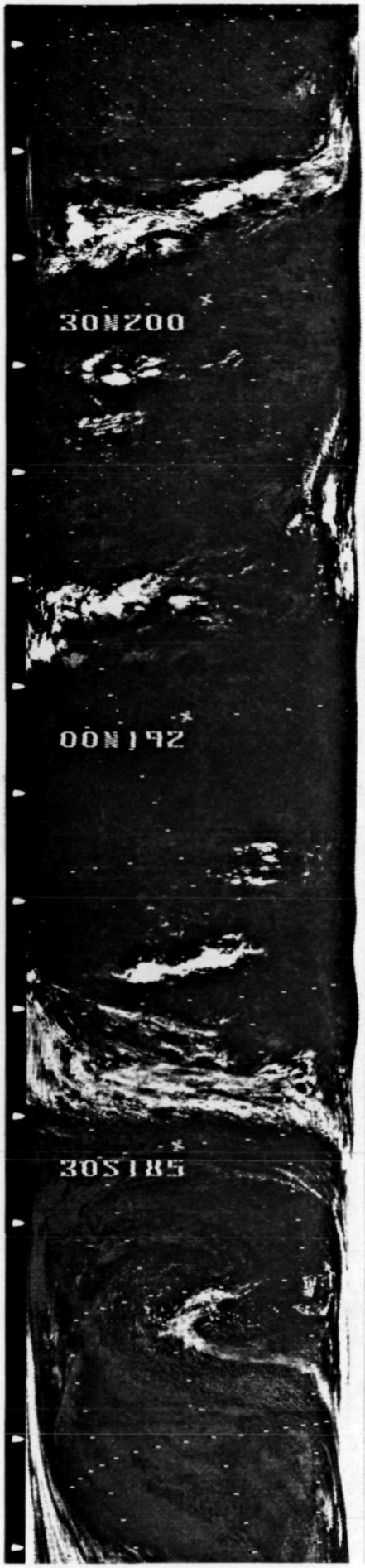

104
71

104
71

106
72

106
72

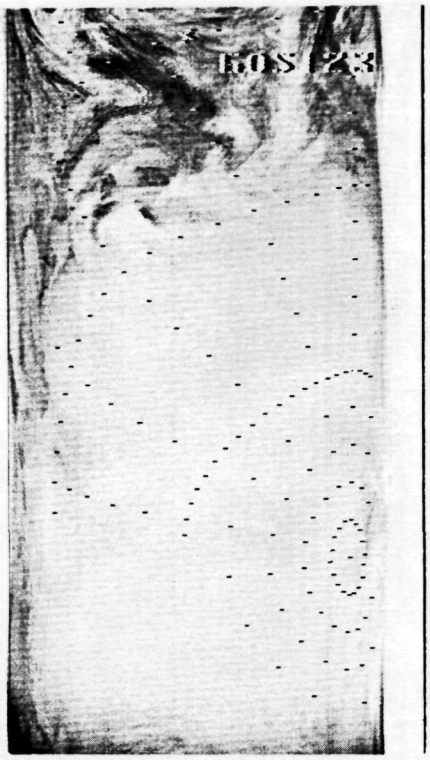

107
73

107
73

107
74

108
75

108
75

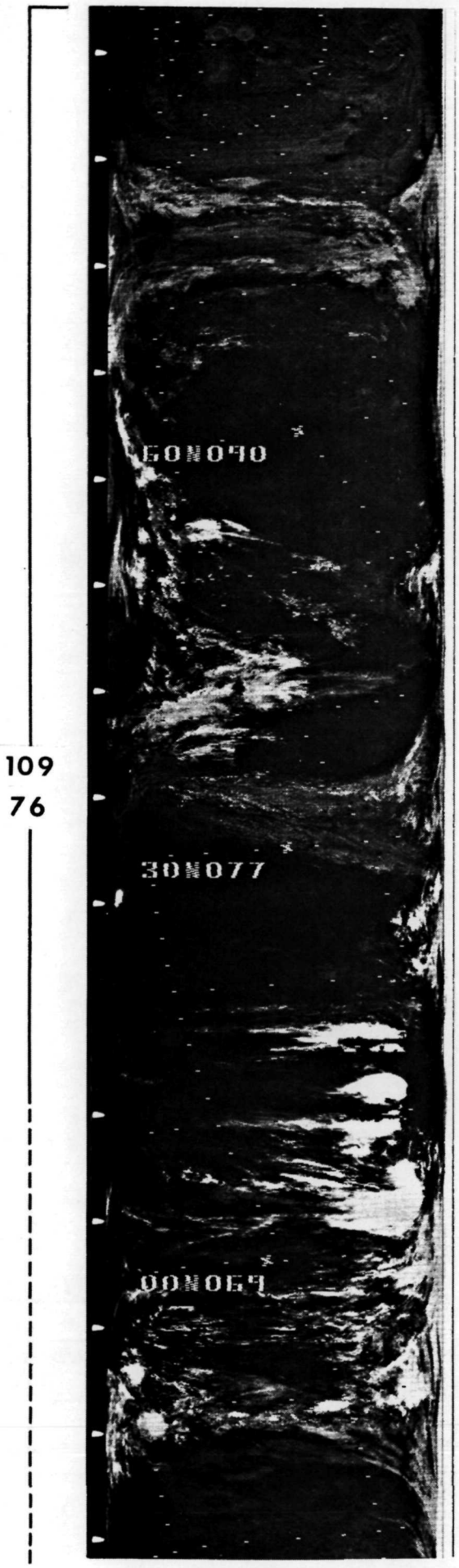

109
76

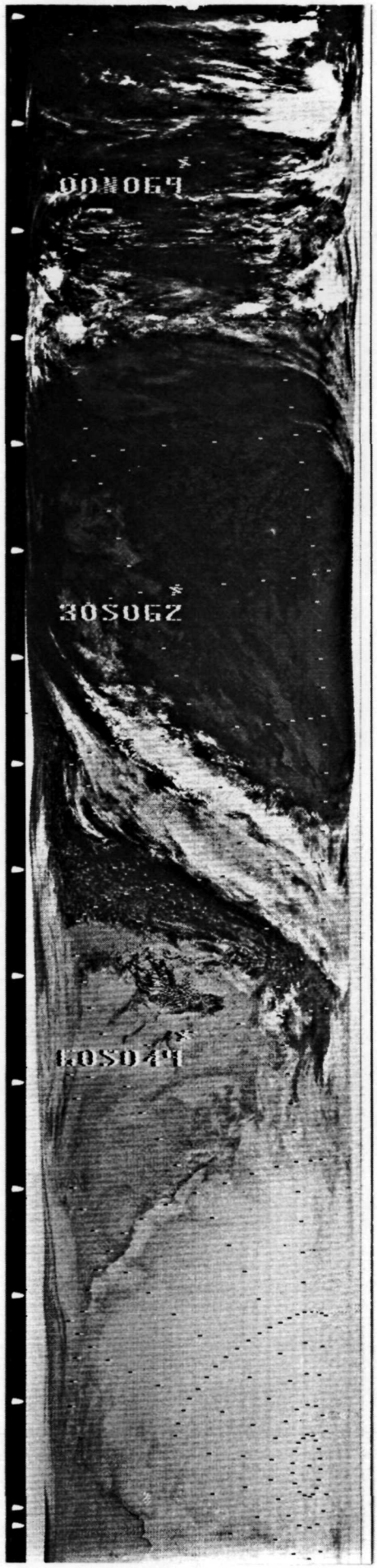

109
76

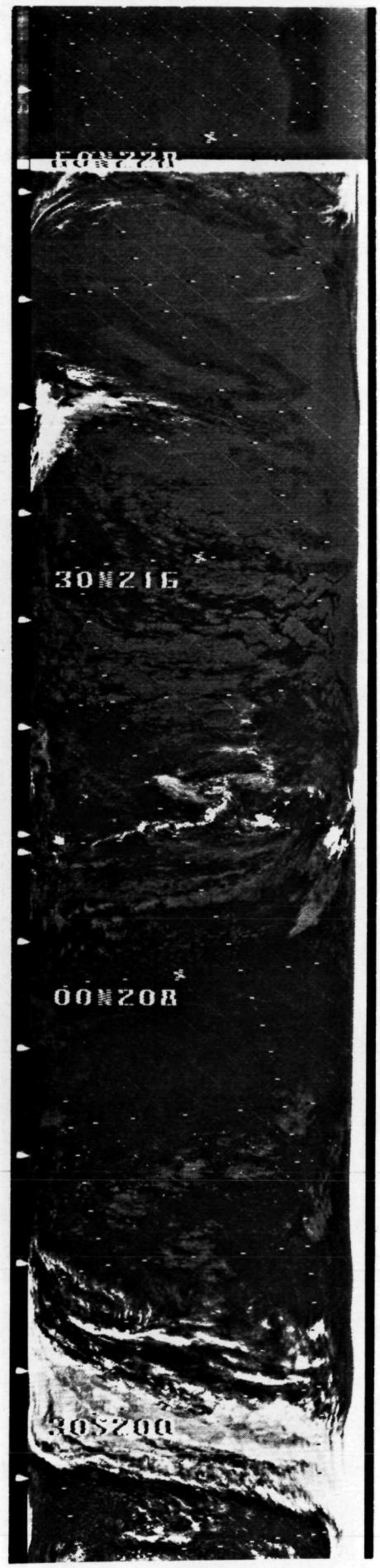

118
77

118
77

119
78

119
78

120
79

120
79

121
80

121
81

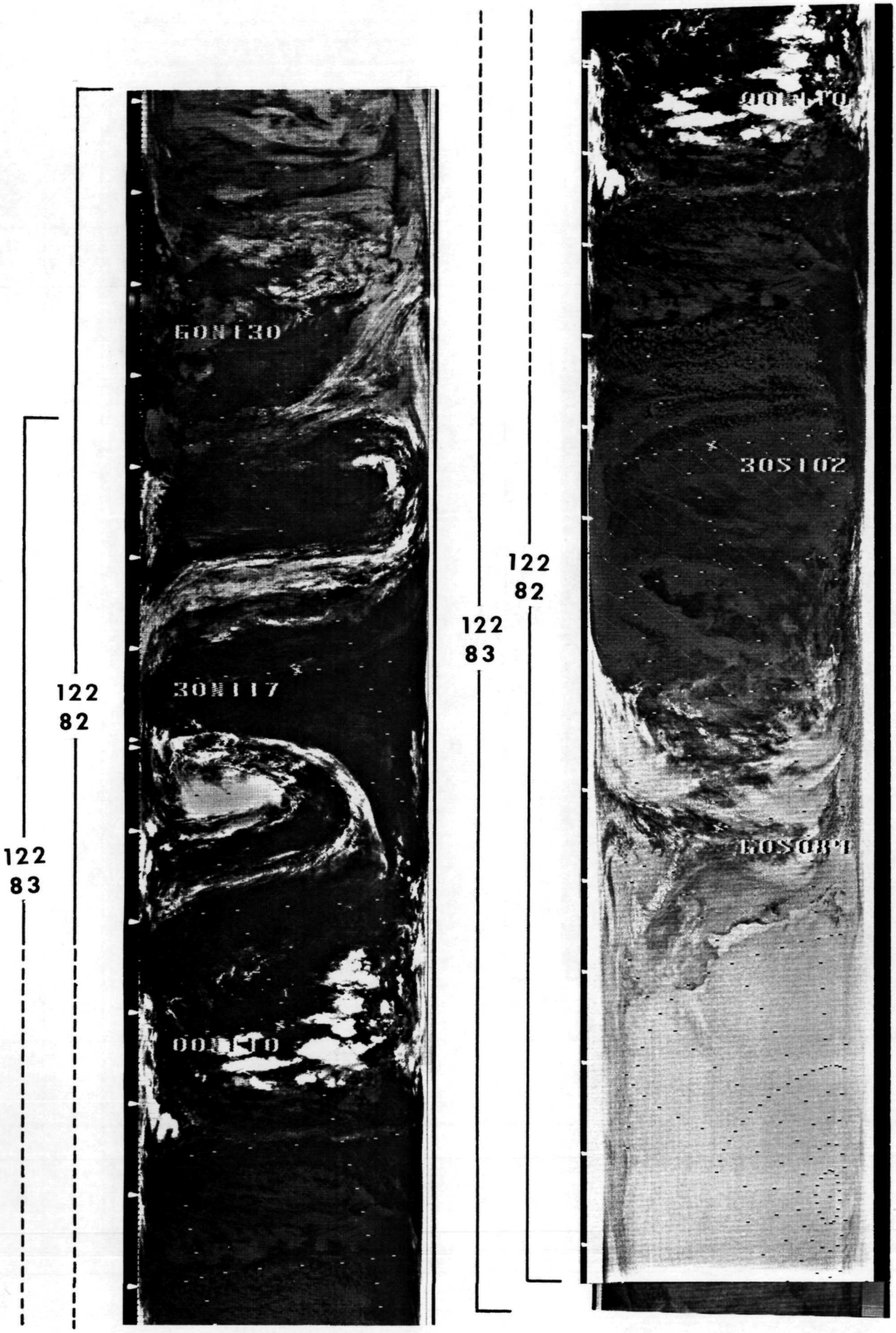
60N130
30N117
00N110
122
82
122
83
00N110
30S102
60S084
122
82
122
83

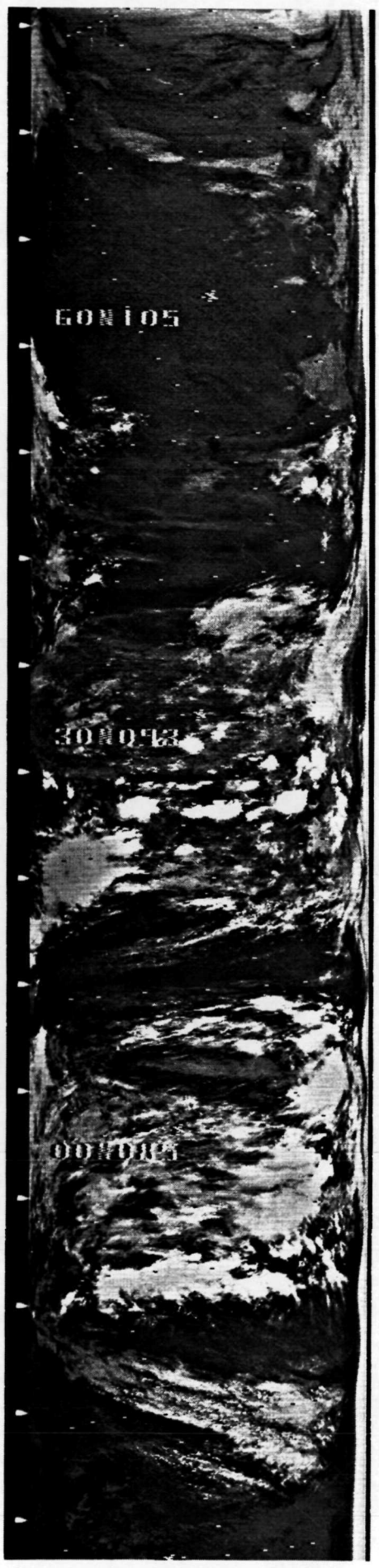

123
84

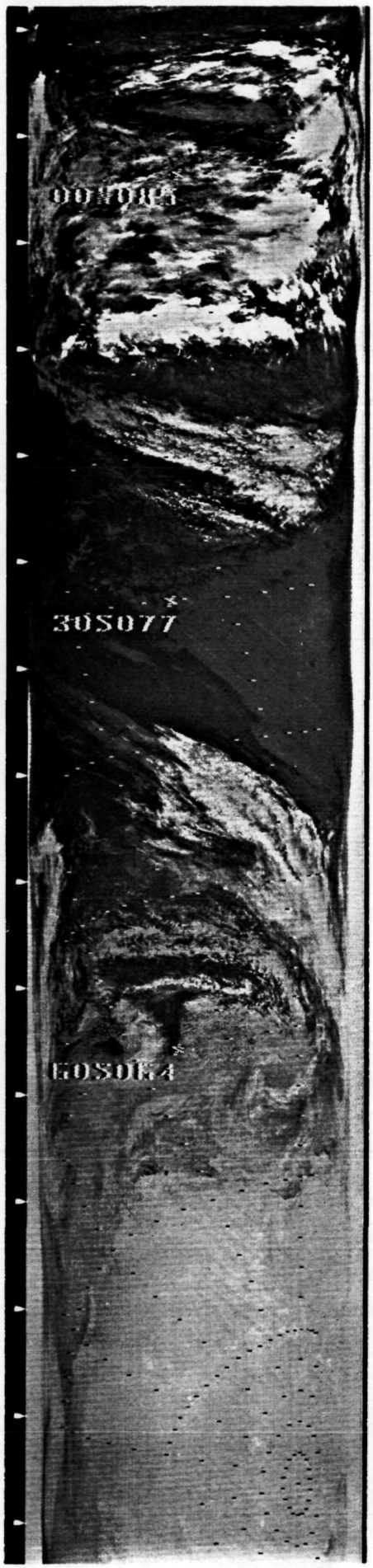

123
84

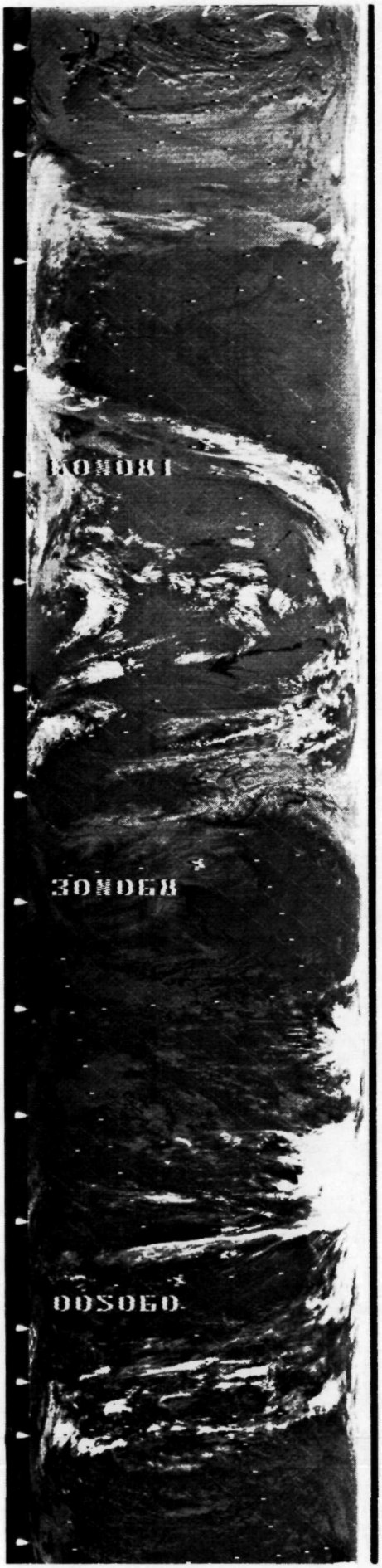
124
85
10N081
30N068
00S060

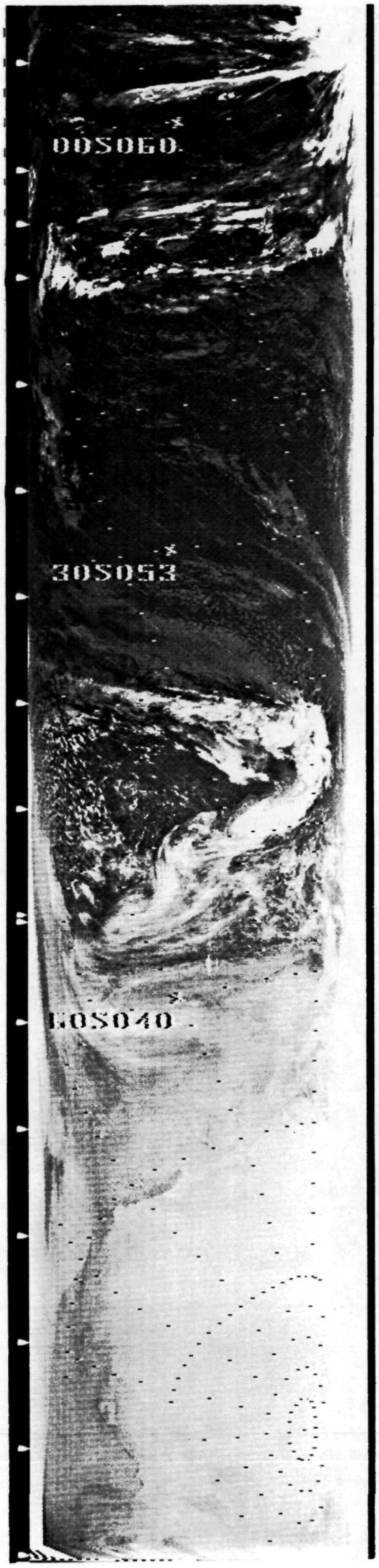
124
85
00S060
30S053
10S040

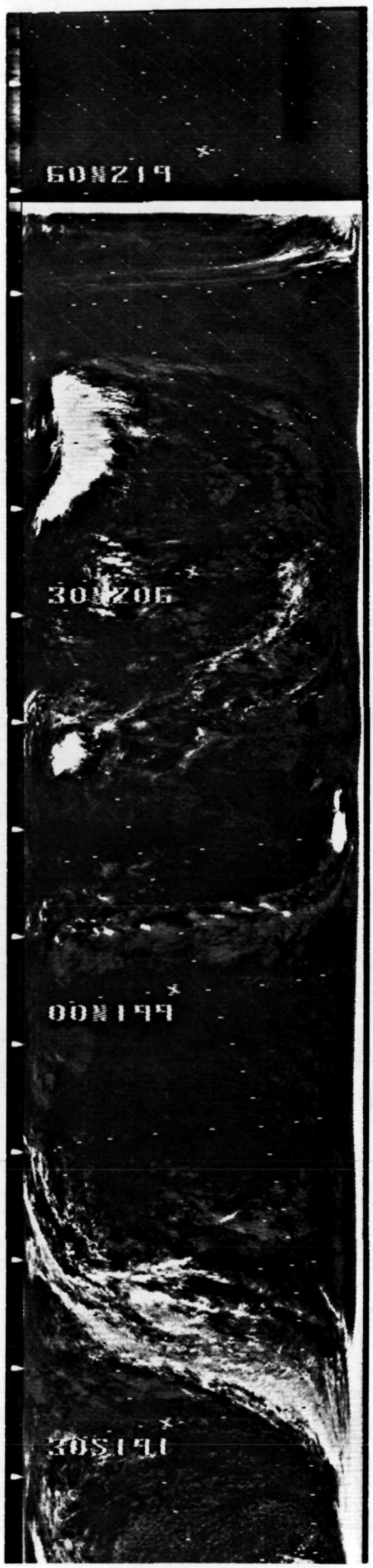

133
86

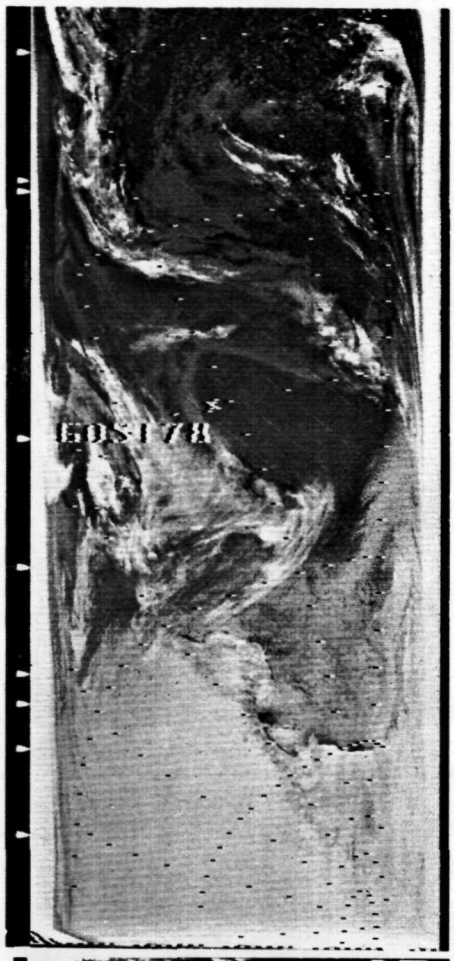

133
86

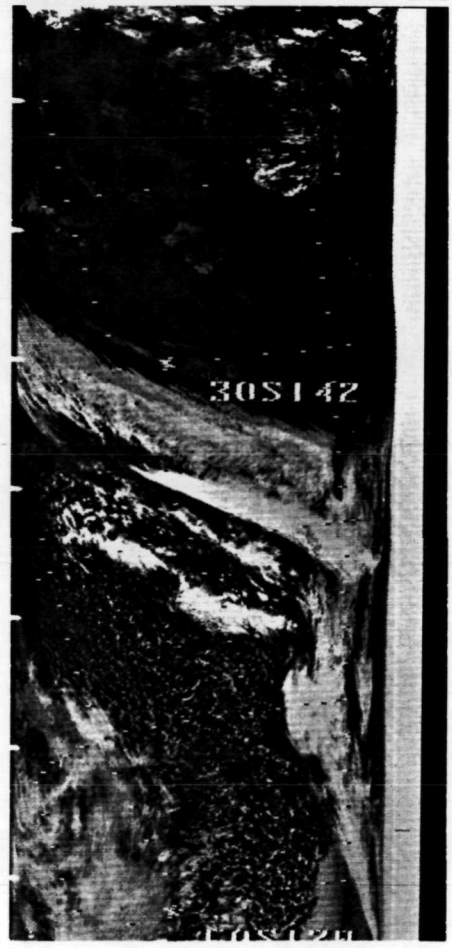

135
87

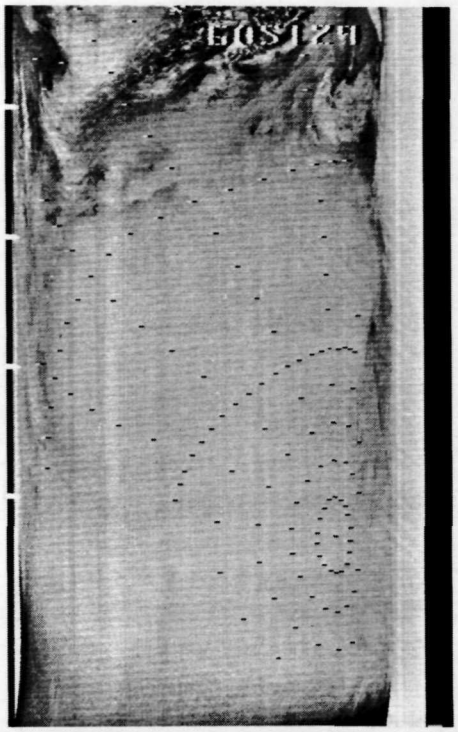
135
87

136
88

136
88
30N133

136
89
30S117

137
90

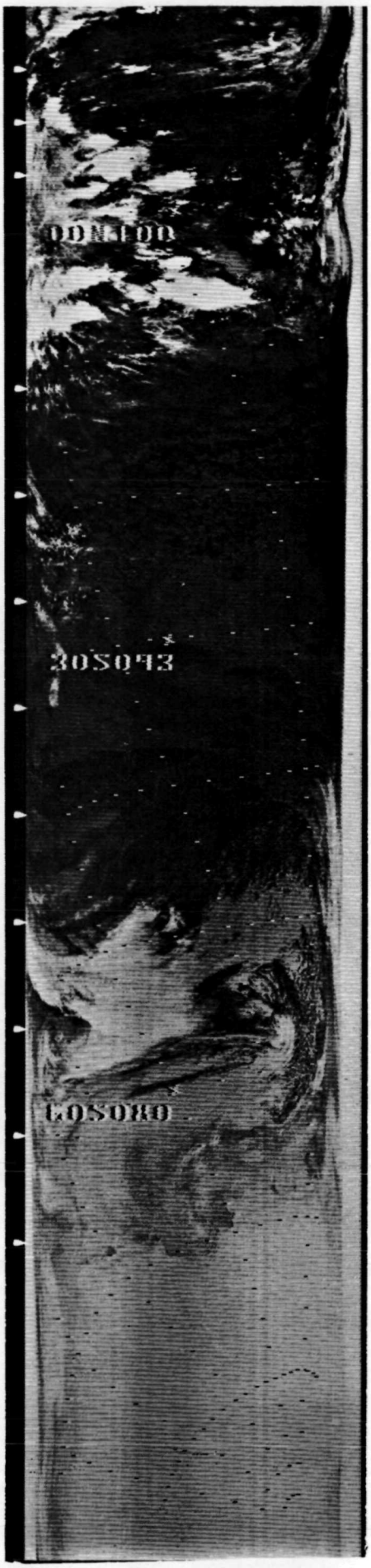

137
90

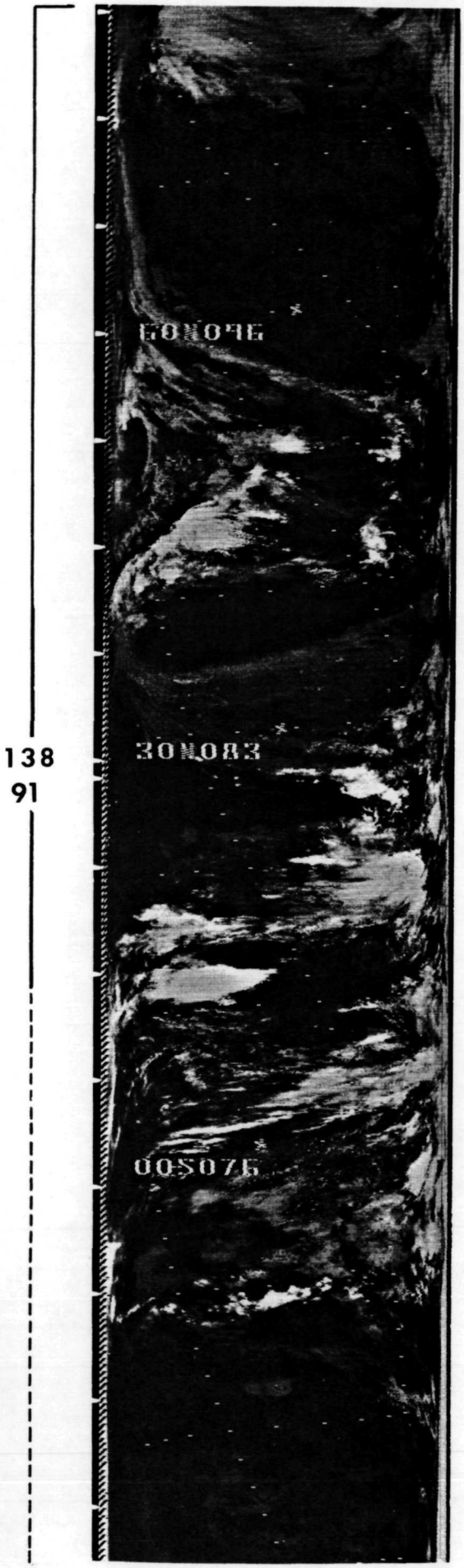
138
91

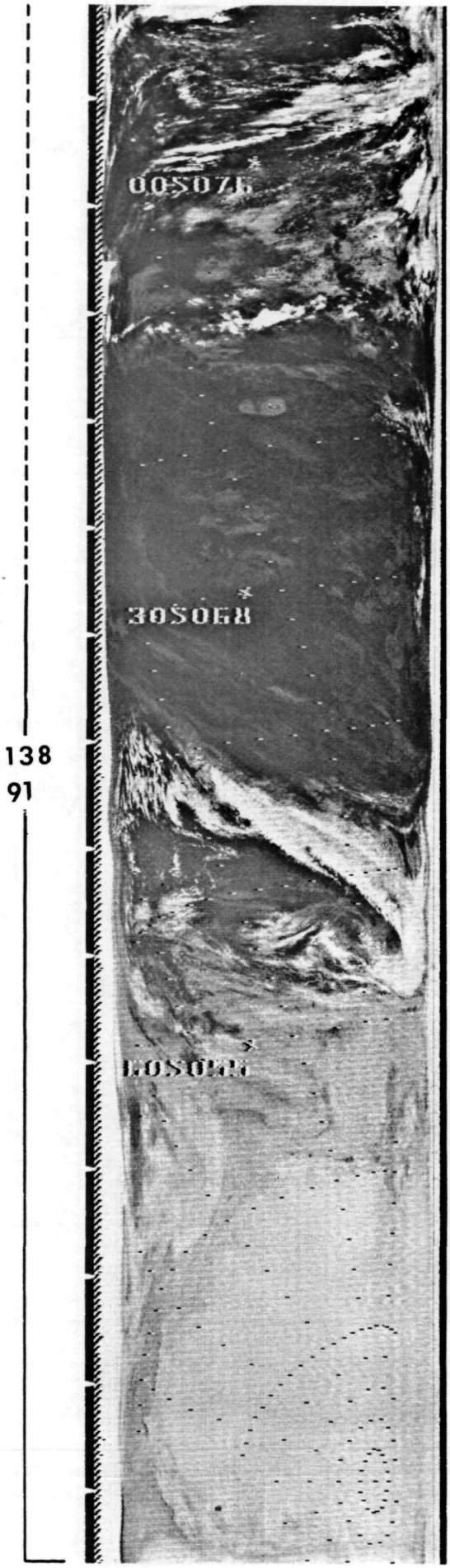
138
91

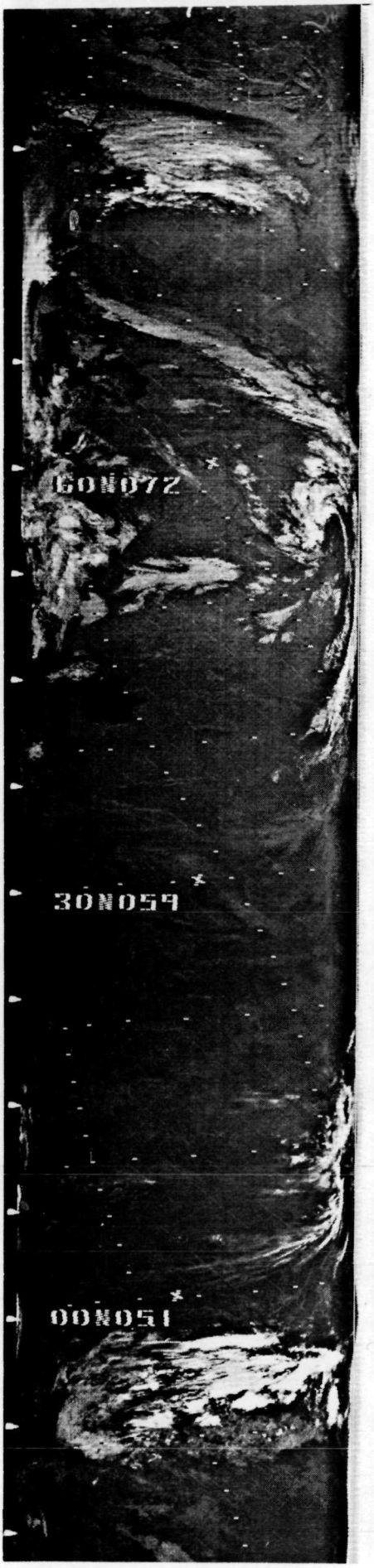

139
92

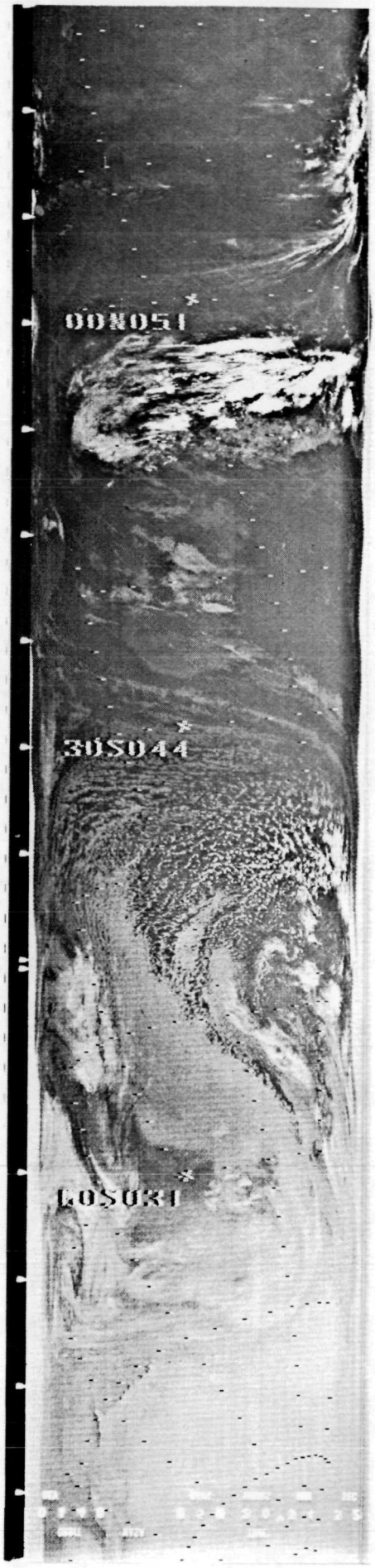

139
92

145
93

145
93

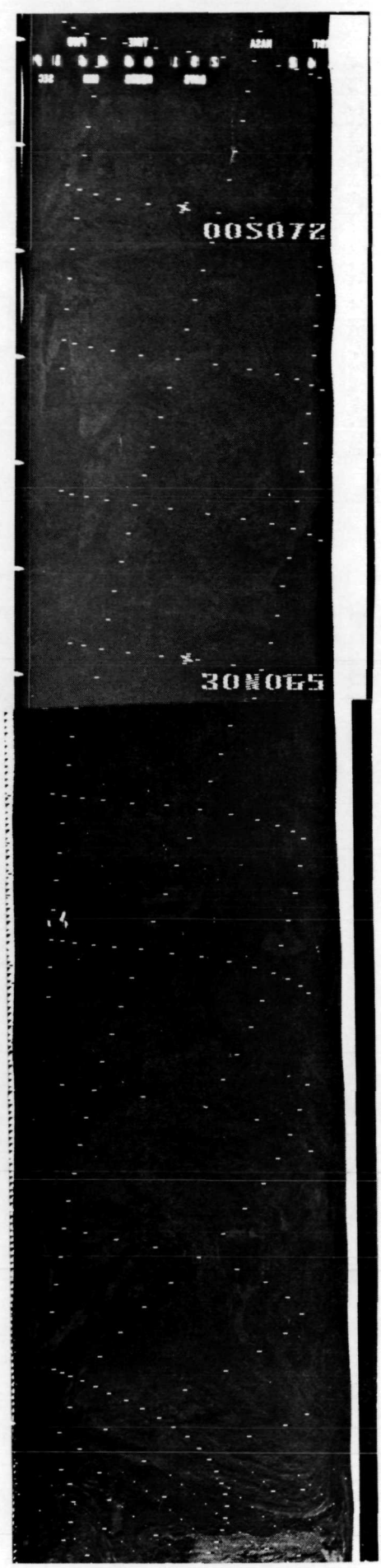

145/146
94

146
95

146
95

159
96

160
97

161
98

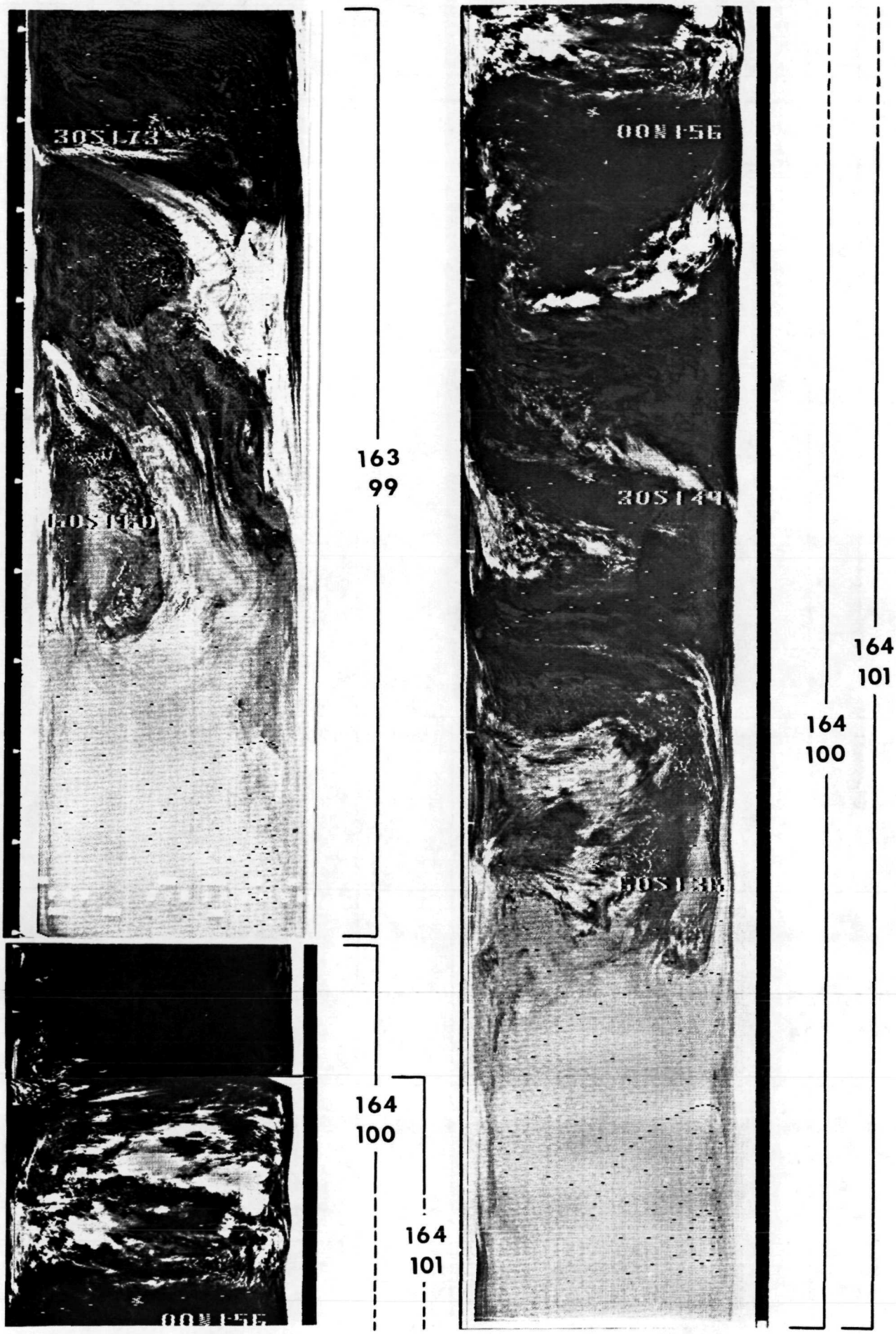
30S173
00N156
30S149
163
99
164
101
164
100
164
100
164
101

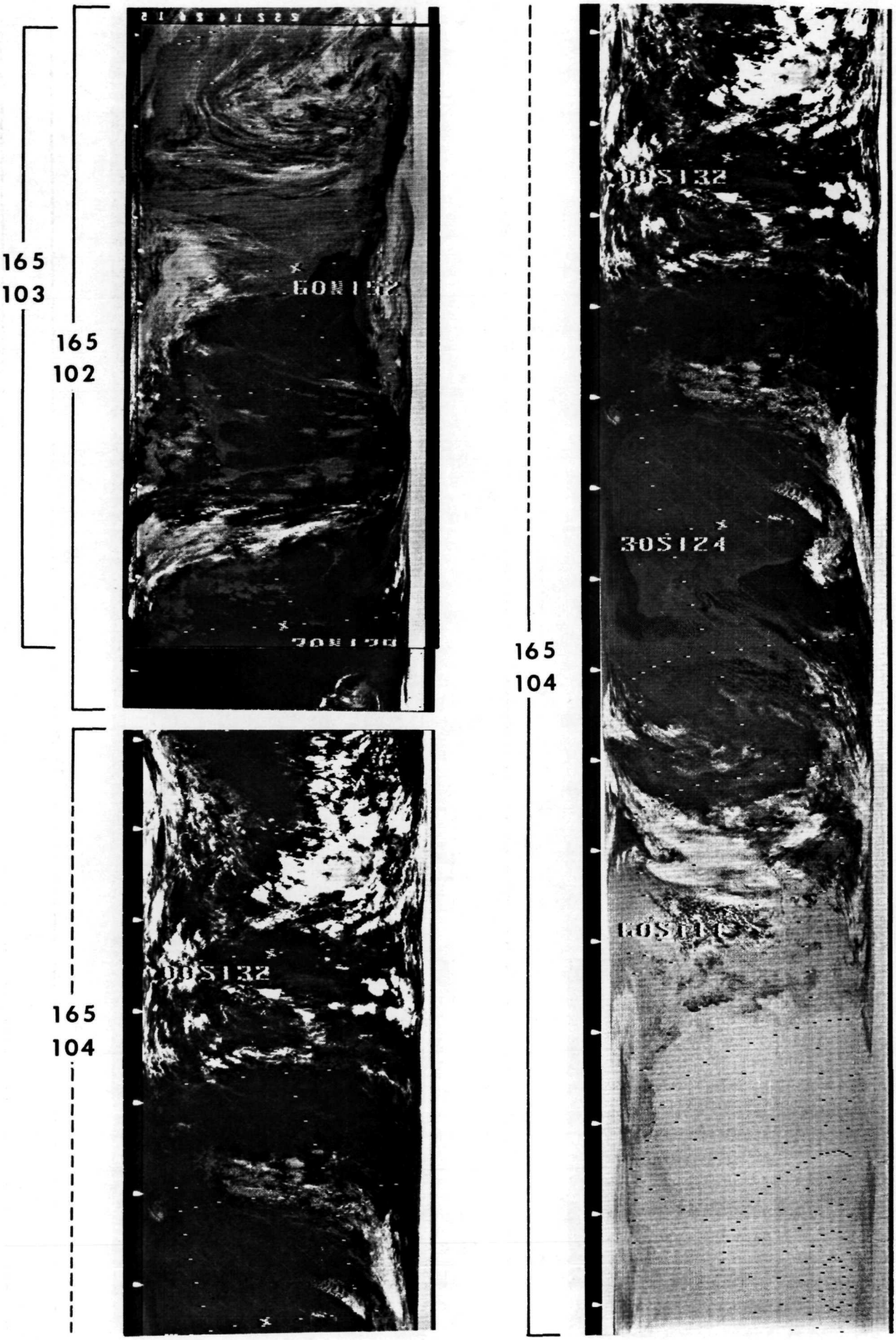
165
103
165
102
165
104
165
104

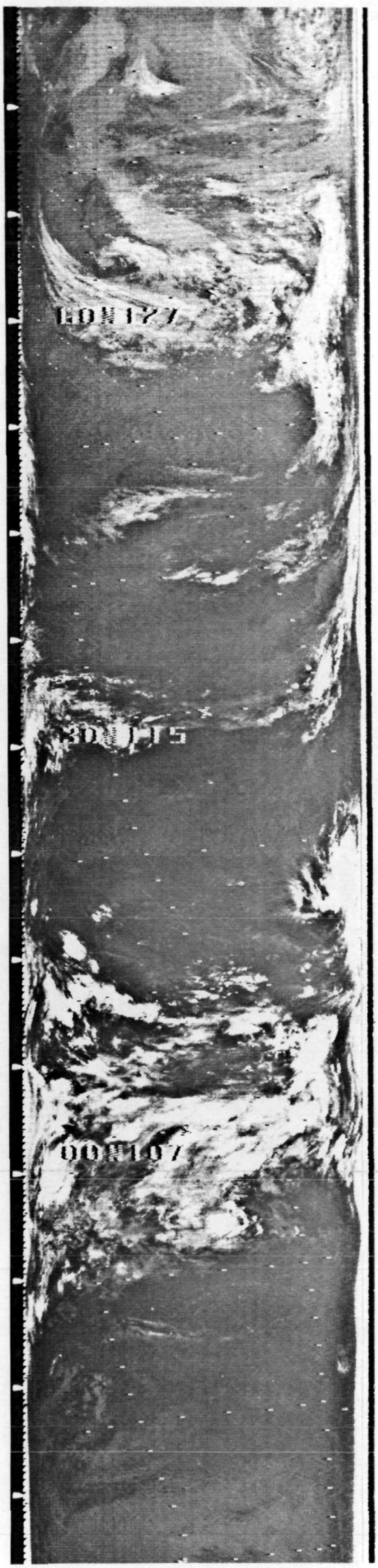
166
105

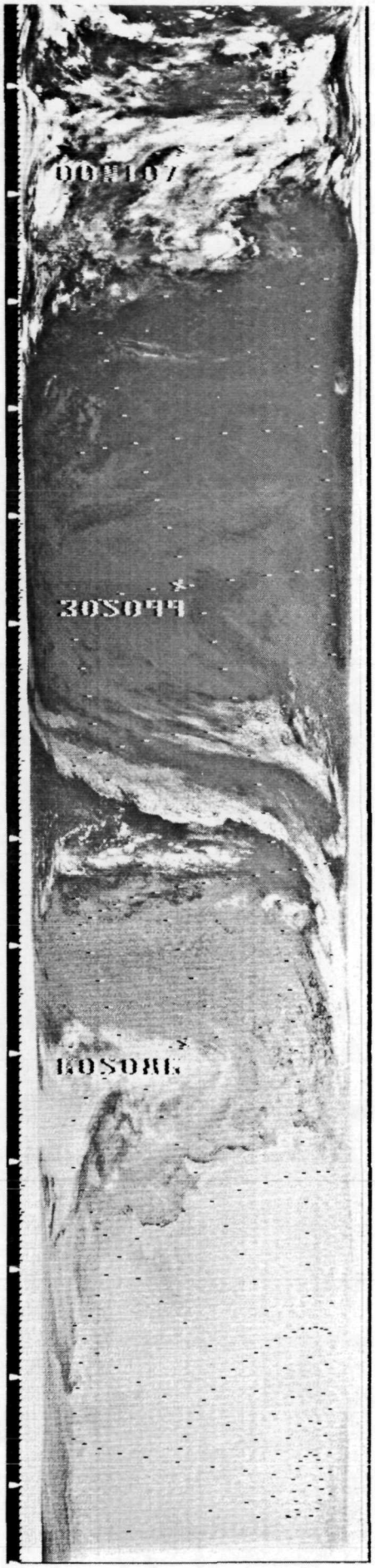
166
105

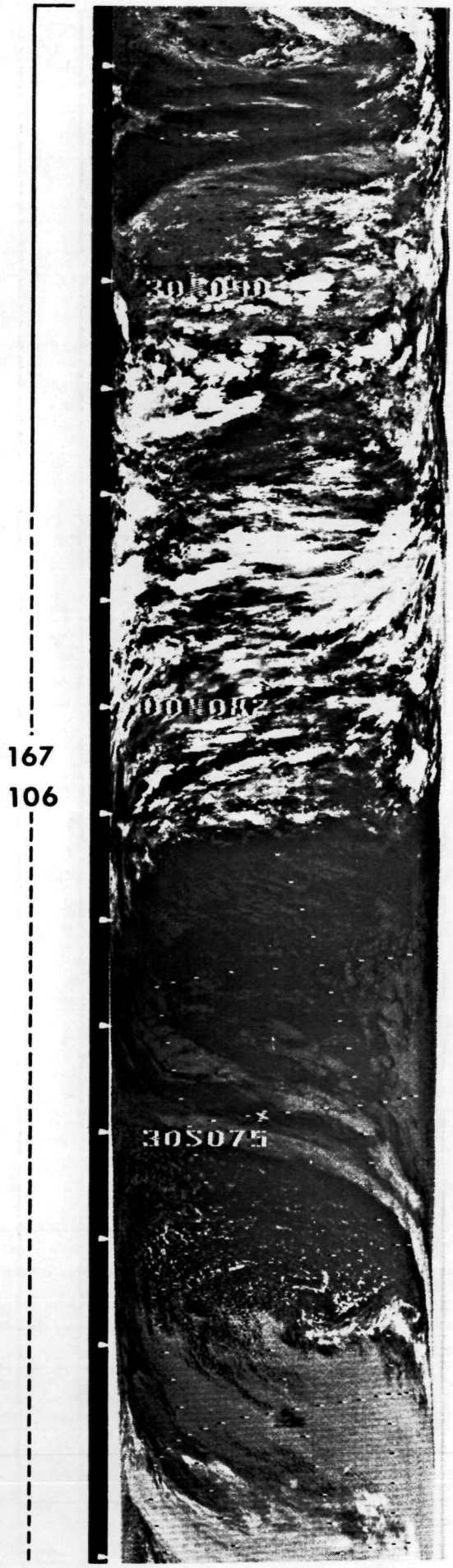
167
106
30S075

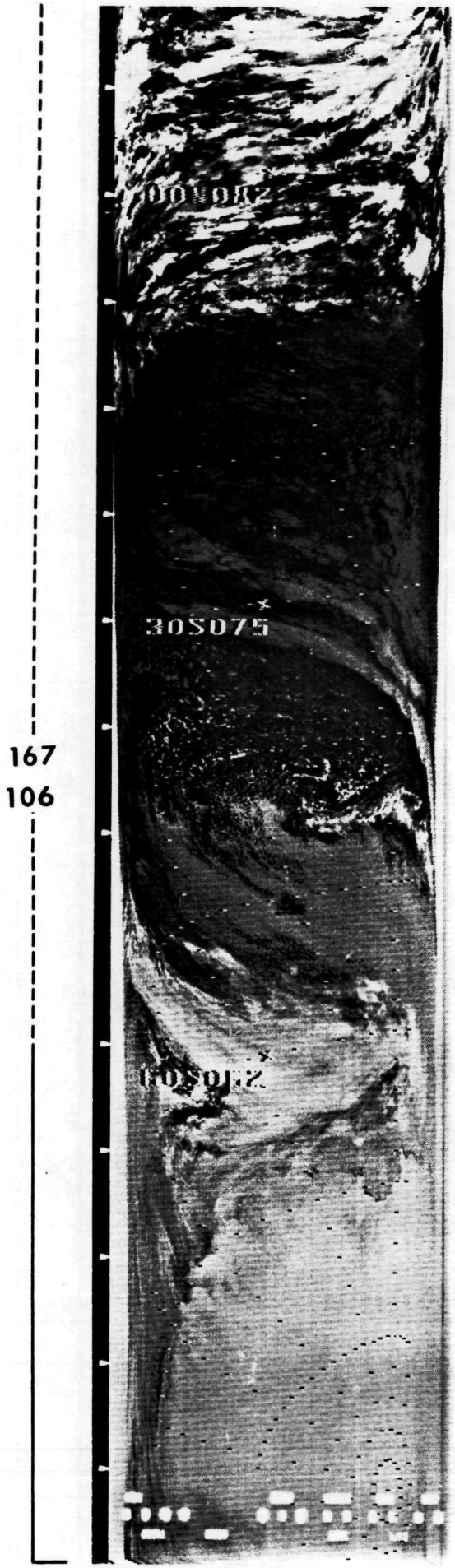
167
106
30S075

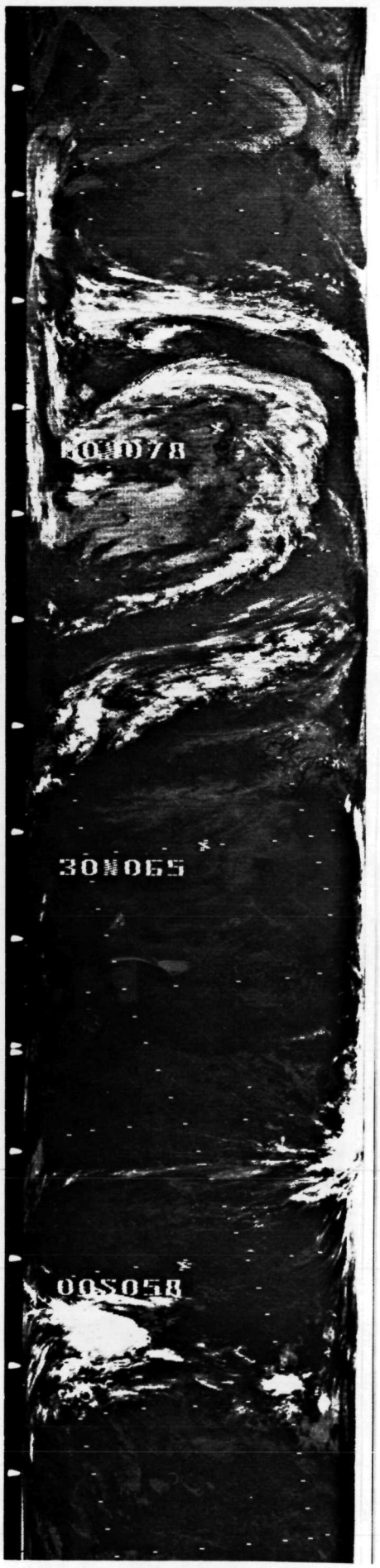

168
107

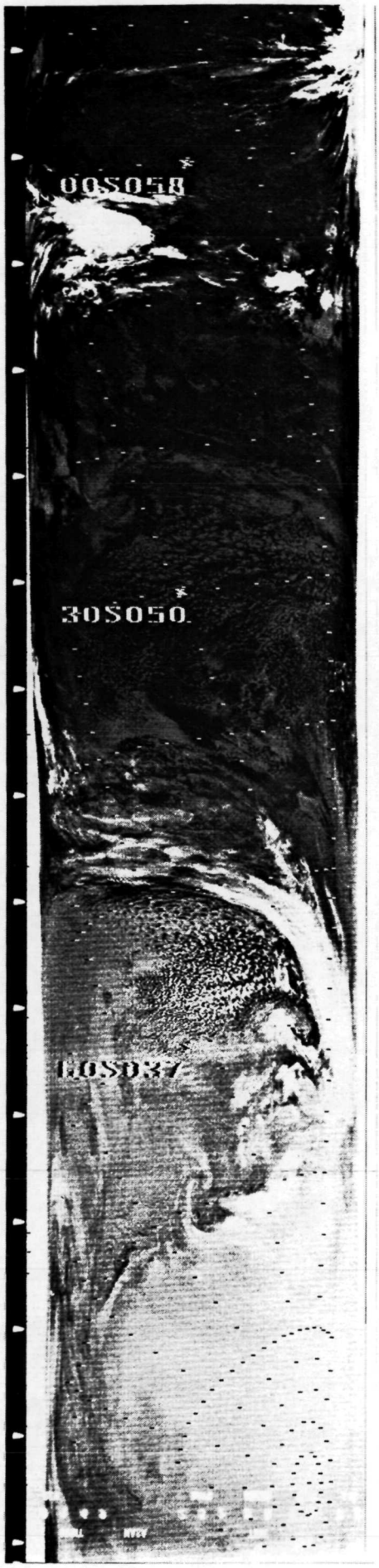

168
107

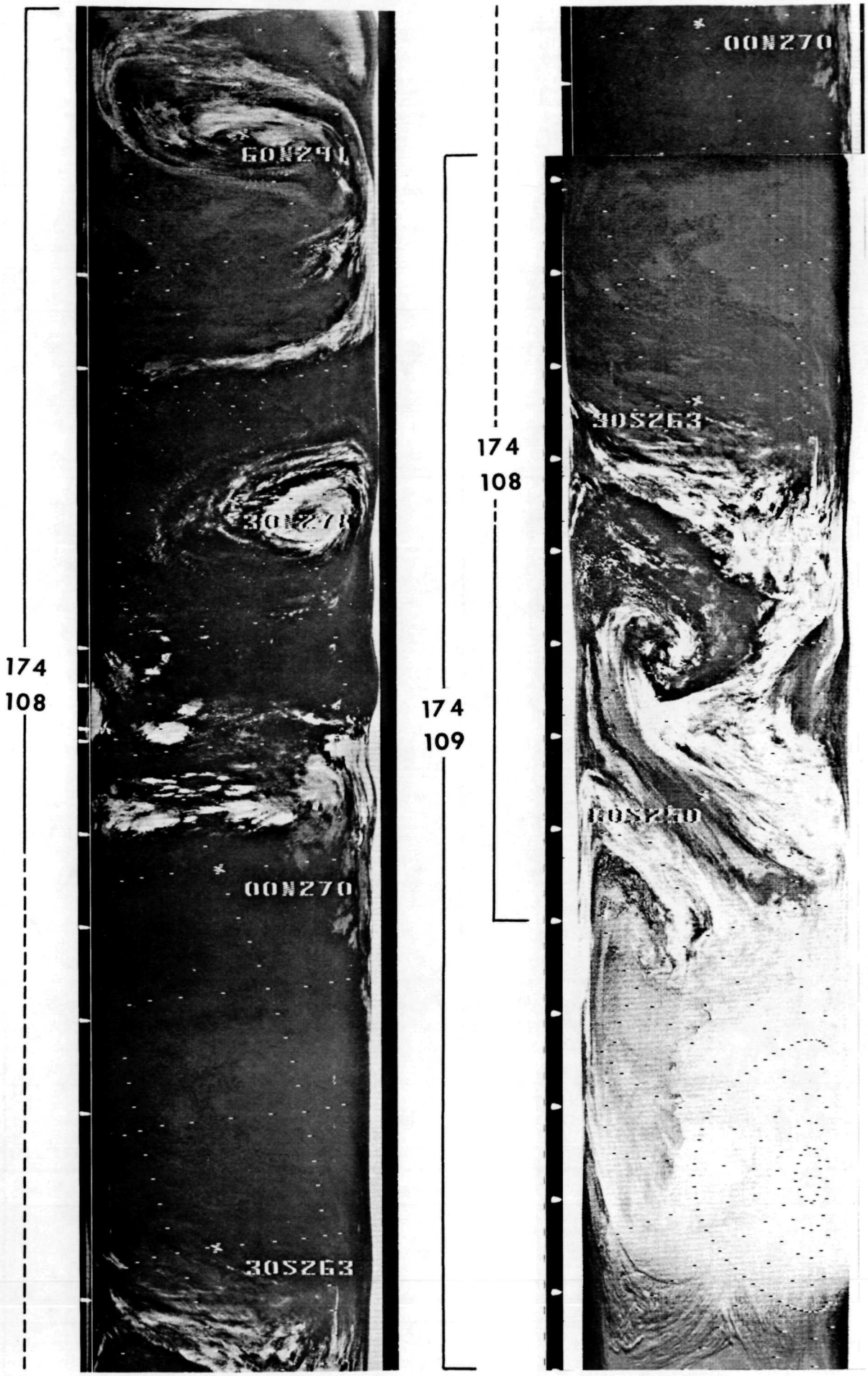
60N291
30N278
00N270
30S263
174
108
174
109
174
108
00N270
30S263
10S250

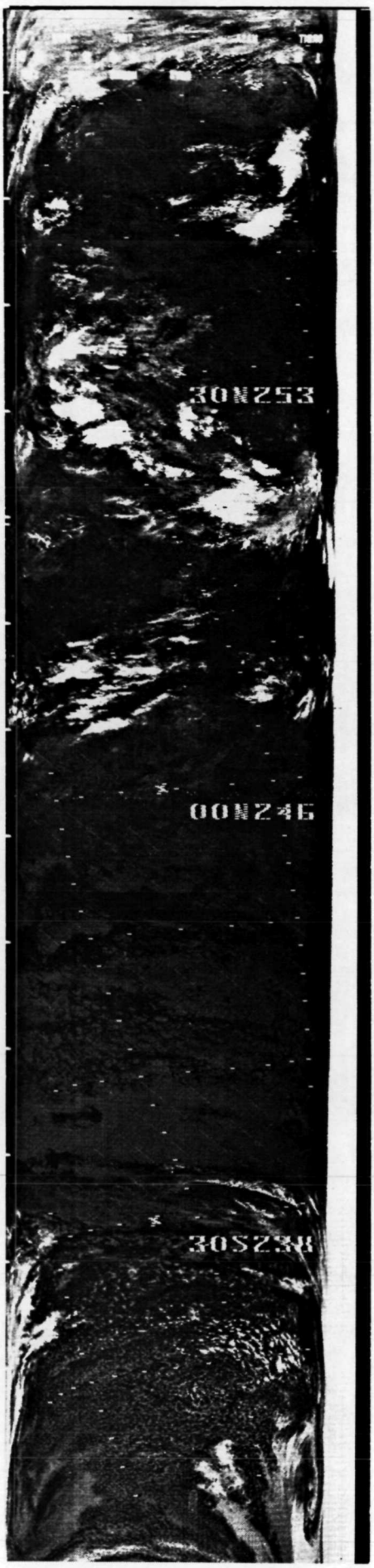

175
110

175
111

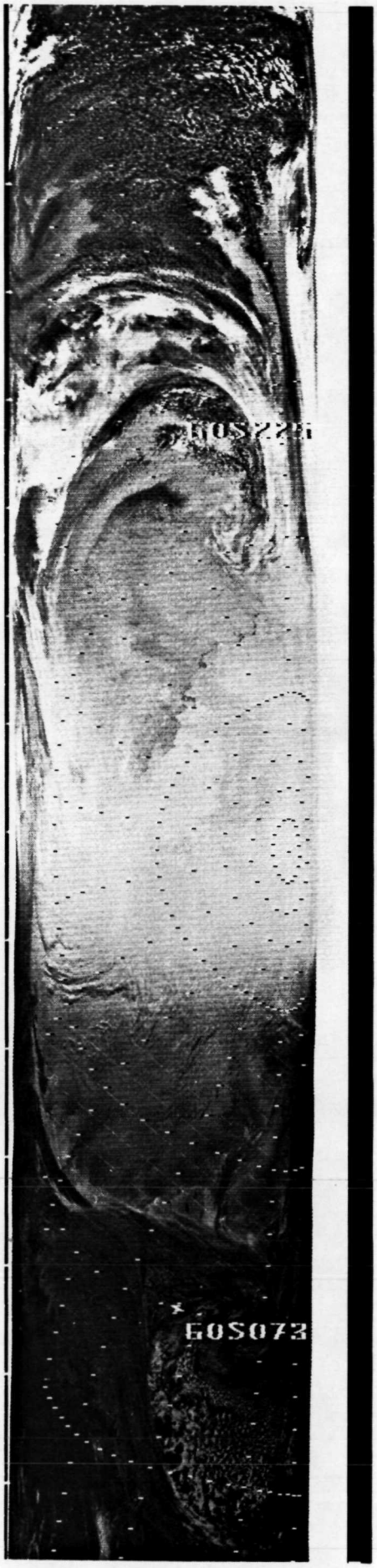

175
111

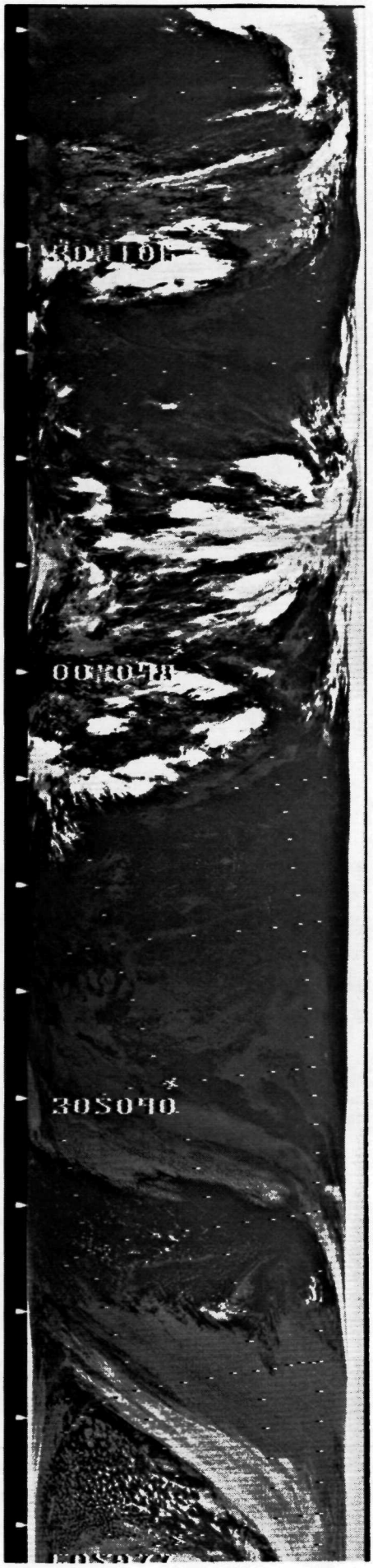

181
112

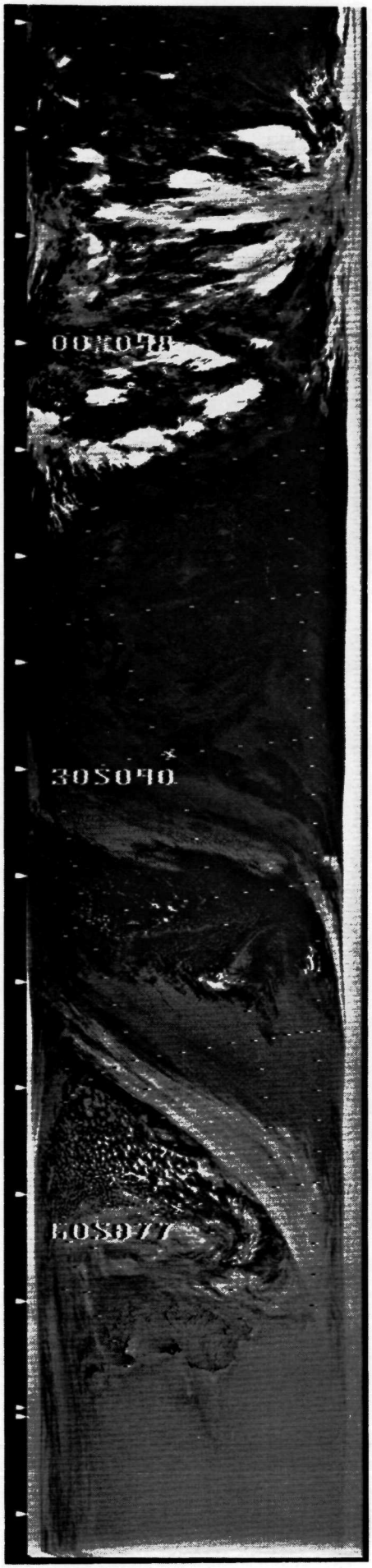

181
112

182
113

182
113

183
114

183
114

188
117

188
116

187
115

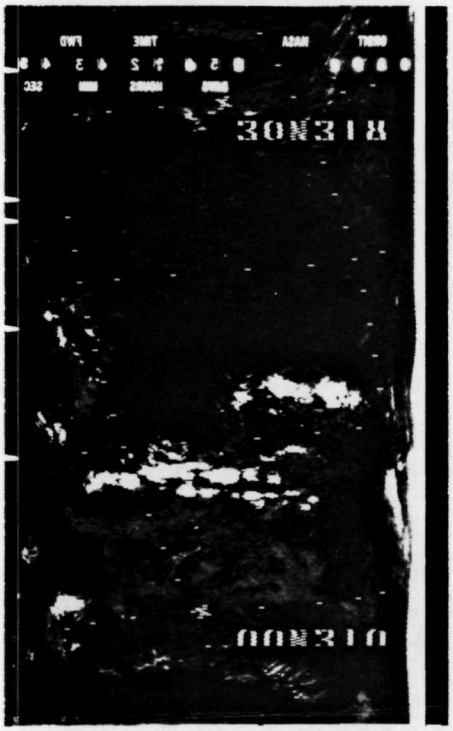

189
118

188
116

189
119

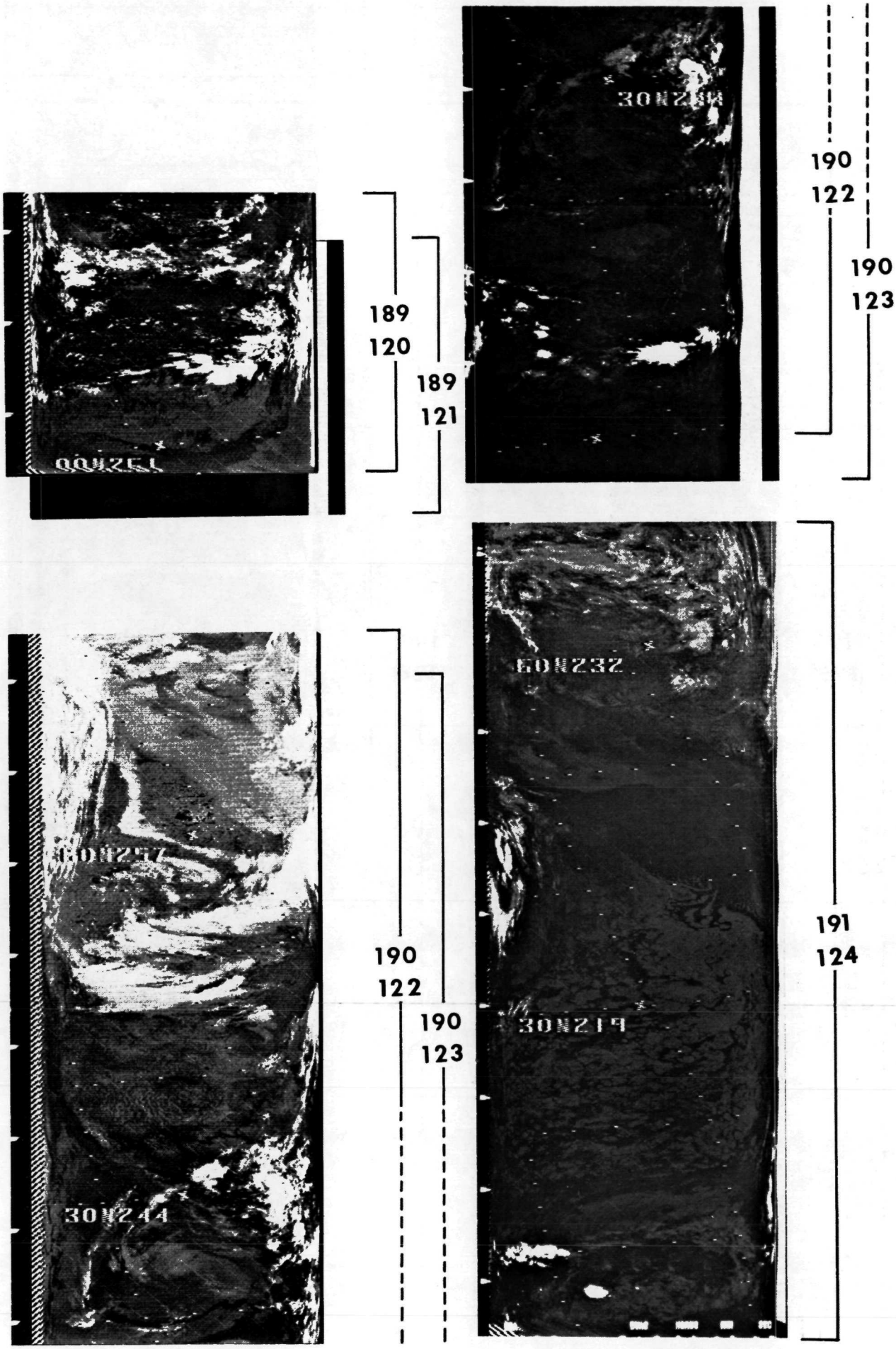
189
120
189
121
190
122
190
123
190
122
190
123
191
124

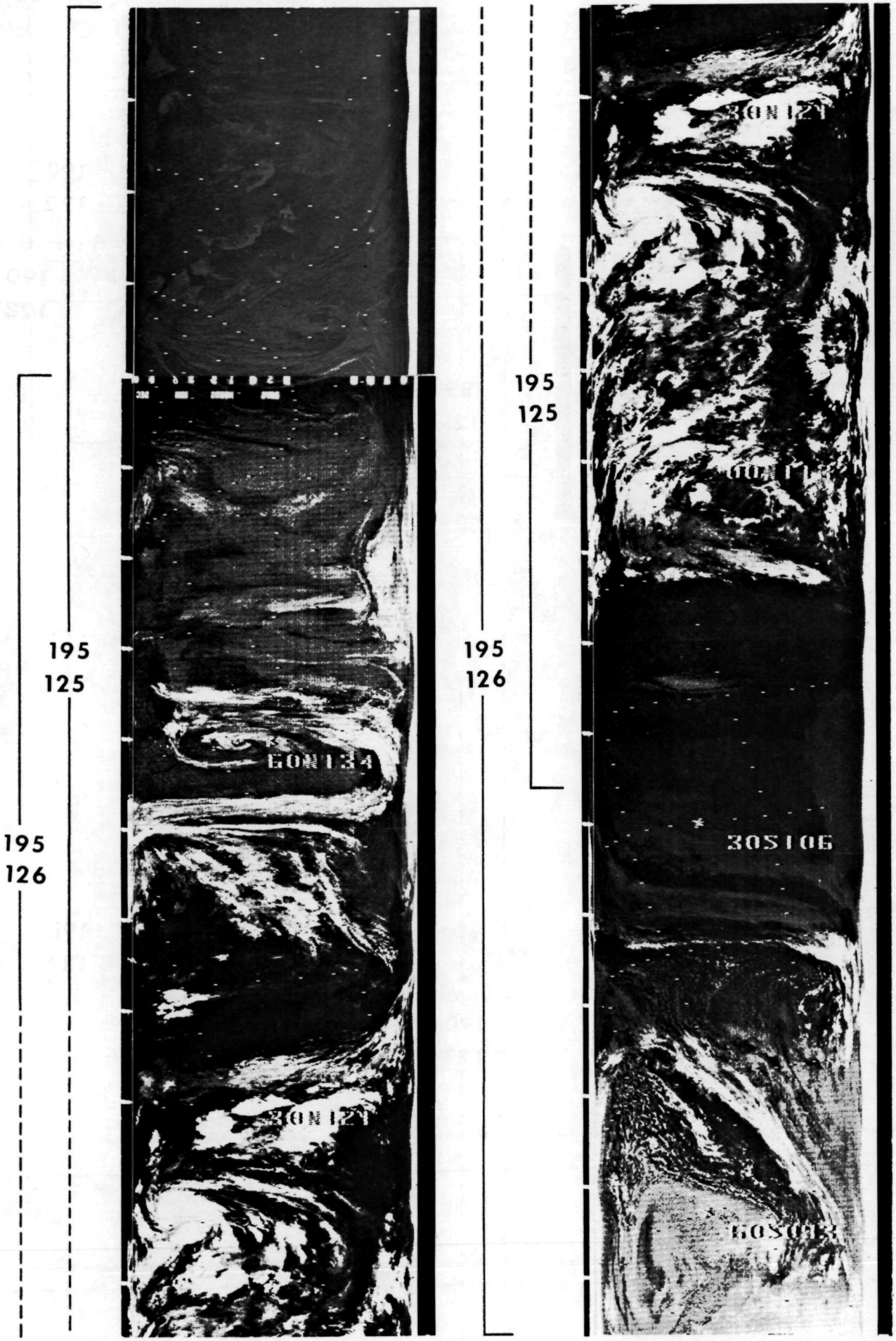
195
125
195
126
60N134
30N121
195
125
195
126
30N121
30S106

195
127

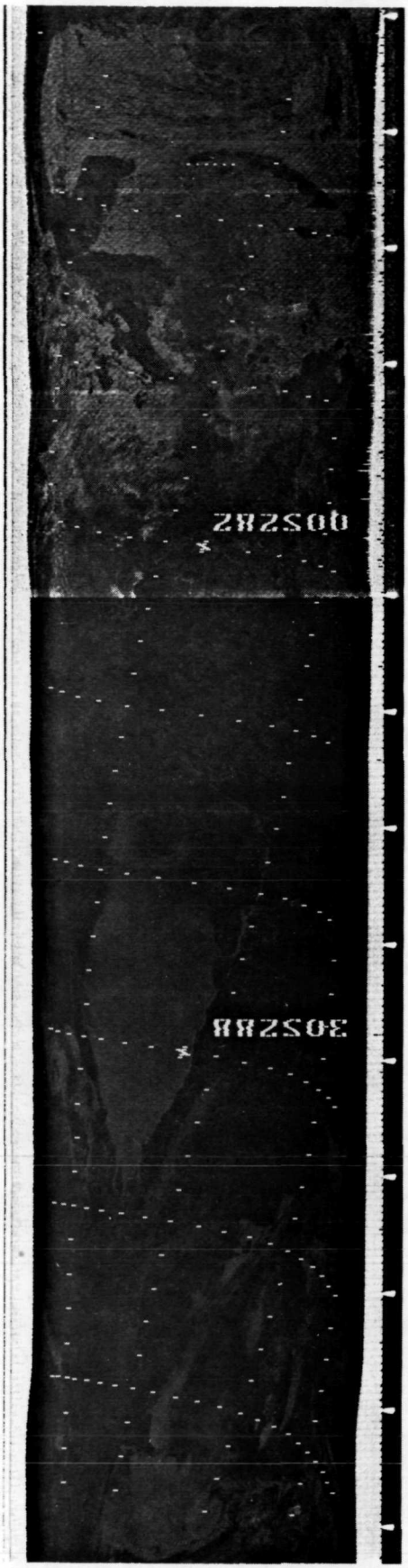

195/196
128

196
129

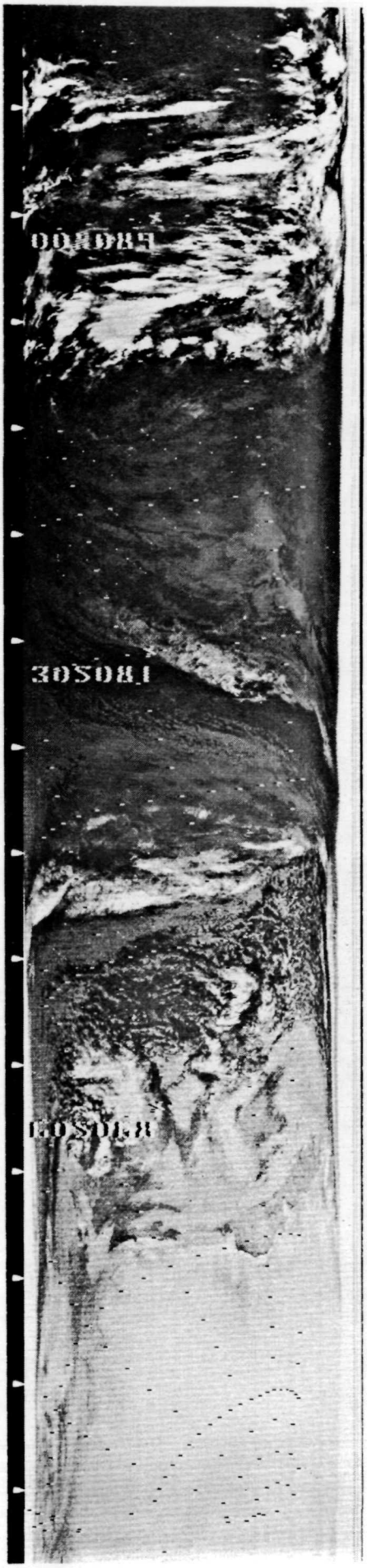

196
129

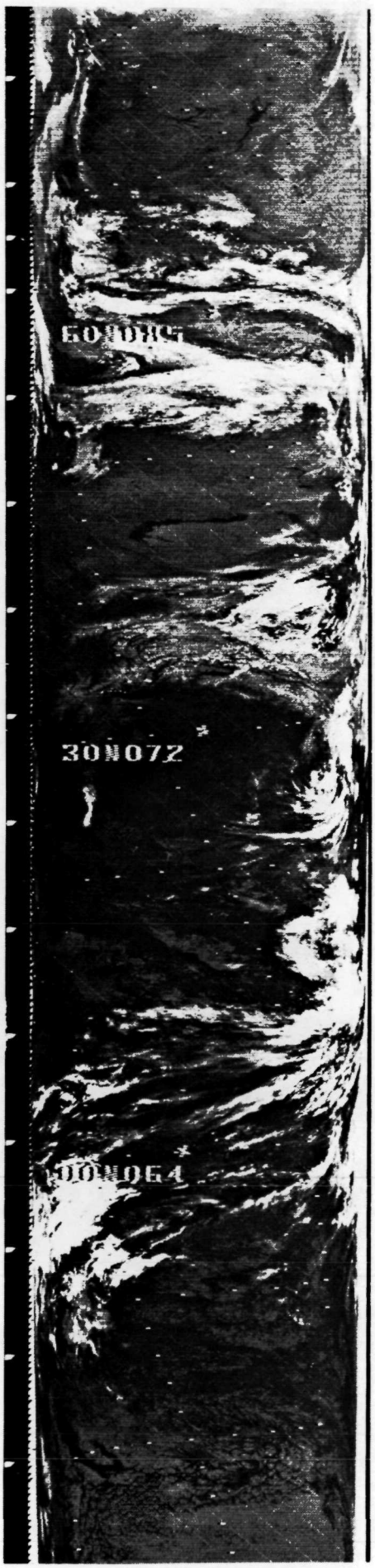

197
130

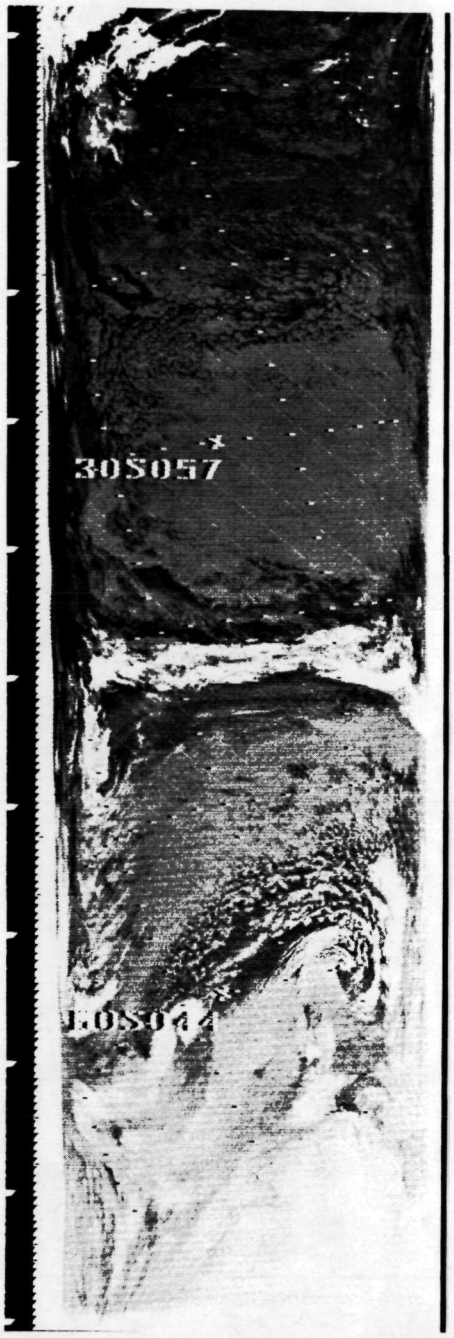

197
130

201
131

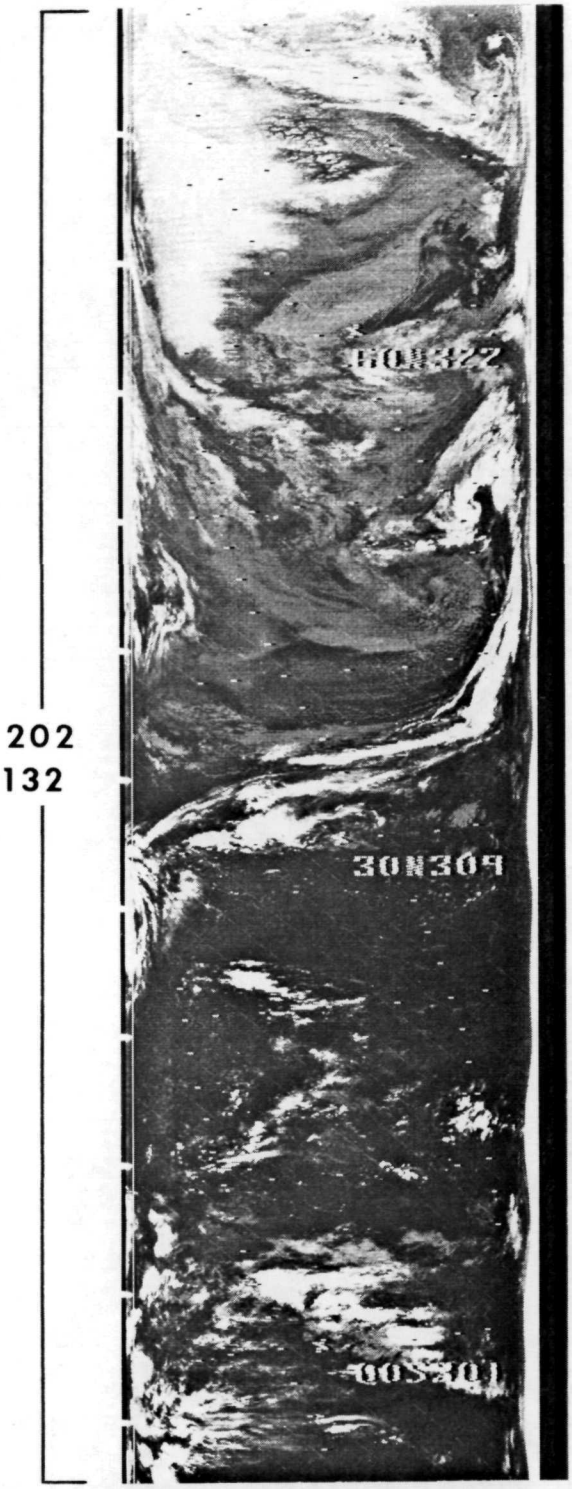
202
132

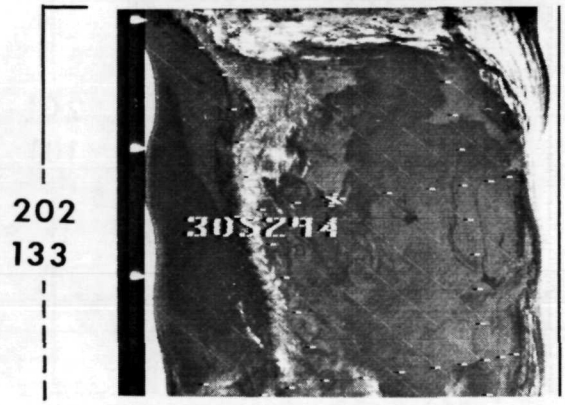
202
133

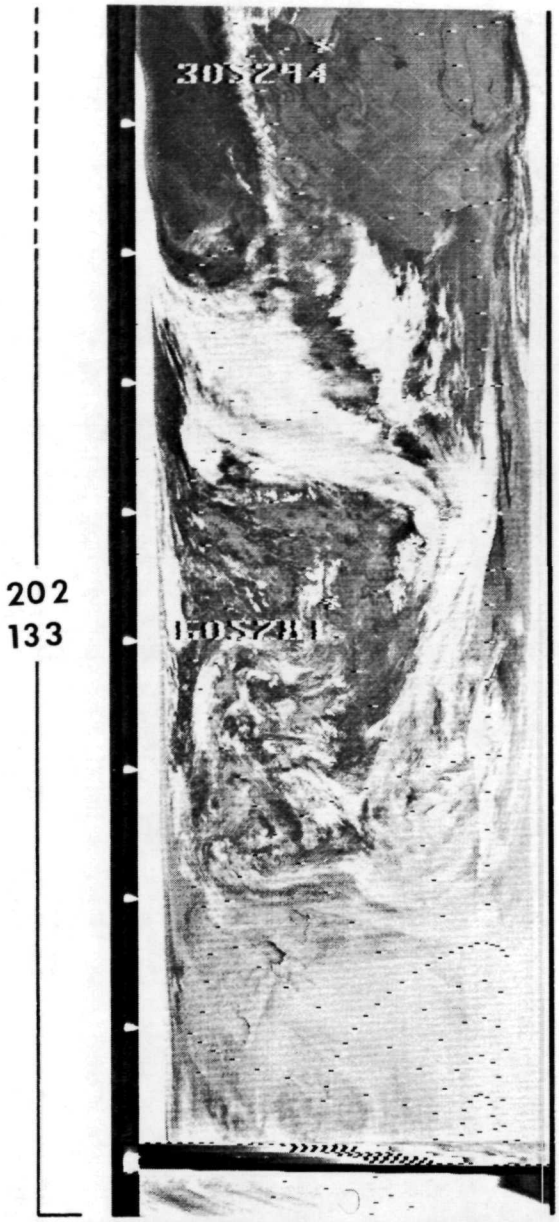
202
133

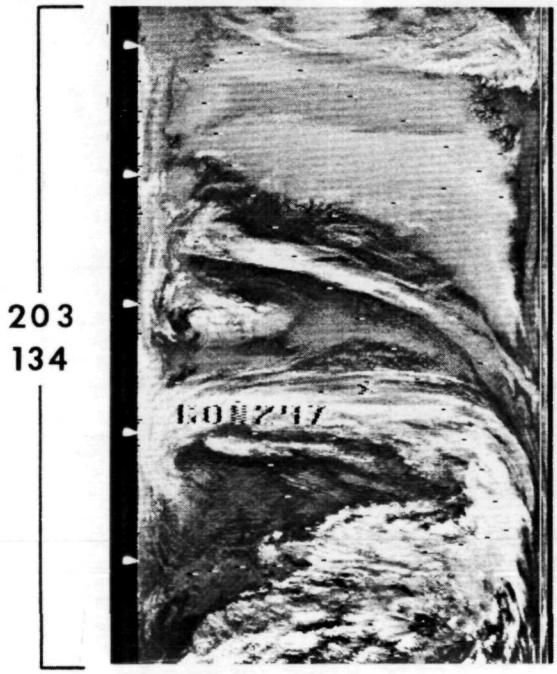
203
134

205
135

205
136

205
137

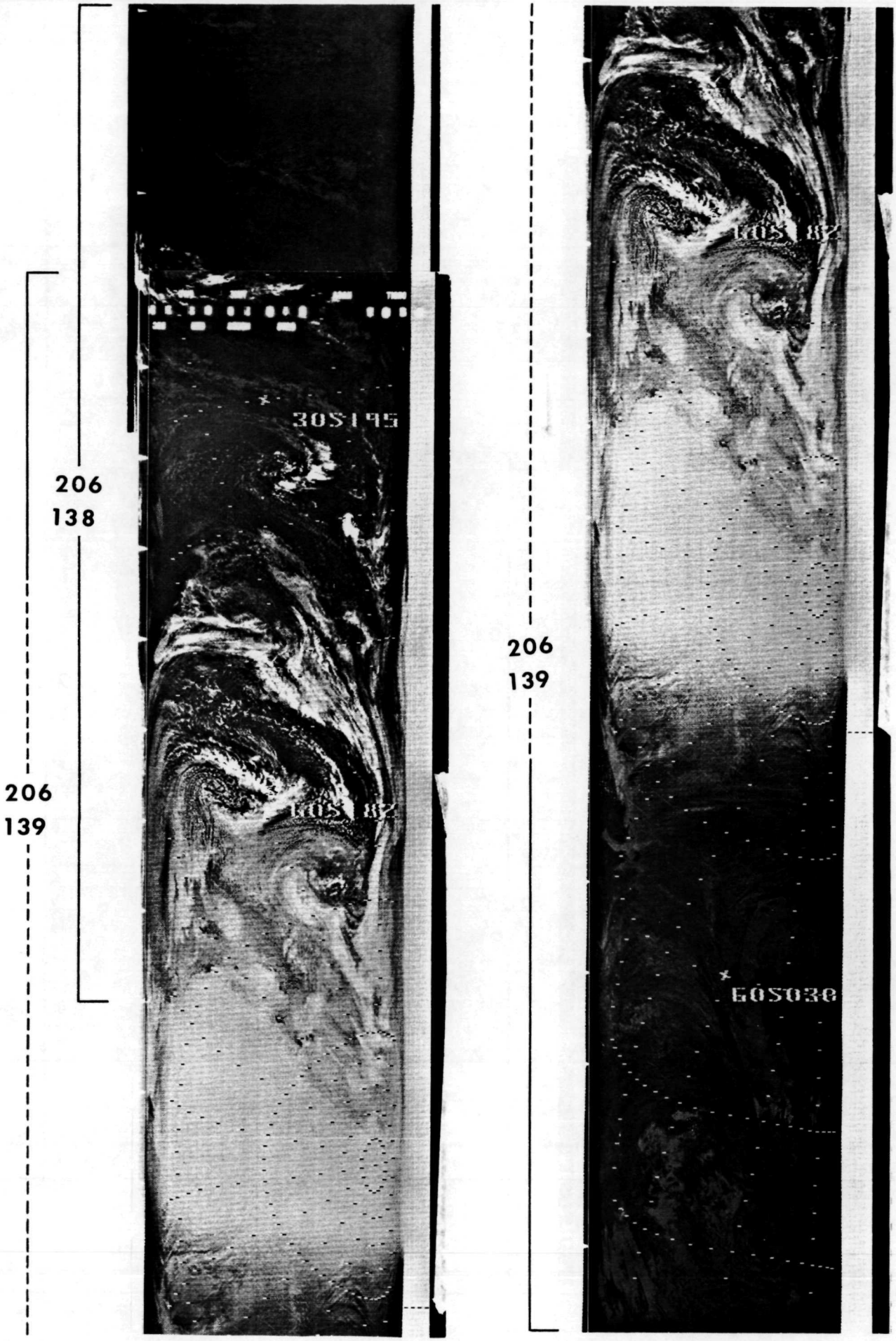
206
138
206
139
305195
605182
206
139
605182
605030

207
141

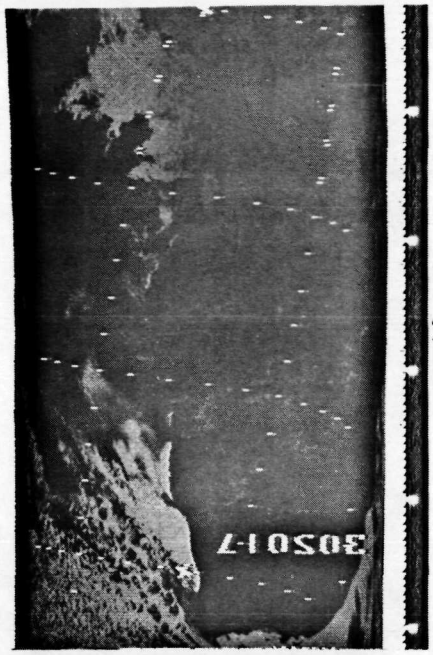

206 / 207
140

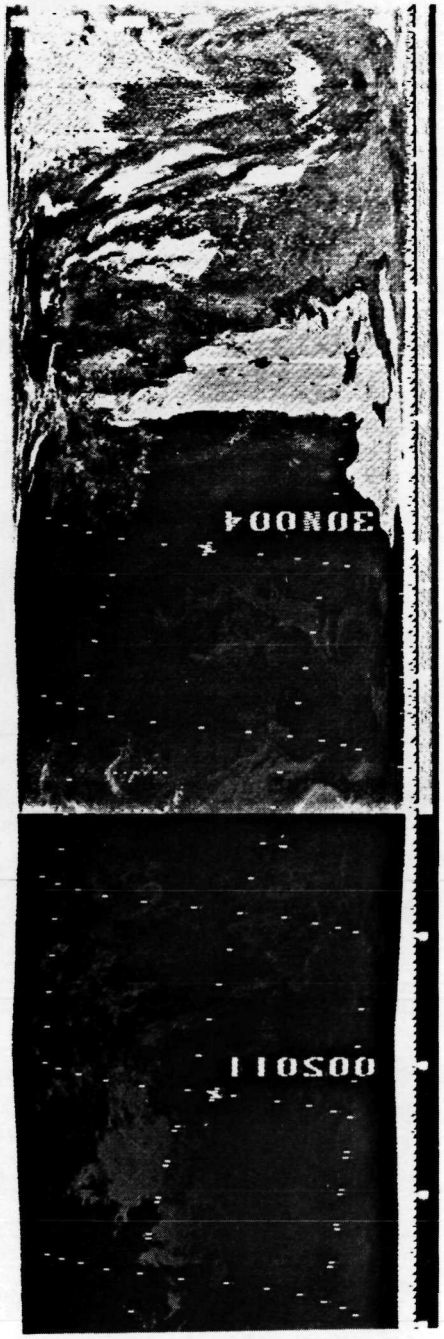

206/207
140

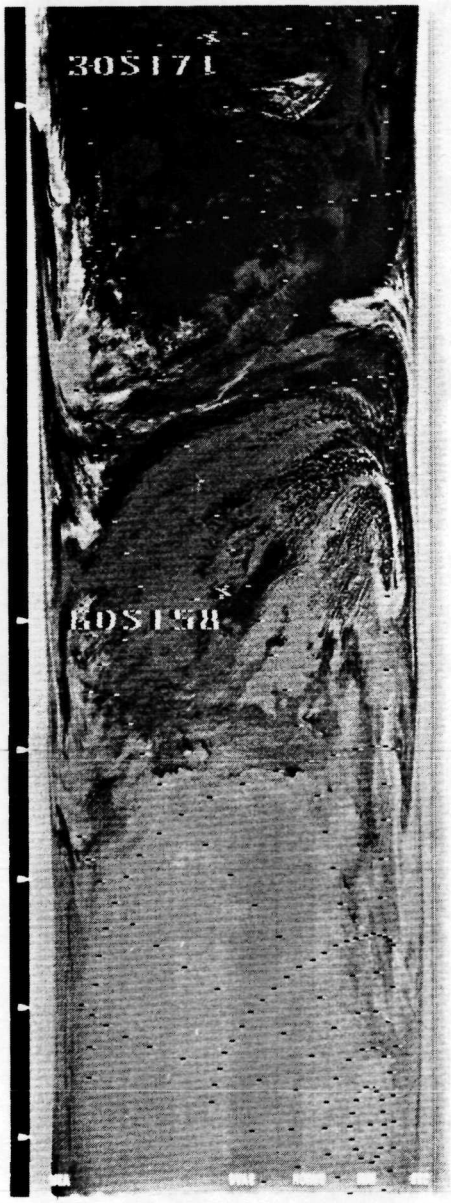

207
142

208
143

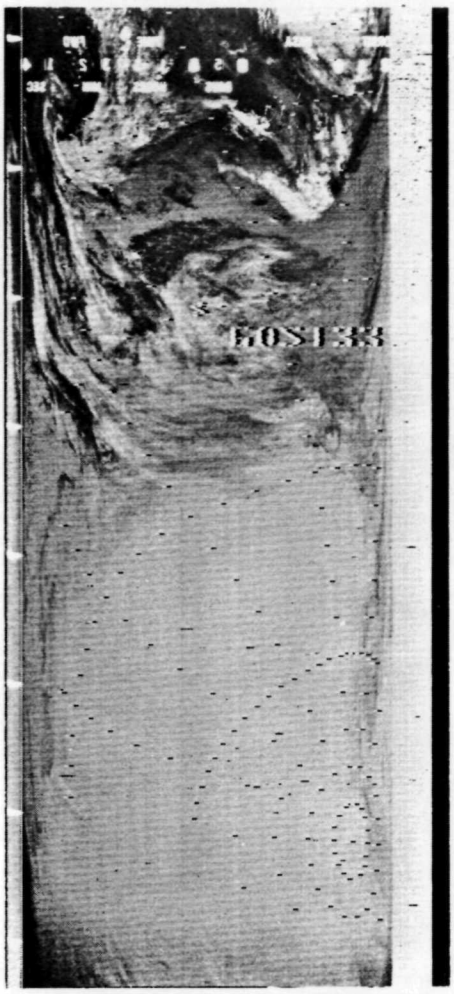

209
144

209
145

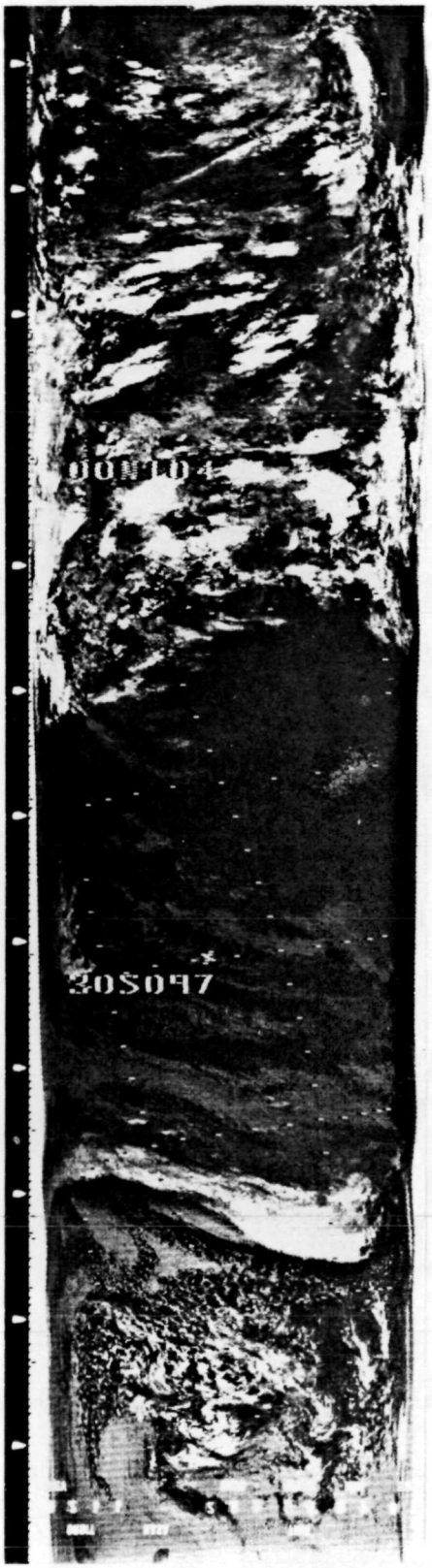

210
146

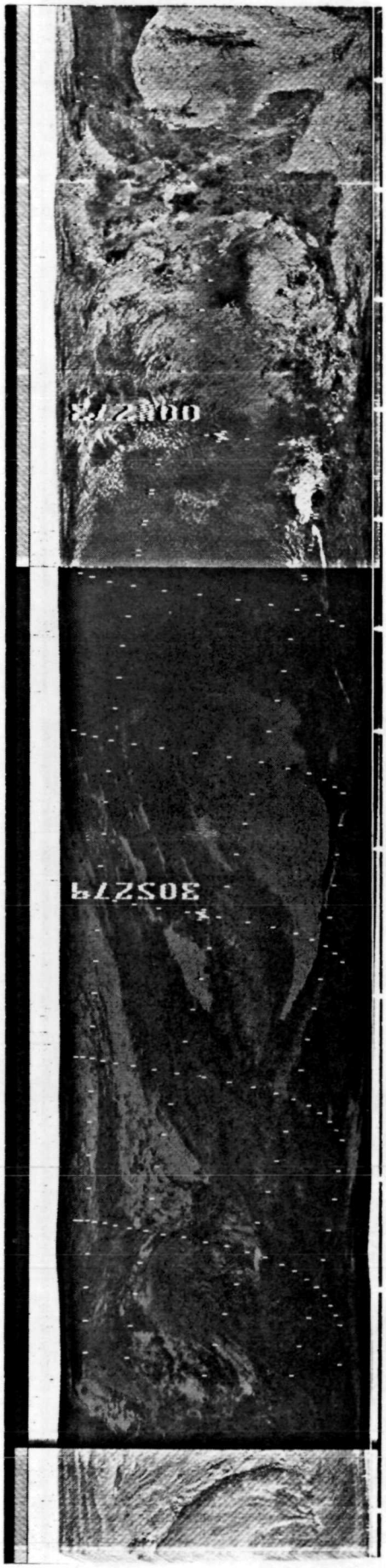

210/211
148

210
147

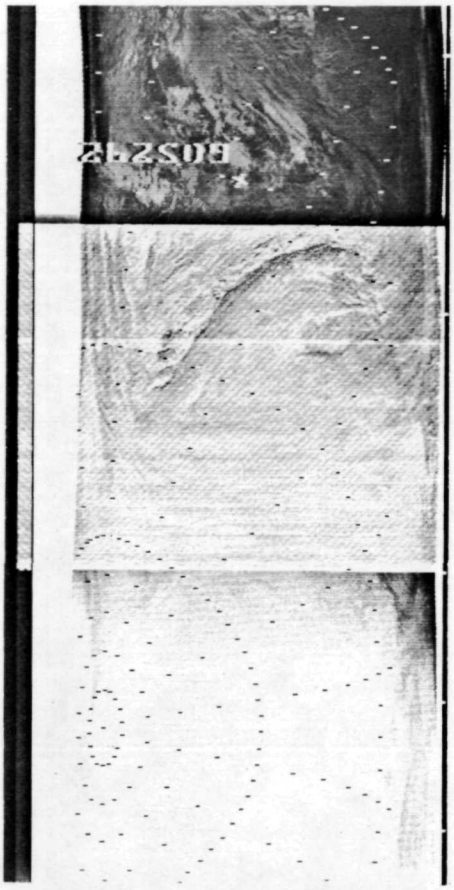

210
147

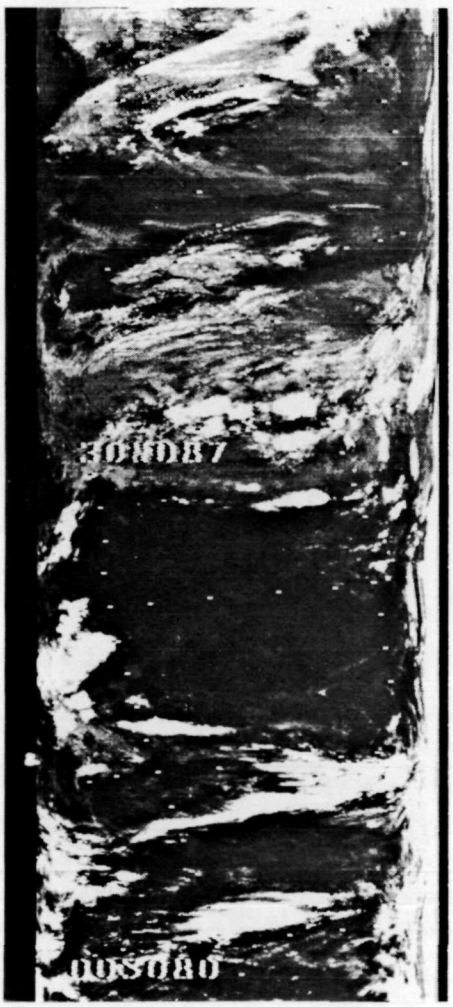

211
149

211
149

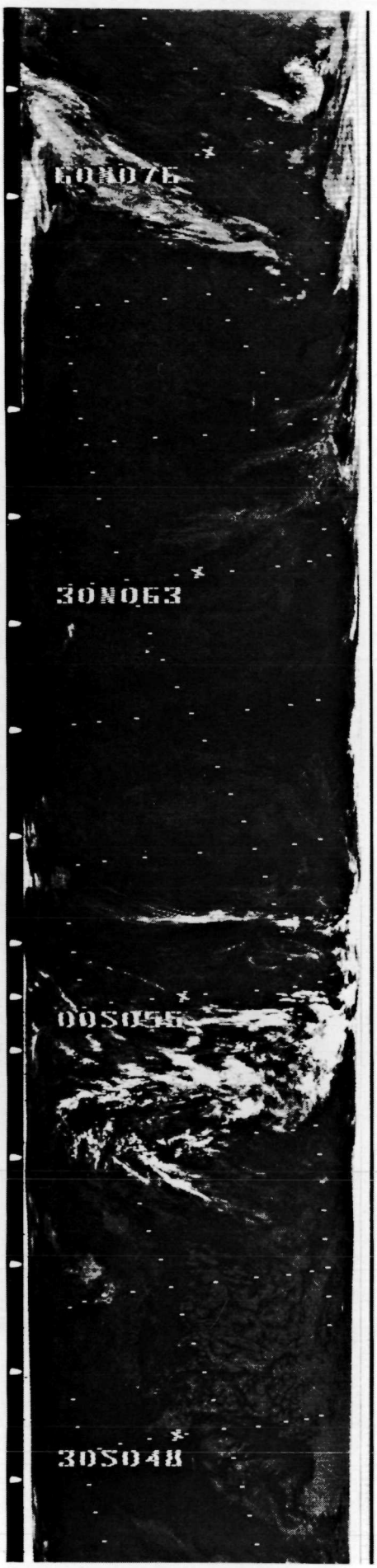

212
150

212
150

216
151

217
152

217
153

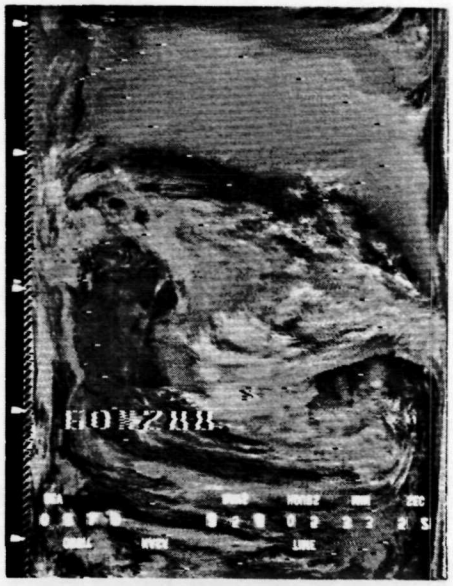

218
154

218
155

218
155

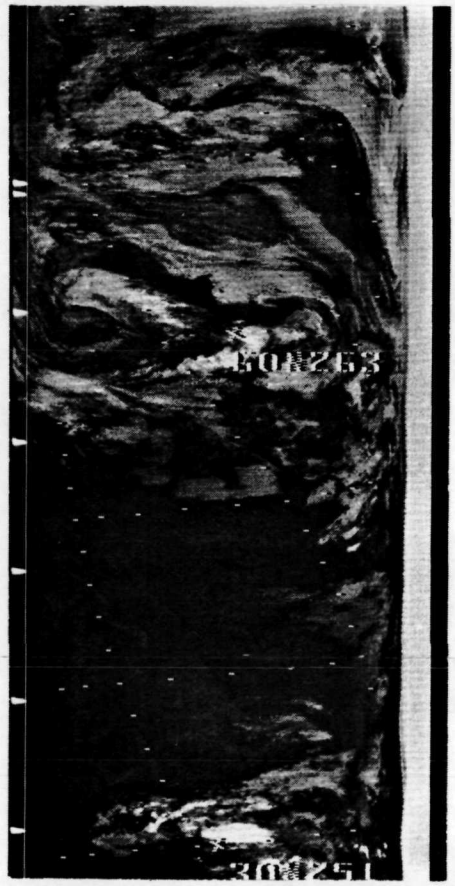

219
156

219
157

219
158

220
159

221
160

221
161

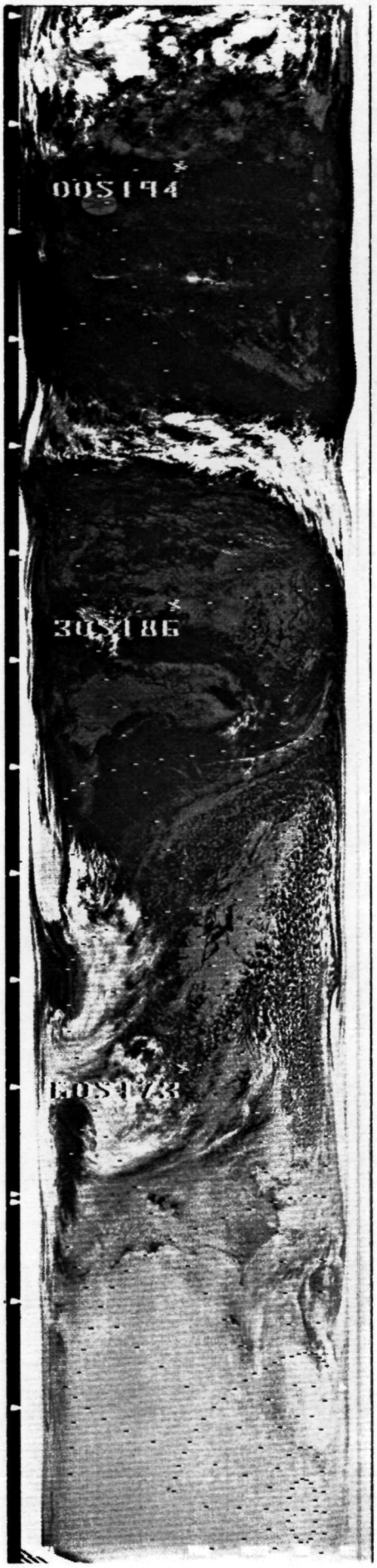

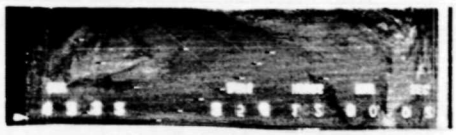

222
162

222
163

223
164

223
165

224
166

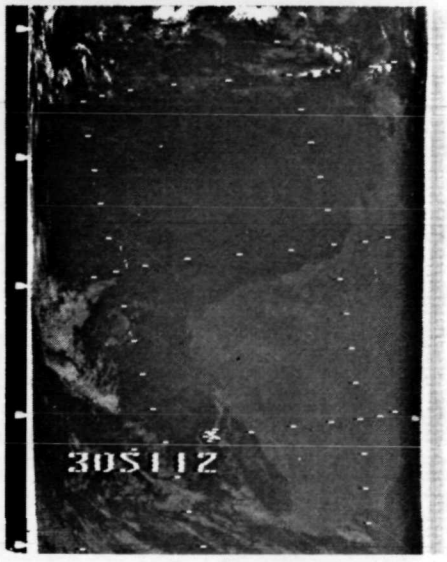

224
167

224
167

224
168

225
169

225
169

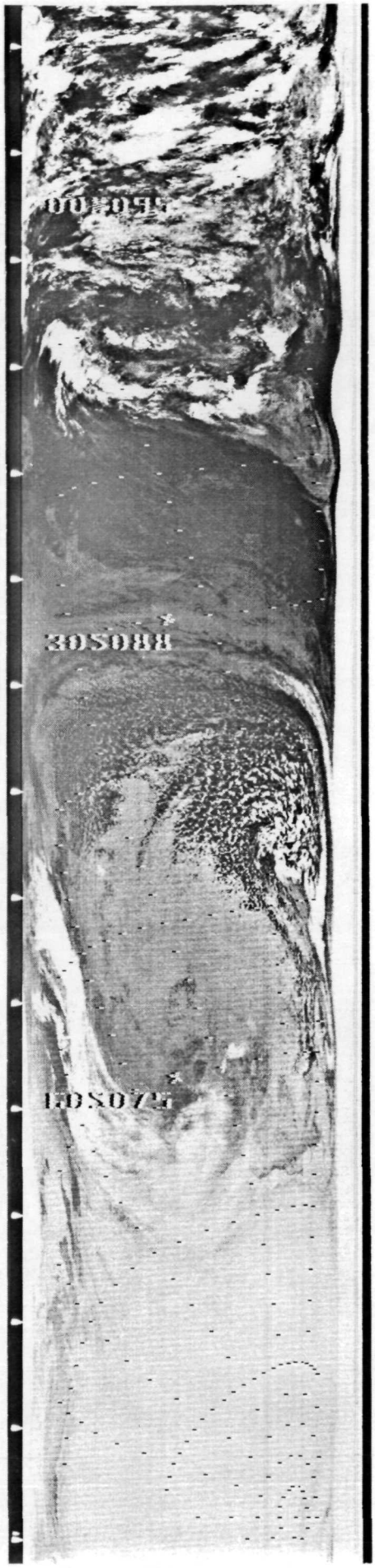

226
170

226
171

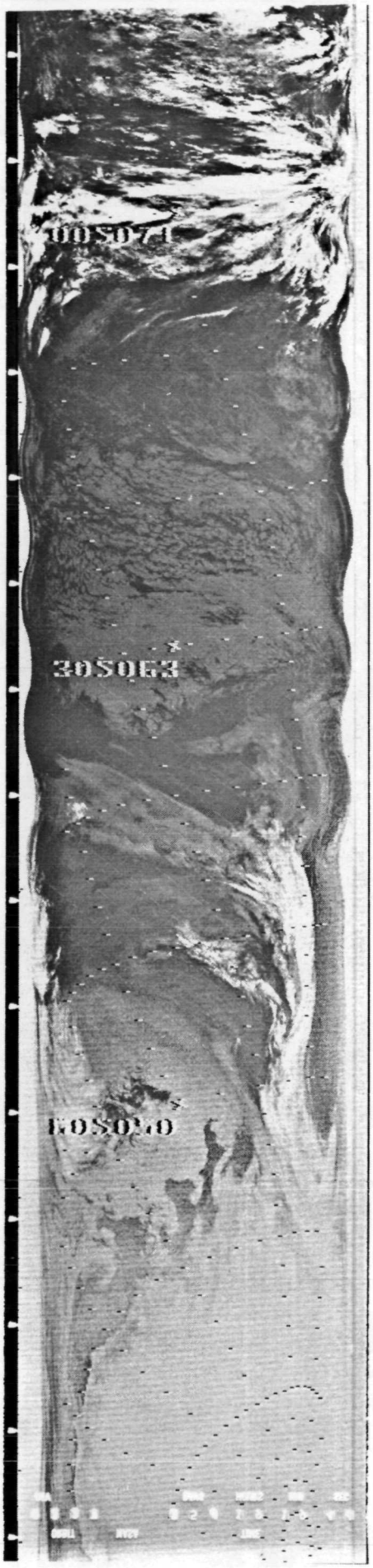

226
171

229
172
30N182

229
172
60N017
30N005

005185
236
173

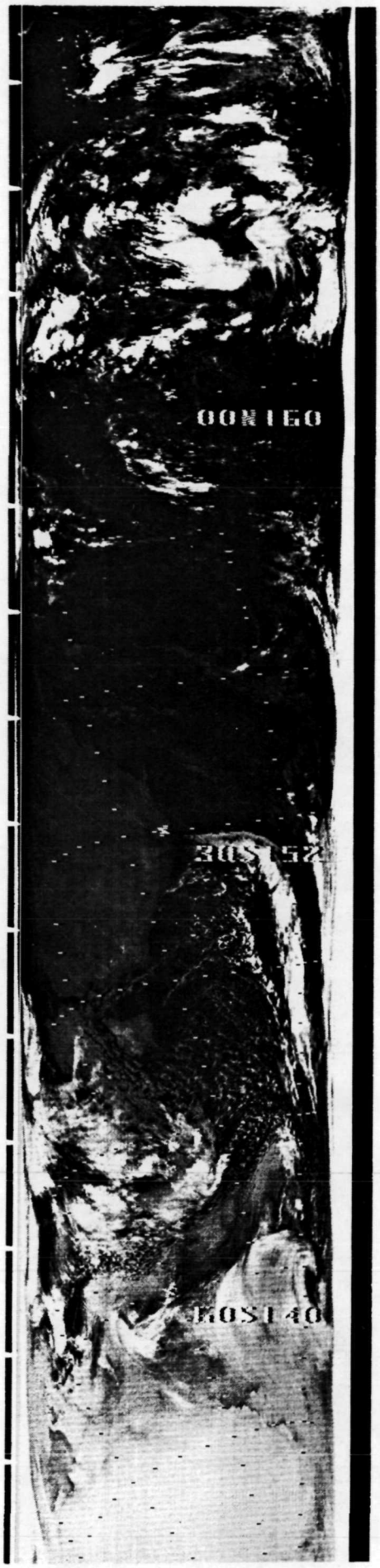
00N160
237
174

237
174

238
175

238
176

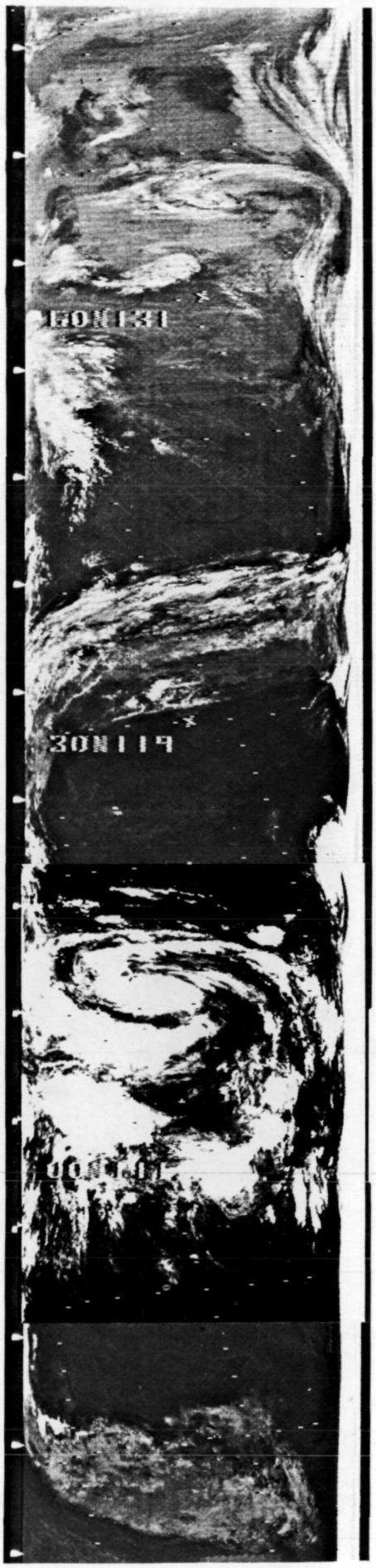

239
177

239
177

239
178

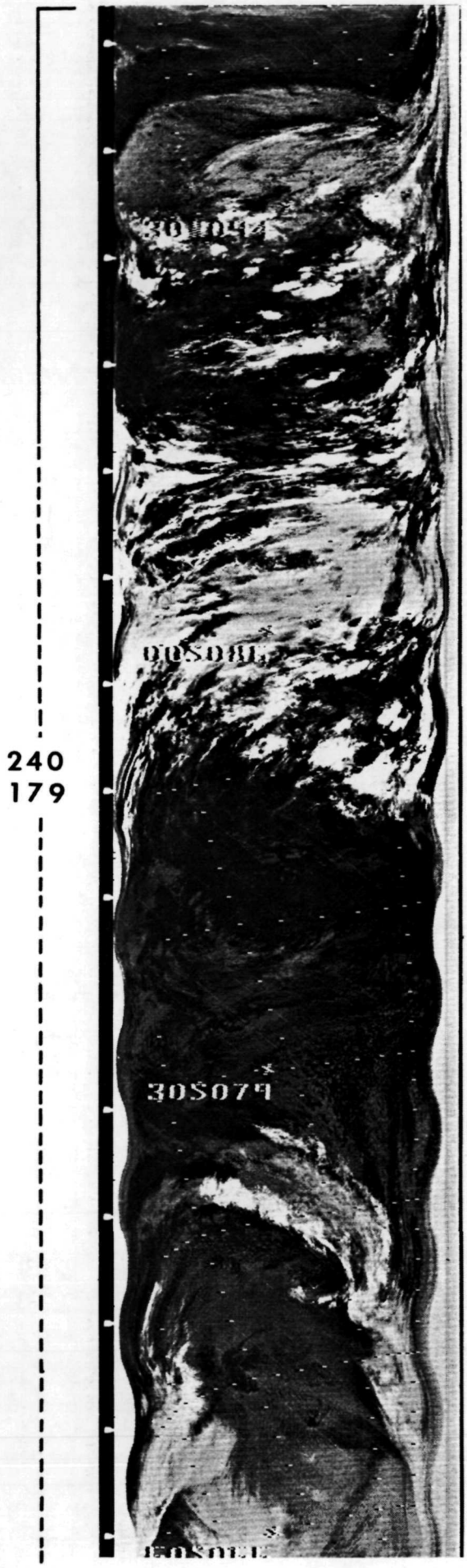
240
179

240
179

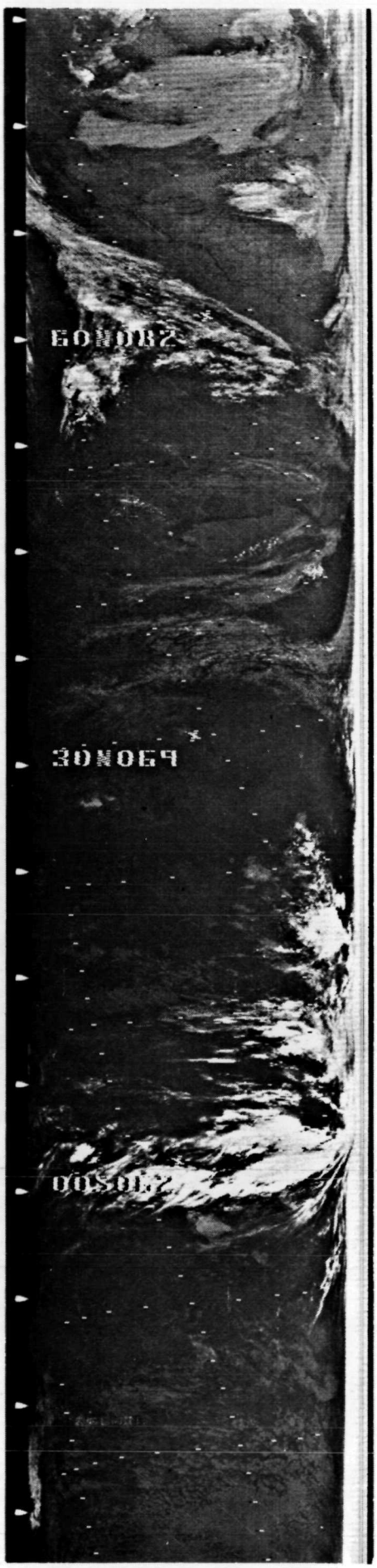

241
180

241
180

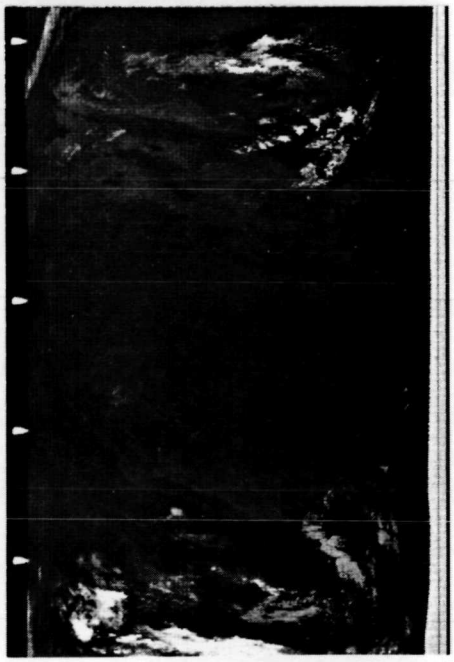

242
181

242
181

245
182

246
183

246
184

246
184

247
185

248
186

249
187

249
188

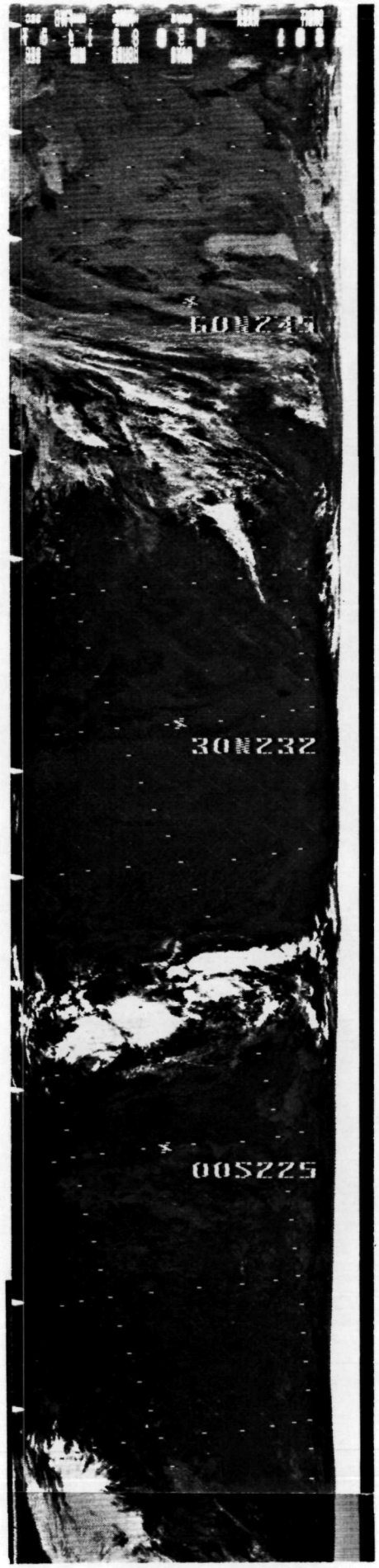

249
189

250
190

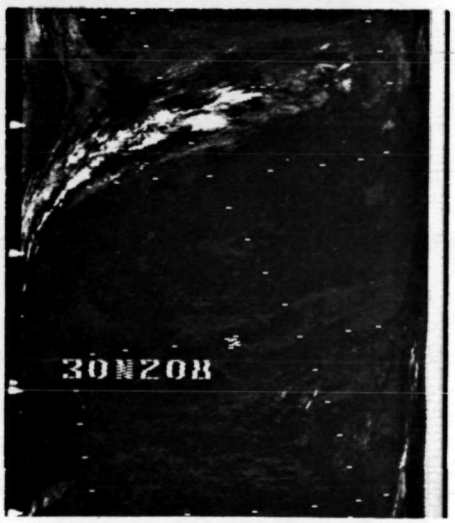

250
191

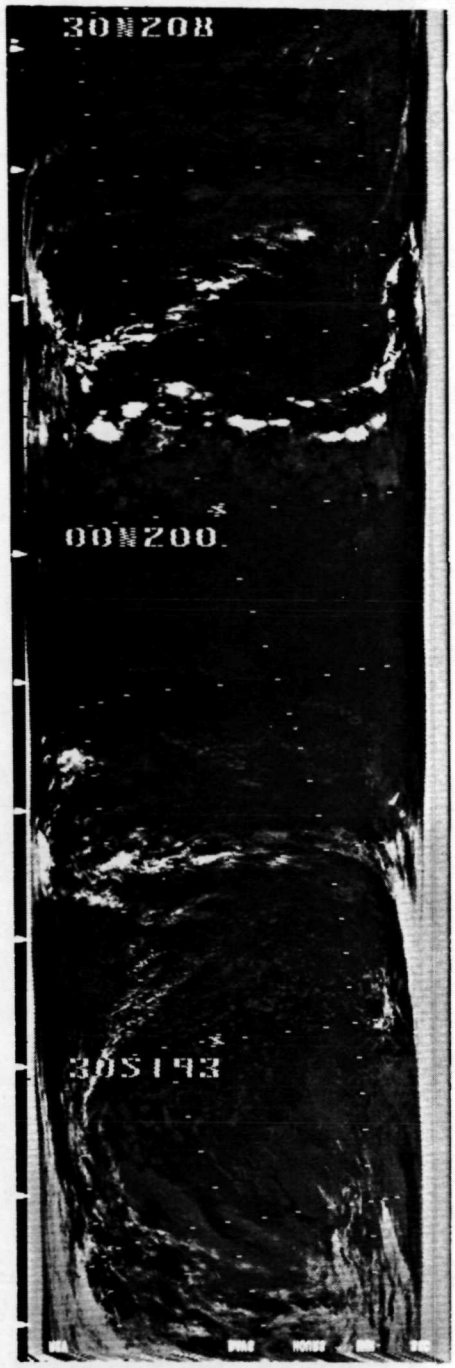

250
191

250
192

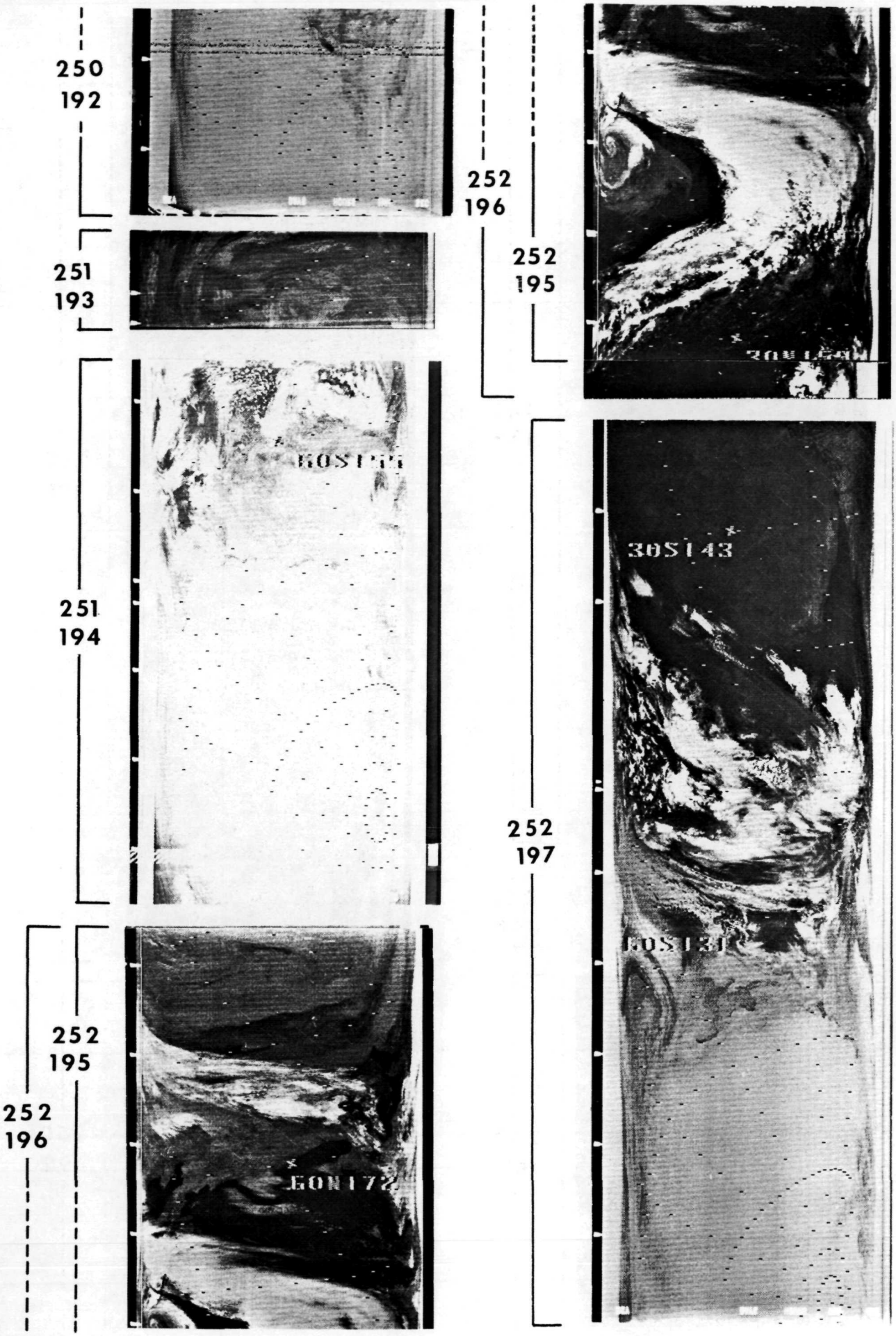
250
192
251
193
251
194
252
195
252
196
252
196
252
195
252
197
30S143

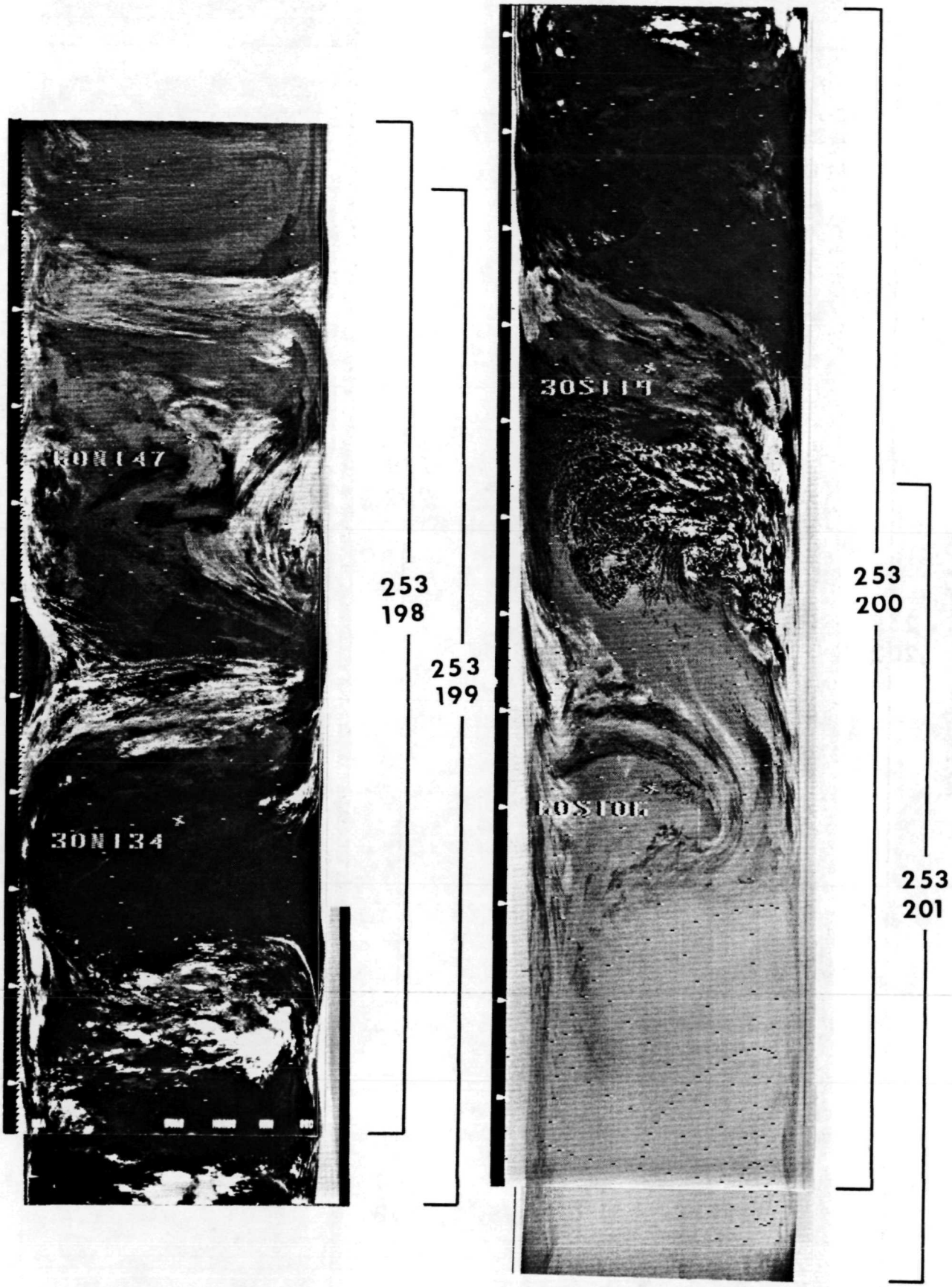
80N147
30N134
30S119
60S101
253
198
253
199
253
200
253
201

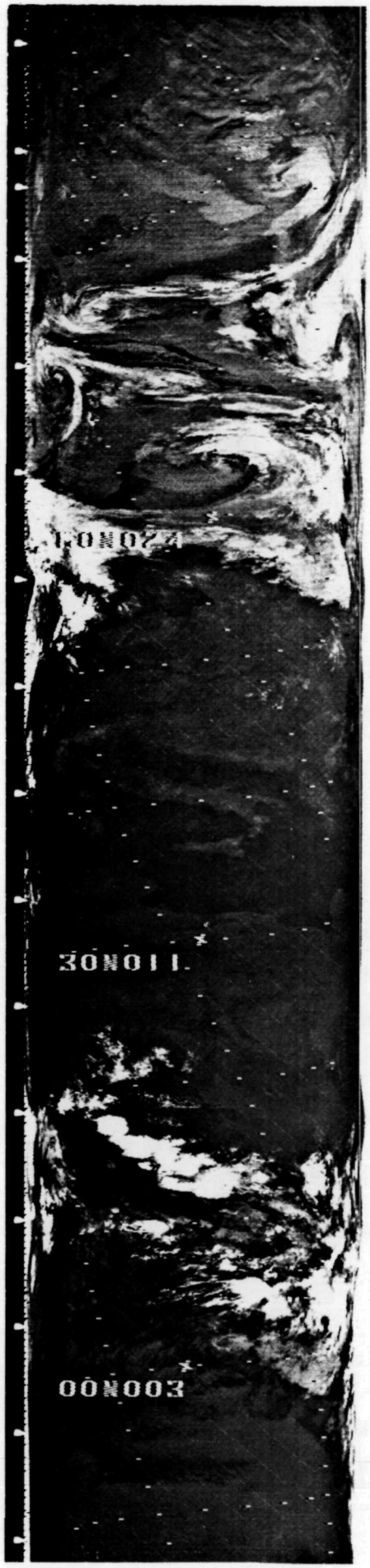

258
202

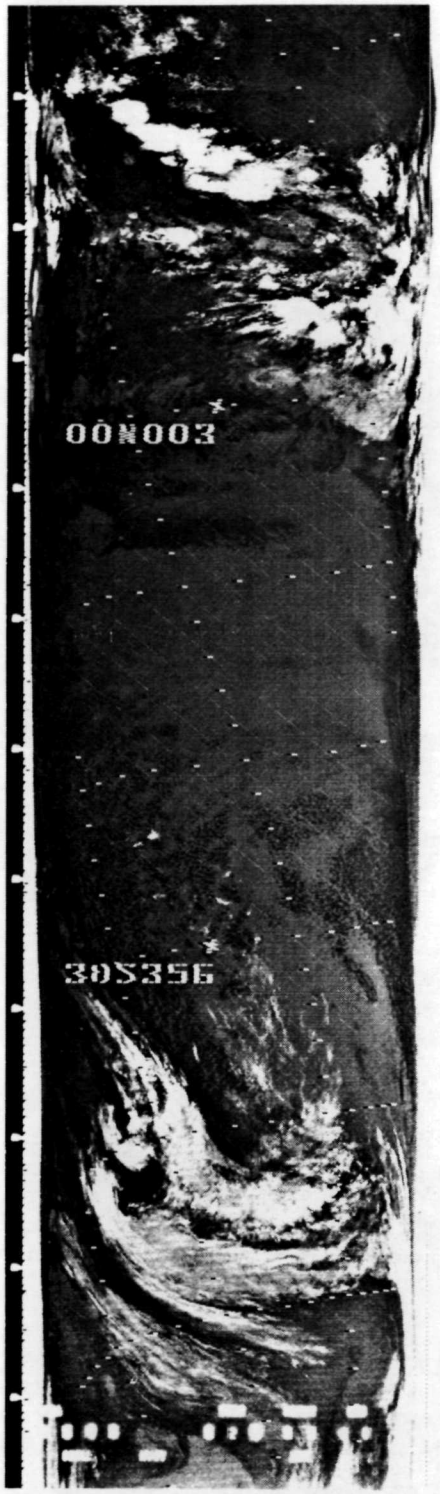

258
202

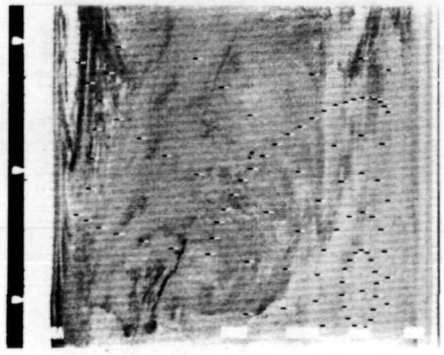

262
203

263
204

263
205

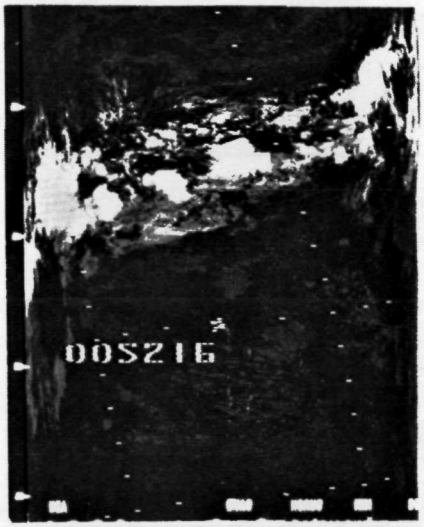

264
206

265
207

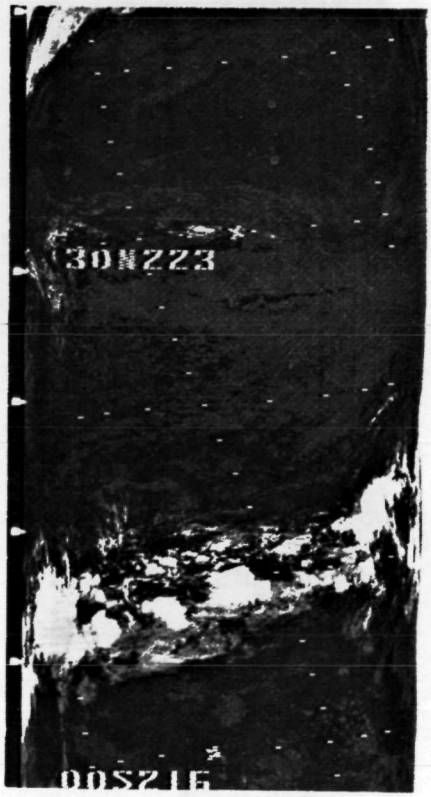

264
206

265
207

266
208

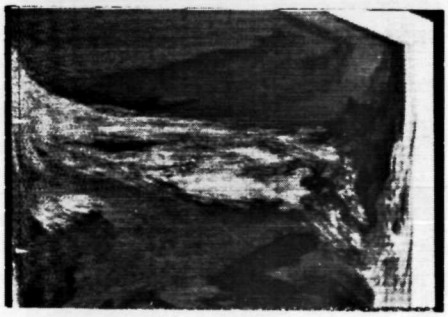

269
209

270
210

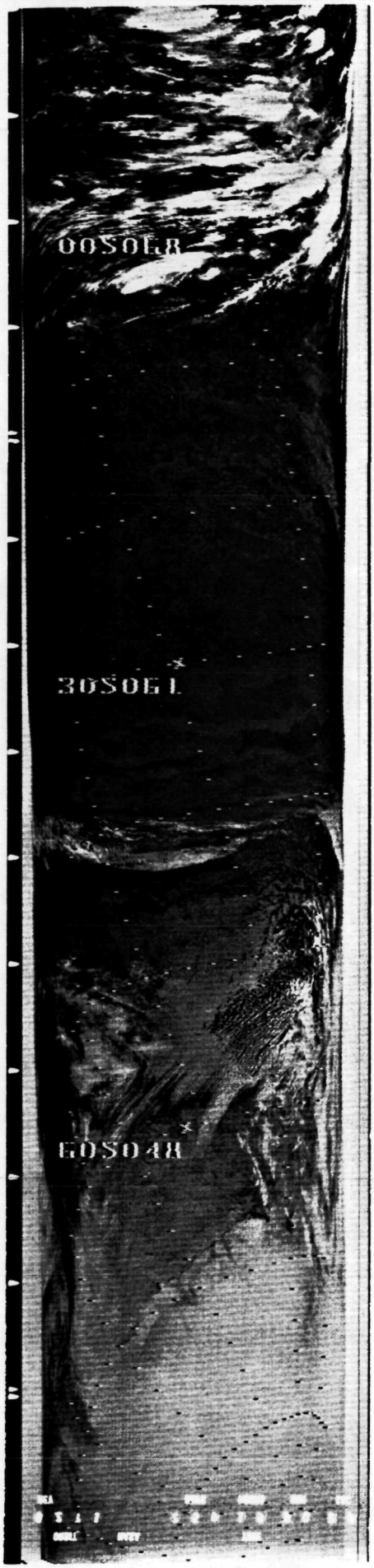

270
210

271
211

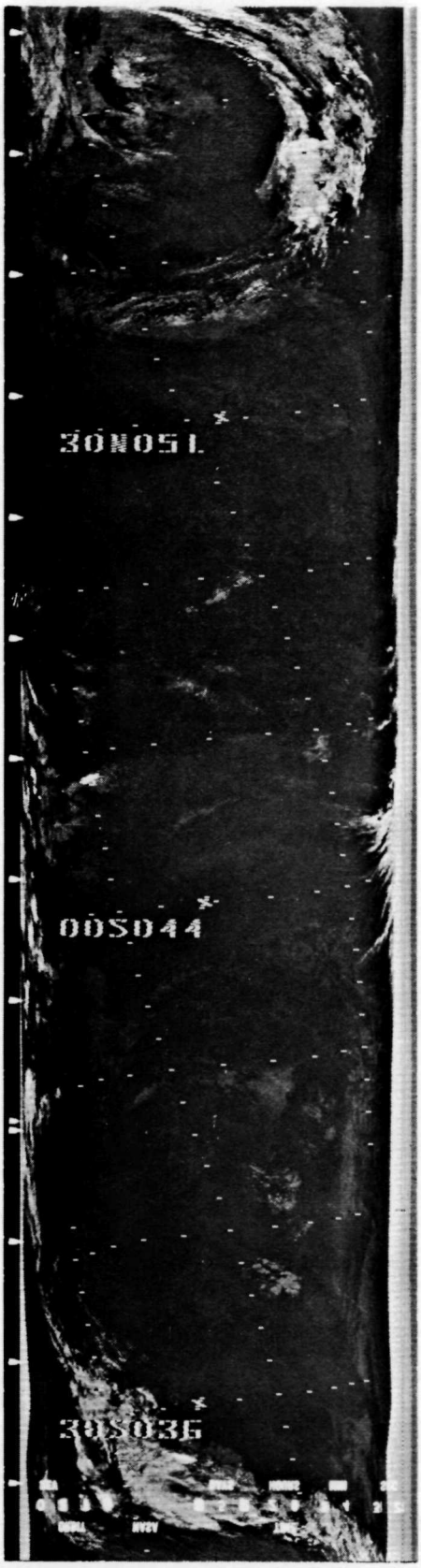

274
212

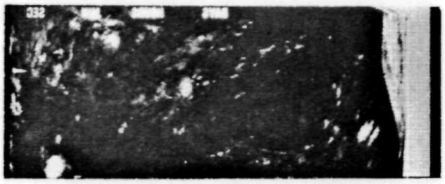

274
213

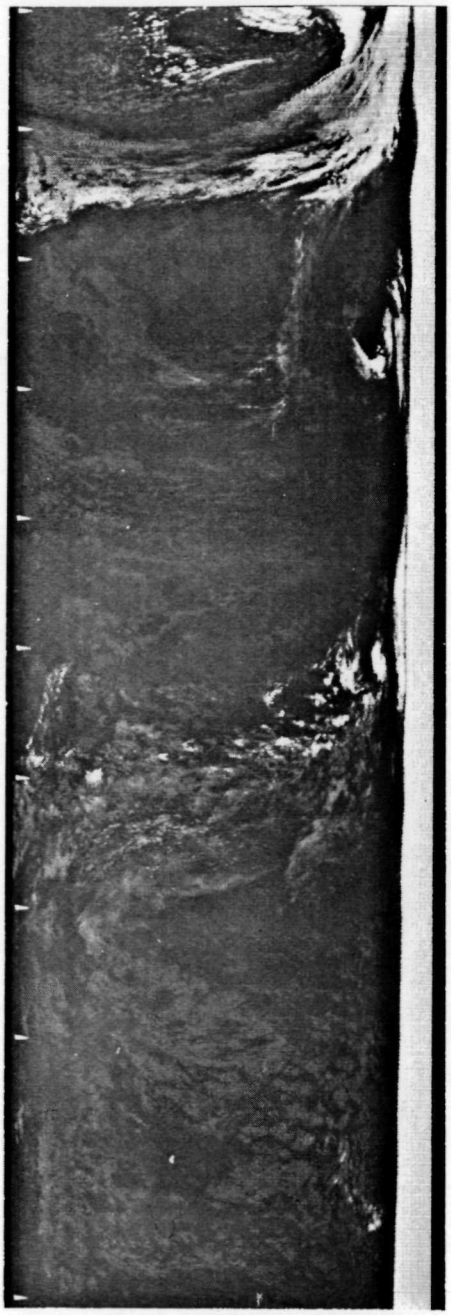

275
214

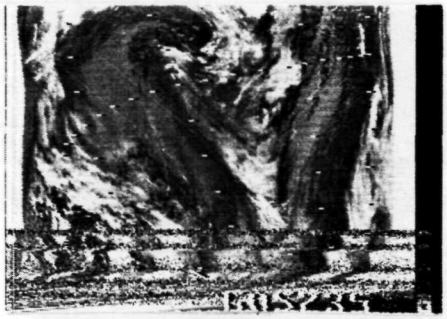

277
217

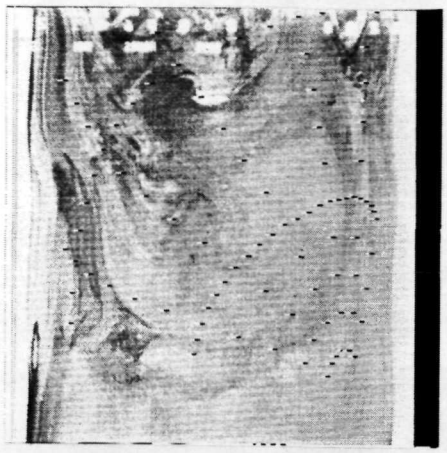

277
218

278
219

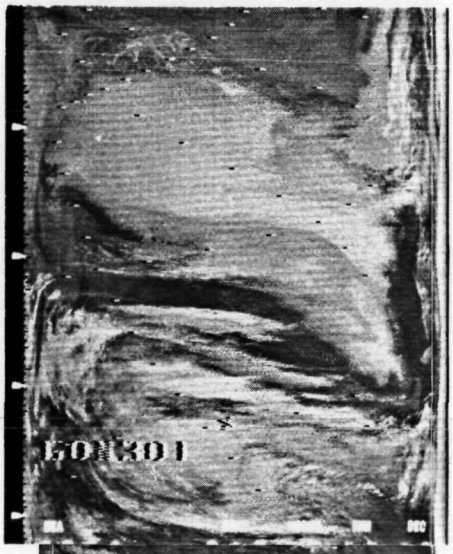

276
215

276
216

278
220

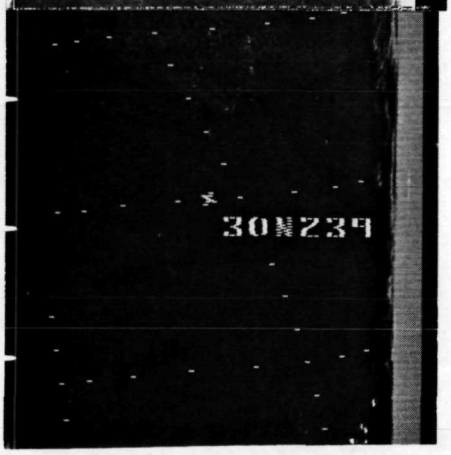

278
221

278
221

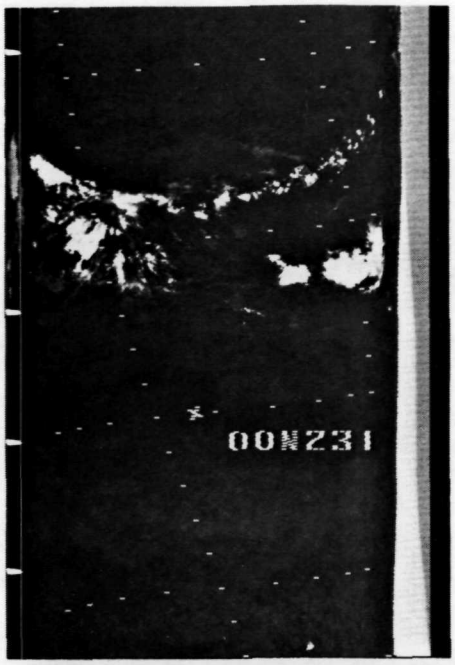

278
222

279
223

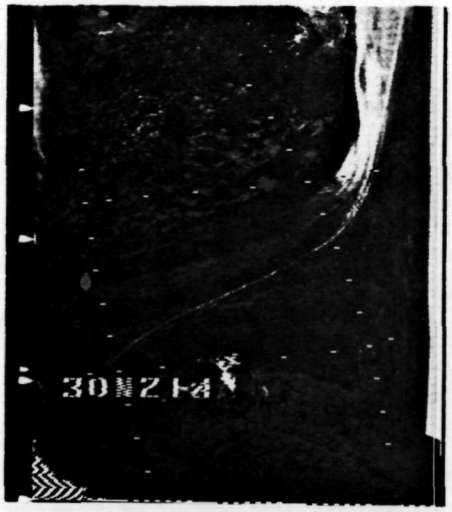

279
224

279
225

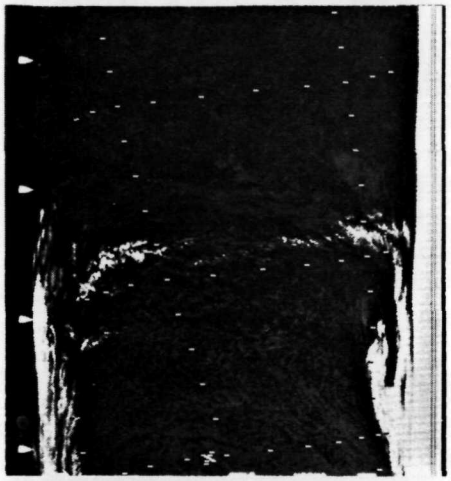

279
226

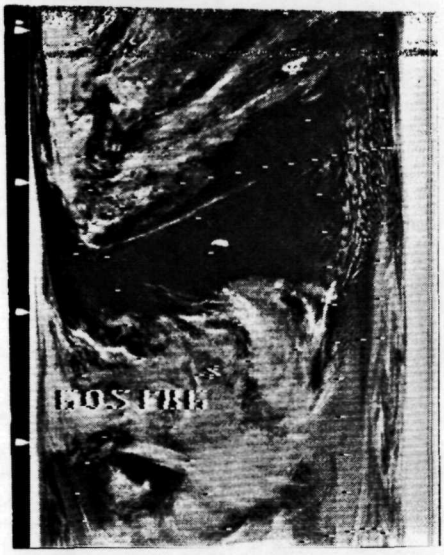

279
227

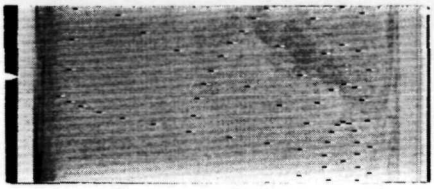

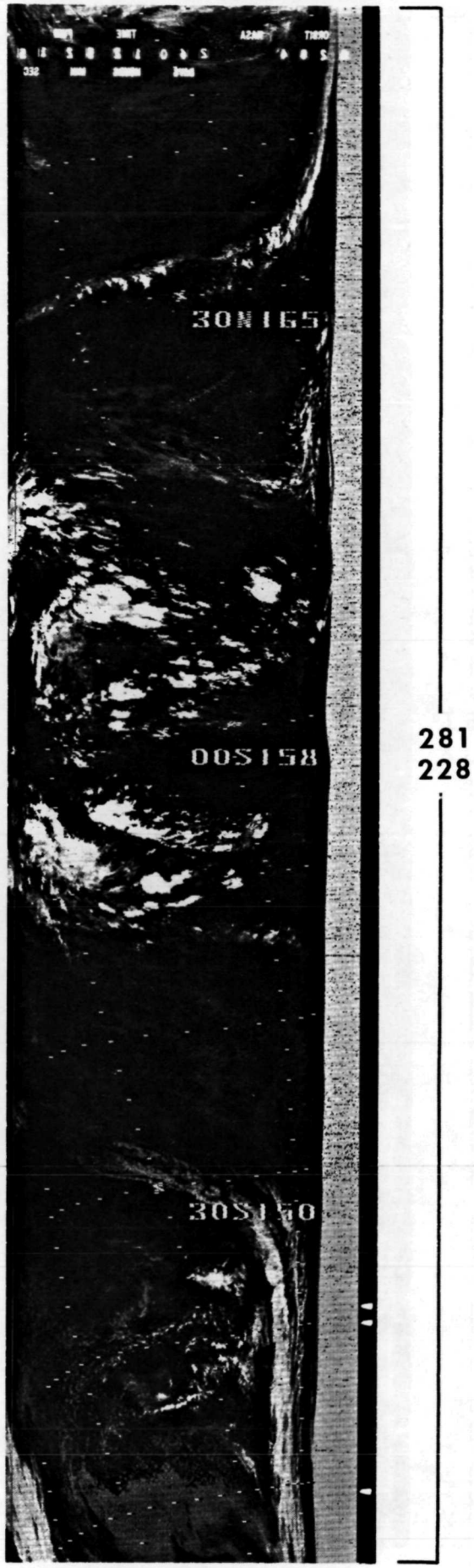
30N165
00S158
30S150
281
228

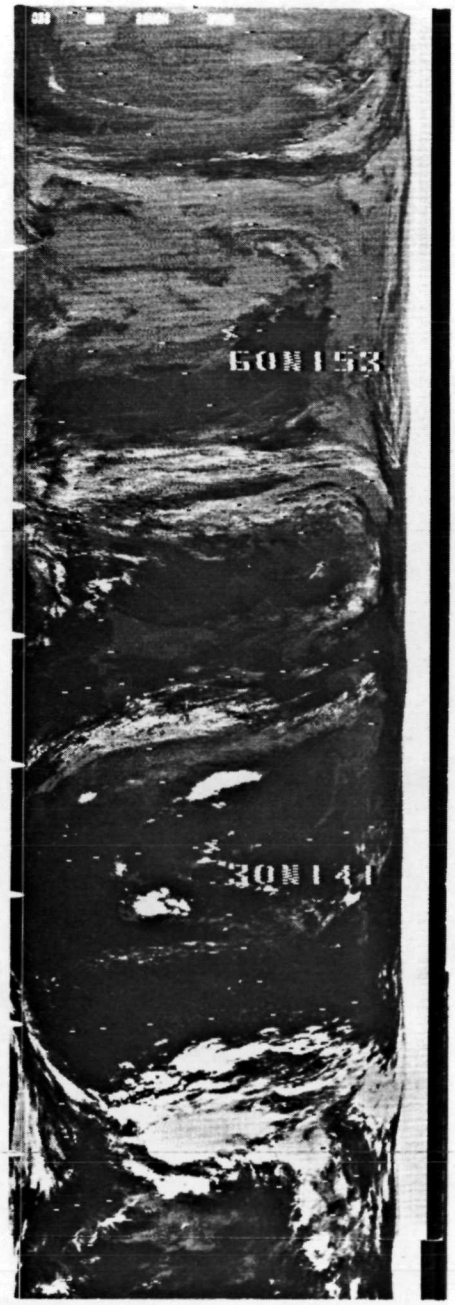
60N153
30N141
282
229
282
230

282
231

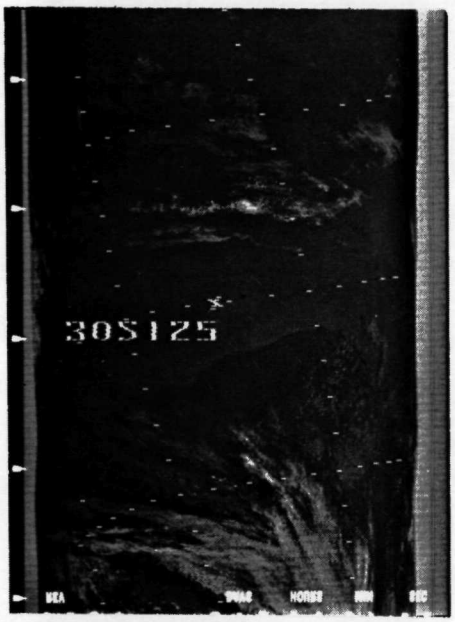

283
232

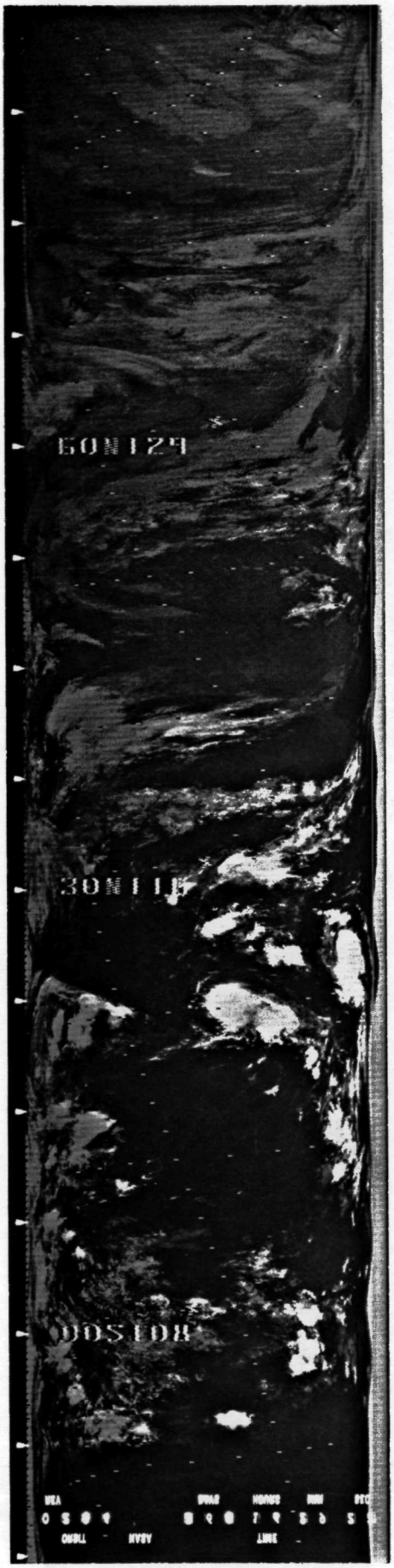

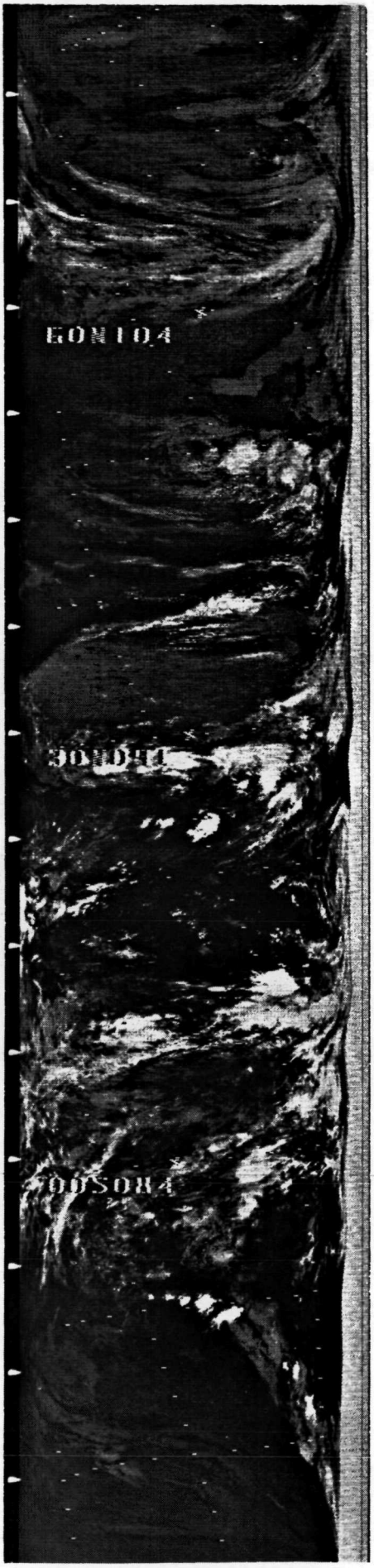

284
233

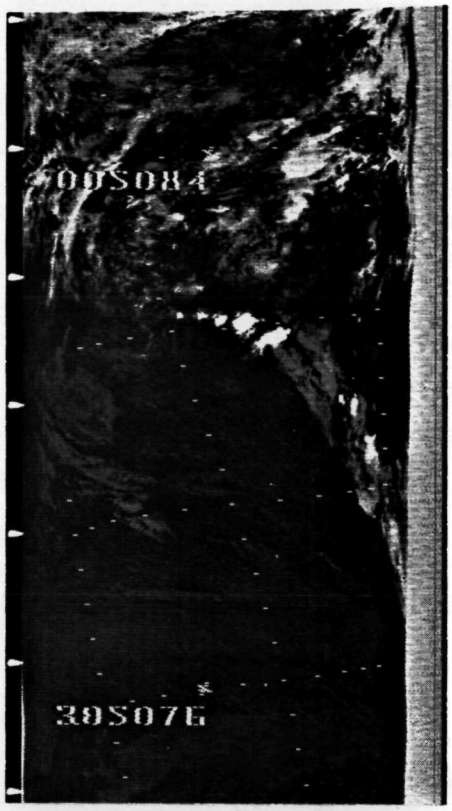

284
233

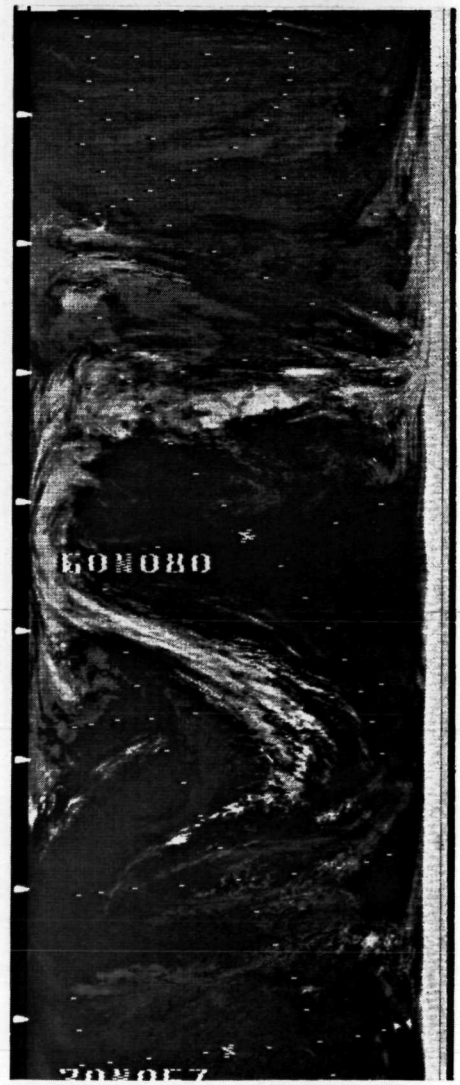

285
234

285
234

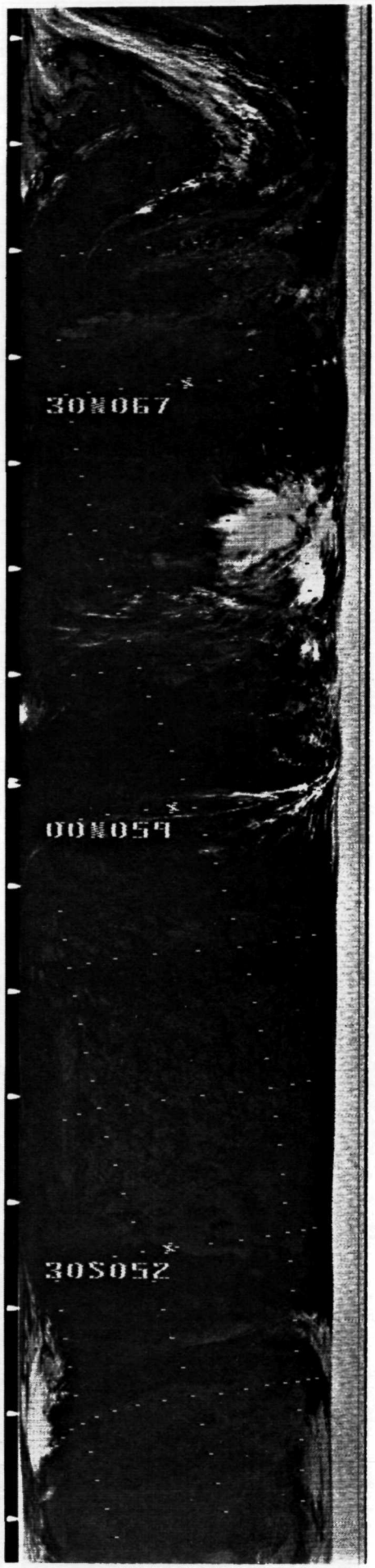

286
235

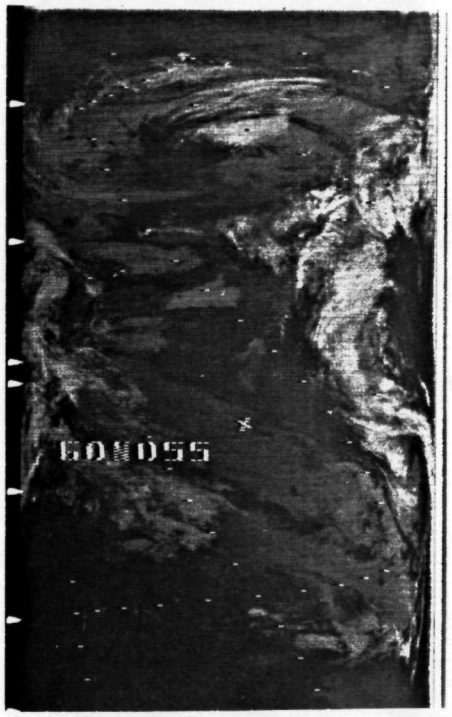

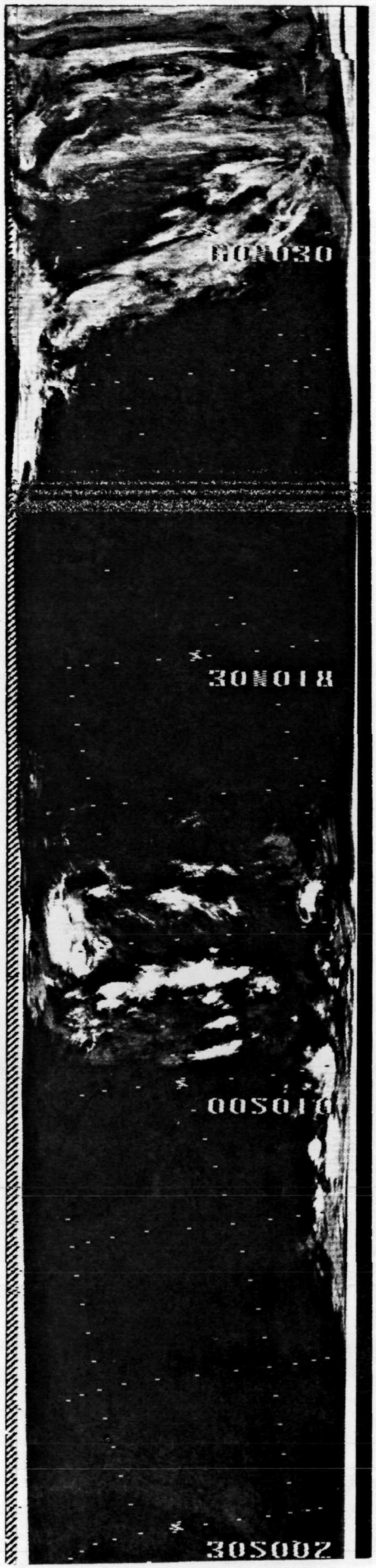

287
236

287
237

287
236

287
237

288
238

288
239

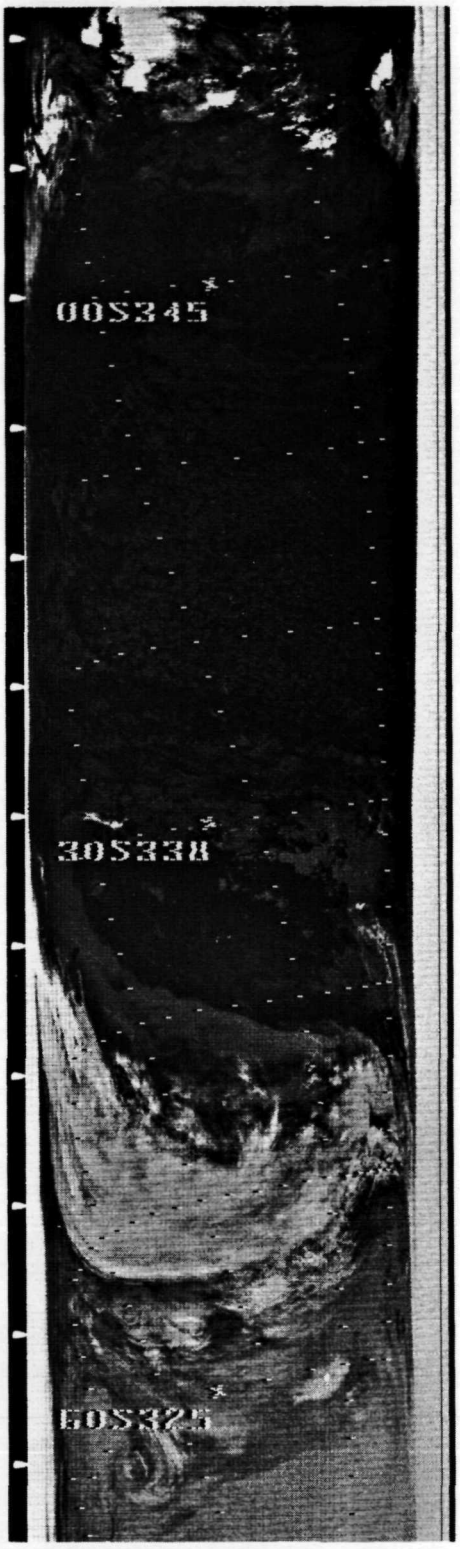

288
239

289
240

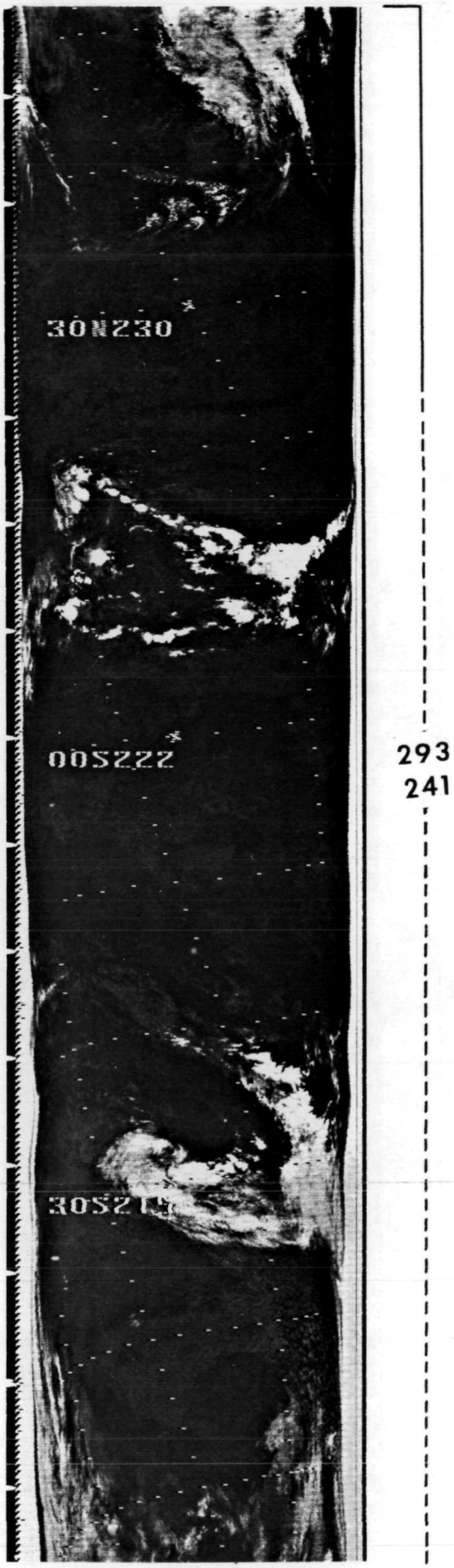

293
241

293
241

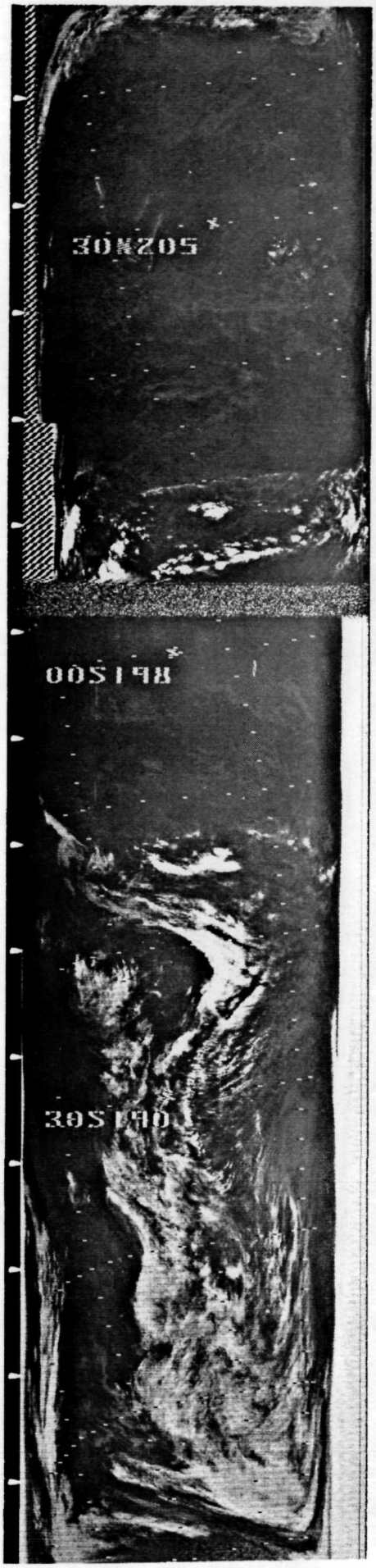

294
242

294
242

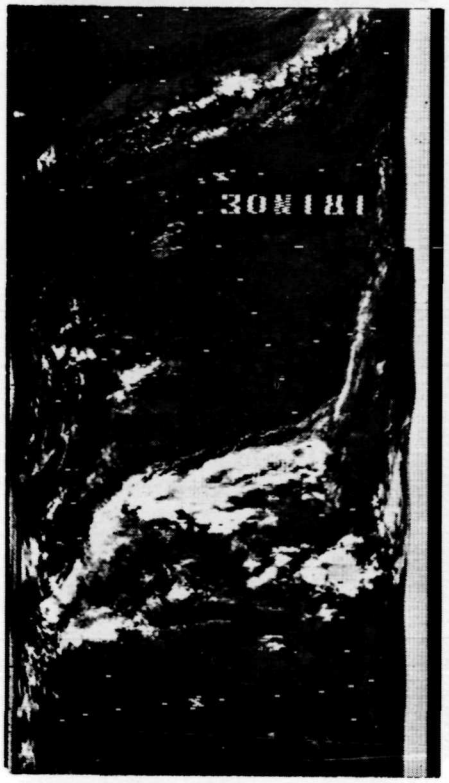

295
243

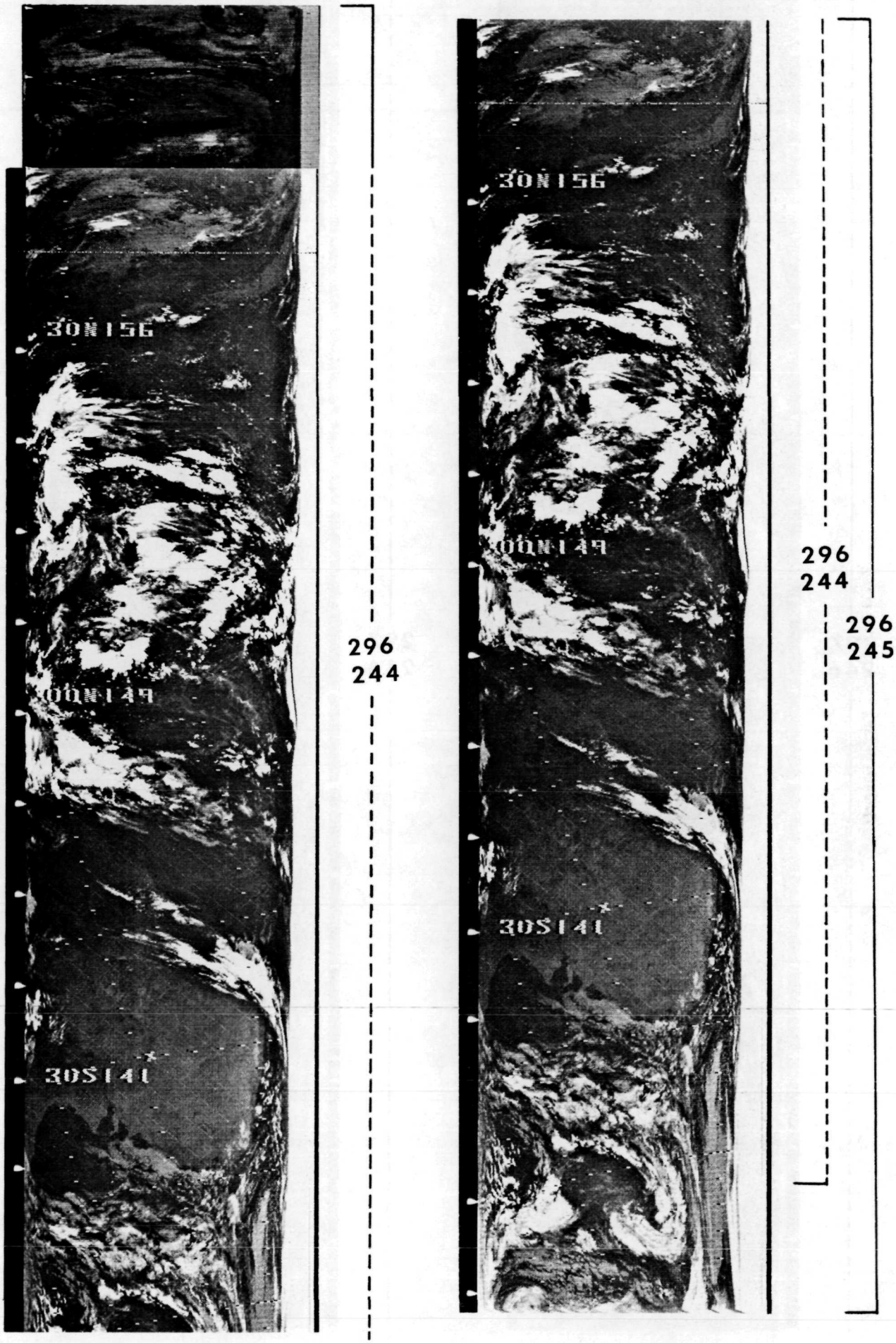
30N156
00N149
30S141
296
244
30N156
00N149
30S141
296
244
296
245

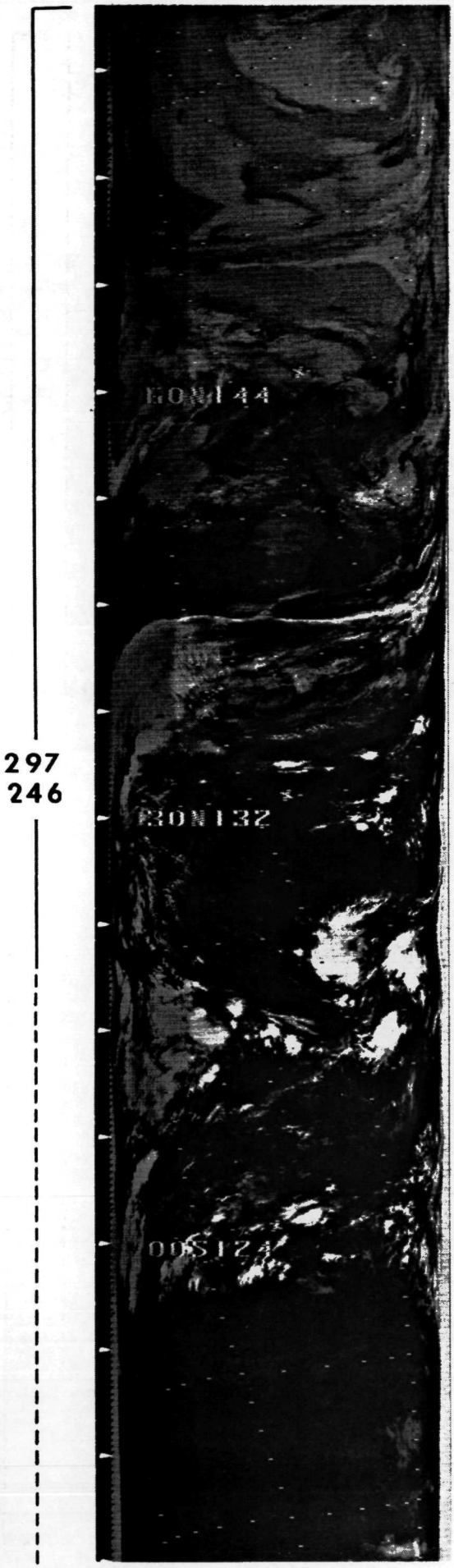
60N144
30N132
00S124
297
246

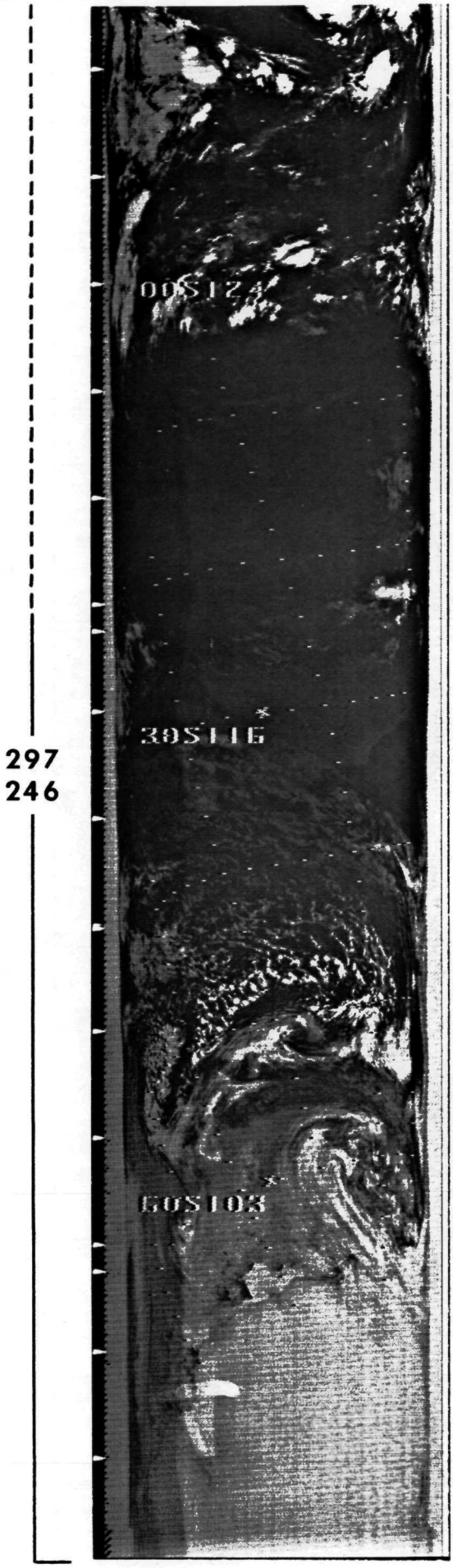
00S124
30S116
60S103
297
246

298
247

298
248

298
248

299
249

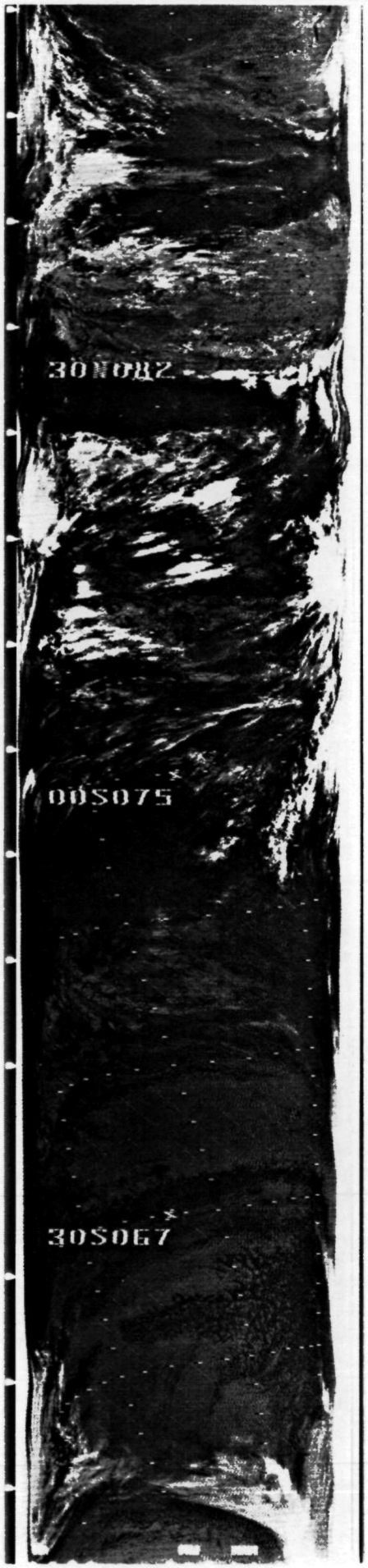

299
249

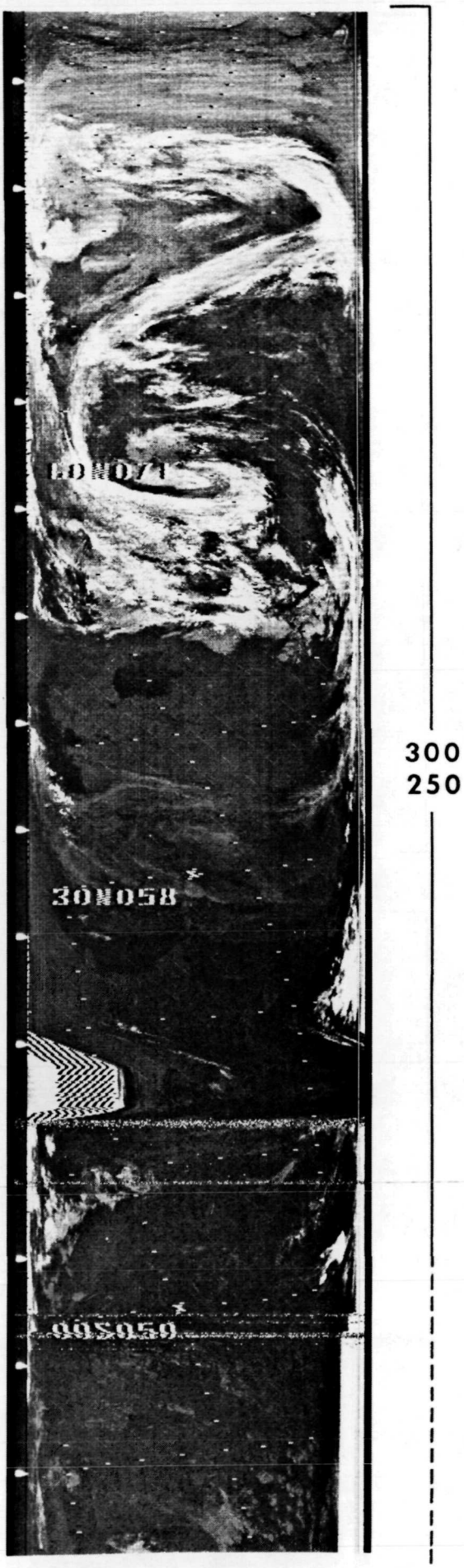

300
250

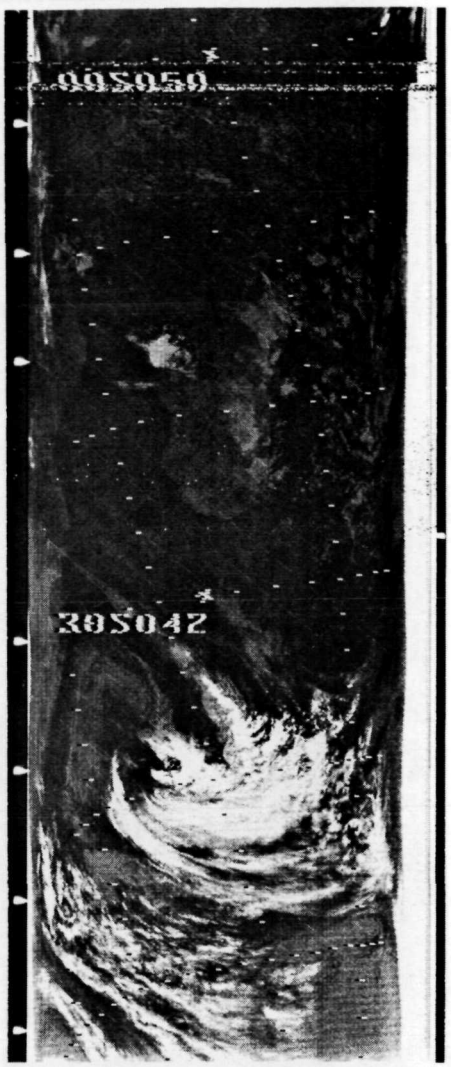

300
250

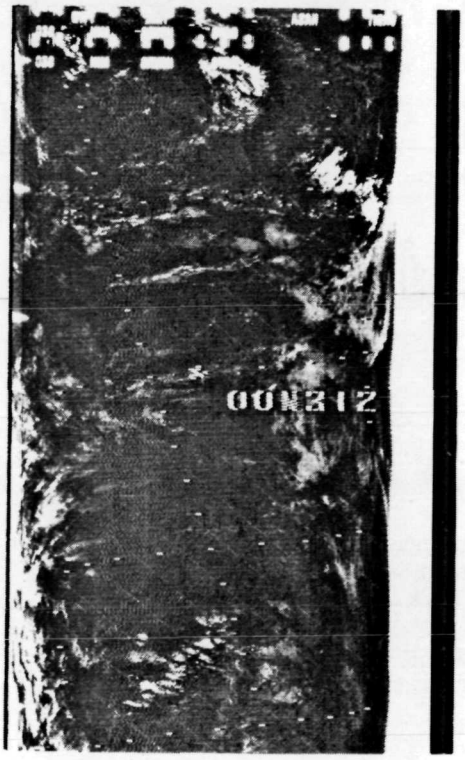

304
251

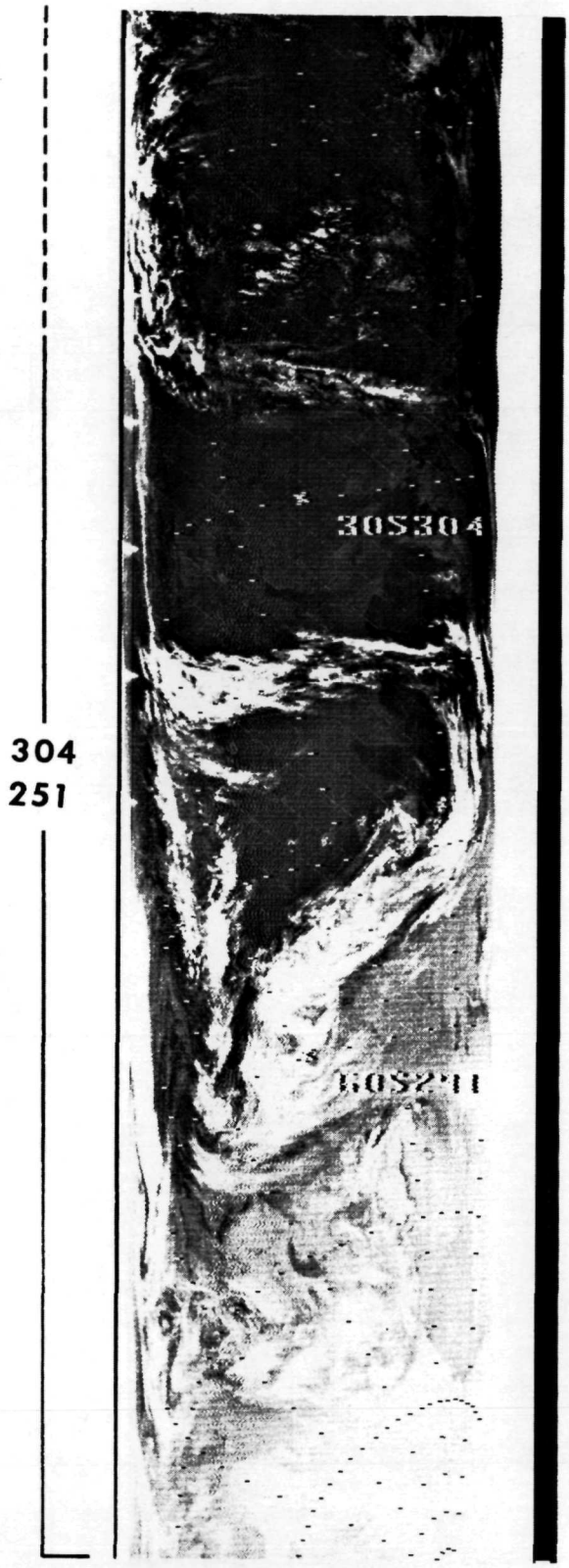
304
251
305304

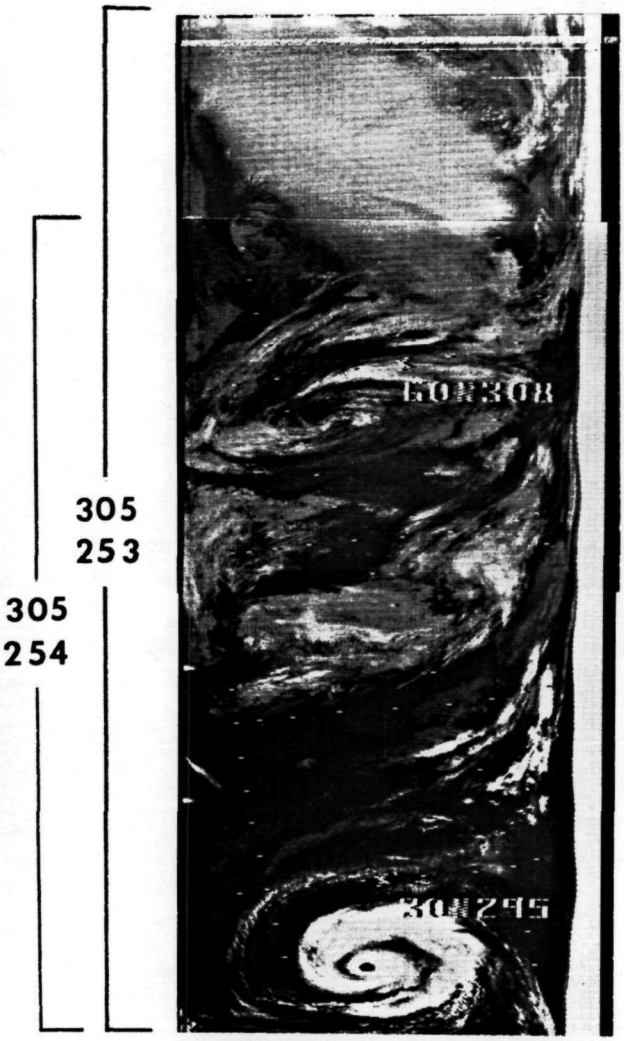
305
253
305
254

305
252

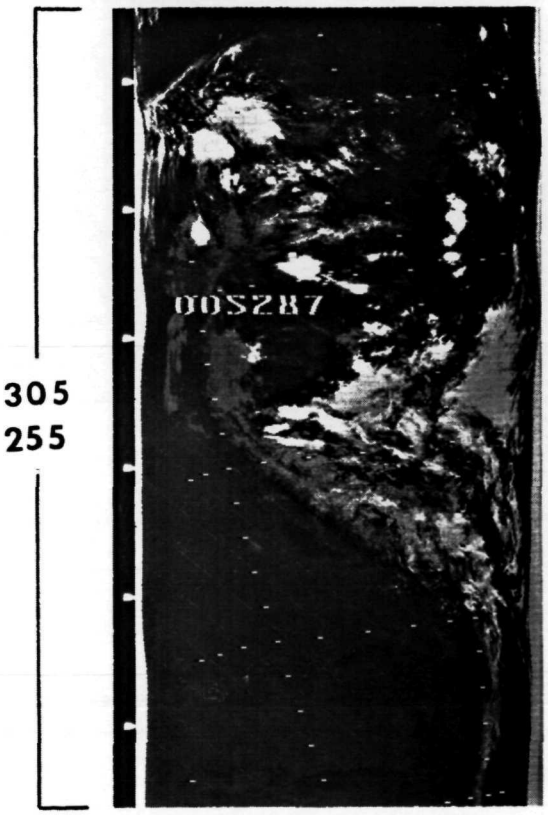
005287
305
255

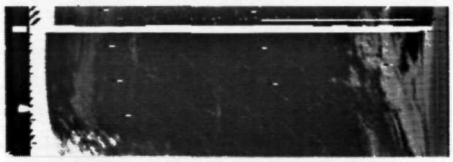

305
256

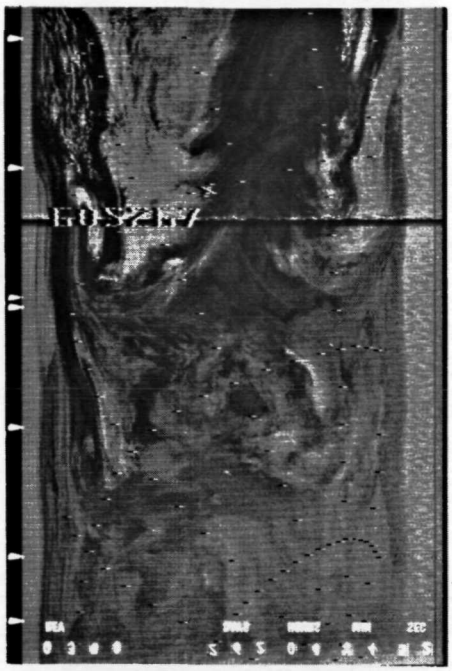

305
257

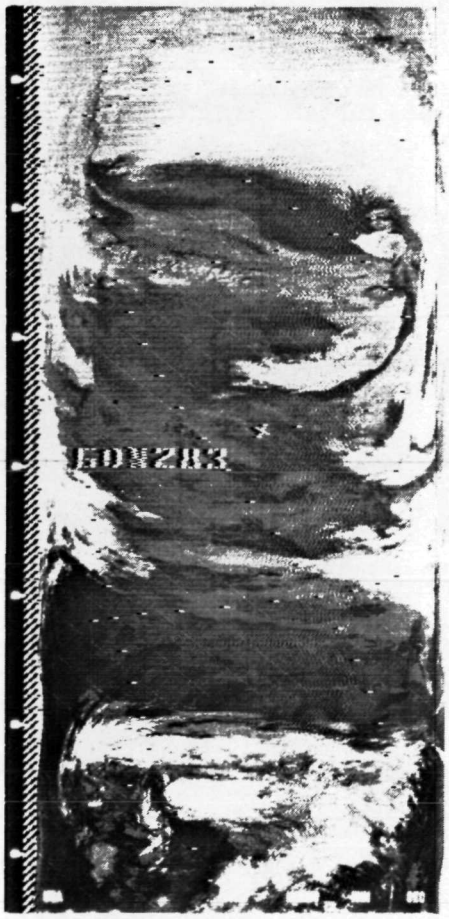

306
258

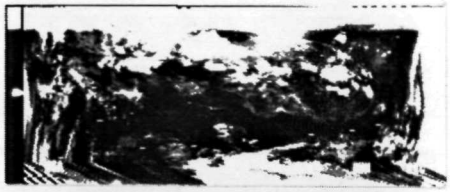

306
259

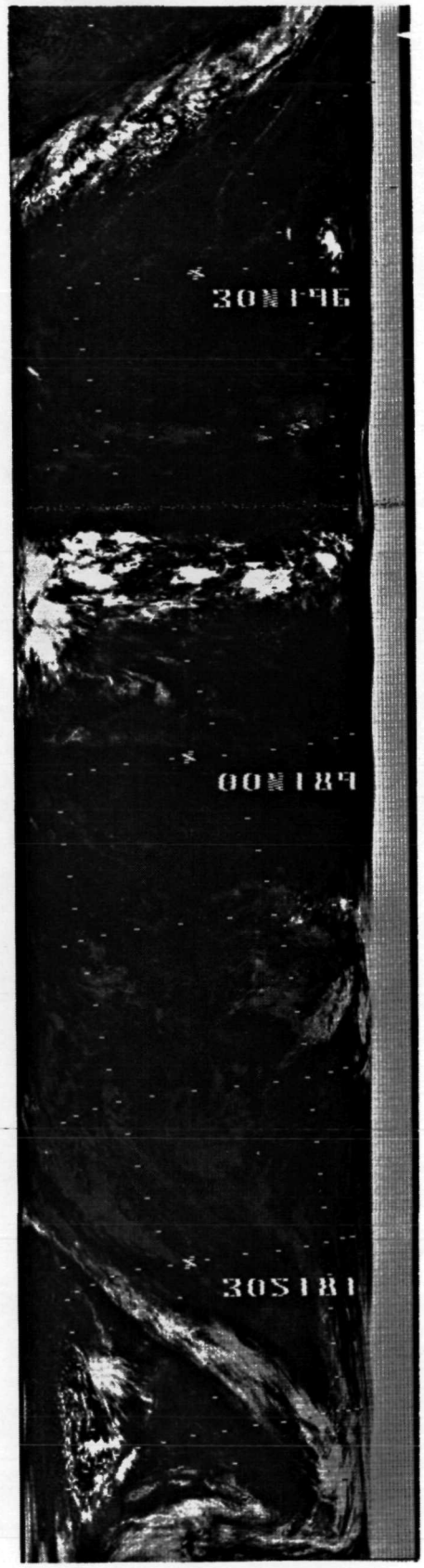

309
260

310
261

310
262

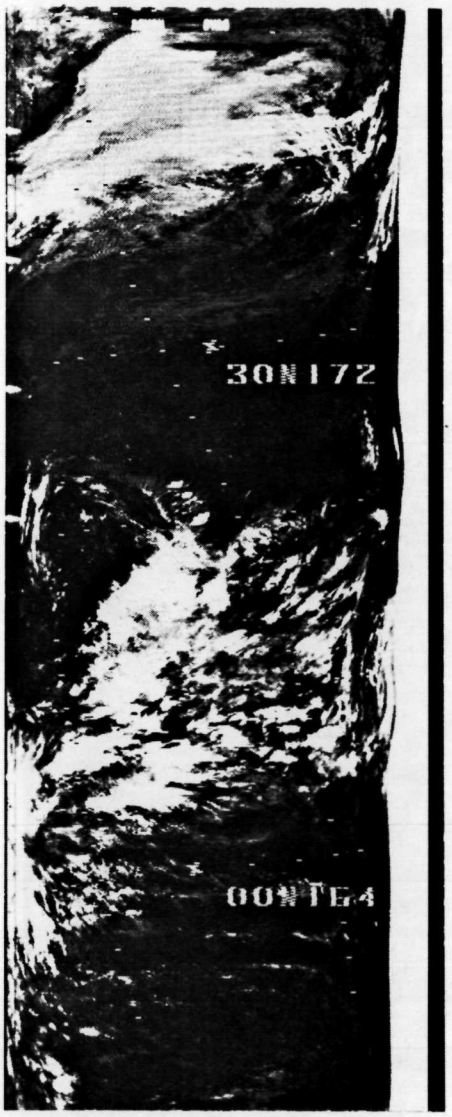

310
263

310
264

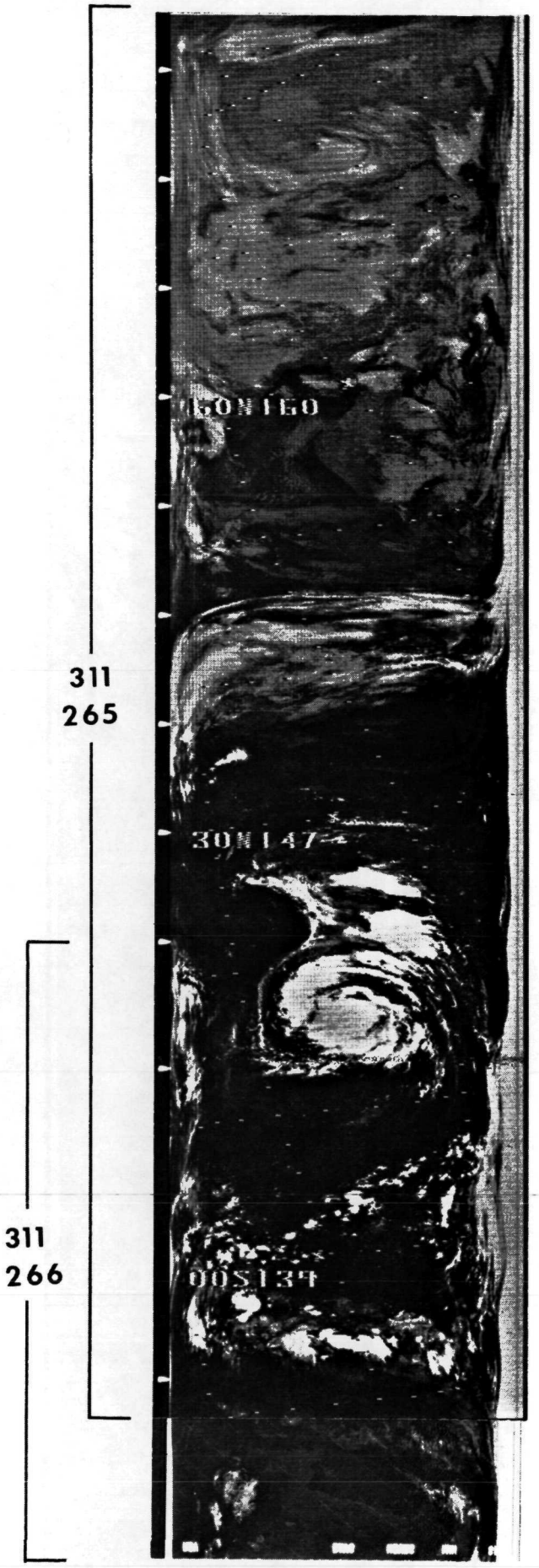
311
265
311
266

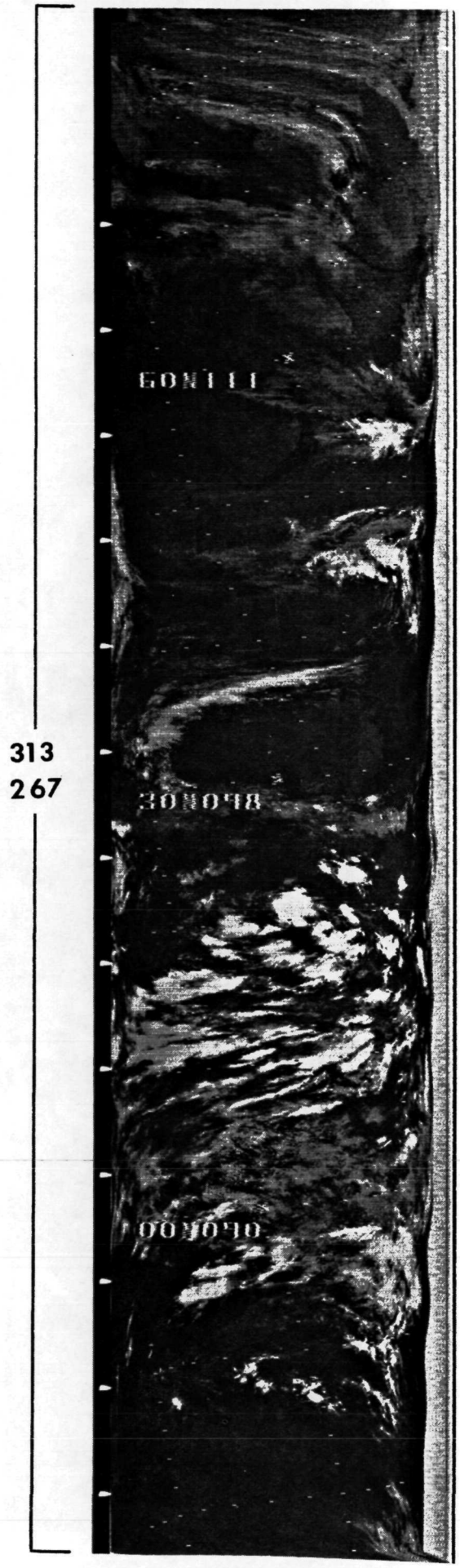
313
267

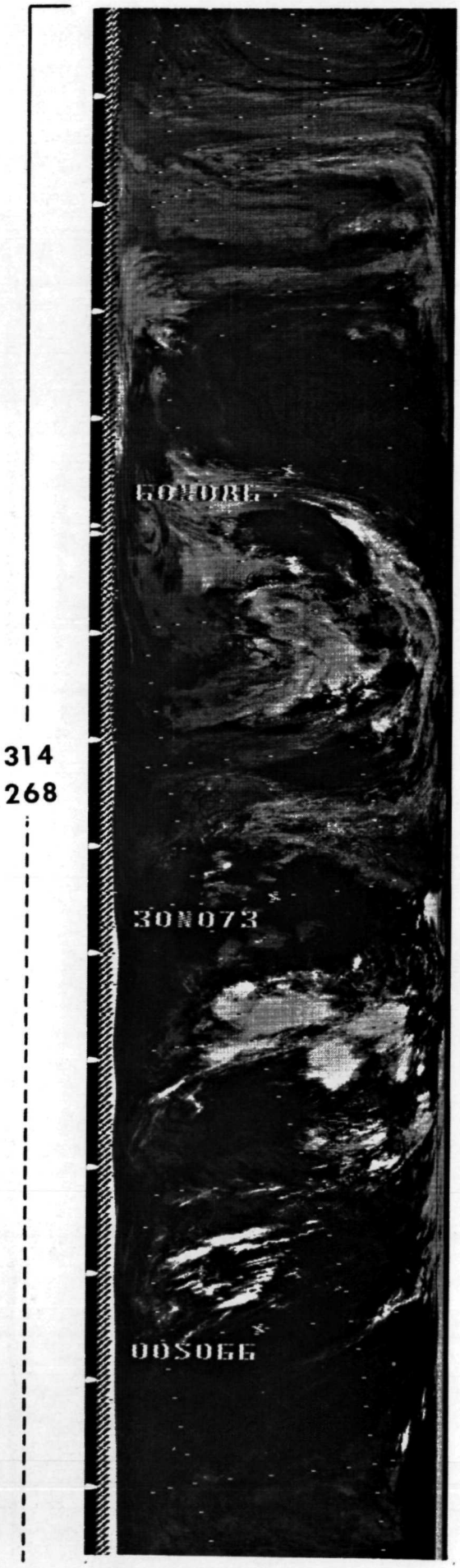
314
268
60N078
30N073
00S066

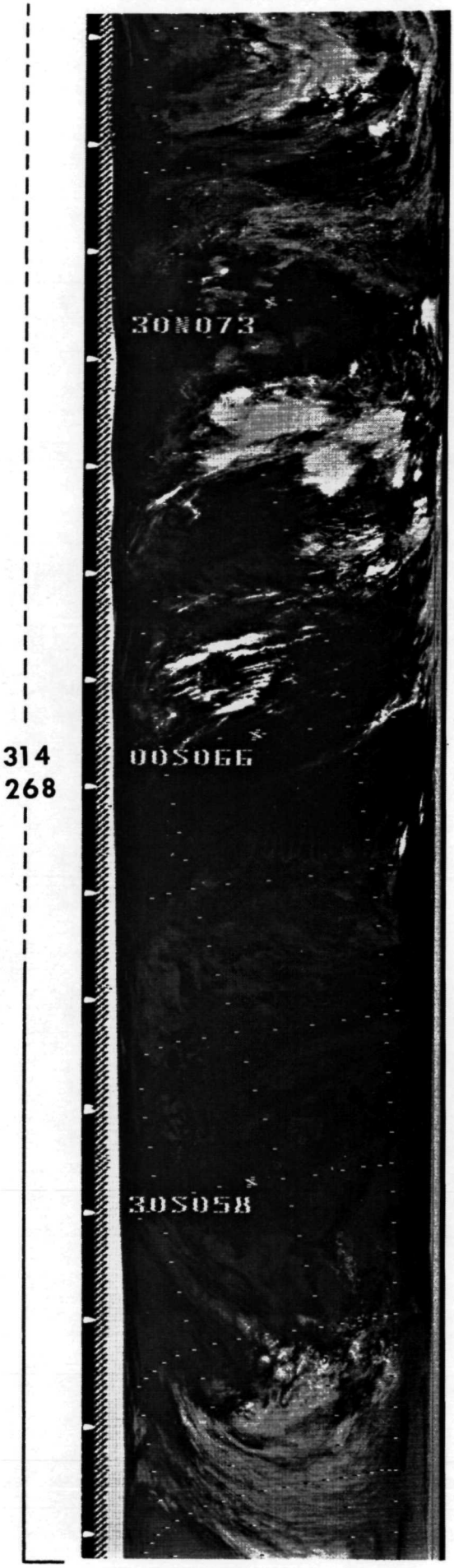
314
268
30N073
00S066
30S058

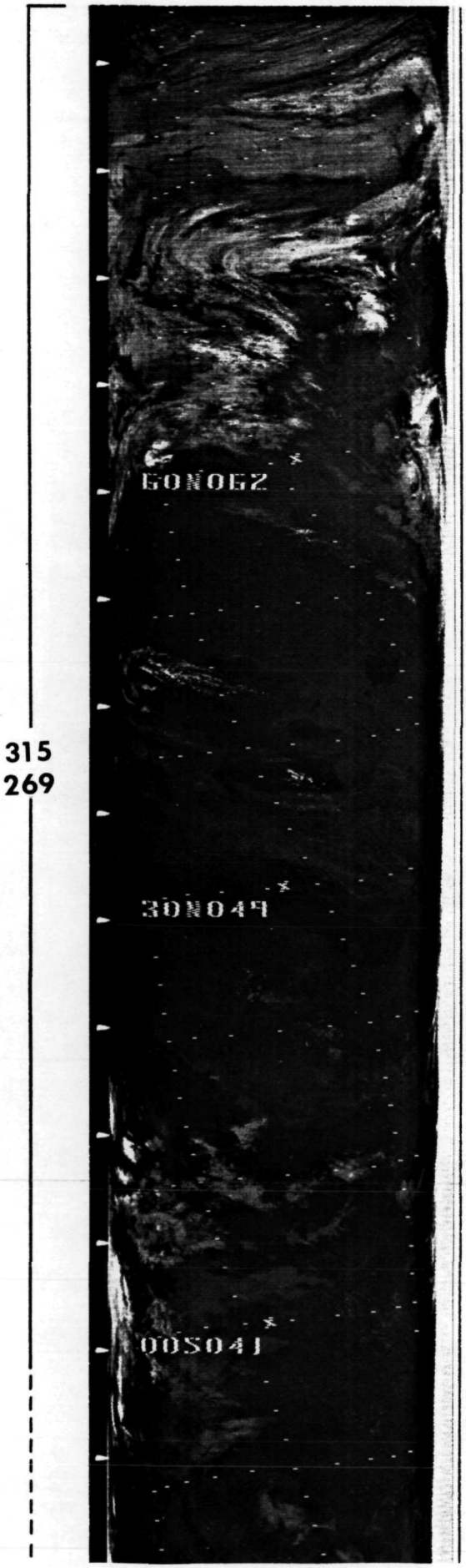
315
269
60N062
30N049
00S041

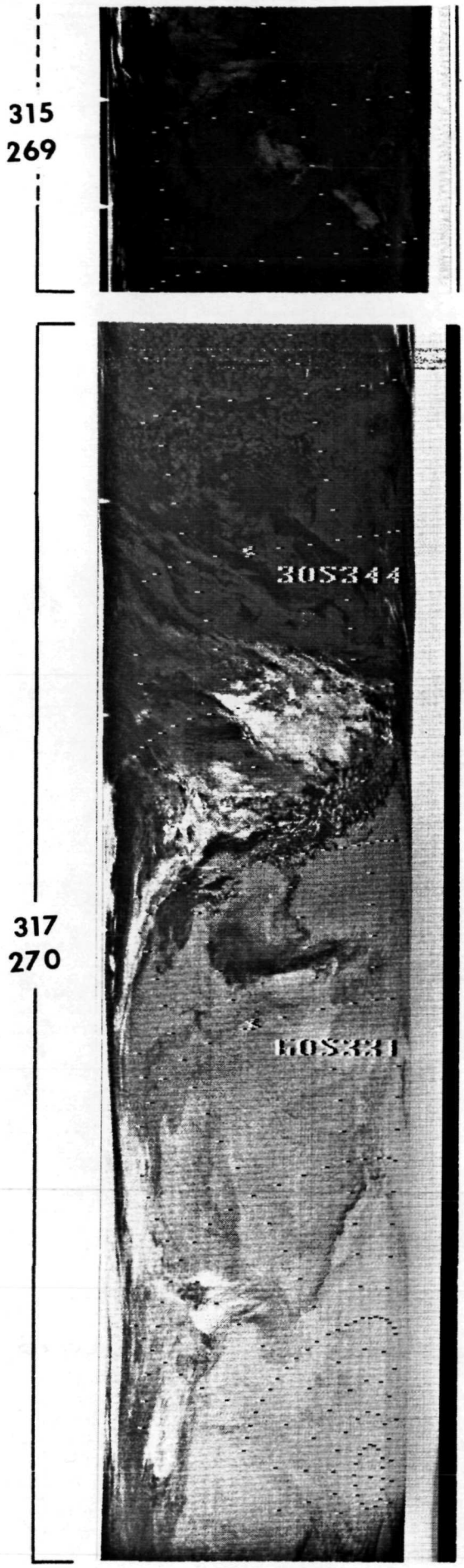
315
269
317
270
30S344
60S341

318
271

318
272

318
273

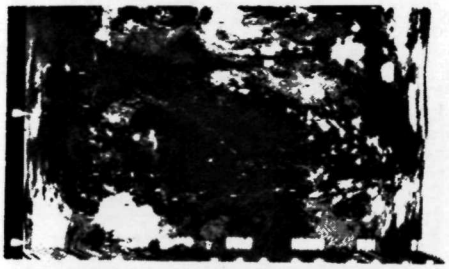

321
274

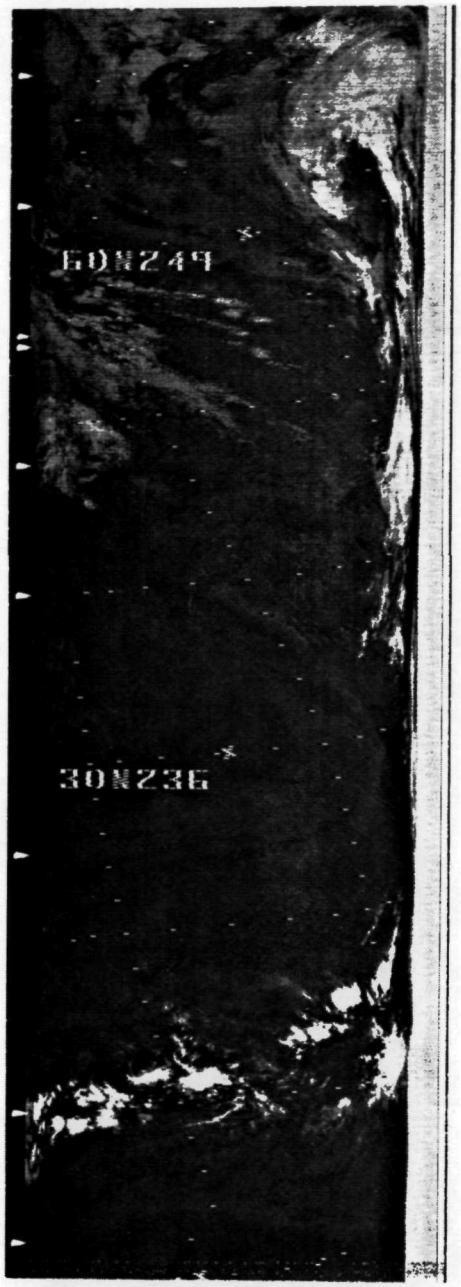

322
275

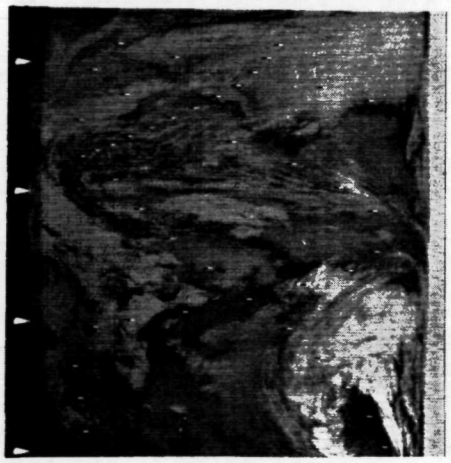

322
275

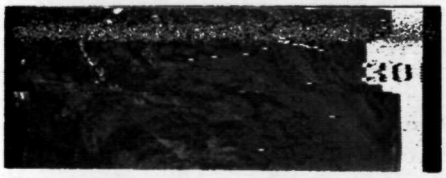

323
276

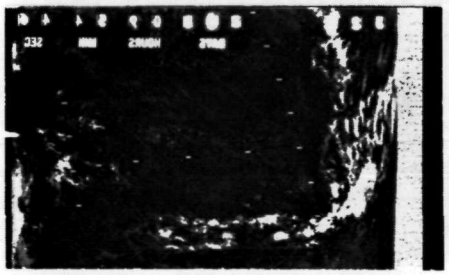

323
277

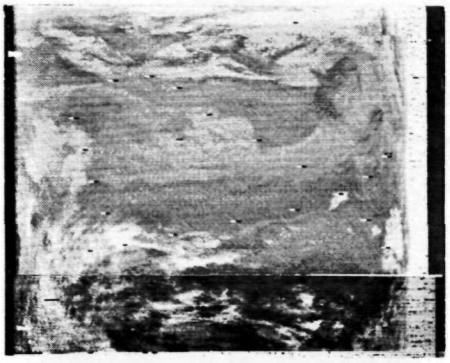

324
278

324
279

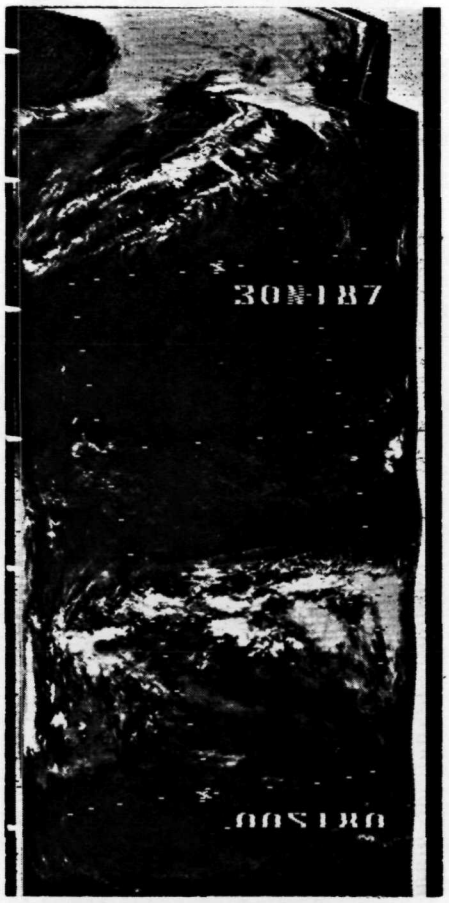

324
280

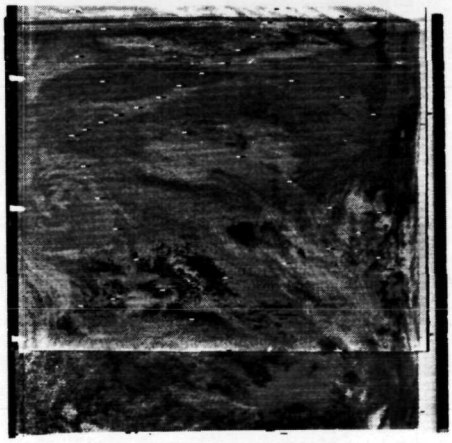

325
281

325
282

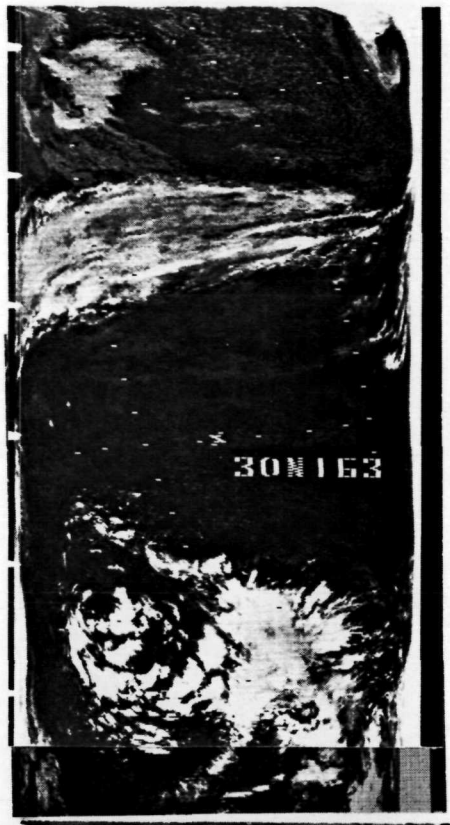

325
283

325
284

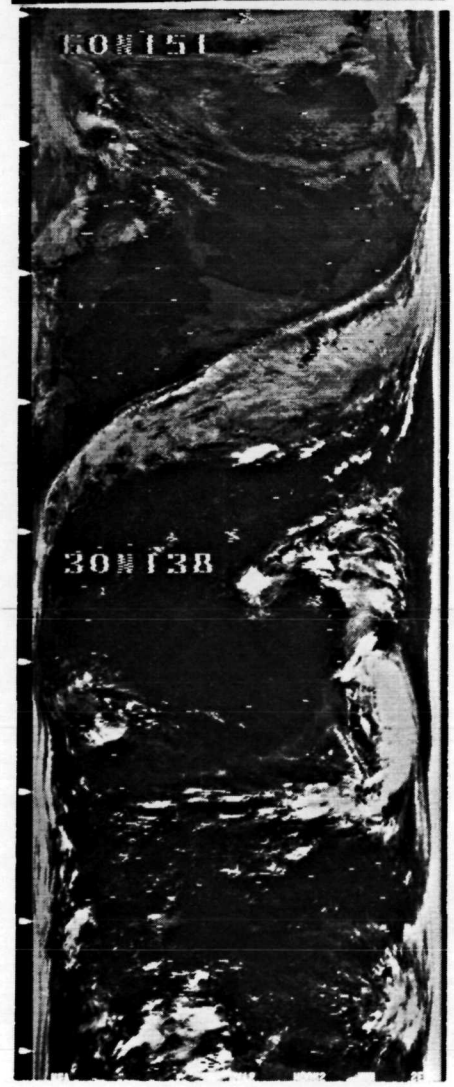

326
285

327
286

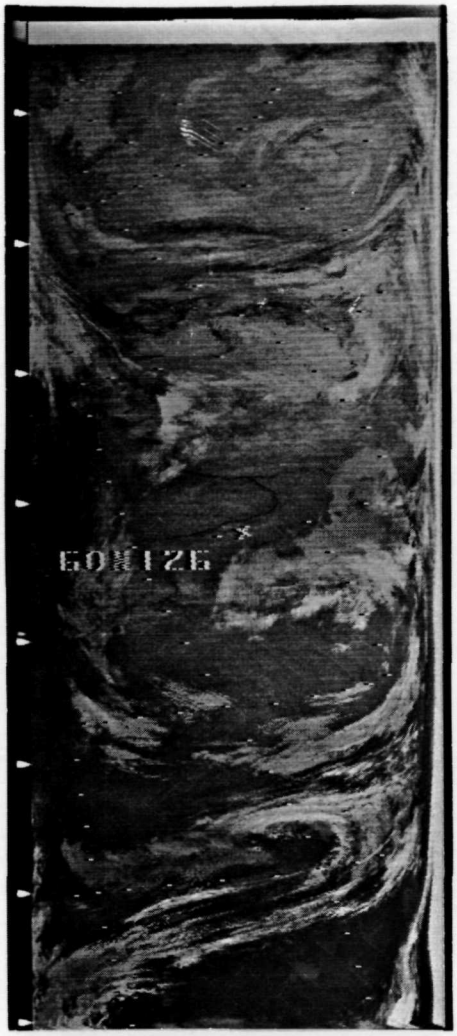

328
287

328
287

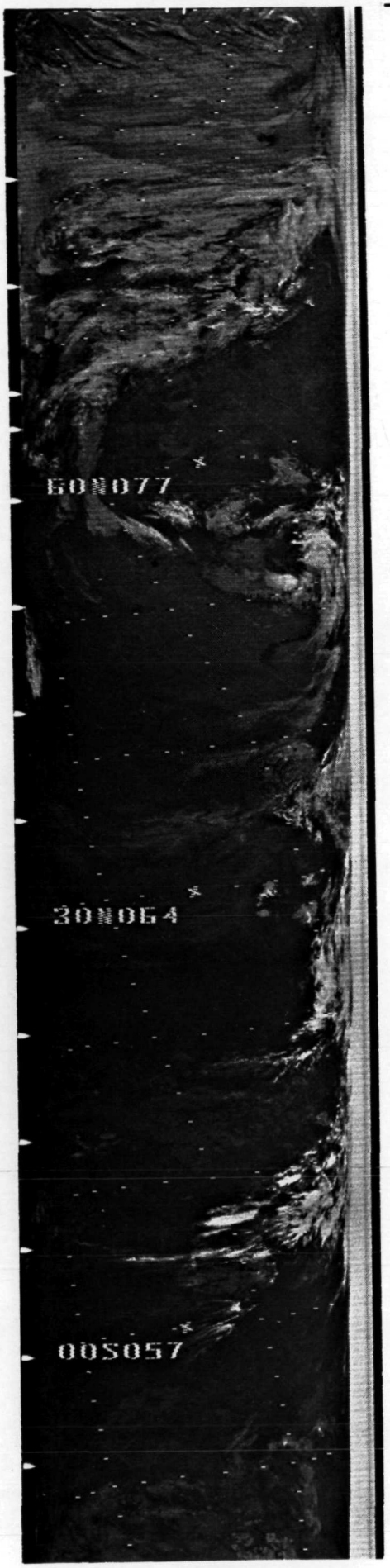

329
288

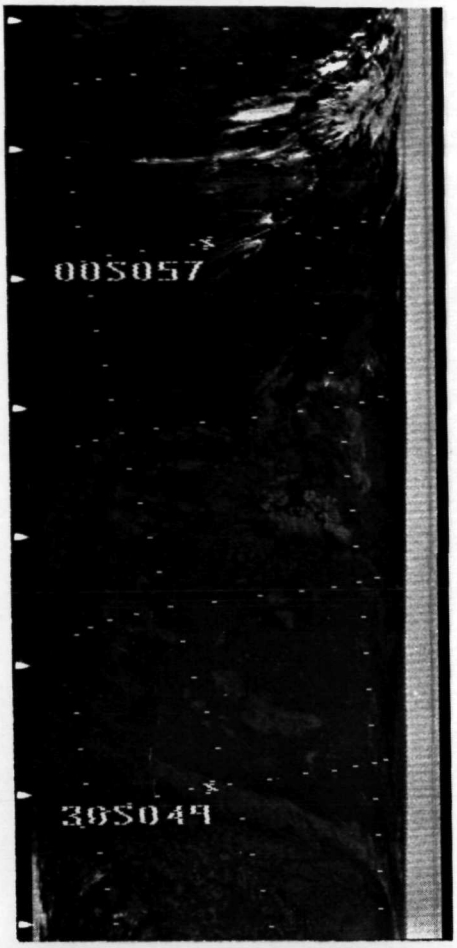

329
288

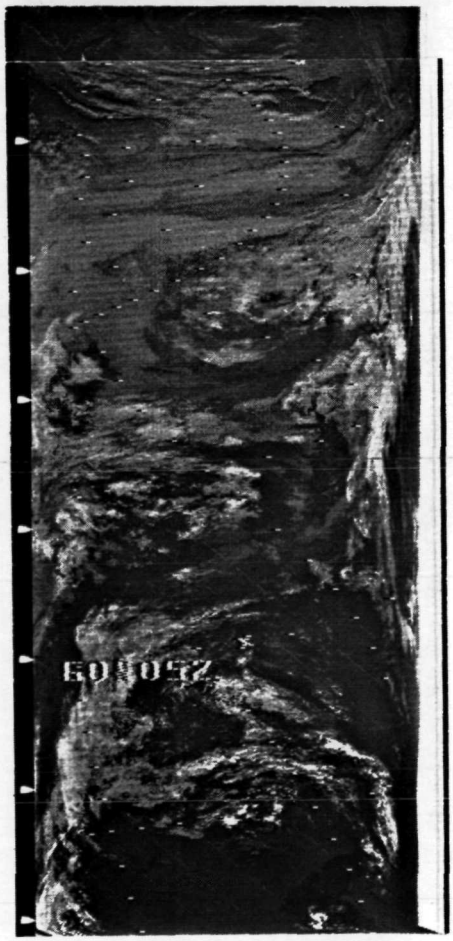

330
289

330
290

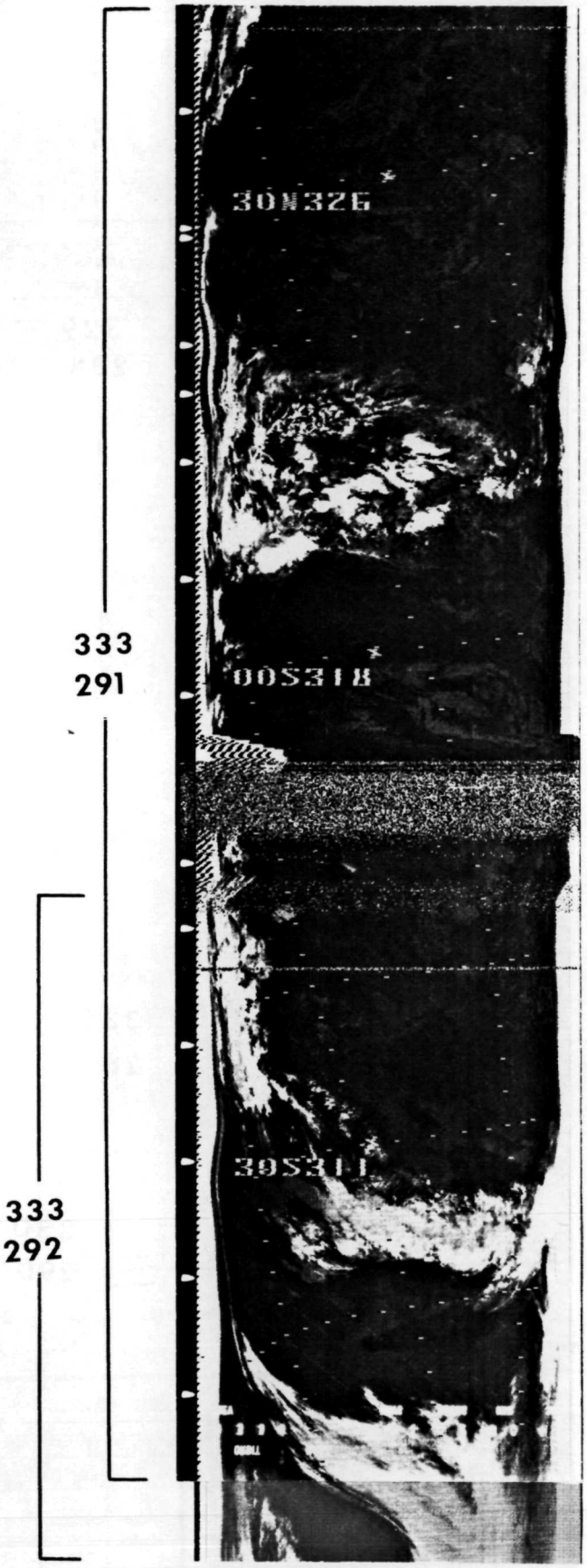
30N326
00S318
30S311
333
291
333
292

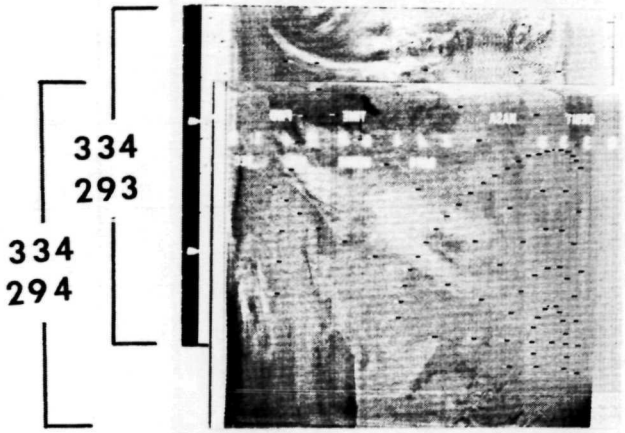
334
293
334
294

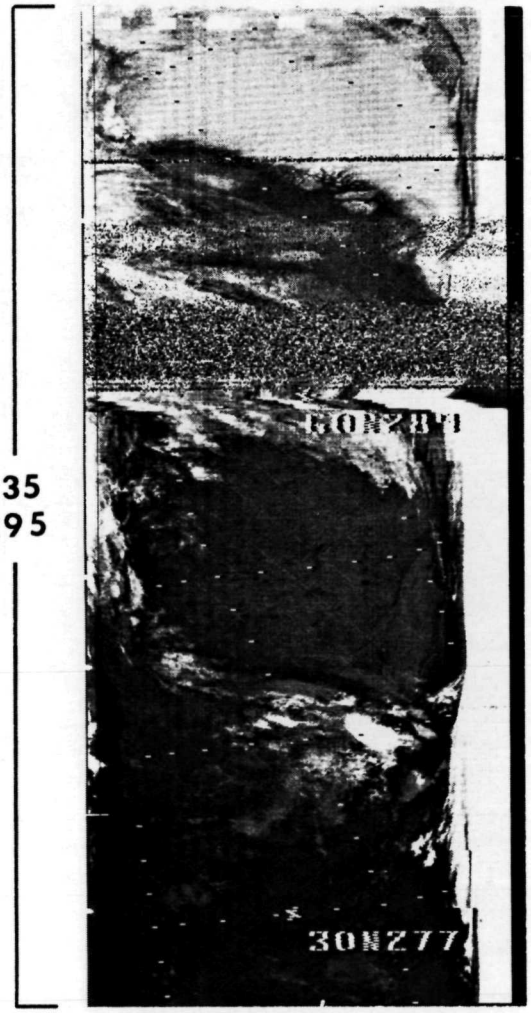
30N277
335
295

339
296

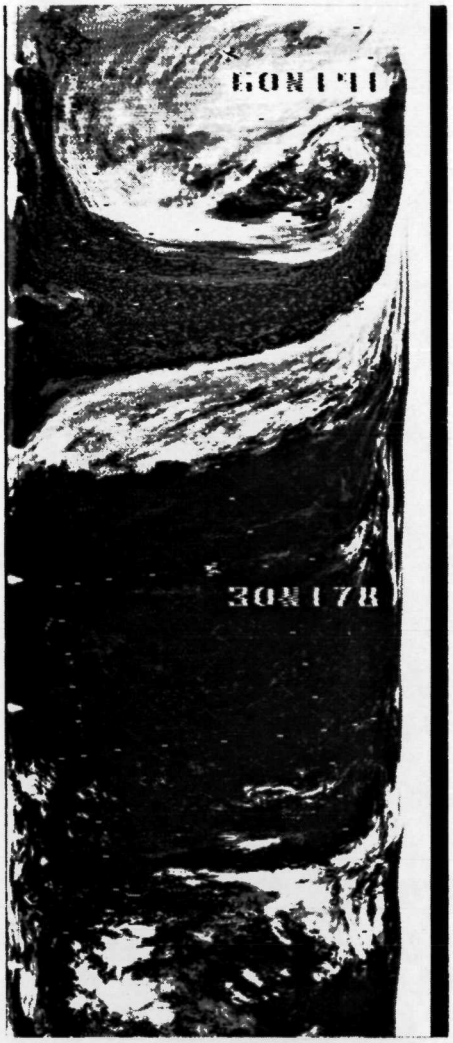

339
297

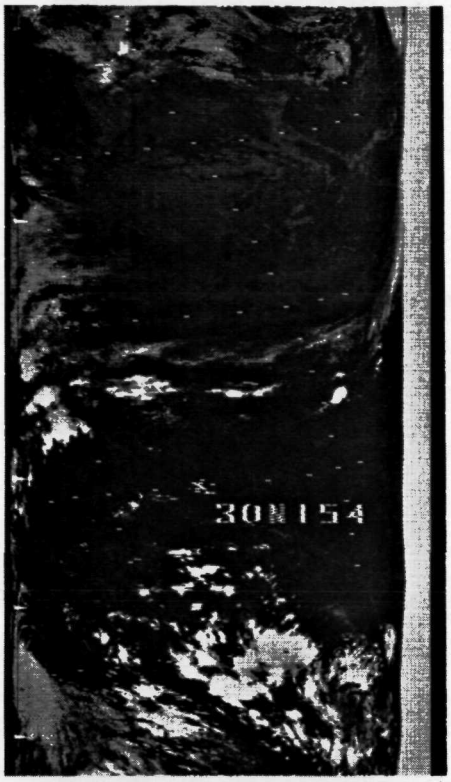

340
298

340
299

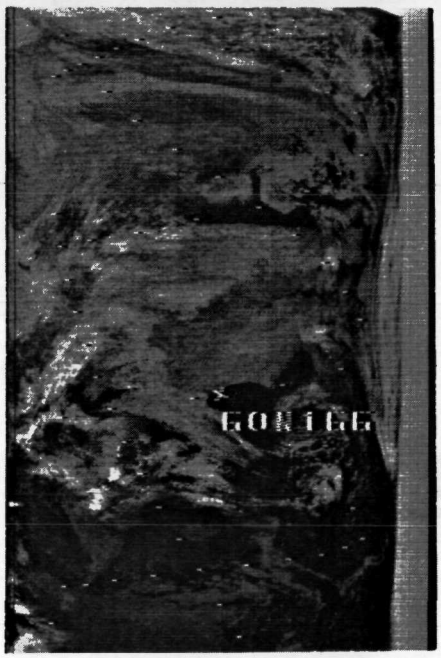

340
298

340
299

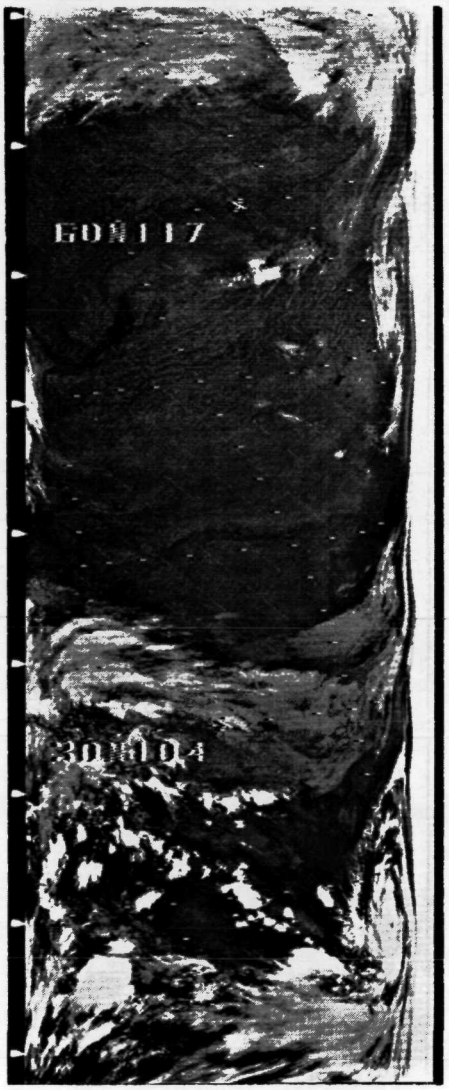

342
300

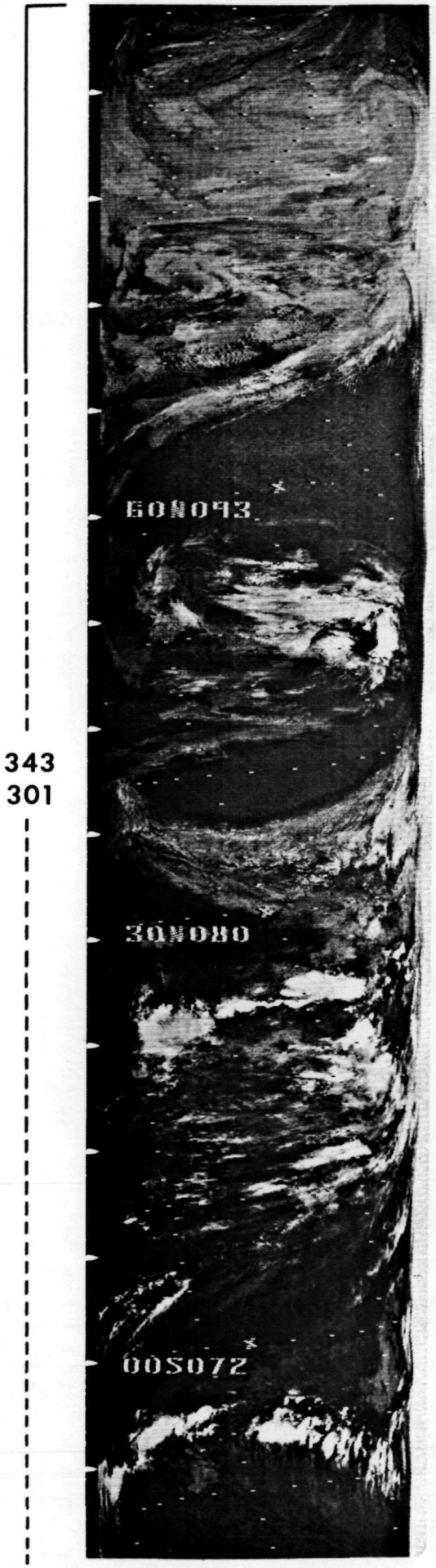
60N093
30N080
00S072
343
301

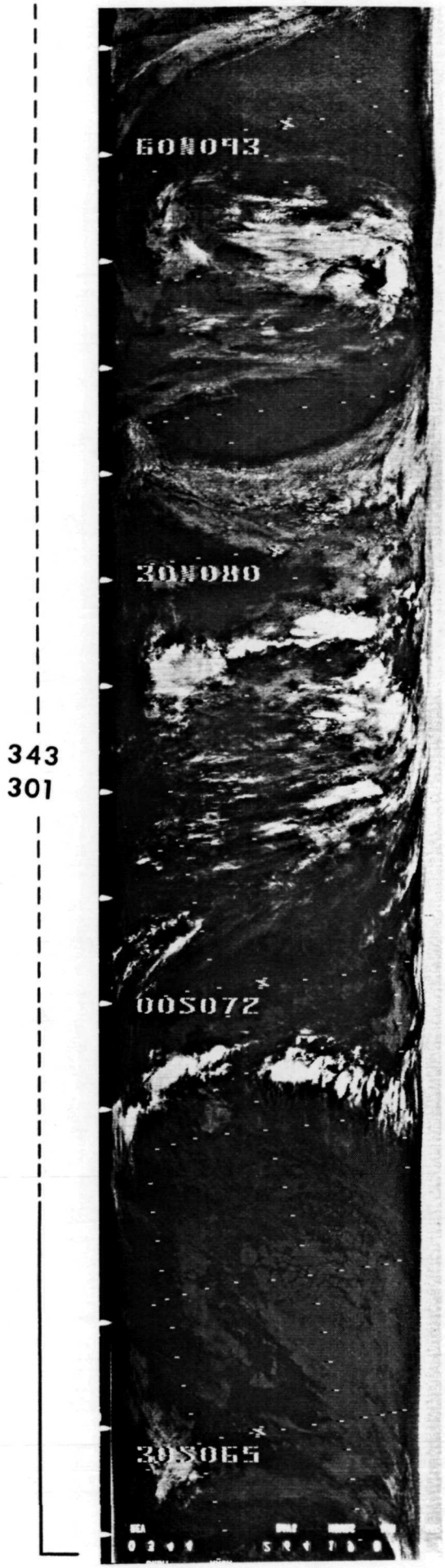
60N093
30N080
00S072
30S065
343
301

344
302

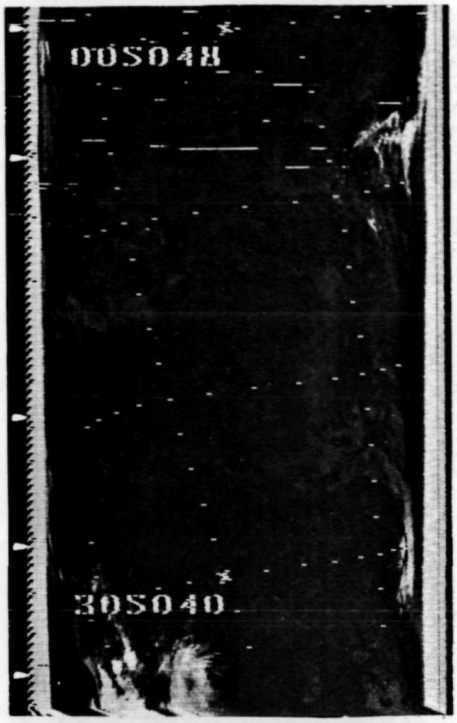

344
302

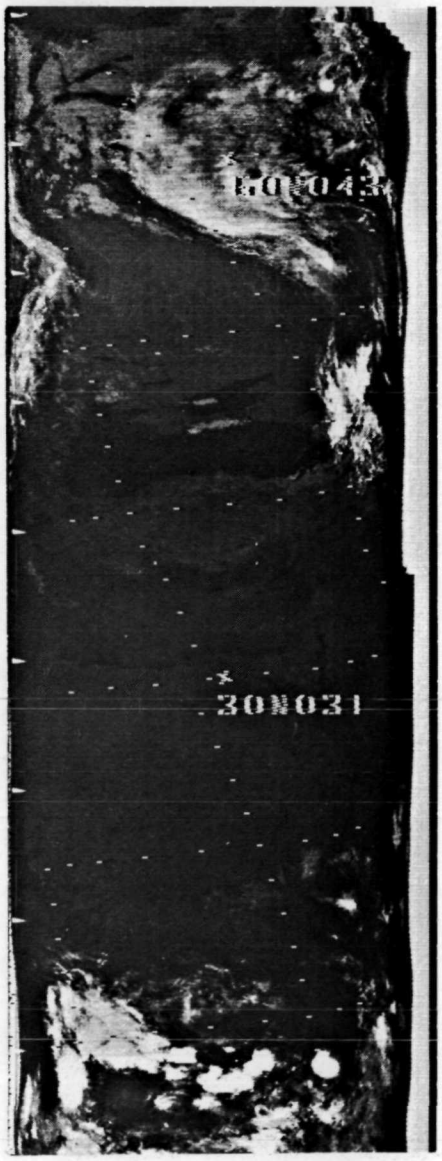

345
303

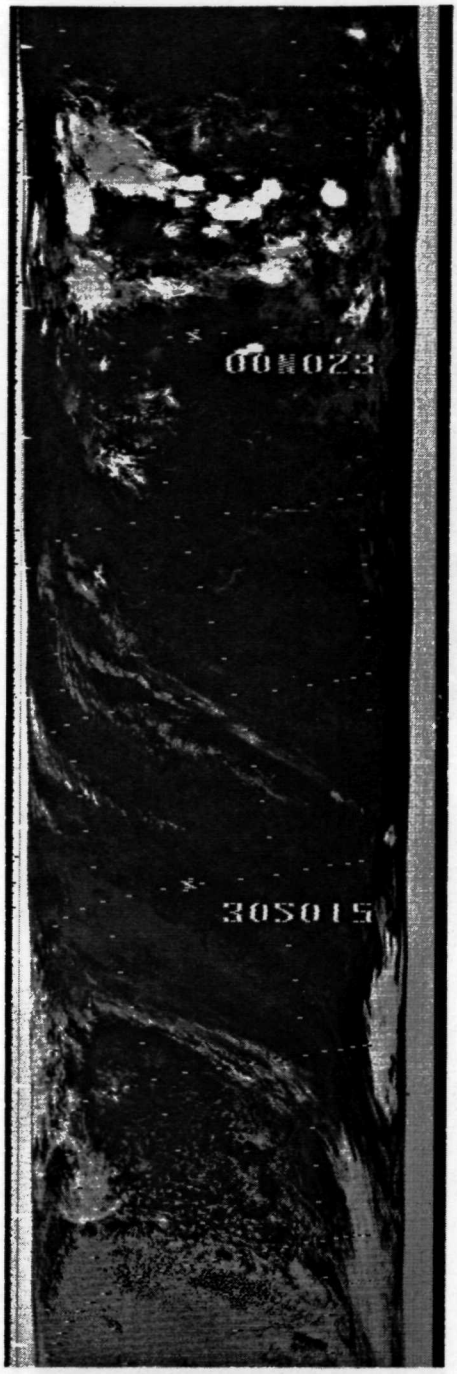

345
303

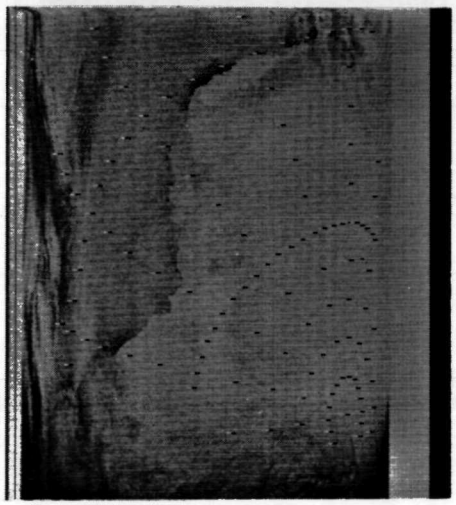

345
304

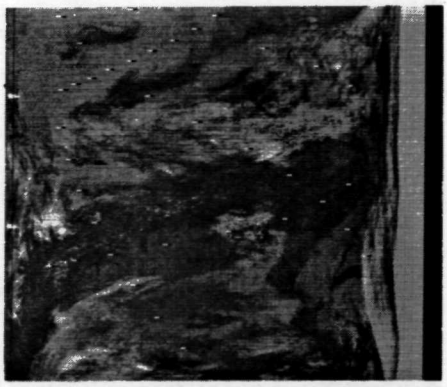

346
305

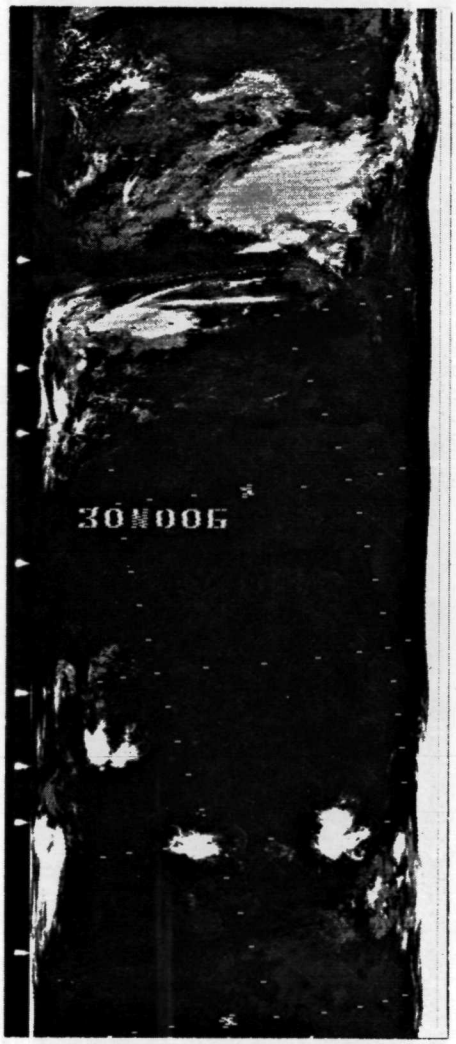

346
306

346
307

346
308

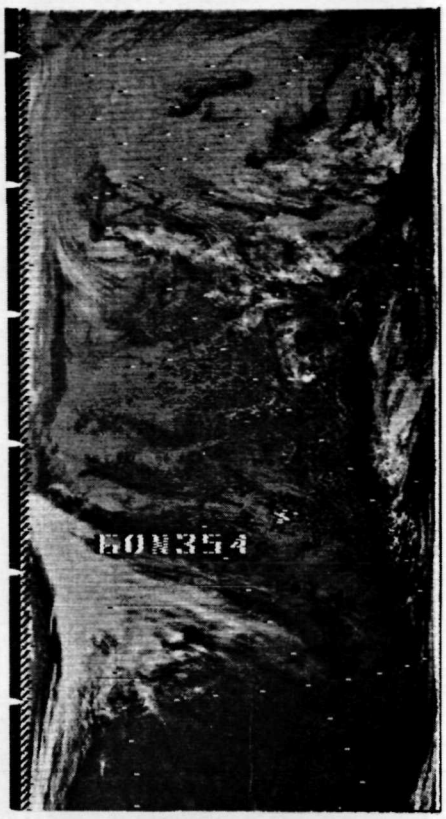

347
309

350
310

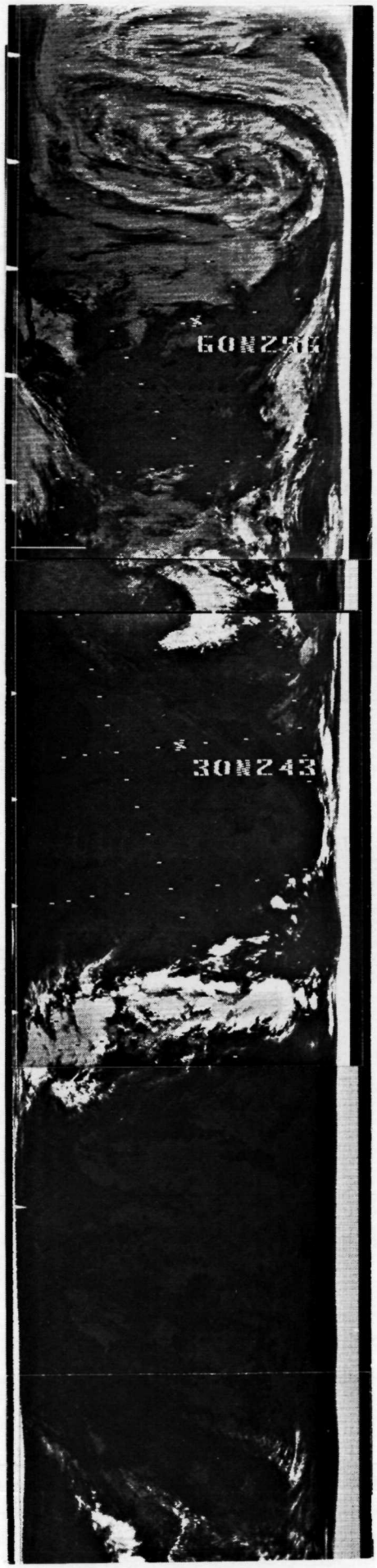

351
312

351
311

351
313

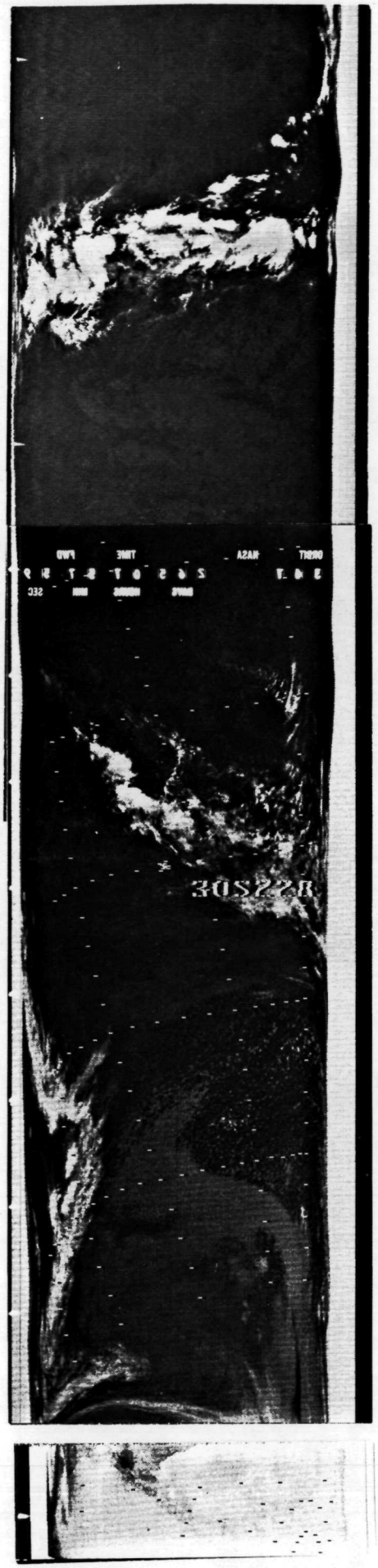

351
311

351
314

351
315

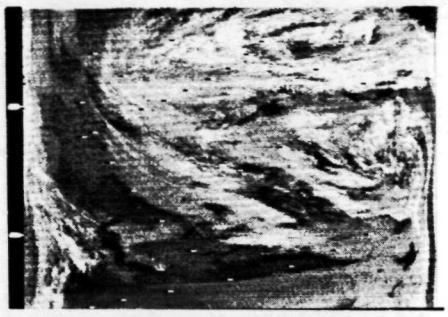

352
316

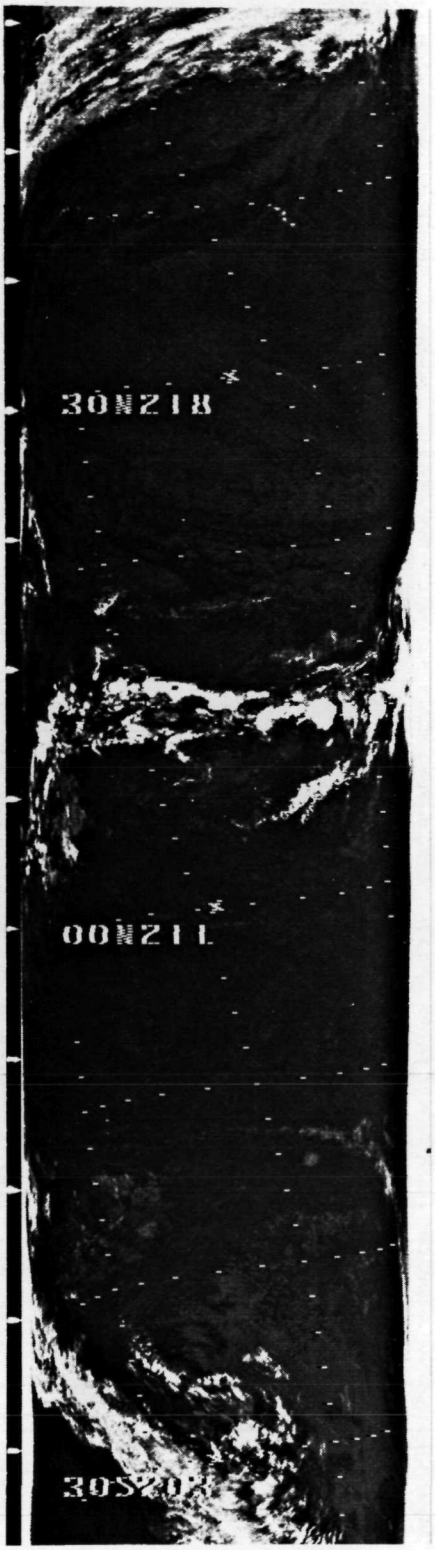

352
317

352
317

353
318

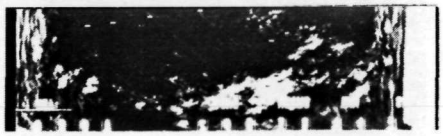

353
319

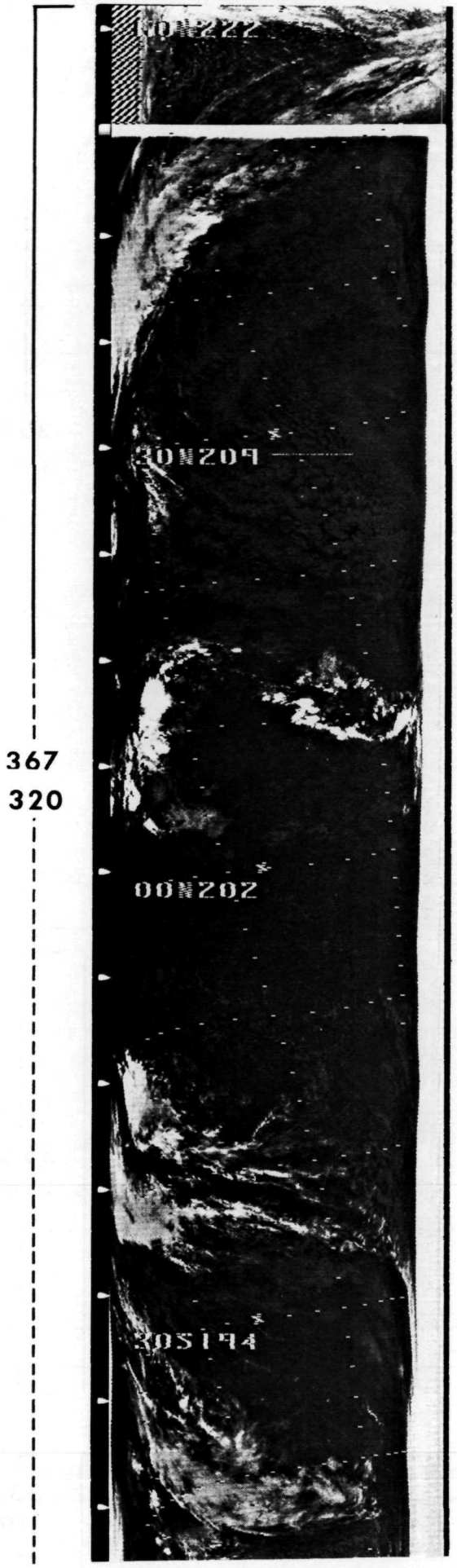
367
320

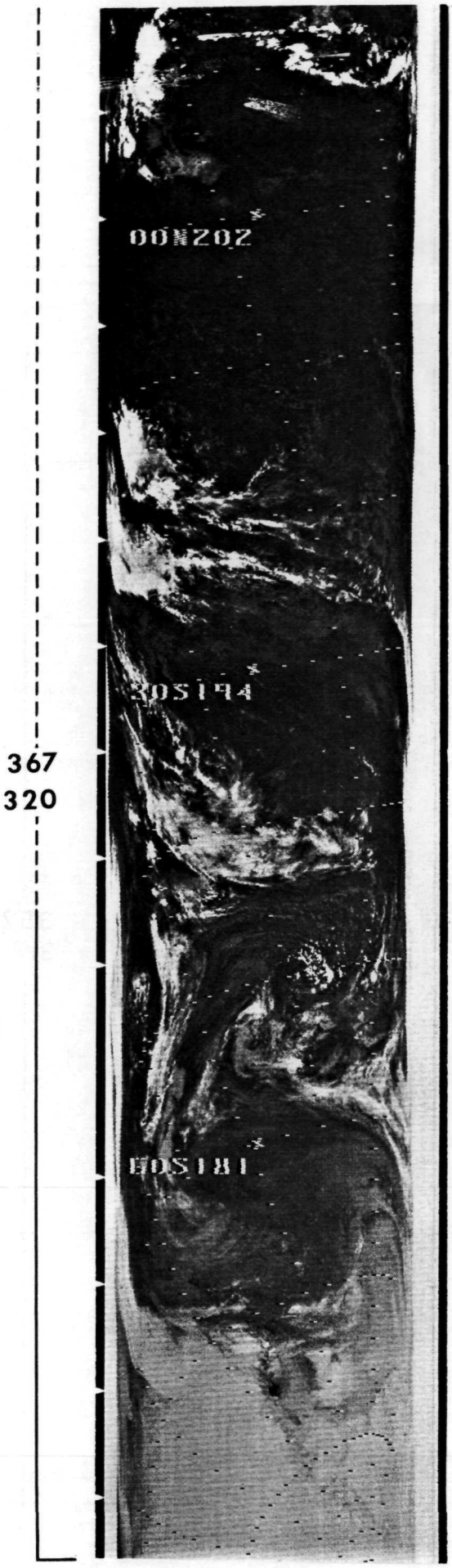
367
320

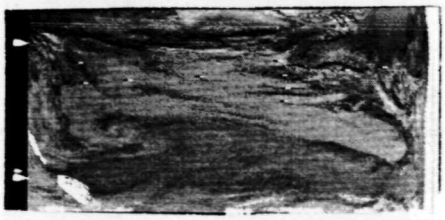

368
321

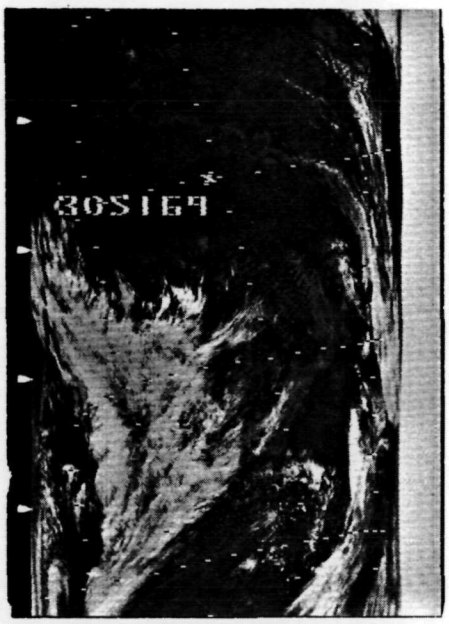

368
322

368
323